Motor axon guidance to the extraocular muscles

Lerner, Oleg

MOTOR AXON GUIDANCE TO THE EXTRAOCULAR MUSCLES

By
Oleg Lerner

A thesis submitted to the University of London for the degree of Doctor of Philosophy (Ph.D)

MRC Centre for Developmental Neurobiology
King's College London

I declare that all work presented in this thesis is my own.

Oleg Lerner

24/06/06

date

Abstract

The six extraocular muscles, which rotate the eyeball, are innervated by three cranial nerves: the oculomotor nerve, which innervates four muscles, the trochlear nerve and the abducens nerve, which innervate one muscle each. In this thesis I investigate the mechanisms which control axon guidance to the extraocular muscles.

Five candidate guidance cues were investigated, whose involvement in axon guidance to the extraocular muscles had been implicated by previous research: class III secreted semaphorins (Sema3F, Sema3C and Sema3A), hepatocyte growth factor (HGF) and stromal cell-derived factor 1 (SDF-1). Expression analysis in the chick embryo revealed that *HGF* is expressed in the dorsal oblique muscle, the target of the trochlear nerve, and in the mesenchyme surrounding several of the oculomotor target muscles. HGF promoted outgrowth from rat embryonic explants containing oculomotor and trochlear neurons and was therefore proposed to act as a chemoattractant for these axons. *Sema3C* was expressed in the lateral rectus muscle, the target of the abducens nerve, and Sema3C promoted outgrowth from abducens explants *in vitro* and was therefore proposed to act as a chemoattractant for abducens axons. Sema3F chemorepelled oculomotor axons *in vitro* and inhibited outgrowth from trochlear explants.

SDF-1 was expressed in the mesenchyme adjoining the oculomotor and trochlear nerves' exit points from the neural tube, at stages when these axons are emerging into the periphery. *In vitro*, SDF-1 promoted trochlear and oculomotor axonal outgrowth and facilitated oculomotor axons' ectopic exit from the explant. This led to the conclusion that SDF-1 acts to enable exit from the neural tube of these axons. This theory was supported by the finding that mice mutant for the receptor for SDF-1 displayed a failure of oculomotor axons to exit the neural tube correctly. In summary, this project has identified distinct attractants and repellents which govern axon guidance to the extraocular muscles.

CONTENTS

List of Figures

Acknowledgements

I would like to thank my supervisor, Sarah Guthrie, for her guidance, encouragement and above all patience throughout my PhD. A debt of gratitude is also owed to Uwe Drescher for deputizing so effectively in Sarah's absence and generously offering to help at every opportunity thereafter. The whole Guthrie lab deserves fulsome praise just for putting up with me, even at my grumpiest in these last few months, but special thanks must go to Rachel for having shown the way, being an unerring source of wisdom, and above all being a great friend, to John for always being ready to help, even when hundreds of miles away, to Fabrice for teaching me most of what I know in the lab, and to Arifa for being a ray of sunshine even on the darkest days. A big thank you also to Valerie, Uma, Ailish and Maria for making it such a fun place to work, for which our neighbours in the Cohen lab: Laura, Natalie, Mathieu, Romke and Jim also deserve much credit.

I'm grateful to everybody who has generously provided the ingredients essential to make this PhD a success: Drs John Chilton and Britta Eickholt for supplying the *in situ* constructs and Drs Ivo Lieberam and Fannie Mann for providing the mutant mice.

Finally a big thank you to all my friends and family for their unstinting support and encouragement and above all to my wife, Nanna, for being such a pillar of strength, without whom I might not have made it to the end.

This work was supported by Guys and St Thomas's Charitable Trust Foundation

Chapter 1: Introduction

The aim of this study is to investigate the mechanisms of axon guidance that control axonal growth towards and innervation of the extraocular muscles. The extraocular muscles rotate the eyeball to move the general field of vision and exert fine control to maintain a steady image on the retina. They act in three antagonistic pairs: the medial and lateral recti move the eye horizontally; the dorsal and ventral recti control vertical movement; the dorsal and ventral oblique muscles provide torsion. Three nerves originating in the brainstem supply the innervation to the extraocular muscles. The relationships between these muscles and the nerves that innervate them have been mapped using retrograde horseradish peroxidise labelling in a variety of species including quail, chick and monkey (Heaton 1981, Heaton and Wayne 1983, Porter et al 1983). The lateral rectus is innervated by the ipsilateral abducens nerve, arising from rhombomeres 5 and 6 in the chick, or rhombomere 5 in mammals. The dorsal oblique is innervated by the contralateral trochlear nerve, whose cell bodies are located in the rostral part of rhombomere 1. The remaining four muscles (the dorsal rectus, the ventral rectus, the medial rectus and the ventral oblique) are innervated by the oculomotor nerve positioned in the caudal midbrain. Figure 1.1 shows a schematic view of the connectivity in the system.

This system has hitherto received relatively sparse attention, but what little is known highlights some very interesting questions with regard to how the complex pattern of innervation is accurately established. One of the issues is that the muscles are located in close proximity to each other, and the navigating axons must distinguish accurately between the correct and incorrect targets. Also, the oculomotor nerve displays an unusual but highly reproducible pattern of innervation. Oculomotor axons extend to the farthest target initially (the ventral oblique) ignoring other developing extraocular muscle masses which lie in close proximity to their trajectory, and only form branches into the other targets (ventral rectus, medial rectus and dorsal rectus) after initial contacts with ventral oblique had been made (Chilton and Guthrie 2004). Once the oculomotor axons have contacted the dorsal rectus, the motor neurons that innervate this

muscle begin to translocate their cell bodies across the midline; the end result being that this branch of the oculomotor nerve projects contralaterally (Puelles 1978, Chilton and Guthrie 2004, see figure 1.1). This study investigates which signals enable the axons to select the right target and ignore the inappropriate ones and what mechanisms determine the precise trajectory of the nerves and the reproducible pattern of branching and innervation.

This introductory chapter will address firstly the patterning events in the early embryonic development, describing the mechanisms that specify the central nervous system (CNS) and subdivide it into broad regions. These regions are subsequently patterned into specific domains which generate different classes of neurons, including the motor neurons that will form the three nerves that innervate the extraocular muscles. I will describe what is known in the sequence of events spanning the formation of an initially homogenous neural plate to the birth of oculomotor, trochlear and abducens neurons. Secondly, the development of craniofacial mesenchyme and neural crest will be considered with particular focus on the formation of head muscles, which is different to myogenesis in the trunk, but is as yet relatively poorly understood. The key events in the patterning and migration of cranial muscles follow a different schedule from those of the trunk muscles and are under the control of different signalling cascades, and the resulting differences in the craniofacial environment compared to the trunk have an impact on and pose particular challenges for the pathfinding of cranial motor axons. Thirdly, I will discuss the mechanisms that enable axons to navigate through their environment focusing on the major families of axon guidance cues and their receptors and illustrating the principles with examples of systems where these cues are known to exercise a major influence on axon pathfinding. Particular emphasis will be placed on the molecules that have been investigated in this study namely the semaphorins, HGF and SDF-1. Subsequently, I will describe in more detail the development of oculomotor, trochlear and abducens nerves, describing the timescale of axonal growth, their trajectory and key decision points. Finally, I will summarize the aims of the project and the experimental approaches employed to pursue the answers to the unresolved questions that this fascinating system poses.

1.1 CNS PATTERNING IN THE EARLY EMBRYO

During embryonic development the central nervous system (CNS) is derived from a sheet of cells known as the neural plate. The neural plate is induced from ectodermal cells, which form the dorsal surface of the embryo, by contact with ingressing mesodermal cells during the gastrulation stage. The precise molecular nature of the inducing signal is unclear, but attention has centred on three secreted proteins: follistatin, noggin and chordin, which are expressed in the Spemann's organizer (Hensen's node in birds and mammals). These are capable of neural induction in naïve ectodermal cells and can directly bind to and antagonise members of the bone morphogenic protein (BMP) family (Piccolo et al 1996). BMP2 and BMP4 are expressed in presumptive neuroectoderm and are thought to repress neural induction. Recently, this 'default' model of neural induction has been challenged by a number of groups, and fibroblast growth factor (FGF) signalling has been shown to be an important contributor, either directly, or through downregulation of BMP signalling and potentially downregulation of other signalling pathways (reviewed in Stern 2005).

Initially neural plate cells are uniformly anterior in their character. It was shown in the chick that during a brief period between HH stages 3-4 (Hamburger and Hamilton 1951) the combined action of four factors (FGFs, retinoids, paraxial mesoderm-derived caudalising factor and a rostralising factor) specifies the neural plate into different rostrocaudal regions: the forebrain, the midbrain, the hindbrain and the spinal cord (Muhr et al 1999). The fate of cells within each domain becomes increasingly restricted through expression of transcription factor cascades and inductive signalling from neighbouring cells. A key role in this process is played by organisers. An organiser is a group of cells that can pattern neighbouring tissues by secreting diffusible signals that influence the fate of cells they bind to. Sometimes these signals act as morphogens and induce different cell fates at different concentrations.

1.1.1 Midbrain-hindbrain boundary organiser.

A crucial centre in the patterning of the anterior-posterior (AP) axis is the midbrain-hindbrain boundary (MHB) organiser. The MHB organiser was identified in transplantation experiments. Transplantation of quail or mammalian midbrain into chick forebrain induces expression of engrailed genes (which are usually expressed in a gradient either side of the midbrain-hindbrain boundary) and subsequently a cerebellar phenotype (Martinez et al 1991). Marin and colleagues (1994) showed that, whilst a rostrocaudal inversion of a presumptive midbrain results in the development of a normal midbrain, rostrocaudal inversion of midbrain with isthmocerebellar tissue, thus including the presumptive organiser, gave rise to an ectopic isthmocerebellar complex plus a symmetric double-caudal midbrain. These cytomorphological changes were preceded by correlated changes in expression of engrailed-2.

The establishment of the midbrain-hindbrain boundary is controlled by two homeodomain transcription factors: *Otx2* and *Gbx2* (*gbx1* in zebrafish). The early neural plate expresses *Otx2* in an anterior domain and *Gbx2* in a posterior domain, with the boundary of the two domains corresponding to MHB. In *Otx2* mutant mice (where part of the coding region is replaced with E. Coli *lacZ* coding sequence) the forebrain and midbrain were not formed, *lacZ* expressing endomesodermal cells failed to localize anteriorly and *lacZ* expression was progressively extinguished in the ectoderm (Acampora et al 1995). In *Gbx2* mutant mice, the *Otx2* expression domain expanded posteriorly with organizer markers expressed at the new caudal border. Transient expression of *Gbx2* in the caudal region of *Otx2* domain in wild type mice resulted in a more rostral organizer and, at E9.5, an expanded hindbrain and a reduced midbrain (Millet et al 1999). Expression of *Otx2* in the anterior hindbrain results in an enlarged inferior colliculus and a caudal shift in the expression of midbrain markers (*Wnt-1*, *EphrinA5*), isthmic markers (*Pax2* and *Fgf8*) and hindbrain marker (*Gbx2*) (Broccoli et al 1999).

The organiser can regenerate following ablation, implying that it is induced by direct

cell-cell interactions (Irving and Mason 1999) and its position is defined by the boundary between *Otx2* and *Gbx2*-expressing domains; this suggests that these transcription factors activate the expression of cell surface molecules that participate in the induction of the organiser. Following induction the transcription of a number of genes is activated including transcription factors of the Pax family, and the diffusible molecules Wnt-1 and Fgf8. The establishment of the organizer is followed by the maintenance phase during which the expression of the above genes becomes dependent on one another (reviewed in Rhinn and Brand 2001). FGF8 can mimic the activity of the organizer, since beads coated with recombinant FGF8 produce ectopic mirror image midbrains as well as lateral protrusions which develop into isthmocerebellar tissue, when implanted into chick caudal diencephalons. The corresponding gene expression changes are a downregulation of *Otx2* and an upregulation of *En1*, *Wnt1* and *Fgf8*. Ectopic *Wnt1* and *Fgf8* expression formed concentric rings around the bead (Martinez et al 1999). Wnt1 functions as a mitogen and to maintain expression of *en* genes, but cannot recreate the organizer on its own. *Wnt1* knockout mice fail to develop midbrain and anterior hindbrain but this is rescued by expression of *En1* in midbrain (Danielian and McMahon 1996). Mice mutant for *Fgf8* fail to gastrulate, probably because they also lack *Fgf4* (Sun et al 1999).

1.1.2 Hindbrain patterning

The hindbrain is a highly regular structure divided into eight segments known as rhombomeres. Rhombomeric segmentation is marked by a series of morphological constrictions in the neuroepithelium at about HH stage 10 in the chick. This divides the hindbrain into autonomous metameric subunits with cells no longer free to move between them (Fraser et al 1990). Each rhombomere has a unique expression profile of developmentally regulated transcription factors which are believed to confer its identity and ensuing cell fate. Figure 1.2 shows a schematic representation of the hindbrain and marks the expression domains of some of the relevant regulatory genes (including the *Hox* genes, *kreisler* and *Krox-20*), which will be discussed in section 1.1.2.2). Firstly, I will discuss mechanisms, which govern the assignment of position along the

rostrocaudal axis to cells within each rhombomere, thereby enabling them to assume their prescribed developmental fate.

1.1.2.1 Assignment of rostrocaudal identity – retinoic acid and FGF8

A key morphogen involved in the assignation of rostrocaudal identity is retinoic acid (and its derivatives). It is produced by perinodal tissue and its synthesis increases threefold between HH stages 4-6 in the chick (Chen et al 1992); it has been shown that genes that are expressed within posterior rhombomeres (e.g. more 5' *Hox* genes) are activated by higher concentrations of retinoic acid (Simeone et al 1990). This has led to the hypothesis that as the node regresses, retinoic acid (RA) synthesis is increased resulting in specification of more posterior tissues. Although a gradient of RA across the hindbrain has never been directly demonstrated, its putative existence is supported by the distribution of its two main metabolic enzymes: RALDH-2, which converts retinaldehyde into RA, and CYP26, a cytochrome P450 related enzyme which oxidatively inactivates it. During early gastrulation in the mouse and chick, *Raldh-2* is expressed in the mesoderm adjacent to the node and the primitive streak and at the headfold stage it remains in the posterior regions of the mesoderm up to the base of the headfolds. In contrast, *Cyp26* is localised in the neural folds and the presumptive midbrain and forebrain, which suggests that the embryo is actively removing RA from the anterior neuroepithelium. Hence the high RA levels found at the hindbrain/spinal cord boundary could diffuse into the adjacent hindbrain region and form a shallow gradient that participates in patterning this tissue. Retinoic acid signals through nuclear receptors which act as ligand-gated transcriptional activators; these fall into two families: RA receptors (RAR: subtypes α,β and γ) and retinoid X receptors (RXR: subtypes α,β and γ). RA in complex with a receptor binds to retinoic acid response elements (RARE), which are found in the enhancers of several *Hox* genes, hence the level of RA can directly influence *Hox* gene expression (reviewed in Gavalas and Krumlauf 2000). Exposing mouse embryos to high concentrations of RA results in a posteriorisation of the hindbrain, as reflected by the expression of rhombomere-specific markers and the transformation of the trigeminal motor nerve (normally resident in

rhombomeres 2/3) to a facial identity (normally resident in rhombomeres 4/5) (Marshall et al 1992). Conversely, RA deficiency results in anteriorisation of the hindbrain. The degree of anteriorisation depends on the level of deficiency. Simultaneous targeted inactivation of RARα and RARβ in mice results in an intermediate RA signalling phenotype. All rhombomeres anterior to r5 are normal, but r5 is expanded, the r5/6 boundary is lost, ectopic otic vesicles are formed and expression of anterior rhombomere markers spreads caudally (Dupe et al 1999). Targeted mutation of *Raldh-2* results in a very low RA signalling phenotype (some residual RA activity remains probably through the conversion of retinol by other enzymes). In this case r5-r8 markers are missing or severely downregulated, and *Hoxb1* and *Wnt8a* expressing cells, instead of forming a defined r4, are scattered throughout the caudal hindbrain (Niederreither et al 2000). The vitamin A deficient quail provides a model of complete absence of RA signalling: here, rhombomeres 4-7 fail to develop. The resulting hindbrain is of approximately normal length, rhombomeres 1 to 3 each approximately double in size. The embryos can be rescued by injection of retinol in to the egg (Gale et al 1999).

In addition to the caudalising signal provided by retinoids, FGF8 signalling from the isthmus is important for the patterning the anterior hindbrain. The FGF8 and retinoid gradients provide the AP positional information within the developing hindbrain which is used to regulate the expression of other genes, which in turn facilitate the segmentation of the hindbrain into rhombomeres, each with a unique identity, and the subsequent differentiation of rhombomere-specific neuronal populations. Particularly important amongst these are the Hox genes – an evolutionarily conserved, large family of homeobox transcription factors (Lumsden and Krumlauf 1996). Rhombomere 1 is unique amongst hindbrain rhombomeres in not expressing any *Hox* genes. Transplantation of r1 tissue to more caudal positions showed it was competent to express *Hox* genes, but this expression was blocked by the addition of isthmic tissue or FGF8 protein. Ectopic addition of FGF8 to r1 blocked expression of *HoxA2* in rhombomere 2, whereas adding FGF8-neutralizing antibody extended *HoxA2* expression into r1 (Irving and Mason 2000). Therefore, the opposing gradients of retinoic acid and FGF8 cooperate in the anterior-posterior (AP) patterning of the hindbrain.

1.1.2.2. Genes that confer segment identity

The Hox gene family demonstrates co-linearity; that is the position of the gene on the chromosome correlates with the expression site on the AP axis, with genes closest to the 3' end being expressed most rostrally. There are four Hox clusters in vertebrates (a-d), containing sets of paralogous genes. Each rhombomere has its own distinct complement of *Hox* gene expression (summarized in figure 1.2) (Lumsden and Krumlauf 1996).

It is difficult to disentangle the role individual *Hox* genes play in patterning, since mutations in single *Hox* genes can often be compensated by other paralogues and, conversely, because *Hox* genes are sometimes involved in the control of expression of other *Hox* genes, so mutations in individual *Hox* genes can have knock on effects. Nonetheless, mutant studies have provided invaluable insights into the function of *Hox* genes in hindbrain development.

HoxA1 mutants have abnormalities in rhombomeres 3-8, including a total absence of r5, suggesting that *HoxA1* is a key gene for the patterning of these rhombomeres and r5 in particular (Carpenter et al 1993). *HoxA2* mutants lack the r1/r2 boundary and have an enlarged r1 territory, implying that HoxA2 confers r2 identity and represses the induction of r1 fate in the cells in which it is expressed (Gavalas et al 1997). *HoxB1* appears to be critical in the development of rhombomere 4. Its expression is confined to that rhombomere; and in the *HoxB1* mutant r4 assumes an r2-like identity. Both facial branchiomotor neurons and contralateral vestibular acoustic neurons, which are born in r4, fail to migrate normally and instead migrate dorsally in the manner of trigeminal neurons (resident in r2) (Studer et al 1996). Conversely, overexpression of *HoxB1* in chick r2 using a retroviral vector results in trigeminal axons acquiring a facial phenotype and projecting to the r4 exit point (Bell et al 1999). Overexpression of *HoxB1* in r1 also produces facial-like motor neurons, and the overexpression of *HoxA2* in r1 produces ectopic branchiomotor neurons with trigeminal characteristics (Jungbluth et al 1999). As the overexpression of *HoxB1* in rhombomeres anterior to r4 is sufficient to confer r4 identity on motor neurons found within those rhombomeres, and the absence of *HoxB1*

results in a failure of motor neurons located in presumptive r4 to assume r4 fate, it can be surmised that *HoxB1* is the key regulatory gene for the establishment of r4 identity. Similarly, overexpression of *HoxA3* in the rostral hindbrain results in the induction of motor neurons normally found in caudal hindbrain (Guidato et al 2003). *Hox* genes also mutually repress the expression of other *Hox* genes in order to further demarcate the AP patterning they induce. For example, in *HoxA3/HoxB3* compound mutant mice, not only are r4 facial branchiomotor neurons duplicated in r6, but *HoxB1* is also upregulated in r6 (Gaufo et al 2003). The complex interconnections between the different *Hox* genes are still being unravelled. The general principles of *Hox* gene function in hindbrain development are emerging, though. As illustrated by the examples above, *Hox* genes play a key role in establishing segment identity and subsequently in directing the specification of neuronal cell types that arise in that segment.

Another two transcription factors that are important in hindbrain segmentation are Krox-20 and kreisler. Krox20 is a zinc-finger transcription factor expressed in r3 and r5 at early stages of hindbrain patterning. Mouse mutants in this gene have a fused region thought to be equivalent to r2/4/6 and lack both r3 and r5 (Schneider-Maunoury et al 1993, Schneider-Maunoury et al 1997). Krox20 regulates expression of *EphA4* which is normally expressed in r3 and r5 and is known to be involved in rhombomere boundary formation, which could explain this phenotype (Theil et al 1998). The expression of *Krox20* in r5 could be controlled by kreisler – a leucine zipper transcription factor, which is expressed in r5 and r6. Mice lacking *kreisler* show a lack of segmentation posterior to r3/r4 and also lack *Krox20* expression in r5 (Manzanares et al 1999). Both *kreisler* and *Krox20* are expressed prior to the activation of *Hox* genes and may therefore be upstream regulators of *Hox* gene expression.

1.1.2.3 Establishment of rhombomere boundaries and periodicity

The boundaries between newly formed rhombomeres consist of loosely-packed cells, suggesting a low affinity for their neighbours. Transplantation experiments have suggested that odd and even rhombomeres have different cell surface properties (Guthrie

and Lumsden 1991). Cells from even-numbered rhombomeres preferentially adhere to cells from other even-numbered rhombomeres, and cells from odd-numbered rhombomeres preferentially adhere to other odd rhombomere-derived cells (Wizenmann et al 1997). A likely explanation for this differential affinity is the alternate expression of Eph receptors and their ligands on different rhombomeres. EphA4, EphB2 and EphB3 are expressed in r3 and r5, whilst ephrinB ligands are expressed in even-numbered rhombomeres (r2, r4 and r6) (Nieto et al 1992). Repulsive EphR-ephrin interactions have been found to mediate cell sorting, facilitating segregation into rhombomeres, defined by surrounding rhombomere boundaries (Xu et al 1999, Mellitzer et al 1999). Once these boundaries are established, they go on to express a number of specific markers such as FGF3, peanut agglutinin, chondroitin sulphate proteoglycan, L1 and laminin, which, in addition to the large intercellular spaces, enable their subsequent occupation by axon tracts later in development (Heyman et al 1993). Interestingly, the odd-even periodicity appears to specify an additional dimension to the positional identity of hindbrain cells. This was demonstrated in transplantation experiments, where grafting of anterior rhombomeres into posterior positions induced posteriorisation but with a preference to retaining the original even or odd identity (i.e. it was easier for r4 to become r6 than r5, for example) (Itasaki et al 1996).

1.1.3 Dorso-ventral patterning

Specification of neuronal fate depends on the assignment of a full set of cartesian coordinates to cells in the developing neural tube. Equally important to specifying the rostro-caudal position is the assignment of dorso-ventral identity. Dorso-ventral (DV) patterning is laid down as a result of morphogens secreted from adjacent tissues on the ventral and dorsal sides of the neural tube inducing the expression of different transcription factors at different points along the DV axis; these transcription factors specify different domains which will give rise to different cell types including motor neurons.

Ventralising signals are secreted from the notochord - a region of axial mesoderm lying

ventrally to the neural tube along the caudal hindbrain and the spinal cord. The absence of the notochord results in a dorsalised neural tube, both in mouse mutants that lack the notochord (Pringle et al 1996), and following surgical ablation in the chick (Placzek et al 1990). Grafting an ectopic notochord laterally to the neural tube in the chick ventralises this lateral region, producing an ectopic floor plate and adjacent spinal motor neurons (Yamada et al 1991). Medium conditioned by the notochord can reproduce this effect, suggesting a diffusible signal (Yamada et al 1993, Placzek et al 1993). Sonic hedgehog (SHH), a homologue of the drosophila hedgehog gene, was identified as the key signal. Mice mutant for this gene lack both the floor plate and the surrounding motor neurons (Chiang et al 1996). Anti-SHH antibodies applied to chick explants *in vitro* produce a similar phenotype (Marti et al 1995). SHH protein induces floor plate at high concentrations and motor neurons at lower concentrations (Roelink et al 1995).

In addition to SHH signalling, retinoic acid produced in paraxial mesoderm promotes ventralisation of the neural tube and prompts differentiation of ventral motor neurons in the spinal cord in an SHH-independent manner (Novitch et al 2003). Retinoids may also be involved in governing the differentiation of two interneuron populations in the spinal cord (Pierani et al 1999). Thus retinoic acid appears to be a key morphogen in the developing nervous system in both the anterior-posterior and the dorso-ventral axes.

Dorsalising signals are secreted from the epidermal ectoderm, a region which flanks the neural plate prior to tube closure and overlies the neural tube subsequently. The epidermal ectoderm secretes bone morphogenic proteins which account for its dorsalising activity. BMP4 and BMP7 are necessary for the induction of neural crest, some interneuron populations and roof plate tissue (Liem et al 1995). The roof plate maintains signalling by producing BMP4 and BMP7 after neural tube closure. Ablation of the roof plate by expressing diphtheria toxin under a Gdf7 promoter (a roof plate gene) prevents the induction of dorsal interneuron populations (Lee at al 2000). *Lhx1α*-deficient mice, which lack the roof plate, have the same phenotype (Millonig et al 2000). However, BMPs do not appear to act in the same concentration-dependent manner that SHH does (Liem et al 1997).

1.1.3.1 Determination of progenitor cell identity in the ventral neural tube

Graded SHH signalling gives rise to multiple progenitor domains in the ventral neural tube. These domains are defined by the complement of homeodomain and bHLH transcription factors that they express. Expression of these factors is controlled by SHH in a concentration-dependent manner (reviewed in Shirasaki and Pfaff 2002). These transcription factors are divided into two classes according to how their expression is affected by SHH. Class I genes are constitutively expressed by the neuroectoderm, but exposure to SHH restricts them to dorsal regions. Class II genes, on the other hand, are activated by SHH and are therefore expressed more ventrally. Different members of each class are sensitive to different concentrations of SHH, which establishes broadly delineated expression domains along the DV axis. The boundaries between the neighbouring but overlapping domains are sharpened by the antagonistic action of Class I and Class II on each other's expression (see figure 1.3).The mutual repression of class I and class II genes is augmented by a group of transcriptional co-repressors called groucho-TLE co-repressors (Muhr et al 2001). These interactions relieve progenitor cells of the need for further morphogenic signalling. Once progenitor domains are established it is likely that cell surface molecules act to prevent cell mixing between neighbouring domains. At the moment it is not clear what these are, although cadherins have been implicated (Espeseth et al 1998, Lele et al 2002).

Figure (1.3) shows the five progenitor domains established along the different axial positions in the ventral neural tube. The two ventral-most domains are of interest with regard to motor neuron formation. The ventral-most domain (P3) is defined by its expression of class II factors *Nkx2.9*, *Nkx2.2*, *Nkx6.2* and *NKx6.1* and its lack of expression of Pax6 (a class I gene). In the spinal cord this domain gives rise to a population of interneurons known as V3 interneurons, but in the hindbrain it gives rise to branchiomotor and visceromotor (BM/VM) neurons (these are dorsally projecting hindbrain motor neurons that innervate branchial arch muscles and parasympathetic ganglia respectively – see figure 1.4). In *Nkx2.2* mutant mice the lack of this class II factor relieves the repression on Pax6, leading to Pax6 expression spreading ventrally;

this results in the development of ectopic motor neurons at the expense of V3 interneurons in the P3 domain in the spinal cord (Briscoe et al 1999). In the hindbrain, however, both BM/VM neuron generation in the P3 domain and somatic motor neuron generation in the dorsally-adjacent pMN domain proceed normally. This can be explained by the longer persistence of *Nkx2.9* expression in this domain in the hindbrain, which compensates for the absence of *Nkx2.2*. In fact a population of serotonergic neurons in the hindbrain P3 domain, which develops after *Nkx2.9* is downregulated, is absent in the *Nkx2.2* mutant (Briscoe et al 1999). A crucial gene for the development of the P3 domain in the hindbrain is *Phox2b* (a paired homeodomain transcription factor). *Phox2b* mutant mice fail to generate BM/VM neurons in the hindbrain Pattyn et al 2000). Its expression is regulated by *Hox* genes (Davenne et al 1999) and *Nkx2.2*. Overexpression of *Nkx2.2* produces ectopic BM/VM neurons (Pattyn et al 2003). *Phox2b* expression in the P3 domain suppresses *Pax6* expression whilst promoting the expression of *Nkx6.1* and *Nkx6.6*, thus creating a feedback loop to consolidate the transcription factor identity of this region (Dubreuil et al 2002).

Dorsal to the P3 domain is the pMN domain which gives rise to spinal motor neurons and to somatic motor neurons in the hindbrain. It is marked by the expression of *Nkx6.1* and *Olig2* (Class II) and *Pax6* (Class I) transcription factors. It is bordered by *Nkx2.2* expression ventrally and *Irx3* expression dorsally. Lack of *Nkx6.1* in mice results in the loss of spinal motor neurons and a ventral spread of V1 interneurons (Sander et al 2000), a phenotype which is mirrored at hindbrain level with the loss of abducens and hypoglossal somatic motor neurons (Pattyn et al 2003). Hindbrain somatic motor neurons were also absent in rats lacking Pax3 (Osumi et al 1997).

1.1.3.2 Generation of motor neurons

Once the pMN domain is established, committed precursors go on to differentiate in an SHH-independent manner. In the spinal cord *Nkx6.1* activates the transcription of *Olig2* MNR2 controls its own expression and drives the motor neuron differentiation program. Misexpression of *Mnr2* in the dorsal spinal cord induces motor neurons without altering

the expression of homeodomain proteins (Tanabe et al 1998). Overexpression of *Olig2* in the chick spinal cord also results in upregulation of *neurogenin2* (Novitch et al 2001). *Neurogenin2* mutant mice display a reduced number of motor neurons (Scardigli et al 2001). Thus it is thought that Olig2 acts on *neurogenin2* and *Mnr2* in parallel to elicit motor neurons. In the hindbrain *Olig2* is also expressed in the pMN domain only, however, it is not sufficient to induce motor neurons, since *Nkx6.1/Nkx6.2* double mutant mice lack somatic motor neurons, but still express *Olig2* (Pattyn et al 2003). Olig2 may be acting in concert with Nkx6.1 and Nkx6.2 to promote the development of somatic motor neurons. As in the spinal cord this action is likely to be mediated by MNR2 as it is expressed in hindbrain somatic motor neurons. The interaction between anterior-posterior and dorso-ventral patterning mechanisms is also important in the hindbrain. The loss of *HoxA3* and *HoxB3* which are key factors for the specification of the posterior hindbrain (see figure 1.2) results in the loss of *Pax6* and *Olig2* expression in the pMN region of the posterior hindbrain and hence to a failure to develop the abducens nucleus (Gaufo et al 2003). This demonstrates that anterior-posterior patterning genes interact closely with dorso-ventral patterning genes to enable the differentiation and precise positioning of motor nuclei.

The trochlear nucleus in r1 and the oculomotor nucleus in the caudal midbrain express *Phox2a*, a close relative of *Phox2b* with an identical homeodomain. This expression is followed by the activation of *Phox2b*. This is the reverse of the order of expression of these two genes in the caudal hindbrain where the expression of *Phox2b* precedes the expression of *Phox2a*. *Phox2a* knock out mice lack both the oculomotor and trochlear nuclei (Pattyn et al 1997) and they are also absent in humans missing this gene (Nakano et al 2001). Other somatic motor nuclei are unaffected in *Phox2a* mutants.

HB9 is another transcription factor whose expression is restricted to the MN domain. Its homeodomain is very similar to MNR2. In chick it is only expressed in postmitotic motor neurons (Tanabe et al 1998). Mice do not express *Mnr2* but express *Hb9* in a pattern similar to the combination of *Hb9* and *Mnr2* in the chick. *Hb9*-deficient mice display a normal number of motor neurons, but these neurons express markers normally

seen in V2 interneurons (Arber et al 1999, Thaler et al 1999).

HB9 (in the mouse) and MNR2 are progenitor-specific motor neuron regulatory genes and are activated in the final mitotic cycle. Once the prospective motor neurons exit the cell cycle they activate the expression of further transcription factors including LIM homeodomain genes (which contain a LIM zinc finger motif). In particular, all motor neurons express *Islet-1* as soon as they leave the cell cycle. In *Islet-1* mutant mice motor neurons undergo apoptosis, suggesting that *Islet-1* activation represents a commitment to the motor neuron fate (Pfaff et al 1996). However, whilst this activation is a necessary step, it does not appear sufficient for motor neuron induction, since overexpression of *Islet-1* in the chick spinal cord fails to elicit motor neurons (Tanabe et al 1998).

Somatic motor neurons, in particular, can be defined by their LIM code. In the chick trochlear and abducens motor neurons express *Islet-1* and *Islet-2*, whilst the hypoglossal motor neurons express *Islet-1*, *Islet-2* and *Lim-3*. (Varela-Echavarria et al 1996). Misexpression of Lim-3 in the caudal chick hindbrain results in an increase of hypoglossal neurons at the expense of surrounding BM and VM neurons (Sharma et al 1998). In the mouse trochlear neurons express only *Islet-1*, abducens and hypoglossal neurons express *Islet-1*, *Islet-2*, *Lim-3* and *Lhx-4*. Loss of *Lim-3* and *Lhx-4* results in the abducens and hypoglossal neurons adopting a BM/VM fate (Sharma et al 1998). In BM/VM neurons all nuclei express only *Islet-1* except contralaterally projecting vestibulo-acoustic neurons, which briefly express *Islet-2* also (Varela-Echavarria et al 1996). Thus they may need other transcription factors to fully specify their identity. For example, Nkx6.1 is involved in regulating migration and axon guidance of branchiomotor neurons despite not being required for p3 domain specification (Muller et al 2003).

1.1.4 Midbrain patterning

The midbrain, which contains the most rostral motor nucleus – the oculomotor nucleus, lacks the regular segmented organisation of the hindbrain, and the adult midbrain

tegmentum features many spherical, ovate and plate-shaped nuclei in a complex cytoarchitecture. However, there is evidence to suggest that during development, neuronal fate in the caudal midbrain is directed by positional information in the rostrocaudal and dorso-ventral axes, bestowed by diffusible morphogens emanating from the midbrain-hindbrain junction and the floor plate respectively. In the rostrocaudal direction FGF8 is thought to be the key effector (Crossley et al 1996, Martinez et al 1999). En1/2 and Pax2/5 are expressed in a double inverted gradient (with the maximum at the isthmus); they activate the expression of *fgf8* and are in turn activated by it, thus forming a positive feedback loop. Grg4 (homologue of the drosophila transcription factor grouchy) is activated by, but represses the expression of the above genes, thus forming a negative feedback loop (reviewed in Sato et al 2004). Pax2 is essential for *fgf8* induction but Grg4 inhibits this activity in the midbrain setting the expression domain of *fgf8* precisely in the isthmus (Ye et al 2001). Interestingly, the ability of FGF8 protein to pattern different brain structures may be isoform-dependent. The *fgf8* gene contains six exons, and there are at least 8 known isoforms. Sato and colleagues (2001) found that overexpression of *fgf8a* in the chick diencephalons confers a midbrain phenotype, but overexpression of *fgf8b* results in an r1-cerebellar phenotype. In the first instance multiple oculomotor nerve trunks were seen, in the second the oculomotor nucleus was not formed, but the trochlear nucleus was observed at the caudal diencephalon level. This suggests that the rostrocaudal positional information conferred by FGF8 is both necessary and sufficient for the formation of these motor nuclei. Electroporation of *fgf8b* at a 100fold lower concentration produced the same phenotype as *fgf8a*. However, co-transfection with Otx2 increased the threshold for cerebellar induction 10fold. These data imply that the strength of the signal is crucial and that Otx2 maybe a key molecule for midbrain competence (Sato et al 2001).

In the hindbrain and the spinal cord neuronal subtypes are arranged into longitudinal columns, each with a specific transcription factor expression profile originally established by the morphogenic gradient of SHH emanating from the floor plate and the underlying notochord (Shirasaki and Pfaff 2002). Work in Ragsdale's lab indicates that a similar patterning mechanism may be operating in the midbrain and subthalamic

tegmentum. They found a periodic pattern of acetylcholinesterase (AChE – a neuronal marker) expression in four arcs, interspersed with $AChE^-$ interarcs, radiating away from the midline in the ventral midbrain. Expression of certain transcription factors such as *Phox2A*, *Evx1* and *Pax3* was confined to particular arcs or interarcs (Sanders et al 2002). This arcuate pattern is produced by a gradient of SHH (expressed at the midline). Unilateral overexpression of *Shh* in the chick midbrain tegmentum results in the upregulation of transcriptional targets of SHH including FoxA2, HNFβ and PATCHED. In addition the entire arcuate pattern of the ventral midbrain, including $Phox2A^+$ oculomotor neurons of arc1 and $GATA2^+$ lateral arcs, was expanded, whilst the arcs' relative positions were maintained. Microelectroporation of SHH into the dorsal midbrain was sufficient to elicit a complete set of arcs, and electroporation into the lateral tegmentum produced mirror image arcs (Agarwala et al 2001). As is the case with *fgf8*, the expression of *Shh* may be confined to the midline by a repressive action of Otx2. In a conditional *Otx2* mutant, a reduction of *Otx2* expression in the ventral midbrain resulted in a dose-dependent dorsal expansion of the expression of *Shh* and its downstream effectors (Puelles et al 2003).

How do these arcs relate to the nuclei subsequently formed? The first arc contains the oculomotor complex as well as the red nucleus (a cerebellar related nucleus mediating outflows to the spinal cord). These nuclei are fully segregated, although overlapping in the rostrocaudal direction. It appears that their relative positions are specified by SHH in the medio-lateral direction and FGF8 in the anterior-posterior direction, as shown by electroporation experiments (Agarwala et al 2002).

1.2 DEVELOPMENT OF CRANIOFACIAL MESODERM AND EXTRAOCULAR MUSCLES

The mesoderm layer underlying the neural tube, as well as being an important source of inductive signals for neural tube patterning, provides the precursor cells, which, in conjunction with migrating neural crest, will form all the non-neural structures of the

vertebrate head, as well as the musculature, bones and connective tissues of the trunk. Of particular interest, in the context of this project, is the development of extraocular muscles, which is currently poorly understood. Extraocular muscles, like other head muscles, are derived from cranial mesoderm and receive patterning signals from the neural crest (which also contributes cells to the muscle sheath). This section will describe the embryology and organisation of head tissues including the cranial mesoderm and the neural crest focussing on its migration and the role it plays in patterning of head tissues.

This section will then focus on head muscle development, with emphasis on the extraocular muscles encompassing their tissue origin, migration, patterning and developmental programme. There are a number of reasons why the development of extraocular muscles is of interest when considering the mechanisms of their innervation.

Firstly, transcription factor cascades that control head muscle differentiation differ somewhat to the trunk myogenic programme and are also different between various groups of head muscles. Elements of the differentiation programme are conserved between the trunk and head programmes, but different upstream regulatory genes are involved, and, generally speaking, much less is known about head muscle differentiation. This endows certain head muscles with a unique identity (the lateral rectus muscle is a good example) that may be crucial in determining which guidance factors they secrete and thus how they are innervated. Another issue is the translocation of the extraocular muscles which coincides with the period when axons are growing towards and contacting the extraocular muscles. This needs to be taken into account when considering the mechanisms of axon guidance because it alters the topography of the system, for example abducens axons contact the lateral rectus primordium when it is located adjacent to the neural tube at rhombomere 2 level, thus the axons have a shorter distance to traverse to contact the target than if it was in its final position, which is more rostral and further away from the neural tube.

1.2.1 Cranifacial mesoderm

Mesoderm is regionalized in the medio-lateral axis. The medial most region is known as axial mesoderm, and posterior to the midbrain-hindbrain boundary it forms the notochord. Rostral to the midbrain-hindbrain boundary and up to the anterior neural fold, it forms a thin strip of tissue known as pre-chordal mesoderm. This will give rise to three of the muscles innervated by the oculomotor nerve, namely the medial rectus, the ventral rectus, and the ventral oblique. Lying caudal to the midbrain-hindbrain boundary and immediately lateral to the axial mesoderm is the paraxial mesoderm, which is the main source of myogenic tissue in the vertebrate embryo. Posterior to the otic vesicle it segments to generate somites, which in turn will give rise to the musculature and skeletal structures of the trunk. Rostral to the otic vesicle the mesenchyme is unsegmented. Scanning electron micrographs suggested a presence of similar somite-like compartments in cranial paraxial mesoderm, which were labelled somitomeres (Meier and Tam 1982). However, the somitomeres do not undergo the structural changes associated with somites (such as epithelialisation), nor do they express the genetic markers seen in somites in a domain-restricted manner; therefore, although the nomenclature persists in the literature, the functional significance of somitomeres is illusory (Couly et al 1992, Noden et al 1999, Mootoosamy and Dietrich 2002). Fate-mapping studies using chick-quail chimeras established that cranial paraxial mesoderm gives rise to the remaining extraocular muscles, namely the dorsal rectus, the dorsal oblique and the lateral rectus, as well as the muscles of the branchial arches (Couly et al 1992, Noden 1983b). A schematic diagram shows the different mesenchyme domains in the chick embryo and their migration routes (figure 1.5)

1.2.2 Neural crest

Neural crest cells (NCCs) are migratory, multipotent progenitor cells of the dorsal neuroepithelium that give rise to a wide variety of tissues including most of the head. In mammalian embryonic development NCCs start to emigrate from the tip (crest) of the still open neural folds. In avian development this emigration occurs after neural tube

closure. Trunk NCCs, derived from spinal levels of the neural tube, form much of the PNS including spinal sensory, parasympathetic and sympathetic ganglia; satellite cells and Schwann cells as well as melanocytes (skin pigment cells). Cranial NCCs (derived from rostral regions of the neural tube) generate a wider variety of mature cell types. In addition to cranial sensory ganglia, parasympathetic ganglia, Schwann cells of cranial nerves, satellite cells and melanocytes they also give rise to most of the head skeletal and connective tissue that in the trunk is somite-derived: face and skull bones, visceral cartilage, dermis, fat and smooth muscle of skin; cornea and dental papilla etc (reviewed in Santagati and Rijli 2003). Rostral cranial NCCs, which emerge from the diencephalon and the midbrain levels, give rise to the frontonasal skeleton, whereas the more posterior (hindbrain) NCCs fill the pharyngeal arches to generate cartilage and bone of the jaw, middle ear and neck. NCCs from the hindbrain migrate in discrete streams. They express Hox genes in accordance with their rostro-caudal position of origin (although the Hox code can be respecified at the beginning of migration; for example, the rostral limit of *Hoxa2* expression is at the r1/r2 boundary, but NCCs from the r2 level do not express any Hox genes). The Hox code of neural crest cells is crucial in conferring their AP identity. For instance in *Hoxa2* mutant mice the second (hyoid) arch, which is populated by r4-derived, *Hoxa2*-expressing NCCs, undergoes a homeotic transformation into the first (mandibular) arch (which is normally populated by r1/r2-derived, Hox^- NCCs), albeit with reverse polarity (Rijli et al 1993). Similarly, ectopic expression of *Hoxa2* in r1/r2 NCCs inhibits the formation of first arch structures and results in a duplicated series of second arch elements (Grammatopoulos et al 2000). Hox^- NCCs rostral to the second arch are specified by other homeobox transcription factors. Otx2, the gene that patterns the neural tube rostral to the midbrain-hindbrain boundary, is expressed in the crest of the fronto-nasal regions and in those first arch NCCs that originate in the midbrain. The $Otx2^+$ NCCs form the distal jaw elements in the first arch, whereas $Otx2^-$ NCCs from r1 and r2 form the proximal parts of the first arch, as shown by the observation that in Otx2 mutant mice only the distal elements were disrupted (Matsuo et al 1995).

There is ongoing debate about the extent to which the fate of neural crest cells is

predetermined prior to their migration. Noden's seminal work (Noden 1983a) postulated that NCCs are specified with respect to their morphogenetic potential prior to their leaving the neural tube. On the other hand he also pointed out that patterning of NCC-derived arch components is a result of a series of interactions between the crest population and the surrounding tissue. The pre-patterning theory appears to hold in relation to the cells' Hox code. Hox^- and Hox^+ NCCs differ in their competence to form pharyngeal arch skeletal derivatives. If individual Hox-positive NCCs are transferred to a Hox-negative environment, they lose their Hox code and re-programme their differentiation course, indicating a responsiveness to inductive signals from paraxial mesoderm. However, if a large block of cells is transposed to an ectopic location, the original Hox code is maintained, indicating that cross-talk amongst cells is necessary to preserve their identity (Prince and Lumsden 1994, Trainor and Krumlauf 2000). Recent observations also favour plasticity of neural crest cells with one group reporting the existence of an ectodermal organiser that can pattern NCCs (Hu et al 2003) and another providing evidence of the role of endoderm in instructing neural crest (Couly et al 2002).

1.2.3 Extraocular muscle development

In the vertebrate head there are around 40 skeletal muscles. Whereas the somite-derived muscles of the trunk effect locomotion, the head muscles are used to move the eye, control cranial openings, facilitate food uptake and produce vocalisations. Hypobronchial muscles, tongue muscles and muscles of posterior pharyngeal arches develop from occipital somites and therefore follow trunk programmes; others are genuine head muscles (these include extraocular muscles and muscles of the first, second and third pharyngeal arches). Three of the extraocular muscles derive from the pre-chordal mesoderm – a strip of axial mesoderm which lies rostral to the notochord up to the anterior neural fold, the other three extraocular muscles derive from the unsegmented cranial paraxial mesoderm which is adjacent to the pre-chordal mesoderm (see figure 1.5)

Many head muscles including extraocular muscles are migratory, i.e. the mesodermal

precursor cells are born and are specified to become muscle cells in a different location to where the muscle eventually ends up. In this respect they are similar to limb muscles which are specified in the lateral somite and migrate to the limb bud. However, the nature of migration is different between the trunk and the head. Limb muscle precursors migrate as individual myoblasts and HGF expressed along the route of the migration is the signal which drives the myoblasts to delaminate from the somite (Brand Saberi et al 1996, Dietrich et al 1999)

Head muscles, on the other hand, do not migrate as individual cells; they form mesenchymal condensations and migrate as a coherent mass. In the case of several extraocular muscles, translocation continues to take place after terminal differentiation has occurred and myotubes have started to form, as evidenced by histomorphology and immunohistochemistry (Borue and Noden 2004). There is no known precedent for such tissues actively migrating. Mootoosamy and Dietrich (2002) have suggested that, in the case of the lateral rectus primordium, this migration is more apparent than real, with differential growth of surrounding tissues accounting for the change of position. Borue and Noden (2004) have proposed a modification of this model, since many of these muscles actually translocate relative to stationary landmarks. They suggest that the muscle primordia become embedded in a tip of proliferating and expanding sheet of neural crest mesenchyme and are thus 'carried' to their final location. Neural crest expands through rapid proliferation to form most of the non-neural tissues in the head; the developing extraocular muscles are enveloped by neural crest and the neural crest forms the connective tissue of the muscle sheath (see figure 1.5). It has also long been suspected that cranial neural crest cells play a key role in the patterning of head musculature. Grafting experiments carried out by Noden indicated that connective tissue forming crest, which surrounds extraocular and jaw muscles, confers spatial patterning information upon myogenic cells that invade it (Noden 1986).

Firstly, it must be noted that the patterning of cranial muscles is still poorly understood, but that it differs considerably from somitic muscles. In somites Wnt signalling from the dorsal neural tube acts synergistically with sonic hedgehog secreted from the notochord

to induce the dermamyotome which is marked by the expression of Pax3 – a key regulator of trunk myogenesis. In the medio-lateral axis the dermamyotome subdivides into cells that will give rise to the epaxial muscles (medially) and hypaxial muscles (laterally) which in limb level somites will migrate into the limb bud. The choice of hypaxial fate is driven by lateralising signals from the lateral mesoderm, notably BMP4 (Pourquie et al 1996). Pax3 lies upstream of genes of the MRF family, the expression of which is the key step that results in commitment to the myogenic lineage. Four members are known to date: myoD (the first to be discovered), myf5, myogenin and MRF4. *Myf5* expression is induced in dorsal medial somites, followed by *MyoD* in dorsal lateral somites. Disruption of both genes leads to the absence of all skeletal muscle (Rudnicki et al 1993). There is considerable redundancy between the two genes. Absence of *myf5* alone produces mild defects in trunk skeletal muscle, whereas lack of *myoD* slightly delays the development of early limb and branchial muscle (Kablar et al 1998). Whereas myf5 and myoD are early effectors of myogenesis, myogenin is critical for terminal differentiation of myoblasts. Mice lacking *myogenin* have very poorly developed skeletal muscle even though myoblasts are present (Hasty et al 1993). MyoD is expressed in myoblasts well before the activation of its target genes, which include a number of transcription factors, cell cycle regulators and muscle structural genes, such as myosin heavy chain. This delay is achieved through association with myogenic antagonists and post-translational modification of myoD (reviewed by Berkes and Tapscott 2005).

In cranial muscles this process is considerably delayed in comparison to the somites. Although the cranial mesoderm gastrulates from the primitive streak before the somitic mesoderm, myogenic differentiation is delayed in the head relative to the trunk. In the chick somitic expression myf5 appears at HH stage 9-10, whereas in the branchial arches for instance, expression of this gene commences considerably later at HH stage 13-14 and the onset of myosin heavy chain expression occurring not before HH stage 21. A clue to the molecular nature of signals that induce myogenesis in the head has been provided by a paper by Tzahor and colleagues. Expression of Wnt3a, Wnt13 or stabilized β-catenin (downstream effector of Wnt signalling) blocked head myogenesis

in vivo or *in vitro*; whereas Wnts stimulate myogenesis in the trunk. BMPs also block head myogenesis (as they do in the trunk (Pourquie et al 1996)). In cranial mesoderm explants noggin and gremlin (BMP inhibitors) were required for myogenesis, and their action was augmented by Frzb (a Wnt inhibitor). Crucially, both BMP and Wnt antagonists are secreted by cranial neural crest cells, and other tissues surrounding cranial muscle anlage suggesting that a signal from the neural crest is required to activate the head myogenic programme *in vivo* (Tzahor et al 2003). BMPs and Wnts may be acting to block premature development of the muscles; both are expressed in the dorsal neural tube, whilst cranial muscles develop at some distance from the neuroepithelium. The role of the neural crest in the patterning of head muscles is supported by the phenotype of zebrafish *chinless* mutant. It lacks neural crest-derived cartilage and mesoderm-derived muscle in all seven branchial arches. Undifferentiated cartilage and muscle precursors were present. Mosaic analyses showed that the mutation blocks differentiation directly in the crest and not in the mesoderm. Therefore, crest signals pattern mesodermally derived myocytes (Schilling et al 1996).

Transcription factor cascades that govern muscle differentiation in the head have not been fully elucidated. Head muscles express members of the MRF family to control differentiation – in the branchial arches *myf5* expression is followed by *myoD* and subsequently *myogenin*, but myogenic cells do not express *Pax3*, which is the key upstream myogenesis regulator in the trunk (Hacker and Guthrie 1998). In the *Pax3/myf5* double mutants all trunk skeletal musculature is absent, but head muscles are unaffected (Tajbakhsh et al 1997). Which transcription factors act as upstream regulators of head myogenesis is not clear, but it appears that distinct pathways operate in subsets of head muscles. For example, double mutants for *myoR* and *capsulin* (members of myoD family) experience a loss of a very specific group of muscles, namely the masticatory muscles derived from the first arch while other first arch muscles are unaffected. *MyoR* and *capsulin* are normally transiently expressed in the precursor cells for this specific group of muscles. This phenotype is strikingly similar to the *Pax3/myf5* mutants, except the phenotype is much more restricted (Lu et al 2002). Also *myf5* expression is controlled by different regulatory sequences in different parts of the body,

again pointing to the existence of distinct myogenesis programmes (Hadchouel et al 2003).

One of the head muscles, the lateral rectus expresses some of the regulatory genes that mark migratory somitic muscles namely *Lbx1*, *Paraxis* and *Pax7*. It does not, however, follow a trunk developmental programme, since upon transplantation of the mesodermal tissue from which this muscle arises to the level of the somites it doesn't activate a myogenic programme, implying that it is unable to respond to trunk myogenic signals (Mootoosamy and Dietrich 2002). And although the lateral rectus primordium migrates from its original location to a more rostral one, the mechanism of migration is thought to be quite different to that of $Lbx1^+$ trunk myoblasts (Mootoosamy and Dietrich 2002, Borue and Noden 2004). None of the other extraocular muscles express these transcription factors which marks the lateral rectus out as somewhat unique and that has consequences with respect to its innervation. As described in section (1.4.3), axon guidance to the lateral rectus muscle has several interesting features. The expression of these regulatory genes is most likely crucial for bestowing the unique identity on the lateral rectus which may manifest itself in the expression and secretion of different guidance cues to those secreted by other extraocular muscles, thus enabling it to attract abducens axons and prevent oculomotor axons from inappropriately innervating it.

1.3 AXON GUIDANCE

1.3.1 Principles of axon guidance

The mechanisms which govern the guidance of axons to their targets have been the subject of extensive research over the past 15 years. At the tip of an axon is the growth cone, a highly motile structure which guides the axon towards its target by responding to molecular cues in the environment. These cues are read by a complement of cell surface receptors, which transduce the signal to the interior of the cell which can lead to the alteration of the morphology of the growth cone and subsequently to the direction of

growth of the extending axon. These morphological alterations that can cause the axon to advance, retract, turn and branch are underpinned by the reorganization of the actin and microtubule cytoskeleton. The question addressed in this section is: what are these extracellular cues that are able to signal to the growth cone to direct the axon?

Tessier-Lavigne and Goodman (1996) proposed four categories of axon guidance cues that can influence the decisions of growth cones and hence the trajectory choices of extending axons. These categories encompass chemoattractants and chemorepellents, which can be either contact-mediated (i.e. permissive and non-permissive) or diffusible. A repulsive cue acts by promoting actin depolymerisation and the retrograde flow of actin filaments, leading to the retraction of lamellopodia and filopodia resulting in growth cone collapse. Conversely, an attractive cue stimulates actin polymerisation and subsequently axonal growth. A growth cone presented with a gradient of an attractive or repulsive cue would be able to turn up or down the gradient because the effect on the cytoskeleton will be greater on one side of the growth cone; in fact it has been shown that growth cones are sensitive even to very shallow gradients (Rosoff et al 2004).

In reality it was an overly simplistic model and increasingly the evidence is pointing to the same guidance cues being able to exert a range of effects on different populations of axons or even different parts of the same neuron (Polleux et al 2000). The response of the growth cone is determined by the complement of receptors it possesses and the downstream machinery to propagate the signals. The intracellular state of the growth cone is also important and changes in Ca^{2+} concentration or levels of cyclic nucleotides can alter the response of the growth cone to a given cue (Wen et al 2004, Hopker et al 1999, Song et al 1998). Also the growth cone is usually subjected to multiple extracellular cues at once and needs to integrate the disparate information to make a pathfinding decision. Therefore, the intracellular signalling pathways downstream of different ligands often interact: this interaction can occur at receptor level or further downstream, either at the second messenger level or through signalling pathways converging onto common effectors. In particular, members of the Rho-GTPase family are common downstream targets for many of the ligands that control axon guidance.

Receptors to guidance cues belonging to the netrin, semaphorin, slit and ephrin families signal through complex pathways to Rho GTPases which include RhoA, Rac1 and Cdc42. Activation of Rac1 and Cdc42 by attractive cues promotes actin polymerisation and causes growth cone extension, whereas activation of Rho by repulsive cues has the opposite effect and results in growth cone collapse (reviewed in Huber et al 2003, Kalil and Dent 2005).

The bifunctionality of many ligands and the complex interactions between different signalling pathways greatly enhance the permutations that are possible with a limited number of signals, thus enabling the establishment of the precise and sophisticated neuronal circuitry witnessed in adult vertebrates. In this section I will discuss the known guidance cues, with particular emphasis on the semaphorins, stromal cell-derived factor 1 and hepatocyte growth factor whose effects on the extraocular system were investigated in this study.

1.3.2 Extracellular matrix proteins

The extracellular matrix (ECM) is rich in molecules that can affect the behaviour of a growth cone including laminin, fibronectin, tenascin, collagen, thrombospondin, vitronectin, proteoglycans and oligosaccharides -- secreted by neighbouring cells and anchored to the ECM. Most of these have permissive effects on axons, and, in fact, are often used in *in vitro* assays to facilitate axonal outgrowth. Laminin, which is found in basal laminae, consists of three polypeptide chains (Paulsson et al 1985). Application of laminin to growth cones can cause acceleration of axon growth within minutes (Rivas et al 1992). Little is known about the action of laminin *in vivo*, but *Drosophila* lacking lamininA exhibit stalling of sensory axons, indicating that it is a permissive substrate for this population of neurons (Garcia-Alonso et al 1996). Another ECM protein, tenascin, has three isoforms expressed in the developing nervous system. Each has distinct effects on different axonal populations *in vitro* (Faissner 1997). Mice lacking tenascin C exhibit defects in motor co-ordination and exploratory behaviour (Fukamanchi et al 1996, Kiernan et al 1999). Extracellular matrix molecules bind to integrins on growth cones.

Integrins are dimeric transmembrane proteins consisting of an α and a β chain. Antibodies against integrin can block axonal extension on a laminin substrate (Tomaselli et al 1988). Integrins are thought to affect the intracellular state of the growth cone. They can modulate a tyrosine kinase in neurons (Wang et al 1993) and alter intracellular calcium levels (Schwarz et al 1992).

1.3.3 Cell-to-cell adhesion molecules

The immunoglobulin superfamily includes cell adhesion molecules (CAMs), which have one or more Ig domains. Neural cell adhesion molecule (N-CAM) is the best characterised. It is present on most neurons and is attractive for growing axons. It has many isoforms produced by differential splicing and post-translational modifications. N-CAM binds to polysialic acid (PSA) with different binding affinity in the embryo and the adult. Removal of PSA affects axonal sorting in the developing limb leading to aberrant muscle innervation. This suggests that N-CAM and PSA act together to promote fasciculation and outgrowth of axons (Tang et al 1992). Fascicilin II (*Drosophila* homologue of N-CAM) promotes fasciculation rather than directing the growth cone (Lin and Goodman 1994). L1-type molecules (L1, Nr-CAM and Ng-CAM) are capable of promoting fasciculation and outgrowth. They interact homophilically and heterophilically with other Ig superfamily members such as DM-GRASP and TAG-1 and also ECM molecules. They are also known to signal *in cis* and *in trans* such that "cis-assisted trans interactions occur" (Kunz et al 2002) meaning that the presence of an IgCAM on a growth cone can potentiate its response to an IgCAM on another cell. This may aid the fasciculation of axons with a similar complement of IgCAMs. Antibodies raised against L1 prevent fasciculation of L1 expressing neurons and reduce axonal growth rate in culture (Chang et al 1987). L1 mutations in humans and in mice result in malformations linked to decussation events, indicating a possible failure of fasciculation (Wong et al 1995, Cohen et al 1998) although it has also been ascribed to the role L1 plays in semaphorin signalling (Castellani et al 2000, see also semaphorin section). L1 has also been shown to be necessary for correct projection of retinal ganglion cells (Demyanenko and Manness 2003).

TAG-1 (in the rat) and axonin-1 (in the chick) are also immunoglobulin family members. In the chick, commissural axons express axonin-1 before crossing the midline, while the floor plate expresses Nr-CAM. Interruption of their binding with antibodies prevents commissural axons from crossing the midline (Stoeckli and Landmesser 1995), implying that the interaction between axonin-1 and Nr-CAM plays an important role in this process.

Cadherins are another class of cell surface molecules whose signalling is dependent on high intracellular calcium concentration. The prototype in this class N-cadherin is a transmembrane glycoprotein whose expression on axons is thought to promote axonal fasciculation in the mouse (Tomaselli et al 1988). It is also required for the outgrowth of retinal ganglion cells from the Xenopus retina (Riehl et al 1996). In spinal motor neurons differential expression of class II cadherins in different motor pools is thought to be crucial in the segregation of these motor pools (Price et al 2002).

1.3.4 Netrins

Netrins are a family of small secreted guidance cues structurally related to laminins, and are capable of interacting with the extracellular matrix which is thought to limit their diffusion capability (Serafini et al 1994). Netrin-1 and netrin-2 were identified in a screen for molecules attracting the commissural axons towards the midline; netrin-1 is expressed in the floor plate, while netrin-2 is expressed in the ventral third of the spinal chord (Kennedy et al 1994). Mice lacking netrin-1 or DCC experience severe midline crossing defects (Fazelli et al 1997, Serafini et al 1996). Cerebellofugal axons and alar plate axons are also attracted to the midline by netrin, suggesting that netrin attraction is a universal cue for circumferentially migrating axons in the neural tube (Shirasaki et al 1995, Shirasaki et al 1996). Netrin-1 also attracts commissural axons from the dentate gyrus and the CA3 regions to the contralateral hippocampus (Steup et al 2000). Expression of netrin-1 at the optic disc attracts axons of retinal ganglion cells (RGCs) to lead them out of the retina. This effect can be replicated in culture and blocked with

antibodies directed against DCC. In netrin-1 or DCC mutant mice RGC axons fail to exit the retina into the optic nerve (Deiner et al 1997).

Like other guidance cues, netrins are in fact bifunctional and can elicit both attractive and repulsive responses, depending on the receptor combination found on the target cell. If netrin binds to a homodimer of DCC (deleted in colorectal cancer - a member of the IgCAM family), it triggers an attractive response in the growth cone. If it binds to a heterodimer of DCC and Unc-5 on Xenopus spinal neurons, the growth cones are repelled away from the source of netrin (Hong et al 1999). The attractive response of Xenopus spinal neurons can, however, be converted into repulsion either by reducing cAMP levels with competitive analogues (Ming et al 1997) or by blocking influx of calcium (Hong et al 2000). Repulsion could also be elicited by addition of laminin, which lowers cAMP levels, highlighting the ability of guidance cues to interact (Hopker et al 1999).

Whilst netrin attracts commissural axons to the midline, it seems plausible that it repels motor axons away from the midline, or prevents motor axons from crossing it. Cranial motor neurons express Unc-5 and DCC in the rat (Barrett and Guthrie 2001) which should render them susceptible to the repulsive action of netrin. In fact, trochlear axons, branchiomotor axons and visceromotor axons are repelled by netrin *in vitro* (Colamarino and Tessier-Lavigne 1995, Varela-Echavarria et al 1997). What these populations of motor neurons have in common is that they all project dorsally within the neural tube possibly as a result of netrin repulsion from the midline. However, somatic motor neurons (which exit the neural tube ventrally) were unaffected by netrin *in vitro* despite expressing the appropriate receptors. Furthermore, mice lacking netrin-1 do not display any abnormalities in cranial motor axon guidance (Serafini et al 1996). So far the only evidence of netrins acting as repellents *in vivo* has come from *Drosophila* where dorsal or ventral trajectory selection by motor neurons is dependent on netrin signalling to different receptors. Ventrally-projecting motor neurons express *frazzled* (fly homologue of DCC) and upregulation of UNC-5 dorsalises them (Labrador et al 2005).

1.3.5 Ephrins

Ephrins are cell surface molecules divided into two classes. Ephrin-As, of which five vertebrate members are known, are linked to the cell-membrane by GPI anchors. Ephrin-Bs, with 3 vertebrate members, are transmembrane proteins. They signal to receptor tyrosine kinases known as Eph receptors. These also come into classes: EphA receptors (1-8) and EphB receptors (1-4). Ephrin-As signal to EphA receptors, and ephrin-Bs signal to EphB receptors, with the exception of ephrin-A4 that can signal to both classes of receptor. Since both ligand and receptor are membrane bound, a cell-to-cell interaction is required. EphB2 and ephrinB2 form a tetramer, in a 2:2 stoichiometry, as revealed by a crystallographic study (Himanen et al 2001). This explains why soluble ephrins must be clustered to have an effect on growth cones *in vitro* (Davis et al 1994). *In vivo*, clustering is facilitated by localisation on lipid rafts (Davy et al 1999). Signalling downstream of EphA receptors is thought to be mediated by ephexin, a guanine-exchange factor that is tyrosine-phosphorylated as a result of ephrin binding and stimulates the RhoA pathway leading to growth cone collapse (Sahin et al 2005).

The role of ephrins has been particularly extensively studied in the developing visual system (reviewed by Knoll and Drescher 2002). RGC project to the tectum (superior colliculus in mammals) and establish a topographic map, a process which relies extensively on ephrin-Eph receptor signalling. Axons from the nasal retina project to the posterior tectum and axons from the temporal retina project to the anterior tectum. Similarly axons from the ventral retina project to the dorsal tectum and vice versa. Topographic mapping means that axons from neighbouring cells project onto neighbouring cells and therefore requires an exquisite precision in the axonal pathfinding. Ephrins and Eph receptors are expressed in inverted gradients in the tectum and the retina. For example, ephrins A2, A5 and A6 are expressed at high levels in the posterior tectum and their amount decreases towards the anterior end. The RGCs are sensitive to ephrin-mediated repulsion (Drescher et al 1995), and they express EphA3 in the opposing gradient, with temporal axons having the highest complement. Higher levels of EphA receptors enhance their axons' response to ephrin signalling, which is

key to the axons identifying the correct termination point along the axis that enables topographic mapping. This was demonstrated in an experiment in which increasing the level of EphA receptor expression in a dispersed subset of retinal axons led to the formation of two overlapping maps, with the axons carrying aberrantly high levels of EphA forming an ectopic map in the anterior tectum and 'pushing' the wild-type axons to the posterior tectum (Brown et al 2000). The situation is further complicated by graded expression of ephrins in the retina and Eph receptors in the tectum. The level of expression of EphA3, EphaA4 and EphA7 in the tectum increases in the anterior direction. Ephrins A2, A5 and A6 are present in a high → low gradient from nasal to temporal in the retina. Since ephrins are capable of reverse signalling to the cell on which they are present, these additional gradients confer a further capacity on retinal axons to discriminate their position along the anterior posterior axis in the tectum which may be necessary to achieve the precision required for topographic mapping (reviewed in Knoll and Drescher '02). For example, retinal axons fail to grow on EphA7 containing stripes, and EphA7 is involved in suppressing RGC branching anterior to the correct termination zone (Rashid et al 2005).

Ephrin-Eph receptor signalling is also involved in midline crossing. Both EphA4 deficient mice and ephrinB3 deficient mice have corticospinal tract axons aberrantly cross the midline, suggesting that the interaction between these two molecules is required for the correct pathfinding of this population of neurons (Kullander et al 2001, Yokoyama et al 2001). The optic chiasm is a prominent midline crossing point where RGC axons either cross to project to the contralateral tectum or make a 90 degree turn to project ipsilaterally. This decision depends on their sensitivity to ephrinB2 expressed at the midline; ipsilaterally-heading axons were repelled by the midline, whereas contralaterally projecting axons were not. This is governed by the EphB1 receptor; in EphB1 null mice much of the ipsilateral projection was lost, and the expression of this receptor is confined to ipsilaterally projecting neurons in wild-type mice (Williams et al 2003).

Ephrins are also capable of retrograde signalling to the cell on which they are present,

upon binding an Eph receptor. This bi-directional signalling is involved in regulating cell sorting during compartmentalisation of the hindbrain into rhombomeres (Mellitzer et al 1999, Xu et al 1999). It is also thought to underlie the repulsion of ephrinB expressing forebrain commissural axons away from areas of EphB expression (Henkemeyer et al 1996). Vomeronasal organ (VNO) is used for pheromone detection in rodents. It sends axons to the accessory olfactory bulb. *In vitro* VNO axons express a preference for EphA covered stripes, suggesting that these axons are attracted to areas of EphA expression. It's not clear how retrograde signalling through ephrin-A5 is achieved, since this class of ephrins lack a cytosolic domain (Knoll et al 2001). The bi-directionality and bi-functionality of ephrin-EphR interactions increases the number of signalling permutations which can guide growth cones to their targets. Another potential increase in the signalling repertoire available to growth cones was highlighted by an intriguing recent paper. Ephrins and their receptors are often co-expressed in the same cells in many different systems including the retinotectal projections and spinal motor axons and it has been widely assumed that the purpose of this is to modulate or mask ephrin-Eph signalling through *cis* interactions. Marquardt and colleagues (2005) showed that in spinal motor axons in any case, ephrinA and EphA are segregated in different membrane domains and do not interact in *cis*, instead they participate in independent *trans* signalling interactions with opposite outcomes: ephrinA to Eph signalling resulting in growth cone collapse and EphA to ephrin signalling resulting in growth cone expansion.

Ephrins play an important role at several stages of the motor axon guidance process. When spinal motor axons exit the neural tube, they grow through the rostral part of the sclerotome in the somite and avoid the caudal sclerotome. The caudal sclerotome expresses ephrinB1 and ephrinB4 (in the chick) and ephrinB2 (in the mouse). It is plausible that the ephrins expressed in this part of the somite act to exclude spinal motor axons from that territory, since the motor neurons express EphB1 (chick) or EphB2 and EphB3 (mouse). Indeed, *in vitro* spinal motor axons preferentially grow on laminin stripes when presented with a choice of laminin or ephrin (Wang and Anderson 1997). The axons of the lateral motor column (LMC) project to the limb plexus as an

intermediate target in a process that appears to depend on ephrin signalling. The plexus expresses EphA7 while the axons express ephrin-A5, and in the absence of EphA7 the axons no longer converge on the plexus, which suggests Eph receptor-mediated attraction (Araujo et al 1998). Another possibility is that this phenomenon is governed by ephrin-A5-EphA7 adhesion; the EphA7 receptor comes in several splice variants: the full length version mediates repulsion while the truncated version mediates adhesion since it can bind the ligand (and the ligand is also membrane-bound) but not transmit the signal thus acting like an endogenous dominant-negative receptor (Holmberg et al 2001).

Once LMC axons reach the limb bud, the lateral subdivision (LMC_L) axons are targeted to the dorsal part of the limb bud and the medial subdivision (LMC_M) axons are targeted to the ventral part. This decision is also thought to be mediated by ephrins. The ventral limb bud expresses ephrin-A2 and ephrin-A5 whilst LMC_L axons express EphA4; thus ephrin-mediated repulsion is thought to exclude these axons from the ventral limb and LMC_M axons which do not express Eph receptors are able to enter this territory (Ohta et al 1996). This idea is reinforced by the observation that overexpression of EphA4 receptor in the LMC_M results in these axons aberrantly targeting to the dorsal limb bud (Eberhart et al 2002). Conversely, in mice lacking EphA4, lateral LMC axons are capable of entering the ventral limb bud (Helmbacher et al 2000).

Ephrins are also believed to play a role in the final part of the spinal motor axons pathfinding namely the innervation of the muscles. EphA receptors are expressed on incoming motor axons while ephrinAs are expressed on the muscles. Disruption of the balance of ephrinA-EphA interactions resulted in a disruption of muscle innervation at the synaptic level in a manner reminiscent of the topographic misprojections seen similar disruptions to the retinotectal pathway (Feng et al 2000). Ephrins also function in the guidance of cranial motor axons. Trigeminal motor neurons are derived from rhombomeres 2 and 3 and target to different muscles in the branchial arches. The muscles express ephrinA5 and the axons express EphA receptors. Overexpression of ephrinA5 in the muscle or overexpression of a dominant negative EphA receptor in

trigeminal neurons leads to a reduction of branching in the muscle (Prin et al 2005).

1.3.6 Slits

Slits are a small family of secreted guidance cues, the first of which was identified in Drosophila as a factor necessary for the repulsion of commissural axons once they have crossed the midline (Kidd et al 1999). Commissural axons are attracted to the midline by netrin, but once they have crossed they lose their sensitivity to netrin attraction and acquire a sensitivity to slit repulsion. The name derives from axons collapsing into a slit along the midline because of a lack of repulsive activity which is necessary to complete the crossing. Slit is a ligand for the Robo receptor; *Robo* mutants cross the midline repeatedly, forming circular pathways (Seeger et al 1993). The discovery of Robo2 and Robo3 explained why the phenotype is not identical to that of *Slit* mutants; the presence of other receptors means some repulsion remains (Simpson et al 2000).

A similar mechanism operates in vertebrates (which possess three Slits and four Robos), as demonstrated by an elegant *in vitro* study by Zou and colleagues (2000). Commissural axons prior to crossing were insensitive to a range of repellents tested, but ones that have crossed the midline were repelled in vitro by Slit2 (and also by Sema3F and Sema3B). Slits at the midline also have a part to play in motor neuron axon guidance. Robo receptors are expressed in cranial motor neurons and Slits repel and inhibit axonal outgrowth from dorsally-projecting cranial motor neurons (but not ventrally-projecting ones) *in vitro*. Analysis of mice deficient in Slit and Robo function shows that cranial motor axons aberrantly enter the midline, while ectopic expression of Slit1 in chick embryos leads to specific motor axon projection errors. Expression of dominant-negative Robo receptors within cranial motor neurons in chick embryos strikingly perturbs their projections, causing some motor axons to enter the midline, and preventing dorsally projecting motor axons from exiting the hindbrain. Therefore Slits may be key components of midline repulsion for dorsally-projecting motor neurons. (Hammond et al 2005).

Slits are also active as repellents in other parts of the vertebrate embryo. The repulsive action of Slit2 confines RGCs to the optic chiasm. It is expressed in the area surrounding the chiasm, while RGCs express Robo1 and Robo2. Slit/Slit2 compound mutant mice experience defasciculation of axons at the chiasm and also form an ectopic chiasm (Plump et al 2002). Olfactory bulb axons project to the olfactory cortex along the lateral olfactory tract (LOT). The LOT passes over the septum, which is secreting Slits. Bulb axons express Robo1 and are repelled by Slit2 *in vitro* (Li et al 1999). Olfactory bulb axons lose their sensitivity to the septum from *slit/slit2* compound mutant mice in a gene dose-dependent manner in culture (Nguyen-Ba-Charvet et al 2002).

Slits are also bifunctional ligands. The axons of pyramidal cortical neurons orientate away from Slit1 in culture, whilst their dendrites show an increase in growth and branching in response to Slit1 (Whitford et al 2002). This is similar to the effect of Sema 3A on these neurons (see section 1.3.8).

1.3.7 Morphogens as guidance cues

Morphogens are defined as secreted proteins produced by a restricted group of cells that emanate away from their sources and induce distinct cellular responses in a concentration-dependent manner. Various members of the hedgehog (Hh), wingless (Wnt), transforming growth factor β (TGFβ) and fibroblast growth factor (FGF) families fall into this category. In addition to their patterning activities a number of these molecules have been implicated in axon guidance.

Fibroblast growth factors are a large family of secreted factors, which bind to cell surface tyrosine kinase receptors, encoded by four genes (FGFR 1-4). FGFR1 is expressed in RGCs, whilst FGF8 and FGF19 are expressed in the region surrounding the optic chiasm. Application of FGFR-blocking antibodies to wholemount rat retinas results in defasciculation and growth dispersion of axons at the optic fissure (Brittis et al 1996). In frogs, addition of FGF to exposed brain preparations induced RGCs to grow around and overshoot their targets (McFarlane et al 1995). *In vitro* RGC growth cones

were shown to be repelled by high levels of FGF2 (Webber et al 2003). It is clear, then, that fibroblast growth factors play an important role in RGC axon guidance.

FGF8 that, in its role as a morphogen, directs the formation of trochlear motor neurons is also involved in the guidance of their axons. FGF8 released from beads attracts trochlear axons *in vitro* and redirects their growth when beads are implanted *in vivo* (Irving et al 2002).

Bone morphogenetic proteins (BMPs) and the related growth differentiation factors (GDFs) are signalling molecules of the TGF-β superfamily. Their graded signalling is required for the specification of the spinal cord dorsal interneurons, including commissural neurons. Both BMP and GDF contribute to the initial guidance of commissural axons in a ventral direction, as indicated by BMP-7 mimicking the repulsive effect of the roof plate on commissural axons *in vitro*, an effect that was augmented by GDF-7. Both BMP-7 and GDF-7 null mice exhibit midline crossing defects in commissural axons, albeit transiently (Butler and Dodd 2003).

Sonic hedgehog has also been implicated in axon guidance. In vertebrates SHH has a conserved expression along the axial midline, with the exception of the optic chiasm region when RGCs are crossing it. Indeed SHH-soaked beads reduced the outgrowth from chick retina explants and direct application of SHH collapses retinal growth cones (Trousse et al 2001). SHH also augments the action of netrin in attracting commissural axons to the midline. In netrin-1/Gli-2 double mutants commissural axons rarely invade the ventral half of the spinal cord; a phenotype that is stronger than either single mutant (Gli-2 is a downstream effector of SHH). SHH also induced attractive turning of commissural axons *in vitro* (Charron et al 2003). Thus SHH is also capable of acting as an attractive and a repulsive cue. In fact, SHH also exerts a repulsive effect on commissural axons after those axons have crossed the midline via Hedgehog interacting protein (Bourikas et al 2005)

Wnts are secreted glycoproteins that bind to Frizzled (Fz) receptors and activate various

intracellular pathways. An elegant study by Lyuksyutova et al (2003) has identified Wnt-4 as the diffusible cue responsible for inducing the rostral turn of commissural axons after they've crossed the midline, via the Fz3 receptor. Wnt-4 is expressed by the floor plate in an anterior-high posterior-low gradient, and can re-orient commissural axons in open-book explants. Conversely, Wnts exert a repulsive effect on cortico-spinal axons that grow in the opposite direction to commissural axons, by acting on the Ryk receptor. Wnts repel corticospinal axons in vitro and injection of anti-Ryk antibodies blocked the posterior growth of cortico-spinal axons (Liu et al 2005).

1.3.8 Semaphorins

Semaphorins are a large family of axon guidance cues conserved throughout the animal kingdom. The first semaphorin was identified in the grasshopper and named fasciclin IV for its role in the fasciculation of axons (Kolodkin et al 1992). The first vertebrate homologue was purified from brain extracts and characterised by its ability to collapse growth cones *in vitro* at very low concentrations (Luo et al 1993). This 100kDa glycoprotein was initially called collapsin I. As more related genes were discovered, they were classed as semaphorins and renamed in a more systematic manner (Semaphorin Nomenclature Committee 1999). Eight classes are now recognised. Class I and II are exclusive to invertebrates, class III-VII contain vertebrate semaphorins, and there is another class of viral semaphorins. Class IV-VI semaphorins are transmembrane, cell surface proteins, class III contains secreted semaphorins and class VII semaphorins are tethered to the membrane by a phosphatydilinositol linkage. All share an N-terminal Sema domain of 500 amino acids containing 17 highly conserved cysteins. This domain is crucial for signalling since it remains biologically active in the truncated form, so long as it is dimeric (Koppel et al 1997, Koppel et al 1998).

Attention has focussed heavily on class III semaphorins, in part because their soluble character facilitates their use in *in vitro* assays. A large body of work has accumulated in support of their role as axonal repellents. *In vitro* Sema3A, the most studied of the semaphorins, repels sympathetic axons (Adams et al 1997, Koppel et al 1997), cranial

motor axons (Varela-Echavarria et al 1997), olfactory sensory axons, as well as trigeminal, facial and vagal ganglionic sensory axons (Kobayashi et al 1997), pontocerebellar mossy fibres (Rabacchi et al 1999), cortical axons (Bagnard et al 1998) and hippocampal axons (Chedotal et al 1998). Sema 3B, 3C and 3F also repel or collapse sympathetic growth cones (Adams et al 1997). In addition Sema 3B repels commissural axons (Zou et al 2000) and Sema 3F repels trochlear axons (Giger et al 2000). It must be noted that some have questioned whether class III semaphorins truly act as diffusible cues because their highly basic C-terminal tail is likely to leave them susceptible to adhesion to cell surfaces and the extracellular matrix (Raper 2000). At the moment little is known about the physiological concentrations of secreted proteins, so results of *in vitro* studies must be interpreted with caution.

Semaphorins signal to the cell through a plexin receptor. This is a large family of transmembrane proteins, distantly related to the semaphorins themselves, divided into four subfamilies (A-D). Invertebrate and transmembrane vertebrate semaphorins can bind directly to plexins; class III secreted semaphorins, however, require the presence of a co-receptor for ligand recognition. Neuropilin 1 (NPN-1) was identified as the functional receptor for Sema3A It binds Sema3A with high affinity, and antibodies against NPN-1 block the ability of Sema3A to repel sensory axons and to induce collapse of their growth cones (He and Tessier-Lavigne 1997). Furthermore ectopic expression of NPN-1 in retinal ganglion cells conferred sensitivity to Sema 3A upon them (Nakamura et al 1998). A second neuropilin (NPN-2) was later identified. *In vitro* binding studies showed that NPN-1 binds Sema3A with a higher affinity than Sema3C and does not bind Sema3F. NPN-2 on the other hand binds Sema3F with a higher affinity than Sema3C or Sema3A. Furthermore, the two neuropilins can heterodimerise as well as forming homodimers. This has led to the hypothesis that a NPN-1 homodimer is the cognate receptor for Sema 3A, a NPN-2 is the cognate receptor for Sema 3F and a heterodimer of the two neuropilins is the cognate receptor for Sema 3C (Chen et al 1998).

Mutant studies in mice appear to confirm this hypothesis. Three *Sema3A* knock outs

have been published. The phenotypes vary according to the genetic background of the mice and their consequent ability to compensate for the loss of the gene. Catalano et al (1998) report few differences to wild type mice in the homozygotes. The other two groups report defasciculation of cranial nerves (trigeminal, facial, vagus, accessory and glossopharyngeal but not oculomotor or trochlear); as well as some misrouting of spinal efferent axons (Behar et al 1996, Taniguchi et al 1997). However, the nerves are still able to reach their targets and those mice that survive display normal locomotion and behaviour, suggesting that innervation is not disrupted (Taniguchi et al 1997). However, axons are seen to enter territory from which they would normally be excluded such as cartilage and the eye (areas which express *Sema3A*). This supports the idea that Sema3A functions as an axonal repellent *in vivo*. The defasciculation and entry into inappropriate regions is probably due to the loss of repulsive activity conferred by the presence of Sema3A. Mice lacking neuropilin-1 have a similar, but more severe phenotype. PNS efferent fibres (again with the exception of the oculomotor and trochlear nerves) display defasciculation, wide spreading in the periphery, overshooting of targets and occasionally ectopic projections (Kawasaki et al 1997). The lesser severity of the phenotype seen in *Sema3A* null mice can be explained by the redundancy amongst different class III semaphorins that can bind neuropilin-1.

In *Sema3F* null mice spinal and most cranial nerves are unaffected (Sahay et al 2003). The exceptions are the oculomotor and trochlear nerves, which are normal in Sema3A and NPN-1 mutants. In *Sema3F* mutants, the oculomotor nerve reaches the vicinity of its extraocular targets but is severely defasciculated. The trochlear nerve is absent altogether due to a failure to exit the neural tube. Several CNS projection pathways are also affected, especially components of the limbic circuitry. Sema3F is required for formation of the anterior commissure, infrapyramidal tract formation, and correct targeting of stria terminalis (major output of the amygdala). As is the case with Sema3A there is an indication of a role for Sema3F in surround repulsion. The oculomotor is defasciculated, as are the axons leaving the medial habenula in the diencephalon, presumably due to the loss of surrounding *Sema3F* expression. The absence of the trochlear nerve is attributed to the loss of *Sema3F* expression surrounding its exit point

which is thought to channel the trochlear axons out of the neural tube (Sahay et al 2003). *Sema3F* is expressed in the caudal midbrain and caudal rhombomere1. Sequestering Sema3F with NPN-2-Fc fusion protein results in trochlear axons invading the midbrain. Therefore, NPN-2 expression in the dorsal part rhombomere1 may be sequestering Sema3F, resulting in a ventral → rostral Sema3F gradient which directs trochlear axons towards their dorsal exit point (Watanabe et al 2004). The phenotype of NPN-2 deficient mice accurately mirrors that of *Sema3F* mutants adding weight to the theory that NPN-2 is the functional receptor for Sema 3F *in vivo* (Chen et al 2000, Giger et al 2000). Sema3F was also found to repel trochlear axons *in vitro* (Giger et al 2000).

There is a nice symmetry in the defects described in the aforementioned mutants. Not only is there a close correlation between the phenotypes of *Sema3A* and *Npn-1* deficient mice, and *Sema3F* and *Npn-2* deficient mice, there is also a complementary pattern in the pathways affected by the two pairs of mutants. The more anterior structures including forebrain tracts and the two most rostral cranial motor nerves are disrupted by the loss of *Sema3F* or *Npn2*, whilst the more posterior structures such as hindbrain and spinal efferent nerves require Sema3A and NPN-1. All nerve tracts that are affected in one pair of mutants are intact in the other. Thus the developing nervous system appears to be subdivided into a rostral domain governed by Sema 3F – NPN-2 signalling and a caudal domain governed by Sema 3A – NPN-1 signalling. Alas, as so often the case, this neat model of semaphorin function turns out to be too simple, after all.

As is the case with many other axon guidance cues *in vitro* experiments indicated that semaphorins were bifunctional and could also function as attractants. Sometimes different semaphorins exert opposite effects on the same population of axons. For example, Sema3B was found to be an attractant for olfactory bulb axons; whilst Sema3F repels them. The expression of the two semaphorins *in vivo* indicated that they could indeed function cooperatively to guide this population of axons (de Castro et al 1999). This result was a surprise since both Sema3B and Sema3F are believed to signal through neuropilin-2. Similarly cortical axons are attracted by a gradient of Sema3C and repelled by Sema3A (Bagnard et al 1998). In addition the same semaphorin could have a

different effect on different parts of the same neuron; Sema3A is repulsive to the axons of cortical pyramidal neurons but an attractant to their apical dendrites (Polleux et al 2000).

A recent paper provided further evidence for a more complex interplay between different class III semaphorins *in vivo* (Falk et al 2005). Both *Sema3F* and *Npn-2* null mice exhibit a drastic reduction of the anterior commissure (Sahay et al 2003, Giger et al 2000, Chen et al 2000). However *Sema3B* mutant mice show a ventral expansion in both arms of the anterior commissure. Interestingly, this effect appears to be dose-dependent with heterozygous mice displaying a smaller but significant expansion. In addition the anterior arm of the commissure is defasciculated. Functional assays then determined that Sema3F repels axons from both arms of the commissure, whist Sema 3B attracts anterior axons and repels posterior axons. Both semaphorins were shown to signal through neuropilin-2 (Falk et al 2005). This mechanism is not restricted to mice; in zebrafish Sema 4D, expressed at the midline, attracts the axons of the anterior commissure, whilst repelling another population of axons, although in zebrafish the opposing actions of Sema 4D are mediated by different neuropilins (Wolman et al 2004).

The more complex behaviours of different populations of axons in response to semaphorin signalling can be explained in a number of ways. Firstly a greater diversity of receptors or receptor complexes could elicit different intracellular responses to different semaphorins. Also, components of receptor complexes or intracellular effectors could be differentially localized both spatially in the same neuron and temporally at different stages of a neuron's development and pathfinding.

As already mentioned, the semaphorin receptor complex requires the presence of a plexin for intracellular signal transduction. In the case of secreted semaphorins this function is performed by plexinAs, of which four have been identified. Indeed neuropilin combinations with different plexins can increase the diversity of semaphorin receptors. It was found that in *plexinA3* mutants dorsal root ganglion (DRG) and sympathetic ganglion (SG) axons lose part of their responsiveness to Sema3A (Cheng et

al 2001). In mice lacking *plexinA4* DRG and SG axons also lose but part of their response to Sema3A (Suto et al 2005). This suggests that either plexin can function to transduce Sema3A signalling. Conversely, in mice lacking plexin A3 SG axons lose their response to Sema3F altogether; the absence of plexinA4, however, actually potentiates their sensitivity to Sema3F (Cheng et al 2001, Suto et al 2005). This indicates that plexinA3 is a better co-receptor for Sema3F in these neurons and the loss of plexinA4 increases the number of more efficient receptor complexes for Sema3F signalling. Interestingly though *plexinA3* (nor *plexinA4*) mutants did not show any defects in the guidance of oculomotor or trochlear nerves, although they are expressed there. This suggests that in those neurons, another plexin is utilized to transduce Sema3F signalling.

Transmembrane semaphorins in vertebrates can signal directly through a plexin receptor and do not require neuropilins for ligand recognition (Tamagnone et al 1999). Suto et al (2005) demonstrated that plexinA4 is a functional receptor for Sema6A and Sema6B *in vitro*. Some of the *in vivo* defects seen in the plexinA4 mutant can be attributed to a loss of Sema6A signalling. For example, the abnormalities in the thalamocortical projection are very similar to those observed in the Sema 6A mutant (Leighton et al 2001). PlexinA1 has been shown to mediate the activities of Sema6D (Toyofuku et al 2004); thus it appears that plexinAs are bifunctional receptors that respond to both class III and class VI semaphorin signalling. One of the more interesting phenotypes of the *plexinA4* mutants is the defect seen in the anterior commissure, which appears to be an intermediate phenotype between those seen in the *Sema3F* and *Sema3B* mutants, suggesting it could contribute to the signalling from both semaphorins. Also like *Sema3B* mutants, *plexinA4* mutants exhibit a gene dose-dependent effect. However, Sema 6A is also expressed in the developing forebrain and could also contribute to the anterior commissure formation through plexinA4 (Suto et al 2005). These data illustrate the difficulties researchers face in trying to unravel the contributions individual molecules make in complex signalling networks.

In addition to plexins and neuropilins, other molecules participate in the formation of

semaphorin receptor complexes further increasing the possible diversity of responses. L1, a member of the cell-adhesion molecule (CAM) family, was found to associate with NPN-1. Corticospinal tract axons and DRG axons from L1 mutant mice lost their responsiveness to Sema3A *in vitro* (Castellani et al 2000). Similarly, a related molecule NrCAM binds to NPN-2 and is required for the responsiveness of anterior commissure axons to Sema3F and Sema3B *in vitro*. Genetic ablation of NrCAM *in vivo* resulted in defects in the anterior commissure formation (Falk et al 2005). Other classes of semaphorins which do not bind neuropilins for signalling require other components in their receptor complexes. Off-track (Otk), an inactive receptor tyrosine kinase associates with PlexA in Drosophila to mediate Sema1a repulsive functions (Winberg et al 2001) and in vertebrates plexinA1 can associate with Otk to respond to Sema6A signals which control cardiac morphogenesis (Toyofuku et al 2004). Met, the hepatocyte growth factor (HGF) receptor with intrinsic kinase activity is required to transduce Sema4D mediated effects in promoting epithelial cell invasive growth and forms a receptor complex with PlexB1 (Giordano et al 2002). Other components of semaphorin receptors continue to be discovered (see Pasterkamp and Kolodkin 2003).

The downstream mechanisms which mediate the effect of semaphorins on growth cones have been extensively researched, but our understanding is still far from complete (reviewed in Huber et al 2003). The Rho family of monomeric GTPases are key mediators of semaphorin signalling. RhoA and Rac1 can bind directly to plexin Bs; RhoA is thought to generally promote growth cone collapse while Rac promotes growth cone extension. RhoD and Rnd1 perform the respective roles downstream of plexinA1. In addition guanine exchange factors and GTPase activating proteins can influence RhoGTPase activity and thus signal transduction. Plexins have been shown to undergo phosphorylation (Tamagnone et al 1999) and a number of kinases have been associated with semaphorin receptor complexes. Met, the HGF receptor, associates with plexinB1, to participate in Sema4D signalling. The Fes tyrosine kinase binds plexinA1 and can phosphorylate it. This phosphorylation is blocked by neuropilin-1 in the absence of ligand. This finding sheds light on the mechanism by which neuropilins participate in semaphorin signalling (Mitsui et al 2002). Fyn, a member of the Src family of non-

receptor tyrosine kinases, associates with plexins A1 and A2, and can phosphorylate PlexinA2. It can also recruit cyclin-dependent kinase 5 (cdk5) to the complex.

Intracellular signalling evoked by any guidance cue is not a simple linear process, where the binding of a ligand results in a series of reproducible steps with a definite outcome, such as growth cone collapse. A number of other factors influence the process. Firstly, as I've already discussed, the same guidance cue can exert different effects on different populations of neurons or even on different parts of the same neuron. This can be partly accounted for by the expression of different receptor components, but other mechanisms are also involved. Secondly, a growth cone must integrate a number of different guidance signals in making correct pathfinding choices. Many of the pathways converge upon Rho GTPases but integration can also occur at receptor level and through regulation of intracellular state. Thirdly, the growth cone of an advancing axon has to change its sensitivity to guidance cues with time, either to adjust to a new concentration of a guidance cue, if it is present in a gradient, or if a new response to the cue is required in a different part of its pathway.

One mechanism which can modulate the response to semaphorins is the concentration of cyclic nucleotides. The repulsive turning response of Xenopus spinal neurons evoked by Sema3A can be converted into attraction by pharmacological elevation of cGMP levels (Song et al 1998). Interestingly, cyclic nucleotides may represent a point of convergence for different signalling pathways. For example, in the case of Xenopus retinal neurons, their normal attractive response to netrin is converted into a repulsive one in the presence of laminin, a non-diffusible axon guidance cue present in the extracellular matrix. This change was effected by a reduction in cAMP levels (Hopker et al 1999). Also changes in cyclic nucleotide levels can alter a localized response to a particular cue. For example, the attraction evoked by Sema3A in apical cortical dendrites, as opposed to the repulsion experienced by the axons of the same neurons, was attributed to the localisation of guanine cyclase in the dendrites (Polleux et al 2000).

The switch from an attractive to a repulsive response can also be governed by the recruitment of different kinases. For example, the attractive response evoked by Sema3B

on anterior commissure axons depends on the recruitment and phosphorylation of fyn src kinase. Pharmacological inhibition of this kinase converts the response into a repulsive one (Falk et al 2005). The switch can also occur through interaction directly at receptor level. For example, application of soluble L1-Fc chimeras to corticospinal tract axons *in vitro* altered the response to Sema3A from repulsion to attraction. Since L1 associates directly with neuropilin-1, the receptor for Sema 3A, and furthermore, L1 molecules can interact homophilically to signal *in trans*, this indicates that the two pathways can combine at receptor level to alter the response of the neuron (Castellani et al 2000).

Growth cone responses are also fine-tuned by localized protein synthesis and degradation. It was shown in retinal growth cones that Sema3A and netrin both stimulate protein synthesis, and that inhibition of protein synthesis abolished their ability to effect chemotropic responses (Campbell and Holt 2001). The MAP kinase pathway appears to be involved in the activation of translation (Campbell and Holt 2003). The purpose of this could be to enable adaptation of the growth cone to a new concentration of ligand when navigating along a gradient of a guidance cue. An elegant study by Ming et al (2002) demonstrated that Xenopus spinal growth cones proceed by a series of desensitization and resensitisation steps when growing along a gradient of netrin-1. The resensitisation required *de novo* protein synthesis. Which proteins are upregulated isn't known, although a recent paper showed that Sema3A induces intra-axonal translation of RhoA mRNA, and this local translation of RhoA is necessary and sufficient for Sema3A-mediated growth cone collapse (Wu et al 2005).

1.3.9 Hepatocyte growth factor

Hepatocyte growth factor (HGF), also known as scatter factor, is a small polypeptide growth factor with a wide range of roles during embryonic development. Mice lacking HGF die during embryogenesis with defects in placenta, liver and muscle (Maina and Klein 1999). HGF signals through Met, a tyrosine kinase cell-surface receptor, which activates cytoplasmic effectors through a multifunctional docking site located in its

carboxy-terminal tail (Ponzetto et al 1994). Various adaptor proteins binding to Met can activate different intracellular signalling pathways including the Ras/MAPK and the PI3K/Akt pathways. It is as yet not clear which signalling cascades are responsible for its effects on axons.

HGF was implicated in axon guidance as a result of a search for diffusible guidance factors for spinal motor axons. HGF can induce spinal neurite outgrowth; and HGF-neutralising antibodies can block the growth-promoting effects of forelimb mesenchyme, suggesting it is a major component of limb chemoattraction (Ebens et al 1996). Forelimb mesenchyme from *hgf* mutant embryos is unable to induce neurite outgrowth. However this could be due to a failure of muscle precursors to migrate to the limb (a process also governed by HGF), and the consequent failure of limb muscle to secrete the appropriate attractants. However, forelimb mesenchyme from *met* mutant embryos, which experience similar muscle migration defects, can induce neurite outgrowth in the normal fashion (Ebens et al 1996). HGF could also orient spinal axons in collagen explants, suggesting it is a chemoattractant rather than simply a growth-promoting factor. Examination of *hgf* and *met* mutant mice revealed defects consistent with effects of HGF *in vitro*. The mutant embryos do not reveal any obvious delay or defect in the convergence of spinal nerves to form the brachial plexus. However, axons emerging from the plexus to form distinct limb nerves show a significant reduction in length. Interestingly, certain nerves appear more affected than others. High levels of *met* expression are restricted to subsets of motor neurons in the parts of the spinal cord that innervate the limbs, suggesting that the affected axons may correspond to muscle-specific pools of Met-positive motor neurons, which beyond the plexus are confined to particular nerve branches (Ebens et al 1996, Maina et al 1997).

HGF is also a chemoattractant for cranial motor nerves that innervate the branchial arches. Branchial arches promoted outgrowth from hindbrain explants *in vitro*; an effect that could be partially blocked with HGF-neutralising antibodies, or mimicked with a HGF-loaded beads (Caton et al 2000). However, cranial nerve abnormalities in *hgf* and *met* mutants were restricted to a delayed outgrowth of the hypoglossal nerve, which suggests other chemoattractants from the branchial arches can compensate for the lack of HGF signalling. In addition to the fact that only part of the chemoattractive activity of

the branchial arches could be blocked with anti-HGF antibodies, HGF was found to chemoattract motor neurons from different hindbrain levels equally, whereas the branchial arches show a preference for more caudal motor neurons. The rest of the chemoattractive activity of the arches is probably accounted for by related neurotrophic factors such as brain-derived neurotrophic factor (BDNF), ciliary neurotrophic factor (CNTF) and cardiotrophin-1 (CT-1), which were found promote outgrowth of cranial motor axons *in vitro* (Naeem et al 2002). *Hgf* expression, as well as being present in the branchial arches and the developing limbs, was identified in the periocular mesenchyme (Caton et al 2000), which is the site of developing extraocular muscles, raising the possibility of it functioning as an attractant for nerves that innervate the extraocular muscles. The authors also found a growth-promoting effect of the branchial arches on oculomotor and trochlear outgrowth, which might be mediated by HGF.

HGF also has neurotrophic capacity. It can promote the survival of rat embryonic motor neurons with a similar efficiency to BDNF and CTNF (Ebens et al 1996). It also enhances the survival of DRG sensory neurons (Maina et al 1997) and sympathetic neurons (Maina et al 1998). It is a common feature of many neurotrophins; molecules that were originally discovered to promote neuronal survival were later shown to have chemoattractive effects on certain populations of axons (Gundersen and Barrett 1979, Song et al 1997, Tucker et al 2001). Different neurotrophins can co-operate to enhance their effects on axonal outgrowth. For example HGF does not increase the outgrowth of DRG and sympathetic neurons in culture, but can potentiate the growth-promoting effect of NGF on both populations of axons. Furthermore, neurotrophins can modulate the effects of other guidance cues. Dontchev and Letourneau (2002) showed that NGF and BDNF can confer resistance to Sema3A-induced collapse on DRG growth cones. Since the Met receptor can associate with certain plexins to participate in semaphorin signalling, it would be interesting to see if HGF can interact with, and modify the response to semaphorins.

1.3.10 Stromal cell-derived factor 1 (SDF-1)

SDF-1, also known as CXCL-12, is a chemokine. Chemokines are relatively short

peptide hormones that bind to seven-transmembrane, G-protein coupled receptors that usually signal through cyclic nucleotide-dependent pathways. Chemokines were originally defined as chemoattractants for leukocytes, but have since been shown to have a much broader spectrum of activities including promotion of angiogenesis, regulation of T cell differentiation and promotion of cell survival.

Recently SDF-1 has also been implicated as having a role in the development of the embryonic nervous system. It was shown to be an attractant for migrating dentate granule cells (Bagri et al 2002) and cerebellar neurons (Zhu et al 2002). The axons of cerebellar neurons were observed to turn away from a source of SDF-1 *in vitro* (Xiang et al 2002); a situation that mirrors the dual effect of Sema 3A on cortical neurons (Polleux et al 2000). The understanding of the role of SDF-1 on cerebellar axon guidance was complicated by the findings of Arakawa et al (2003) who showed that SDF-1 promoted axonal elongation at low concentrations *in vitro*, but switched to repulsion at a higher concentration. The uncertainty with regard to physiological concentrations of guidance cues meant that *in vivo* evidence was required to shed light on the conflicting *in vitro* results with respect to the action of SDF-1.

The first *in vivo* evidence of a role for SDF-1 in axon guidance came from zebrafish. The CXCR4 receptor is expressed in zebrafish RGCs, whilst SDF-1 is expressed in the optic stalk. Antisense knockdown of CXCR4 resulted in aberrant trajectories of retinal axons and a failure to exit into the optic nerve. Furthermore, misexpression of SDF-1 in the retina caused retinal axons to deviate towards the ectopic source of SDF-1, strongly implying that SDF-1 is functioning as an attractant for retinal axons in zebrafish (Li et al 2005).

A similar phenotype was seen in *Sdf-1* and *Cxcr4* mutant mice with relation to spinal motor neurons and cranial somatic motor neurons. These populations of neurons normally have their axons exit ventrally from the neural tube. They transiently express *Cxcr4* at the time of the early axonal projection and the mesenchyme underlying the exit region expresses *Sdf-1*. In *Sdf*-1 or *Cxcr4* mutants motor axons projected dorsally within the neural tube, and at axial levels where dorsally exiting motor neurons were present, the axons often extended out of the dorsal exit point, sometimes aberrantly innervating muscles that are targeted by the dorsal nerves (Lieberam et al, 2005). The conversion of

ventrally-projecting motor neurons into dorsally-projecting ones is similar to the phenotype observed in *Pax6* mutant mice (Ericson et al 1997), and indeed *pax6* mutants lose CXCR4 expression in motor neurons of the caudal hindbrain and rostral spinal cord. By which mechanism does SDF-1 induce this switch? Chalasani and colleagues published a study (2003) where they found that SDF-1 alleviates the effects of chemorepellents both in co-cultures and growth cone collapse studies without exerting an effect on axons alone. In the presence of SDF-1, a much higher concentration of Slit2 was necessary to collapse retinal growth cones, and similarly a higher concentration of Sema3A was required to collapse DRG growth cones, and more Sema3C was needed to collapse sympathetic growth cones. This effect was attributed to the elevation of intracellular cAMP by SDF-1, which is in agreement with previous studies that highlighted the role of cyclic nucleotides in modulating the effects of different guidance cues (Song et al 1998, Hopker et al 1999). Thus the ventral exit of motor neurons in wild-type mice could be due to the protective effect of SDF-1 on the effects of various chemorepellents expressed in the floor plate (Guthrie and Pini 1995, Varela-Echavarria et al 1997, Hammond et al 2005), or perhaps the shielding of repulsive cues found in the ventral mesenchyme. Alternatively it could be due to a more direct attractive effect of SDF-1 on ventrally-projecting motor axons, similar to the one shown for zebrafish retinal axons (Li et al 2005). The two mechanisms need not be mutually exclusive. Indeed there is evidence that SDF-1 can activate multiple intracellular signalling cascades and thus affect neurons in different ways. As well as elevating cAMP (Chalasani et al 2003), SDF-1 has been reported to activate two distinct Rho-dependent pathways (Arakawa et al 2003), and two phospholipase C-dependent pathways (Xiang et al 2002).

The demonstration of attractive effects of SDF-1 on certain axonal populations *in vivo*, and the lack of known attractants for nerves innervating the extraocular muscles, merits the investigation of its possible role in this system.

1.4 DEVELOPMENT OF THE NERVES INNERVATING THE EXTRAOCULAR MUSCLES.

In this section I will describe the key events in the axonal pathfinding of the nerves innervating the extraocular muscles: the stages at which the motor neurons are born, their axonal trajectory both within the neural tube and in the periphery, the timing of growth and the main decision points such as exit point choice, intermediate targets and target muscle selection. I will summarise the current state of knowledge with regard to which guidance cues influence the pathfinding of these axons at each given stage and the main questions that remain unresolved. The pattern of connectivity and the timeframe of innervation in the oculomotor system are complex, conserved and reproducible, but the mechanisms which govern this process remain to a large degree enigmatic. This thesis has attempted to address some of these unknowns, and at the end of this section I will summarise the aims of the project and the approaches used to address them.

To recapitulate there are six muscles which rotate the eyeball and they are innervated by three nerves. The oculomotor nerve innervates four of the muscles while the trochlear and the abducens nerves innervate one each. The final connectivity pattern and progress of axon growth at different stages in the chick are shown in figure 1.1.)

1.4.1 Oculomotor nerve

The cell bodies of oculomotor neurons are located in the caudal midbrain. The patterning events that lead to their generation have been described in section (1.1.4). Once oculomotor progenitors exit the cell cycle, they, in common with other cranial somatic motor neurons, turn on the expression of *Islet-1* and *Islet-2* (LIM homeodomain transcription factors, which are known to specify neuronal fate) (Varela-Echavarria et al 1996). These genes presumably control the expression of various proteins including receptors for axon guidance cues, which will determine the behaviour of oculomotor axons with respect to pathway selection, exit from the neural tube and navigation in the

periphery, which will ensure the innervation of the appropriate targets of the nerve.

Within the oculomotor nucleus, the motor neurons innervating the different muscles are organized into pools, each corresponding to one muscle. This organization into spatially segregated pools is especially prominent in the chicken embryo, where three clusters (or subnuclei) can be discerned purely from cytoarchitectonic features. All four pools can be easily discerned with the help of retrograde tracing: the dorsolateral oculomotor subnucleus innervates the ventral rectus muscle, the dorsomedial subnucleus innervates the medial rectus muscle, a lateral division of the ventromedial subnucleus innervates the ventral oblique muscle, and a medial division of the ventromedial subnucleus innervates the dorsal rectus muscle (Heaton and Wayne 1983). In addition, the oculomotor nucleus contains a pool of parasympathetic neurons (known as the Edinger-Westphal nucleus in mammals or the accessory nucleus in chick), which innervate the ciliary ganglion and control the ciliary muscle and pupillary constriction muscles. This pool is also segregated within the complex. Most strikingly the subset of motor neurons that innervate the dorsal rectus project their axons from their exit point and then translocate their cell bodies across the midline between HH stages 27-35 in the chick, thus projecting to the contralateral side as a result. This translocation was first surmised by analysis of Golgi stained sections (Puelles 1978) and more recently confirmed using Islet-1 as a motor neuron marker (Chilton and Guthrie 2004).

The wiring of the oculomotor system is highly conserved across species, but the development of the oculomotor nerve has been particularly carefully documented in the chick. In the chick axonal outgrowth from the oculomotor nucleus and the innervation of its targets occur in a stereotyped and highly reproducible manner, in a series of discrete steps which always follow in the same sequence at specific times. The oculomotor axons exit the neural tube ventrally, with the first pioneers emerging into the periphery at HH stage 16 in the chick. The first phase of growth is toward the dorsoposterior edge of the eye, which is reached by HH stage 19. Here the axons pause until HH stage 23, possibly awaiting signals from the developing extraocular muscle masses or the maturation of the ciliary ganglion (an intermediate target). Subsequently, the axons extend towards the

ventral oblique, the furthest target, which is innervated by HH stage 25. Branches into the other targets are issued between HH stages 27-29 (Chilton and Guthrie 2004). It is not clear whether the branches are formed by existing axons branching or *de novo* growth. In contrast, in mammals there is no delay prior to the innervation of the more proximal target muscles (Fritzsch et al 1995).

Very little is known about what cues direct the guidance of oculomotor axons. Neuropilins 1 and 2 (the receptors for diffusible class III semaphorins) are expressed in oculomotor neurons, as are two of their ligands Sema3A and Sema3C. At HH stage 26 (just prior to initial contact with the ventral oblique) both neuropilins are expressed by the whole nucleus, by HH stage 31, however, *NPN-1* expression is restricted to the ventral subnuclei and *NPN-2* is more highly expressed in the dorsal subnuclei. *Sema3A* and *Sema3C* are expressed throughout the nucleus between HH stages 26-31. In addition several of the secreted semaphorins including Sema3A and Sema3C are expressed in the head mesenchyme at HH stage 19, i.e. in the region that oculomotor axons will traverse en route to their targets (Chilton and Guthrie 2003). The specific pattern of neuropilin expression in the oculomotor nucleus highlights the possibility that semaphorins may be involved in target selection by the different subpopulations of oculomotor neurons. Studies in mutant mice provided additional support for the role of semaphorin signalling in oculomotor axon guidance. The oculomotor nerve developed normally in mice lacking *neuropilin-1* (Kitsukawa et al 1997) and in mice mutant for *Sema3A* (Taniguchi et al 1997, Behar et al 1996). Sema 3A had no effect on oculomotor outgrowth *in vitro* (Varela-Echavarria et al 1997). *Neuropilin-2* knockout mice, on the other hand, displayed a defasciculation of the oculomotor nerve, although it still reached its target territory (Giger et al 2000, Chen et al 2000). This phenotype was copied in the mutant for the ligand of neuropilin-2, Sema3F (Sahay et al 2003). Sema3F signalling to neuropilin-2 clearly performs an important function in oculomotor axon guidance; other semaphorins may also be involved in this process.

1.4.2 Trochlear nerve

Trochlear motor neurons are born in the rostral half of rhombomere 1; the first neurons are detected at HH stage 17 in the chick, and they continue to proliferate until HH stage 25. Uniquely amongst motor neurons, trochlear axons project dorsally in the neural tube all the way to the roof plate at the isthmus, where they decussate at the midline before exiting the brain on the contralateral side. The neurons within the isthmus project dorsally, while those lying in the adjacent anterior r1 project anterodorsally. The rostral population sends out the pioneer axons, followed by the more caudal neurons. By HH stage 20 the axons approach the dorsal exit point and by HH stage 23 all have exited and are extending through the periphery. The nerve extends as a series of fibre bundles around the dorsal edge of the eye, and by HH stage 26 it has contacted the dorsal oblique precursor (Watanabe et al 2004, Irving et al 2002, Chilton and Guthrie 2004).

The dorsal trajectory of the nerve is thought to be a result of its sensitivity to a multitude of repellent cues emanating from the ventral midline. Trochlear axons are repelled by Slits *in vitro*, which are expressed in the floor plate (Hammond et al 2005) as well as by netrin, also expressed in the floor plate (Colamarino and Tessier-Lavigne 1995). Sema 3A, which is secreted from the notochord (Anderson et al 2003), was also found to repel trochlear axons *in vitro* (Varela-Echavarria et al 1997), although others have failed to replicate this result (Giger et al 2000).

FGF8, which is expressed in a narrow band in the isthmus, is an attractant for trochlear axons *in vitro* and redirects them *in vivo* when misexpressed in posterior r1 (Irving et al 2002). Thus it could be guiding the axons of the more caudally lying neurons in a rostral direction towards the isthmus where they can fasciculate with the axons of the more anterior neurons. Sema3F signalling is also important for trochlear pathfinding. In both neuropilin-2 mutant mice and Sema3F mutant mice trochlear neurons are born but fail to coalesce into a nerve or exit the neural tube (Chen et al 2000, Giger et al 2000, Sahay et al 2003). Sema3F repels trochlear axons *in vitro* (Giger et al 2000, this study) and an ectopic source of Sema3F deflects trochlear axons *in vivo* (Watanabe et al 2004).

Sema3F is expressed along the caudal edge of the midbrain at the time when trochlear axons are extending to their exit point, preventing their inappropriate entry into the midbrain. Also neuropilin-2 is expressed near the dorsal exit point of the nerve, where it could be acting as a sink for the repulsive ligand enabling trochlear axons to grow towards it. This interpretation is supported by the finding that overexpression of neuropilin-2 in the midbrain results in trochlear axons invading that tissue (Watanabe et al 2004).

Whilst the guidance of trochlear axons in the brain has received some attention, little is known about what cues prompt them to exit the neural tube, what directs the contralateral projection and which signals enable the correct pathfinding to the dorsal oblique. The aim was to investigate these in more detail.

1.4.3 Abducens nerve

The abducens motor neurons arise in rhombomeres 5 and 6 in the chick and in rhombomere 5 in mammals (Wahl et al 1994). They are generated between HH stages 16-22 in the chick and their axons exit the neural tube ventrally in multiple rootlets starting at HH stage 16. The axons then course rostrally close to the neuroepithelium traversing the distance of three rhombomeres before making contact with the LR primordium at HH stage 18. This trajectory is highly unusual for cranial motor neurons most of which arise at the same axial level as their targets and do not make large deviations along the rostrocaudal axis. It is also precocious; the LR primordium is contacted two days earlier then other extraocular muscle precursors. The lateral rectus does develop faster than other EOM precursors but at HH stage 18 it shows no evidence of either myotube formation or myosin synthesis (Wahl et al 1994).

By HH stage 21 a subset of axons splits off from the main nerve and makes contact with the rostral part of the muscle mass. These are accessory abducens axons; the muscles they innervate are the pyramidalis and quadratus (P and Q) muscles, which move the nictitating membrane. The P and Q muscle precursors will start to dissociate form the

LR muscle mass at HH stage 22 and they follow a slower development course only maturing around embryonic day 8. The accessory abducens somata which are only found in r5 start to move laterally from HH stage 22 to form a discrete nucleus (Wahl et al 1994). At the same time they downregulate Islet-2 and turn on Lim3 expression, a genetic switch that could be responsible for their segregation from the main abducens nucleus (Varela-Echavarria et al 1996).

Little is known about the signals which direct abducens axons guidance. Sema3A was found to exert a repulsive effect *in vitro*, whilst netrin-1 had no effect (Varela-Echavarria et al 1997). Slits also showed no effect on abducens axons *in vitro* (Hammond et al 2005). SDF-1 was found to facilitate their ventral exit from the neural tube *in vivo* (Lieberam et al 2005). So far nothing is known about which attractants direct the nerve's rostral growth in the paraxial mesoderm towards its target.

1.5 AIMS AND OBJECTIVES

There remain a number of unanswered questions about how the innervation of the extraocular muscles is achieved. In the sequence of events that comprises the pathfinding of these nerves the first important decision point is exit from the neural tube. Oculomotor, trochlear and abducens neurons are all somatic motor neurons, however, whilst oculomotor and abducens axons exit immediately adjacent to the ventral midline, trochlear axons (atypically) extend a considerable distance within the neuroepithelium to exit in the dorsal roof plate, where they decussate and project contralaterally. What signals are directing the atypical behaviour of trochlear axons? The possibilities include: trochlear axons are more sensitive to floor plate repulsion which drives them onto a dorsal trajectory; there is an attractant for trochlear axons in the dorsal neural tube or adjacent mesoderm; or oculomotor and abducens axons exit ventrally because of an attractive signal in the underlying mesoderm which is absent at the r1 level, or which trochlear axons are insensitive to.

Once axons have exited the neural tube they extend through the mesenchyme towards the target. The developing extraocular muscles are not fully differentiated and are still undergoing apparent migration at this stage which poses an additional challenge for the navigating axons. It seems likely the muscles secrete attractant signals to guide the axons towards them, and plausibly that different cues are involved to attract different axonal populations to ensure accurate target selection. So far no attractive signals have been identified for oculomotor or abducens axons. For trochlear axons FGF8 has been shown to be an attractant both *in vitro* and *in vivo* for guidance within the neural tube (Irving et al 2002), but other attractants may be required for trochlear axon growth in the periphery towards the target. Generally, since the nerve trajectories for all three nerves are well conserved between different vertebrate species and the innervation patterns are very reproducible from embryo to embryo (Chilton and Guthrie 2004), there are probably a number of guidance cues both attractive and repulsive (to prevent axons from straying into inappropriate regions) which serve to tightly regulate each step of the guidance process.

In the process of extension towards the target the axons of each nerve exhibit unusual and interesting features. Abducens axons turn rostrally after exiting the neuroepithelium and extend close to and parallel to the neural tube for several rhombomeres; this behaviour is unique since most other cranial motor nerves innervate targets at roughly the same point on the anterior-posterior axis as the motor nucleus itself. This indicates that abducens axons are subject to strong attraction from the lateral rectus (or other tissue at that rostrocaudal level) which is specific for this population of axons. Trochlear axons project contralaterally after decussating at the dorsal roof plate, which is interesting because if the left and right trochlear nuclei are identical, their axons should be subject to the same attractive forces from both sides of the head and it is difficult to explain why the axons cross over. The oculomotor nerve exhibits the most interesting behaviour of all three nerves: in the initial stages of growth in the periphery axons grow lowly and stall, which indicates either a lack of an attractive cue or the presence of repellents; after HH stage 23 the axons elongate quicker but they grow towards the most distal target, ignoring both one inappropriate target (lateral rectus) and several cognate

ones (dorsal rectus, medial rectus, ventral rectus); only after contacts with the ventral oblique have been made do oculomotor branches form to innervate the other muscles. Again there are several possibilities to account for this phenomenon: if the identities of the different pools within the oculomotor nucleus are already clearly established prior to innervation then they may complete their axon guidance on different schedules with neurons that innervate the dorsal rectus, medial rectus and ventral rectus sending their axons later because of a lack of an attractant emanating from these muscles, the presence of a repellent until a later stage, or the need for a retrograde signal from the ventral oblique. If the identities of the different pools are not clearly defined, there is a possibility that contact with the ventral oblique promotes branching into the other muscles and the original branch into the ventral oblique is eventually pruned. Finally there is the question of what induces the translocation across the midline by the cells of the ventromedial subnucleus, which results in a contralateral projection to the dorsal rectus muscle. It may rely on a signal from the target muscle, which is innervated prior to the translocation, or it maybe driven by signals within the midbrain with the timing with respect to the target innervation merely a coincidence.

This project has attempted to resolve some of the mysteries still inherent in the regulation of this system. The conceptual framework to guide the approach was that each population of axons which is destined to innervate a particular muscle carries a specific complement of cell-surface receptors that enable it to interpret the head environment in a unique way. This complement of receptors may be liable to change over the course of the axonal pathfinding with some receptors being up or downregulated to meet the needs of each phase of the process. At the same time a diverse range of guidance cues is expressed in the targets and other key regions along the trajectories of the nerves or adjacent territories; these cues will attract, repel or have no effect on various populations of axons depending on what receptors are present on the surface of the growth cone and what downstream signalling machinery is available to transduce the signals. The expression patterns of the guidance cues are also subject to change and this maybe an important part of the mechanism, for example the formation of a nerve branch into a muscle may be delayed until that muscle activates the

expression of an attractive cue. The approach in this project has been to focus on several candidate guidance cues, where previous evidence indicated a possible role for these cues in this process, and to try to ascertain what that role may be.

The attention was concentrated on the following cues: the secreted semaphorins (Sema3A, Sema3C and Sema3F), hepatocyte growth factor (HGF) and stromal-derived factor 1 (SDF-1). There are several reasons why these candidates were selected. Previous work in this lab has highlighted the differences in the expression of neuropilins (semaphorin receptors) in the three nuclei in question: abducens neurons express solely neuropilin-1 (NPN-1), trochlear neurons express both NPN-1 and NPN-2 at high levels and oculomotor neurons express both receptors uniformly at HH stage 26 but subsequently NPN-1 expression becomes restricted to the ventral subnuclei, whereas NPN-2 expression is higher in the dorsal subnuclei (Chilton and Guthrie 2004). Thus neuropilins fit the profile of receptors that can confer different responses in abducens, trochlear and oculomotor axons to various semaphorins and thereby enable the semaphorins to act in the target selection and discrimination by these axons. It is worth recapping at this point that Sema3A is believed to signal through a NPN-1 homodimer, Sema3F is thought to signal through a NPN-2 heterodimer and Sema3C is thought to signal through a NPN-1/NPN-2 heterodimer, therefore expression of one, other or both neuropilins should render an axon sensitive to the action of different semaphorins. Furthermore, at HH stage 19 in the chick Sema3A, Sema3F and Sema3C are all expressed in different locations in the chick periocular mesenchyme and at other points along the trajectory of the nerves innervating the extraocular muscles making them likely candidate cues (Chilton and Guthrie 2003).

HGF has been shown to be an attractant for other cranial nerves plus its expression has been reported in the periocular mesenchyme (Caton et al 2000). In the absence of known target-derived attractants for the oculomotor and trochlear nerves, HGF is a good candidate to investigate for this role. SDF-1 has recently been implicated in axon guidance in a number of systems (Arakawa et al 2003, Chalasani et al 2003, Li et al 2005); in particular it plays an important part in motor axon exit point selection (including abducens motor axons (Lieberam et al 2005)). The expression of *SDF-1* was

seen in the periocular mesenchyme at early stages in the chick (B. Eickholt – personal communication). Therefore SDF-1 was chosen, to study its potential role in oculomotor and trochlear axon guidance.

The investigation of the role of the selected candidate guidance cues in axon guidance to the extraocular muscles followed a three-pronged approach:

1) The expression of the guidance cue in the target and regions along and surrounding the trajectory of the nerves, was studied at the relevant developmental stages using *in situ* hybridisation. In order to precisely resolve the spatial location of any region of expression, these experiments were performed on cryosections and combined with immunohistochemistry to reveal the location of the nerves and the extraocular muscles

2) The response of oculomotor, trochlear and abducens axons to the candidate guidance cues *in vitro* was tested by culturing embryonic rat explants containing the relevant motor neurons in collagen with the guidance cue in question added to the medium or presented from a graded source.

3) The combination of expression data and the results of co-culture experiments can allow the construction of simple models to explain the observed innervation sequence and eventual pattern. To further validate the ensuing models, their relevance was tested *in vivo*. Two types of in vivo experiment were carried out: mice mutant in genes coding for a candidate guidance cue or its receptor were examined for potential abnormalities in the projections to the extraocular muscles; and in the chick semaphorin signalling to abducens neurons was disrupted using in ovo electroporation of a dominant-negative neuropilin receptor.

The next chapter describes the methods employed in carrying out these experiments and subsequent chapters detail the results obtained.

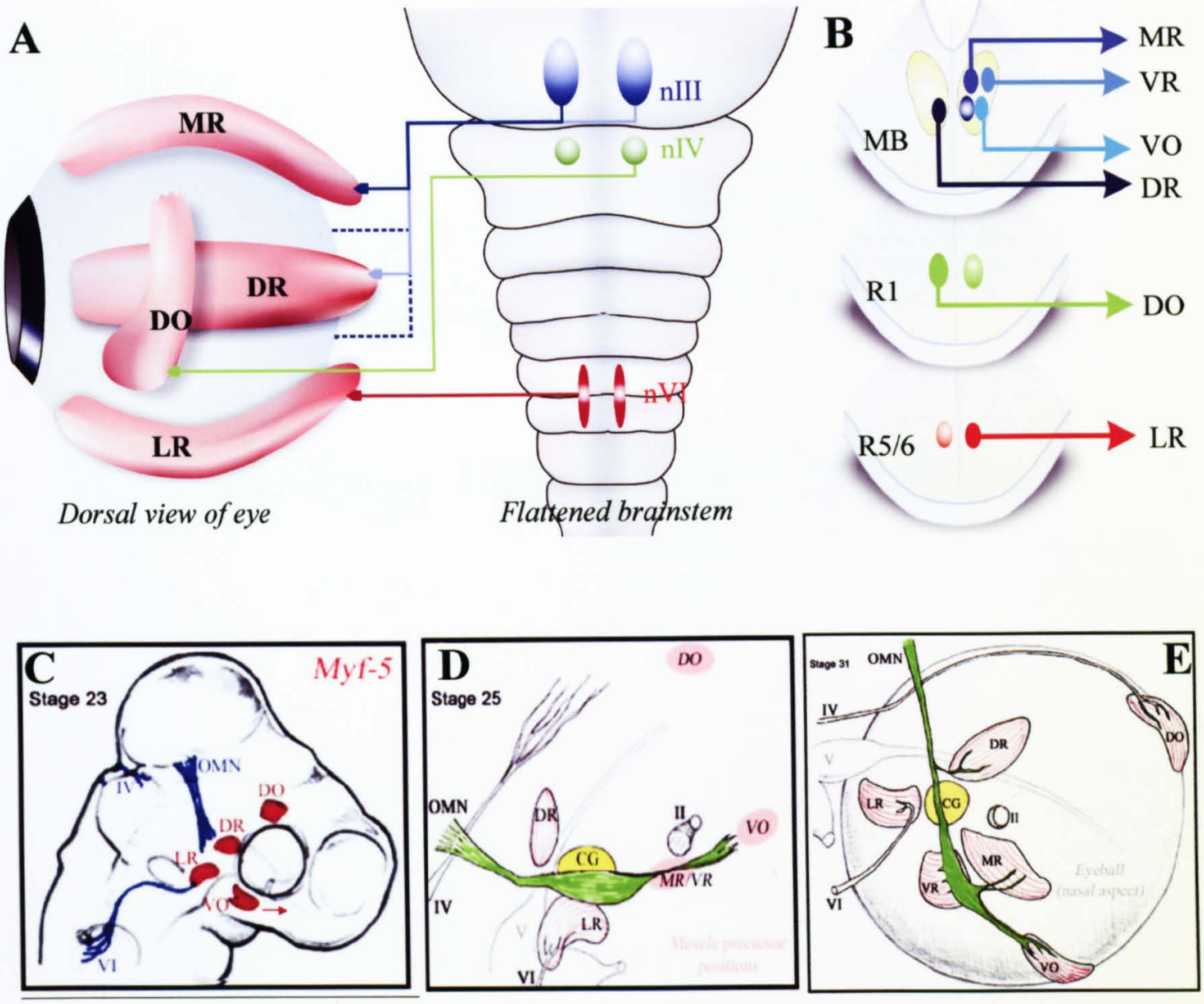

Figure 1.1

Axon growth and connectivity in the chick extraocular system

A, B—Schematic representation of the connectivity in the extraocular muscles. Oculomotor nerve, which stems from the caudal midbrain supplies innervation to four extraocular muscles (2 shown). The trochlear nerve projects contralaterally from rhombomere1 to innervate the dorsal oblique. The abducens nerve projects ipsilaterally from rhombomeres 5 and 6 to innervate the lateral rectus.
C—Extent of axon growth at HH stage 23. The abducens nerve (VI) has innervated the lateral rectus, the oculomotor nerve (OMN) has reached the ventro-posterior edge of the eye, and the trochlear nerve (IV) has emerged from the neural tube.
D—Extent of axon growth at HH stage 25. The oculomotor axons have reached the vicinity of the ventral oblique, but are yet to innervate it, and trochlear axons are approaching the dorsal oblique.
E—Stage 31. All muscles are innervated. Oculomotor axons have innervated the ventral oblique and have formed branches with the remaining targets.

Abbreviations: DR - dorsal rectus, VO - ventral oblique, VR - ventral rectus, MR - medial rectus, LR - lateral rectus, DO - dorsal oblique, OMN - oculomotor nerve, IV- trochlear nerve, VI - abducens nerve, nIII - oculomotor nucleus, nIV - trochlear nucleus, nVI - abducens nucleus, CG - ciliary ganglion, II - optic nerve, MB - midbrain, R1 - rhombomere1, R5/6 - rhombomere 5/6

This figure was compiled using images kindly provided by Dr John Chilton

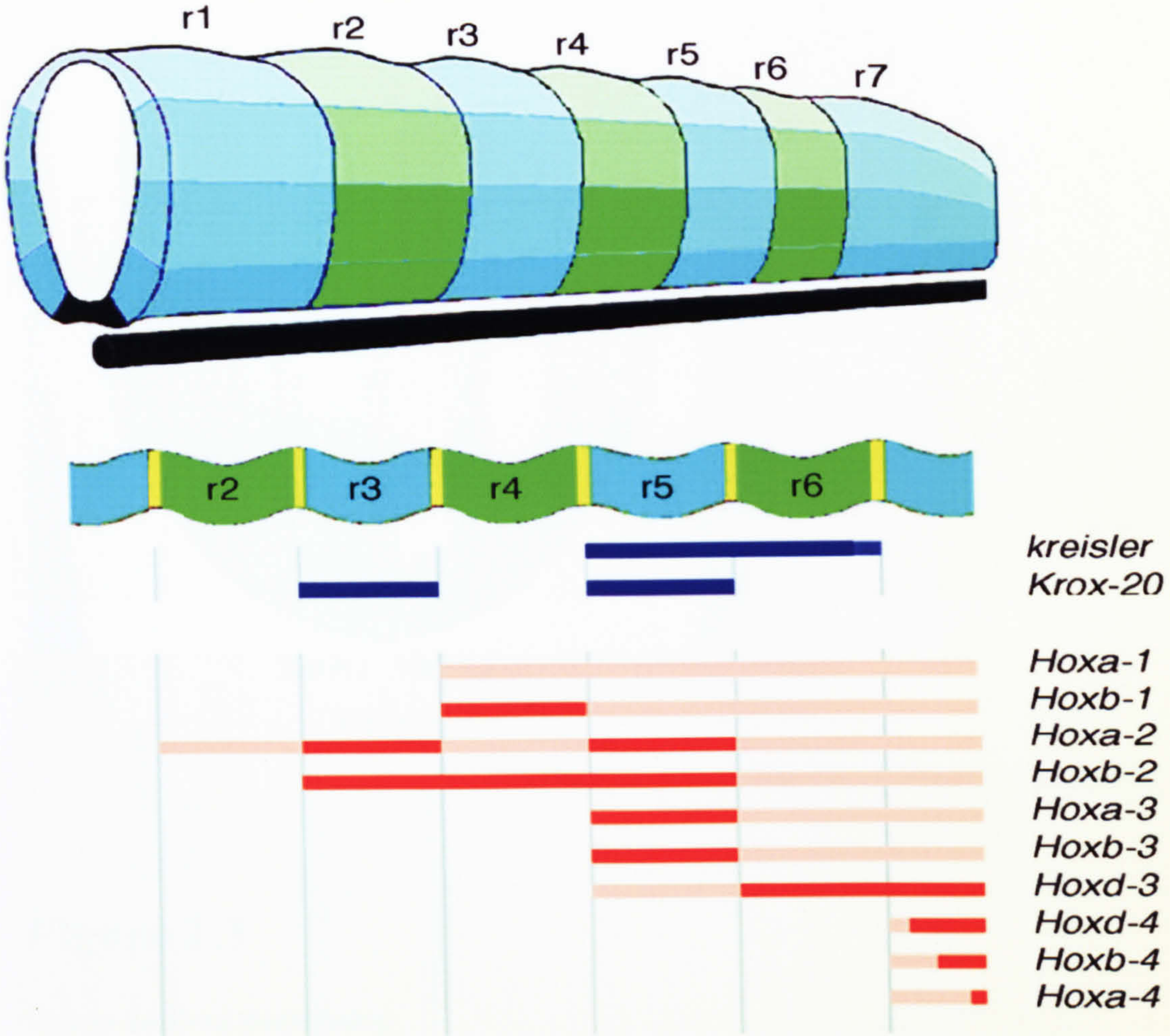

(modified from Lumsden and Krumlauf, 1996)

Figure 1.2

Genes patterning the hindbrain

Schematic representing the segmentation of the hindbrain into rhombomeres, and the differential gene expression of each rhombomere as a result of early anterior-posterior patterning events. *kreisler* is expressed in r5 and r6, while Krox-20 is expressed in r3 and r5. Furthermore each rhombomere expresses a distinct complement of *Hox* genes. Together the expression profiles of these transcription factor genes serve to provide each rhombomere with a distinct identity, enabling each rhombomere to establish distinct combinations of motor neuronal subpopulations later in development.

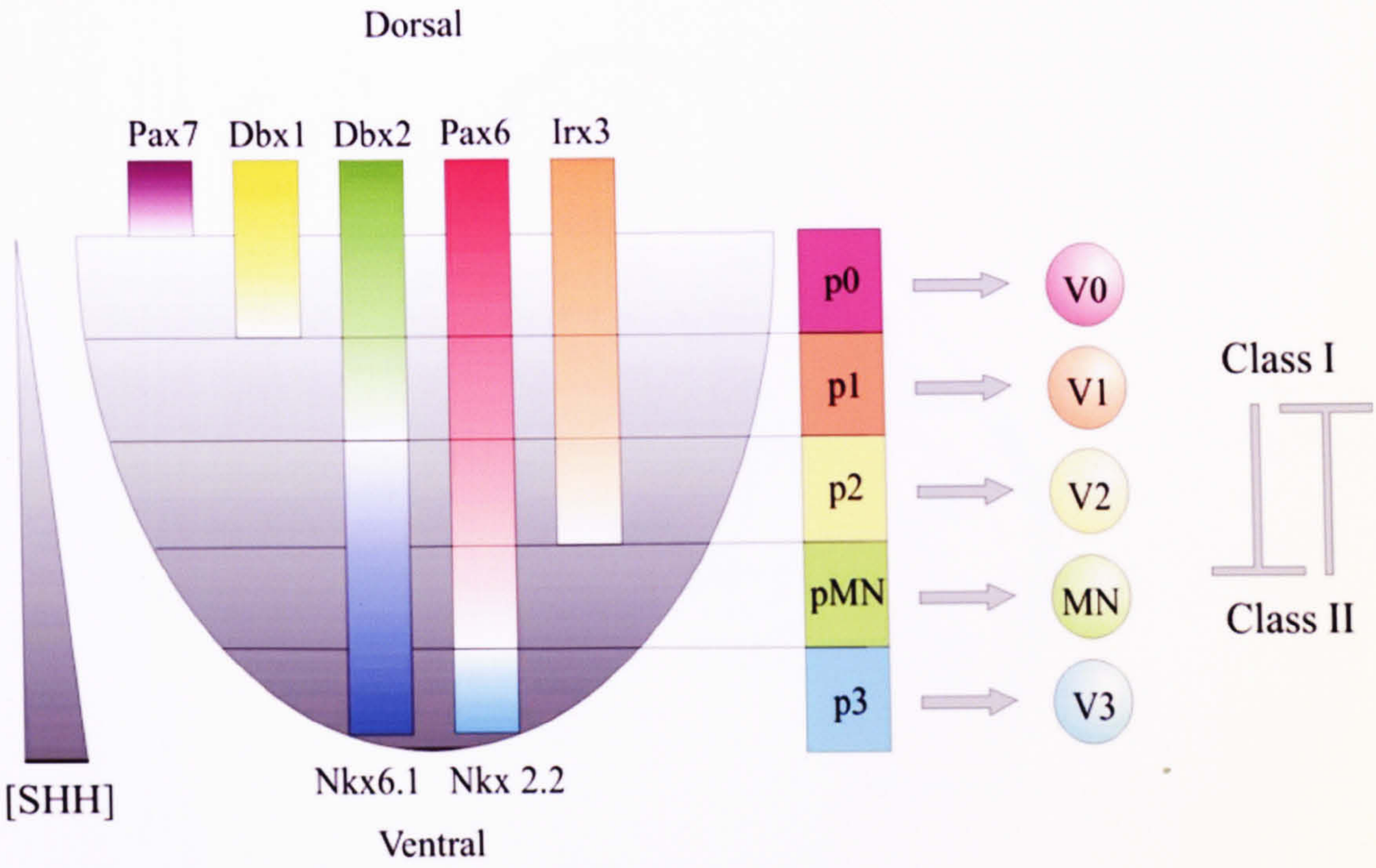

(Modified from Shirasaki and Pfaff, 2002)

Figure 1.3

Dorso-ventral patterning

Schematic representing the transcription factor interactions which specify the ventral portion of the hindbrain and spinal cord. SHH protein is secreted by the underlying notochord and later the floor plate, and forms a protein gradient through the ventral neural tube (indicated in grey) (reviewed in Shirasaki and Pfaff, 2002). The concentration of SHH a region is exposed to governs the transcription factor expression of that region. Class I genes (*Pax7*, *Dbx1*, *Dbx2*, *Pax6* and *Irx3*) are repressed by SHH, while Class II genes (*Nkx6.1* and *Nkx2.2*) are activated by SHH. These classes are mutually repressive, and able to define the ventral neural tube such that five progenitor (p) domains are established. The p3 domain gives rise to the branchiomotor and visceral motor neuronal subpopulations in the hindbrain, and interneuronal populations in the spinal cord. The pMN domain produces the cranial somatic motor neurons, and the spinal motor neurons. The p0, p1 and p2 domains generate various classes of interneurons in both the hindbrain and spinal cord.

A

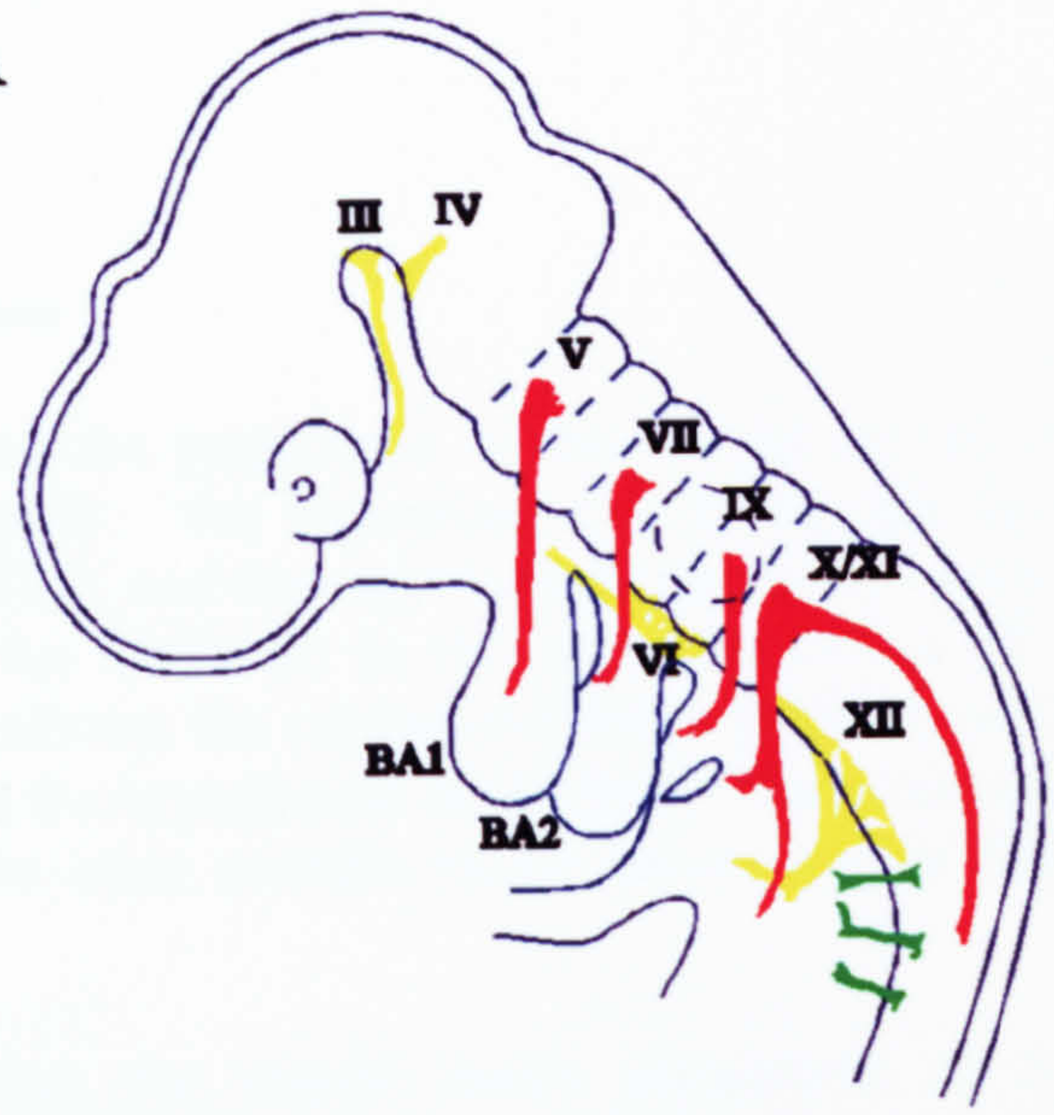

(Jacob et al., 2001)

B

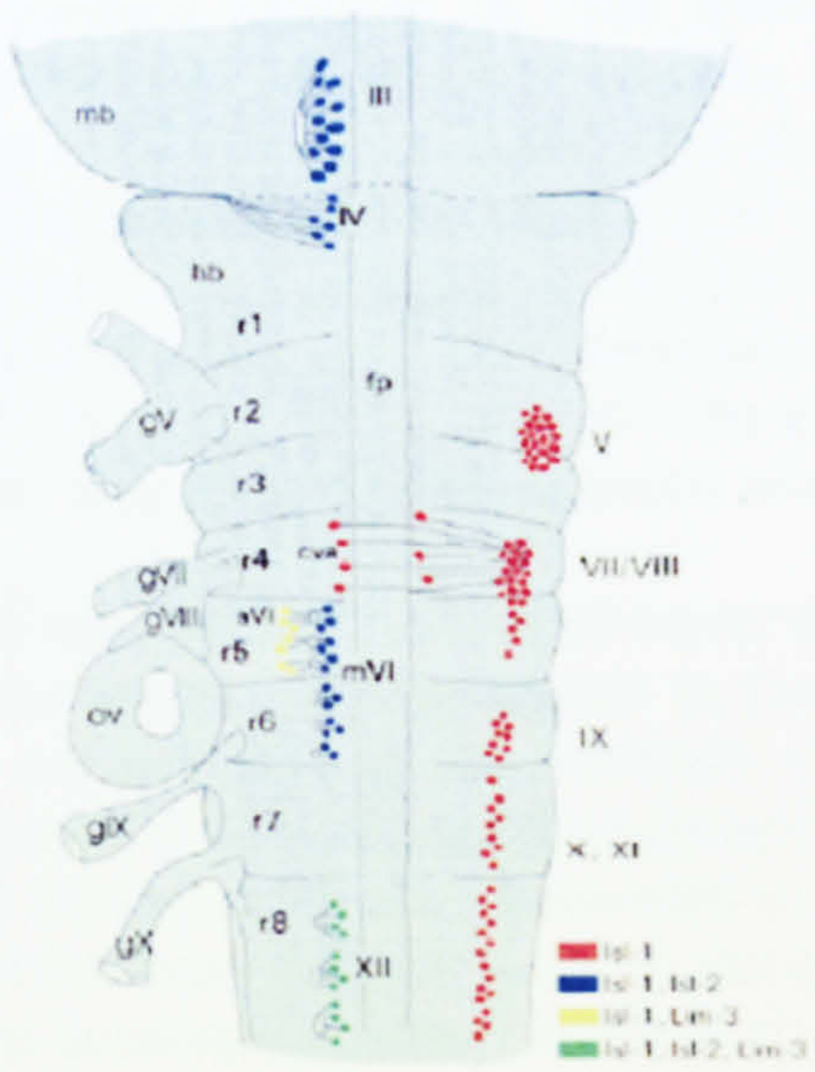

(Varela-Echavarria et al., 1996)

C

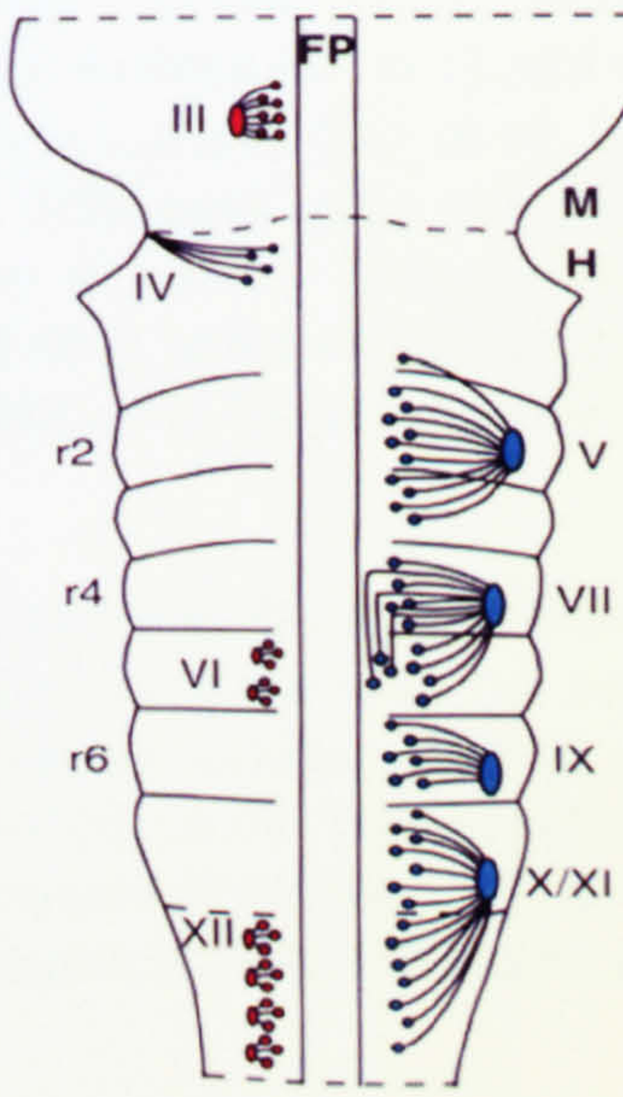

(Varela-Echavarria et al., 1997)

Figure 1.4

Figure 1.4

Cranial nerve projections

A Schematic representing the projections of the cranial nerves in the periphery. The branchiomotor nerves (red): the trigeminal (V) nerve, the facial nerve (VII), the glossopharyngeal nerve (IX), and the vagus/cranial accessory nerve (X/XI), project from dorsal positions along the hindbrain to the branchial arches (BA1 and BA2). The somatic motor nerves (yellow): the oculomotor nerve (III), the trochlear (IV) nerve, the abducens nerve (VI) and the hypoglossal nerve (XII). The trochlear nerve exits from the dorsal midline, while the other somatic motor nerves project from the ventral neural tube.

B Schematic representing the cranial motor projections in the developing chick brainstem. To the left of the ventral floor plate (fp) the somatic motor nuclei are represented; the oculomotor nucleus (III) in the midbrain (mb), the trochlear nucleus in r1, the abducens nucleus (mVI) in r5 and r6, the accessory abducens (aVI) in r5, and the hypoglossal nucleus (XII) in r8. The branchiomotor and visceral motor nuclei are illustrated on the right side of the floor plate; the trigeminal nucleus (V) in r2 and r3, the facial nucleus (VII/VIII) in r4 and r5, the glossopharyngeal nucleus (IX) in r6, and the vagus/cranial accessory nucleus (X,XI) in r7 and r8. The '*LIM* code' gene expression by these nuclei, as further detailed in Varela-Echavarria et al., 1996, is represented by colour in this schematic; red - *Isl-1* alone, blue - *Isl-1* and *Isl-2*, yellow - *Isl-1* and *Lim-3*, green - *Isl-1*, *Isl-2* and *Lim-3*. gV-gX - the cranial ganglia, ov – the otic vesicle, cva – contralaterally migrating vesitulo-acoustic neurons.

C Schematic representing the cranial motor neuron projections in the art hindbrain. The somatic motor nuclei are represented to the left of the floor plate (FP) (in red); the oculomotor nucleus (III) in the midbrain (M), the trochlear nucleus (IV) in r1, the abducens nucleus (VI) in r5, and the hypoglossal nucleus (XII) in r8. The branchiomotor and visceral motor nuclei are represented in blue; the trigeminal nucleus (V) in r2 and r3, the facial nucleus (VII) in r4 and r5, the glossopharyngeal nucleus (IX) in r6 and the vagus/cranial accessory nucleus (X/XI) in r7 and r8.

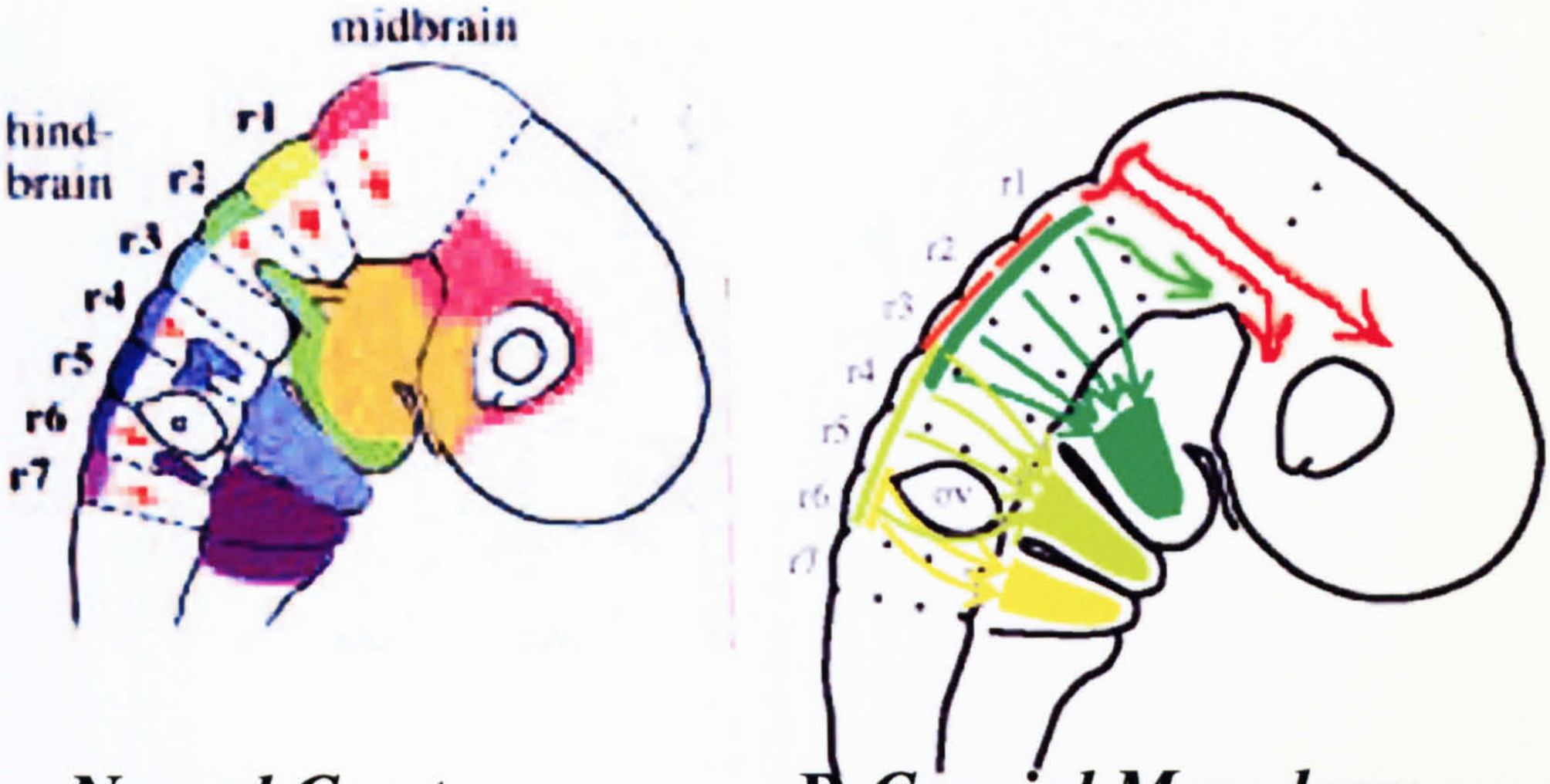

A ***Neural Crest***
(modified from Koentges & Lumsden 1996)

B ***Cranial Mesoderm***
(modified from Hacker & Guthrie 1998)

Figure 1.5

Schematic diagram showing the origin of mesenchymal tissue in the chick head. **(A)** is showing the migration pathways of neural crest. Most of the periocular mesenchyme is derived from the neural crest that has migrated from the midbrain (shown in red) or from the midbrain and rhombomere 1 (shown in orange). (B) is showing the spread of mesodermal tissue. Three of the extraocular muscles are derived from pre-chordal mesoderm (red) - a strip of axial mesoderm rostral to the notochord (orange). The other three extraocular muscles are derived from rostral cranial paraxial mesoderm.

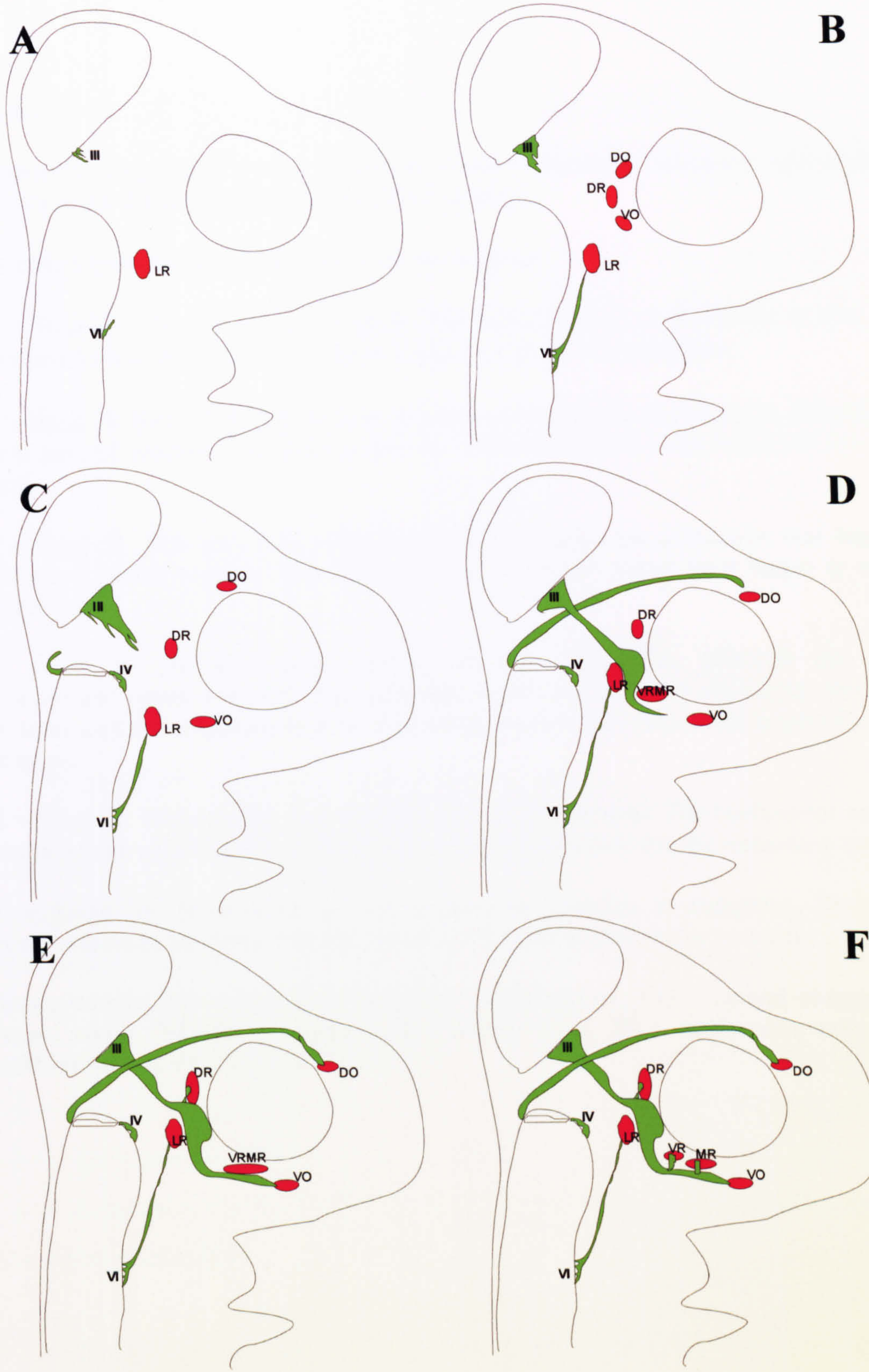

Figure 1.6

Schematic diagram of the development of the oculomotor, trochlear and abducens nerves at six different stages in the chick embryo

Figure 1.6

Schematic diagram of the development of the oculomotor, trochlear and abducens nerves at six different stages in the chick embryo

Muscles are shown in red, nerves are shown in green

A – Stage 16. One extraocular muscle (the lateral rectus) is detectable at this stage. Oculomotor and abducens axons have begun to exit into the periphery.

B – Stage 18. Four of the extraocular muscles are detectable at this stage, although they have not yet reached their final positions. Abducens axons have contacted the lateral rectus

C – Stage 21. Still only four of the extraocular muscles are detectable, and they have advanced further towards their final position. Trochlear axons have begun to exit the neural tube.

D- Stage 26. All extraocular muscle are now detectable, although the VRMR primordium remains fused. The trochlear nerve has reached its target (the dorsal oblique) and the oculomotor nerve is growing towards the most distal target (the ventral oblique).

E – Stage 28. The muscles have reached their final positions. The oculomotor nerve has contacted the ventral oblique and is about to issue branches into the remaining targets.

F – Stage 31. Innervation of the extraocular muscles is complete. The VRMR primordium has separated into the ventral rectus and medial rectus muscles.

Abbreviations: DO – dorsal oblique, DR – dorsal rectus, VO – ventral oblique, LR – lateral rectus, VRMR – ventral rectus/medial rectus, III – oculomotor nerve, IV – trochlear nerve, VI – abducens nerve.

Chapter 2: Materials and Methods

2.1 TECHNIQUES USED IN DETERMINING THE RNA AND PROTEIN EXPRESSION PATTERNS IN THE CHICK EMBRYO

2.1.1 Preparation of plasmid DNA

Several DNA plasmids were used over the course of this project. All of these were amplified and prepared using the Qiagen (UK) Hi-Speed Maxi-prep kit. The DNA concentration of the product was assessed using spectrophotometry, and the identity of the product was confirmed using a double restriction enzyme digest, using enzymes specific to sites either side of the insert (enzymes from Roche, Germany).

2.1.2 Preparation of RNA *in situ* hybridization probes

DNA plasmids used for probe production were prepared as above and linearised using enzymes specific to sites at the opposing end of the insert to the transcription site to be used, such that no transcription could occur from the sense promoter site (in the case of an antisense probe). This involved setting up an enzyme digest in a total volume of 50µl, consisting of 10 µg of plasmid DNA, 10U of the appropriate restriction enzyme (Roche, Germany), 5µl of buffer appropriate for the enzyme (Roche, Germany) and DEPC (diethylpyrocarbonate) treated water. This was incubated at 37°C for 3 hours, and then 1µl of the mixture was electrophoresed on a 1% agarose gel to check that the digest was completed successfully.

The DNA from this linearization was then precipitated using sodium acetate and ethanol. 0.1 volume of 3M sodium acetate solution (pH 5.2) and 2.5 volumes of cold ethanol (-20°C) were added, and the sample was left at -80°C for 20 minutes. The mixture was then centrifuged at 13,000 rpm for 15 minutes, which led to the formation of a pellet in

the base of the tube. The supernatant was removed and the pellet washed with 70% ethanol, vortexed and again centrifuged at 13,000 rpm for 5 minutes. The supernatant was removed and the pellet was allowed to dry at room temperature before being resuspended in 11µl DEPC-treated water. The concentration was estimated by electrophoresis of 0.5µl of the sample on a 1% agarose gel and comparison to the band intensity of DNA of known concentration.

In order to produce RNA probes from these linearised plasmids a transcription reaction was set up. This consisted of 4µg of linearised plasmid, 2µl of 10x transcription buffer, 2µl of 10x dioxygenin labelled nucleotide mix, 20U of RNase inhibitor and 20U of the appropriate RNA polymerase (Roche, Germany). The volume was made up to 20µl with DEPC-treated water. This mixture was then incubated at 37°C for 2 hours, after which 20U of DNase I (RNase free) was added to digest the DNA.

The RNA was obtained from this mixture using a Mini Quick Spin RNA column (Roche, Germany), which was prepared by centrifugation at 1000g for one minute to remove the storage buffer. Then 40µl of DEPC treated water was added to the transcription reaction mixture, which was put onto the column and centrifuged for four minutes at 1000g. The collected liquid contained only the full length probe RNA, 1µl of which was then electrophoresed for 20 minutes at 100V on an RNase free, 0.7% agarose gel to confirm the size of the transcript, and estimate the concentration. The sample was then split into aliquots containing ~1mg of the probe.

Probe	**Vector**	**Source**
Sema3A	pBS	Dr J. Raper
Sema3C	pBS	Dr J. Raper
Sema3F	pCRII	Dr J. Chilton
HGF	pBS KS-	Dr C. Stern
SDF	RT-PCR product	Dr B. Eickholt
CXCR4	RT-PCR product	Dr B. Eickholt

2.1.3 Preparation of chick embryos for cryosectioning

Fertilized hens' eggs (Henry Stewart Farm, UK) were incubated at 37°C for 3-6 days depending on the stage required. Embryos were removed from the eggs and dissected in DEPC treated PBS. Extra-embryonic tissue was removed. Branchial arches and all tissue posterior to the hindbrain were also removed and the roof plate opened to allow better penetration of the fixative. The dissected embryos were fixed in 3.5% paraformaldehyde (PFA) overnight at 4°C. The following day the fixed embryos were washed three times in DEPC-treated PBS for 15 minutes each, followed by immersion in a sucrose gradient (wash in DEPC-PBS/10% sucrose for 1 hour, then in DEPC-PBS/20%sucrose for 1 hour, then in DEPC-PBS/30% sucrose for 1 hour). The embryos were left in a 1:1 mixture of DEPC-PBS/30% sucrose and OCT (VWR International Ltd, UK) overnight, and then were transferred into OCT for 1hour. The embryos were frozen in OCT blocks in different orientations (transverse, parasagittal, coronal) on a 100% ethanol/dry ice bath and stored at -80°C until use. The embryos embedded in OCT blocks were sectioned at 20μm on a cryostat (Bright Instrument Company Ltd, UK), and transferred onto Superfrost Plus™ slides (VWR International Ltd, UK). *In situ* hybridisation was then either performed immediately, or the slides were kept at -20°C for up to one week.

2.1.4 *In situ* hybridisation on cryosections

The slides were allowed to defrost for 1 hour, and were then washed in DEPC-treated PBS for 15 minutes. Meanwhile 1ml of hybridisation buffer* was added to aliquots containing 1mg of RNA hybridisation probe, and the mixture was heated to 65°C for 5 minutes to denature the probe. The slides containing the sections were dried thoroughly and 150μl of hybridization mix was added to each. The probe was left to anneal overnight at 65°C in a humidified chamber.

The slides were washed three times in SSC*/50%formamide/0.1% tween-20, pre-warmed to 65°C. The first wash was for 15 minutes to allow the removal of coverslips; the following two washes were for 30 minutes. This was followed by two washes in

MABT* for 30 minutes. The sections were blocked by the addition of 300µl of blocking solution* for one hour. Meanwhile anti-DIG antibody (Roche, Germany) was diluted 1 in 2000 in blocking solution. 300µl of antibody mix was added to each slide and left overnight in a humidified chamber. The following day the slides were washed 5 times for 20 minutes in MABT and then rinsed twice for 10 minutes in AP buffer*. Meanwhile the staining solution* was prepared. 300µl of the staining solution was added to each slide and left to develop in the dark in a humidified chamber for 3hours – overnight, depending on the probe. The reaction was stopped by three washes in PBS/0.25%TritonX/2mM EDTA (Strahle et al 1994).

*Reagents

Hybridisation buffer – 50% deionised formamide (Fluka, USA), 10% dextran sulphate (Fluka, USA), 1mg/ml yeast RNA, 1x Denhardt's (Fluka, USA), 0.2M NaCL, 10mM Tris, 5mM sodium dihydrogen phosphate.

SSC- 100mM NaCl, 15mM sodium citrate (Sigma, USA)

MABT – 100mM maleic acid (Sigma, USA), 150mM NaCl (Sigma, USA), 0.1% Tween-20 (Sigma, USA).

Blocking solution – 2% Blocking reagent (Roche, Germany) dissolved in MABT + 20% heat-inactivated sheep serum (Sigma, USA).

AP buffer – 100mM NaCl, 50mM MgCl2, 100mM Tris, 0.1% Tween-20 (all from Sigma)

Staining solution - 20µl/ml NBT/BCIP (Roche, Germany) in 5% polyvinyl alcohol (Sigma, USA)/AP buffer.

2.1.5 Immunohistochemistry on hybridised sections

After *in situ* hybridisation had been performed the sections were immunostained using indirect immunofluorescence according to the following protocol. The sections were rinsed in PBS for 5 minutes. Then they were blocked for 30 minutes in PBS/1% Bovine Serum Albumin (Sigma, USA)/0.25% TritonX. Primary antibodies (Mf20, anti-myosin mouse monoclonal antibody, gift of Dr D. Fischman, 1:150; anti-neurofilament H rabbit

polyclonal antibody, Chemicon UK, 1:500, Prin et al 2005) were diluted in PBS/3% BSA/0.25%TritonX and the mix was added to the sections, 300µl to each slide, and left overnight in a humidified chamber. Subsequently the sections were washed three times for 10 minutes in PBS/0.1% BSA/0.05% TritonX. Fluorophore-linked secondary antibodies (Cy3-conjugated goat anti-mouse Fc, Jackson Immunoresearch USA, 1:300; Alexa488-conjugated goat anti-rabbit Fc, Molecular Probes USA, 1:500, Prin et al 2005) were diluted in PBS/3% BSA/0.25%TritonX and the mix was added to the sections, 300µl to each slide, and left overnight in a humidified chamber. Then the sections were, again, washed three times for 10 minutes in PBS/0.1% BSA/0.05% TritonX. The slides were dried and coverslips mounted using Fluorsave™ (Chemicon, UK). Photographs were taken on a Olympus BX21 microscope using a Zeiss Axiocam MRc digital camera. Images were processed using AxioVisionRel 4.2 (Zeiss, Germany) and Photoshop 6.0 (Adobe, USA) software.

2.2 COLLAGEN CO-CULTURE ASSAYS TO ASSESS THE RESPONSE OF MOTOR AXONS TO DIFFERENT GUIDANCE CUES *IN VITRO*

2.2.1 Cell transfection

Cells from the HEK293T (human embryonic kidney) cell line were plated on 30mm tissue culture dishes at $3.5x10^5$ cells/dish (as assessed by cell counts using a haemocytometer) and incubated at 37°C for 6 hours in Dulbecco's Modified Eagles medium (DMEM) (Gibco, UK)/10% fetal calf serum. The cells were then transfected with 1µg of the Sema3F-AP expression construct (obtained from Dr A. Chedotal, Chen et al 1997) using 3µl of Fugene transfection reagent (Roche, Germany) in 100µl DMEM. Mock-transfected HEK293T cells served as controls. For experiments assessing the effects of Sema3A and Sema3C, cell lines (obtained form Dr A. Puschel) stably expressing these molecules were used, and HEK293T cells served as controls.

2.2.2 Cell cluster formation

Cell clusters for use in the collagen co-culture assay were produced according to the method described in Varela-Echavarria et al. (1997). Thus Sema3F or mock transfected cells were removed from the dishes using a PBS wash followed by the application of 150µl of trypsin to each 30mm dish. Sema3A, Sema3C or control (293) cells were harvested directly from 50ml tissue culture flasks using a PBS wash followed by the application of 1ml of trypsin (Invitrogen, UK). The cells were resuspended in DMEM/10% fetal calf serum then centrifuged at 20°C at 2,000rpm for 5 minutes. The pellets were resuspended to a concentration of $3x10^7$ cells/ml. 15µl of this suspension was used to make each hanging droplet of cells on the lids of tissue culture dishes containing 2 ml of PBS. These droplets were incubated overnight at 37°C during which time they cluster together to form cell clusters that can be cut with mounted tungsten needles into appropriate pieces.

2.2.3 Preparation of SDF-coated beads

Heparin-coated beads (Sigma, USA) were rinsed in autoclaved PBS three times. 100µl of beads were added to a well of a 4-well plastic tissue culture dish and excess PBS was removed. The beads were incubated in 12µl of SDF (20µg/ml, R&D Systems), or in the case of control beads, 12µl of PBS, overnight at 4°C. Following this incubation, the beads were rinsed once in PBS and used in collagen co-culture experiments with oculomotor or trochlear explants (see section 2.2.5).

2.2.4 Fluorescent dextran labelling of the abducens nerve

E12 rat embryos were dissected out in Hank's balanced salt solution (Gibco, UK) and extra-embryonic membranes removed. The embryos were pinned out on sylgard-coated dishes and partially dissected to reveal the ventral hindbrain. The mesenchyme layer was peeled back around rhombomere 5 to sever the abducens nerve roots. Fluorescein-conjugated dextran amine crystals (10,000MW, Molecular Probes, Oregon) were

dissolved in distilled water and allowed to dry down to a viscous consistency. Forceps coated in this gel were then used to apply it to the exposed abducens nerve roots. Thus the abducens neurons retrogradely transported the dextran along their axons, as described in Glover et al (1986).

To allow maximum transport of the dextran, the embryos were incubated in Earle's Balanced Salt solution (Gibco, UK) that has been oxygenated using 95% O_2/5% CO_2, for 2 hours at 33°C in an airtight container. Rat embryos were then dissected further for use in the collagen co-culture assay.

2.2.5 Collagen co-cultures

E12 rat embryos were dissected in Hank's balanced salts solution (Gibco, UK) removing extra-embryonic tissue, the mesenchyme ventral to the neural tube, the forebrain and the spinal cord. To ensure the full removal of mesenchymal tissue, the dissected embryos were treated with dispase solution (Roche, Germany) containing DNase (50μg/ml, Sigma, USA). Bilateral explants containing the ventral third of the neuroepithelium were isolated by cutting with mounted tungsten needles. The explants thus contained motor neurons and the floor plate region. Further dissection was dependent on the tissue type required; for oculomotor explants the caudal part of the midbrain was used, for trochlear explants isthmus/rostral r1 were used and for abducens explants (following dextran labelling) r5 tissue was used (see figure 2.1).

The cell clusters prepared the previous day were cut into rectangular strips and placed along with the relevant explant of neuroepithelium on a base of collagen gel. This gel comprises rat tail collagen, (extraction described in Guthrie and Lumsden, 1994) and 3x MEM (Invitrogen, UK) in a 1:1 ratio, 20μl of which is placed on a 4 well tissue culture prepared plastic dish. 40μl of this gel was added to cover the explant and cell cluster, thus sandwiching them in a 3D matrix of collagen. The explants were positioned at a distance of 300-500μm to the cell cluster with one of the lateral edges facing the cluster, or in some experiments with oculomotor explants, the caudal edge was facing the

cluster. Alternatively, in experiments with SDF-coated beads, 5 or 6 beads were placed in a cluster in the centre of the gel and the explants positioned lateral side on, 300-500μm away. The gels were allowed to set for 30 minutes at 37°C before the addition of 'optimix' (70% Optimem with glutamax (Gibco, UK), 23% F12 Nutmix (Gibco, UK), 2% 2M glucose, 5% fetal calf serum (Sigma, USA)); (Colamarino and Tessier-Lavigne, 1995). In the experiments were the effects of HGF or SDF on oculomotor or trochlear axonal outgrowth were being tested, explants were plated out alone and 10ng/ml of HGF (R&D systems) or 100ng/ml of SDF-1 (R&D Systems) were added to the medium. 10ng/ml is the concentration of HGF deemed to be maximally effective for cranial motor axon growth-promotion by previous work in this lab (Naeem et al 2002). Similarly, a report published by Chalasani and colleagues (2003) identified 100ng/ml as an optimal concentration of SDF-1 for use in collagen explant cultures. All co-cultures were then incubated at 37°C for 42 hours to allow explant axons to extend into the collagen matrix.

2.2.6 Immunohistochemistry on explant co-cultures

Collagen co-culture gels were fixed in PFA overnight at 4°C, and then washed three times in PBS/1%TritonX for 30 minutes. They were then blocked for 1 hour (in PBS/1% TritonX/10% sheep serum/0.1% hydrogen peroxide), and washed three times in PBS/1% TritonX. The gels were then incubated for 3 days with the F84.1 antibody (kind gift of W. Stallcup, Prince et al 1992) diluted 1:100 in PBS/1%TritonX/10% sheep serum, at 4°C. This antibody specifically labels oculomotor and trochlear axons as it binds to the surface glycoprotein SC1/ DM-GRASP present on these axons. The gels were then washed six times for one hour with PBS/1% TritonX, followed by an overnight incubation with a peroxidase-conjugated goat anti-mouse antibody (Jackson Immunoresearch, USA) at 1:100 in PBS/1% TritonX/10% sheep serum at 4°C. The gels were washed with PBS/1% TritonX five times for one hour and once overnight, followed by two washes for one hour with 0.1M TrisHCl pH 7.2. The gels were then incubated in 0.5mg/ml diaminobenzidine (DAB) (Sigma, USA) in 0.1M TrisHCl pH 7.2 in the dark, and developed using 0.5mg/ml of DAB in 0.1M TrisHCl pH 7.2 with 0.02%

hydrogen peroxide for 10 minutes. PBS washes were used to stop the reaction and the gels were mounted on slides in 90% glycerol/PBS.

2.3 METHODS OF QUANTIFYING THE *IN VITRO* RESPONSES OF OCULOMOTOR, TROCHLEAR AND ABDUCENS AXONS TO DIFFERENT GUIDANCE CUES.

The normal pattern of outgrowth from oculomotor explants is shown in figure 2.2A and it consists of two broad, brush-like bundles emerging from the caudal edge of the explant either side of the midline (Varela-Echavarria et al 1997). Trochlear axons, which exit the neural tube dorsally *in vivo*, extend inside the explant away from the midline and grow out laterally in fasciculated bundles, as shown in figure 2.2B (Giger et al 2000, Irving et al 2002, Hammond et al 2005). Abducens axons exit the neural tube ventrally in vivo and also in explants; abducens axons do not fasciculate but extend independently through the collagen in random directions (see figure 2.2C) (Varela-Echavarria et al 1997, Hammond et al 2005).

In order to assess the response of axons when presented with a particular guidance compared with the control situation, several methods of measuring axonal outgrowth were used. For oculomotor and trochlear explants both semi-quantitative and quantitative approaches were used to measure axonal outgrowth. The semi-quantitative approach consisted of scoring explants on a 0-5 scale and comparing the scores for the control and experimental groups. This method is described in section 2.3.1. The quantitative approach included measuring the length of axonal bundles, the angle of deflection of axons when presented with a graded source of the cue and the angle of spread of axons. This method is described in section 2.3.2. All scoring and measurements were performed on oculomotor and trochlear explants stained with the F84.1 antibody. Outgrowth from stained explants was similar to outgrowth before staining as assessed with phase-contrast microscopy. Outgrowth from abducens explants was measured quantitatively using pixel counting, as described in section 2.3.3.

2.3.1 Semi-quantitative approach for measuring axonal outgrowth from oculomotor and trochlear explants

Outgrowth from trochlear and oculomotor explants was measured on the semi-quantitative 0-5 scale, where 0 represents no outgrowth and 5 the most prolific outgrowth seen with a particular type of explant (figure 2.3). To avoid bias the scoring was done blind. In experiments in which guidance cues were added to the growth medium, or oculomotor explants were cultured with the caudal edge facing the cluster, comparisons between the control and experimental samples were made using the overall explant score (i.e. measuring the total outgrowth from the explant). The Mann-Whitney U test was used to measure the probability (p) that the experimental group was not significantly different to the control group and any difference in the distribution of scores for the two groups had occurred merely by chance. A p value of <0.05 was taken to be statistically significant. Statistical significance was measured using the Mann-Whitney U test, since the discrete nature of the distribution means that parametric statistical measures such as the Student's t-test are not applicable. For experiments in which the explants were cultured with the lateral side facing the cluster of cells or beads, the outgrowth from the proximal half and the distal half were scored separately, and the distal score was subtracted from the proximal score, giving a net score for the explant of between -5 and 5, where -5 indicates a strong growth-inhibiting effect of the cluster, and +5 a strong growth-promoting effect of the cluster. Statistical comparisons between control and experimental groups were done using the Mann-Whitney U test.

2.3.2 Quantitative approaches for assessing axonal outgrowth from oculomotor and trochlear explants

For experiments in which HGF or SDF-1 were added to the culture medium, axonal outgrowth was also quantified by measuring the length and the angle of spread of axons

(figure 2.4A, B). The length was measured by drawing a line through the middle of the bundle from the edge of the explant to the end of the axon in the centre of the bundle. The angle of spread was measured from the centre of the nucleus to encompass the entire bundle – an increase in the angle of spread indicates an increase in the number of axons, a decrease in the extent of fasciculation, or both. For some of the experiments in which explants were cultured laterally to the cluster a relative length was also calculated, by subtracting the length on the distal side of the explant from the length on the proximal side of the explant. Thus a negative value for the relative length indicated that there was less outgrowth towards the cluster, and a positive value indicated that there was more outgrowth towards the cluster. For each sample, the mean percentage value for the proximal outgrowth was calculated, and the estimated standard error was calculated by the following formula:

$$\text{Estimated standard error} = \frac{\text{standard deviation}}{\sqrt{(n-1)}}$$ (where n is the number of explants in the sample)

Statistical comparison between the control and experimental samples was carried out by using Student's two-tailed t-test, which calculates the probability (p) of the null hypothesis (i.e. that there is no difference between the control and the experimental groups). A p value of less than 0.05 was taken to be statistically significant.

An attractive or growth-promoting cue would be expected to increase the length of axonal bundles, or if presented from a graded source, increase the relative length in experimental explants compared to the control group. A repulsive or growth-inhibiting cue would be expected to reduce the length of axons, or reduce the relative length if presented from a graded source in experimental explants compared to control explants. Similarly, an attractive cue would be expected to increase the angle of spread by enabling more axons to exit the explant and a repulsive cue would be expected to decrease the angle of spread by reducing the number of axons that exit the explant and possibly by increasing the fasciculation of axons that exit into the collagen.

To quantify the amount of chemorepulsion or chemoattraction experienced by the axons cultured with a particular type of cluster, the angle of deflection was measured. This was done by subtracting the angle the bundle on the proximal side makes with the midline (α) and the angle the bundle on the distal side makes with the midline (β) (figure 2.4C,D). A positive value for α-β means that α is larger than β, therefore the axons have been deflected towards the cluster, and therefore they are experiencing chemoattraction. A negative value means that α is smaller β, i.e. the axons have been deflected away from the cluster, therefore they are experiencing chemorepulsion. A mean angle of deflection and estimated standard error for each sample were calculated and statistical comparisons between the experimental and control groups were made using the Student's t-test, with $p<0.05$ taken to be statistically significant.

An exception to the above method was made for calculating the angle of deflection for oculomotor explants cultured with Sema3F-secreting clusters, and the corresponding control group. Because of the strong growth-inhibiting effect of Sema3F on these axons, it was not possible to measure the angle for the proximal bundle, since very few axons emerged from the explant on the facing side. Therefore, the measure of axonal deflection in this experiment was the angle made by the distal bundle to the midline (β) (figure 2.4E).

2.3.3 Quantitative approach for assessing axonal outgrowth from abducens explants

Abducens explants which had their axons retrogradely labelled with FITC-conjugated dextran were not subjected to immunostaining, but rather were photographed immediately using an Olympus Fluoview AX70 laser scanning microscope. The Z-stack images that were collected were flattened and quantification was performed by pixel counting using the Scion Image software. This was done in the following way. The image of each explant was divided into two halves along the midline of the explant, the proximal half of the explant referring to the side which is facing the cluster, and the distal half referring to the side which is facing away from the cluster. The amount of

outgrowth towards the cluster was measured by counting all the pixels, above a given threshold, of axons emerging into the proximal half. Amount of outgrowth away from the cluster was measured by counting all the pixels, above a given threshold, of axons emerging into the distal half. These amounts were given as percentages of total pixel count. Therefore, a score of >50% for the proximal half indicates that more than half the outgrowth has occurred towards the cluster, and the cluster is therefore potentially exerting a growth promoting effect. If the score for the proximal half is <50%, less than half the outgrowth has occurred towards the cluster, and therefore it is potentially exerting an inhibitory effect. For each sample a mean value for all the explants and the estimated standard error were calculated and statistical comparisons between the experimental and control groups were made using the Student's t-test. It must be noted that the number of dextran-labelled cells in the two halves of an abducens explant was rarely equal, which introduced a certain amount of asymmetry into each explant. However, because this asymmetry was unbiased with respect to the orientation of the explant, in a sample of 20+ explants any difference in the outgrowth between the proximal and distal sides should largely average out. The resulting noise in the system should not significantly affect the result.

2.4 METHODS FOR INVESTIGATING THE *IN VIVO* RESPONSES OF AXONS INNERVATING THE EXTRAOCULAR MUSCLES

2.4.1 Electroporation of chick embryos *in ovo*

This work was carried out according to the method described in Momose et al. (1999). Therefore, fertilized hens' eggs (Henry Stewart Farm, UK) were incubated at 37°C for approximately 40 hours until HH stage 11-13. 3ml of egg white was syringed out of the egg, to allow better access to the embryo, without piercing the yolk. The shell above the embryo was cut away and the embryo was injected with ink (using Indian ink in a 1:20 dilution in Ringer solution containing 1% penicillin/streptomycin (Gibco, UK)) from below to increase contrast and improve visibility of the embryo. (Ringer solution is a salt

solution used to hydrate the embryo and consists of 120mM NaCl, 15mM $CaCl_2$, and 5mM KCl in distilled water).

The IVth ventricle within the neural tube that corresponds to the hindbrain level was microinjected with a 1:1 mixture of the dominant-negative NPN-1 expression construct and tau-GFP expression construct (each at a concentration of 1μg/μl, overall DNA concentration of 2μg/μl, with 5% fast green dye to determine the area injected) using a capillary glass needle. The dominant-negative NPN-1 construct contained a chick β-actin promoter to facilitate expression in neural cells and their precursors and a myc tag to enable visualisation of transfected cells with immunohistochemistry. The dominant-negative capacity was conferred by the deletion of the C-domain of the extracellular part of the protein (the C-domain contains motifs found in a variety of proteins involved in homophilic interactions, therefore its loss is likely to prevent either the dimerisation of the neuropilin or binding to other parts of the receptor complex, as a result sequestering the ligand on an inactive receptor) (Renzi et al 1999).The tau-GFP construct was a full length cDNA clone with a chick β-actin promoter (Guidato et al 2003). A 10 volt square pulse was then passed across the hindbrain using a dual pulse isolated stimulator (Intracel, USA) with pieces of 0.5mm diameter silver wire acting as the electrodes. The anode was flattened and placed underneath the ventral surface of the hindbrain, while the cathode was rested on the dorsal surface of the opposing side of the hindbrain. Passing the current across these electrodes temporarily permeabilises the cell membranes and attracts the negatively charged DNA towards the positive electrode. Thus in this configuration the plasmids enter cells in the ventral part of the hindbrain including abducens motor neurons.

About 1ml of Ringer solution/1% penicillin/streptomycin was then added to the electroporated eggs to prevent dehydration and bacterial contamination, and the eggs were sealed with Sellotape. Eggs were then incubated for a further 40 hours at 37°C to reach HH stages 19-21. The area and extent of electroporation was assessed by directly visualizing the GFP expression with fluorescence microscopy and by immunostaining for the myc tag on the dominant negative NPN-1 construct.

2.4.2 Immunohistochemistry on electroporated chick embryos

Embryos were dissected to remove extra-embryonic tissue, the branchial arches and tissues posterior to the hindbrain in PBS, and the roof plate opened to increase the perfusion of fixative, then the embryos were fixed in 3.5% PFA overnight at 4°C. They were washed three times in PBS for one hour each, followed by three one hour washes with PBS/1%TritonX. The embryos were blocked overnight in 20% sheep serum/ PBS/1%TritonX, and then the primary antibodies were added for 3 days at 4°C in 20% sheep serum/ PBS/1%TritonX.

The primary antibodies that were used were: rabbit polyclonal anti-neurofilament H (1:500, Chemicon UK), which stains axonal tracts and mouse monoclonal anti-myc (1:1000, Sigma, USA), which identified cells expressing the electroporated construct. The unbound primary antibodies were removed with six washes in PBS/1%TritonX/10%sheep serum (5x1hour, and once overnight). Secondary antibodies (Cy3-conjugated goat anti-mouse Fc, 1:300 and Cy5-conjugated goat anti-rabbit Fc, 1:150; both from Jackson Immunoresearch, USA) in PBS/1%TritonX/20%sheep serum were added for 2 days. The embryos were then washed six times (5x1hr and once overnight) in PBS/1%TritonX/10%sheep serum and flat-mounted on slides in 2.5% DABCO (Fluka, USA) in 90% glycerol/10% PBS.

2.4.3 Immunohistochemistry on mouse embryos

Sema3A/Sema3C mutant embryos were generously provided by Drs F. Mann and C. Henderson. *CXCR4* mutants were a kind gift from Dr I. Lieberam (Lieberam et al 2005). *Sema3A/Sema3C* mutants (and wild-type littermates) were received as fixed whole embryos aged E10.5. They bisected sagittally to allow better access for the antibodies. They were then washed three times for one hour in PBS and three times for one hour in PBS/1%TritonX. Primary antibody (2H3, mouse anti-neurofilament monoclonal antibody, gift of Drs T. Jessell and J. Dodd; Caton et al 2000) was added at 1:10 dilution

in PBS/1%TritonX/20% sheep serum for 3 days. This antibody stains axon tracts. Embryos were washed six times (5x1hr and once overnight) in PBS/1%TritonX/10% sheep serum. Secondary antibody (Cy3-conjugated goat anti-mouse Fc, 1:300) in PBS/1%TritonX/20% sheep serum was added for 2 days. Embryos were again washed six times (5x1hr and once overnight) in PBS/1%TritonX/10% sheep serum. They were then flat-mounted using DABCO-glycerol.

CXCR4 mutants (and wild-type littermates) were received as fixed whole embryos aged E12.5. The following day the fixed embryos were washed three times in PBS for 15 minutes each, followed by immersion in a sucrose gradient (wash in PBS/10% sucrose for 1 hour, PBS/20% sucrose for 1 hour, PBS/30% sucrose for 1 hour). The embryos were left in a 1:1 mixture of PBS/30%sucrose and OCT (VWR International Ltd, UK) overnight, and then transferred into OCT for 1 hour. The embryos were frozen in OCT blocks in a transverse or saggittal orientation on a 100% ethanol/dry ice bath and stored at -80°C until use. The embryos embedded in OCT blocks were cut into 20μm sections on a cryostat (Bright Instrument Company Ltd, UK), and transferred onto Superfrost Plus™ slides (VWR International Ltd, UK). The sections were washed in PBS for 15 minutes. Then they were blocked for 30 minutes in PBS/1% Bovine Serum Albumin (Sigma, USA)/0.25% TritonX. Primary antibodies (2H3, anti-neurofilament mouse monoclonal, gift of T. Jessell and J. Dodd, 1:20, Caton et al 2000; A8, anti-Islet1 rabbit polyclonal antibody, gift of T. Jessell, 1:500, Chilton and Guthrie 2004) were diluted in PBS/3% BSA/0.25%TritonX and the mix was added to the sections, 300μl to each slide, and left overnight in a humidified chamber. These antibodies stain axons and motor neuron cell bodies, respectively. Subsequently, the sections were washed three times for 10 minutes in PBS/0.1% BSA/0.05% TritonX. Secondary antibodies (Cy3-conjugated goat anti-mouse Fc, Jackson Immunoresearch USA, 1:300; Alexa488-conjugated goat anti-rabbit Fc, Molecular Probes USA, 1:500) were diluted in PBS/3% BSA/0.25%TritonX and the mix was added to the sections, 300μl to each slide, and left overnight in a humidified chamber. Then the sections were, again, washed three times for 10 minutes in PBS/0.1% BSA/0.05% TritonX. The slides were dried and coverslips mounted using Fluorsave™ (Chemicon, UK). Photographs were taken on an Olympus

BX51 microscope using a Zeiss Axiocam MRc digital camera. Images were processed using AxioVisionRel 4.2 (Zeiss, Germany) and Photoshop 6.0 (Adobe, USA) software. In Photoshop the 'Levels' on fluorescent red and green images were altered to maximise signal and reduce noise, then the red and green channels were copied and pasted over the top of the brightfield image, to give the combined images which showed the relative location of expression of the gene in question (at the mRNA level) and protein markers that identified muscle fibres, axons or neuron cell bodies.

List of abbreviations

AP – alkaline phosphatase

DABCO - diazobicyclooctane

DEPC – diethylpyrocarbonate

DIG – digoxygenin

DMEM – Dulbecco's modified eagle's medium

EDTA – ethylenediaminetetraacetic acid

HGF – hepatocyte growth factor

M – molar

MABT – maleic acid buffer with tween20

PBS – phosphate-buffered saline

rpm – revolutions per minute

r1 – rhombomere 1

SDF – stromal-derived factor 1

U – units (of enzyme activity)

V – volts

µl – microlitre

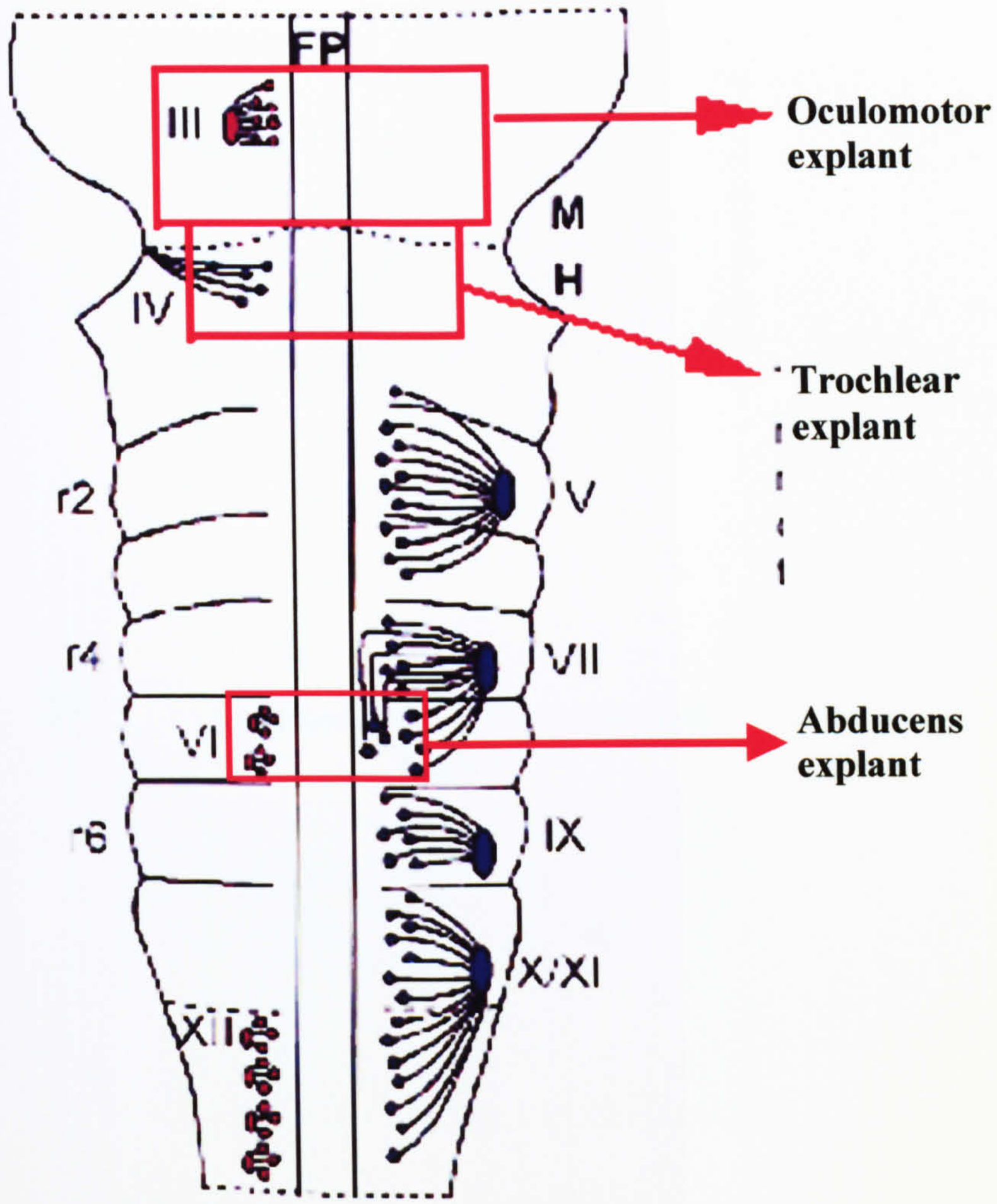

Figure 2.1

Schematic diagram of the hindbrain and caudal midbrain (flat mount)

Red boxes mark the explants dissected out in the rat
FP - floor plate
M - midbrain, H - hindbrain, dotted area indicates the midbrain-hindbrain boundary
III - oculomotor nucleus
IV - trochlear nucleus
VI - abducens nucleus

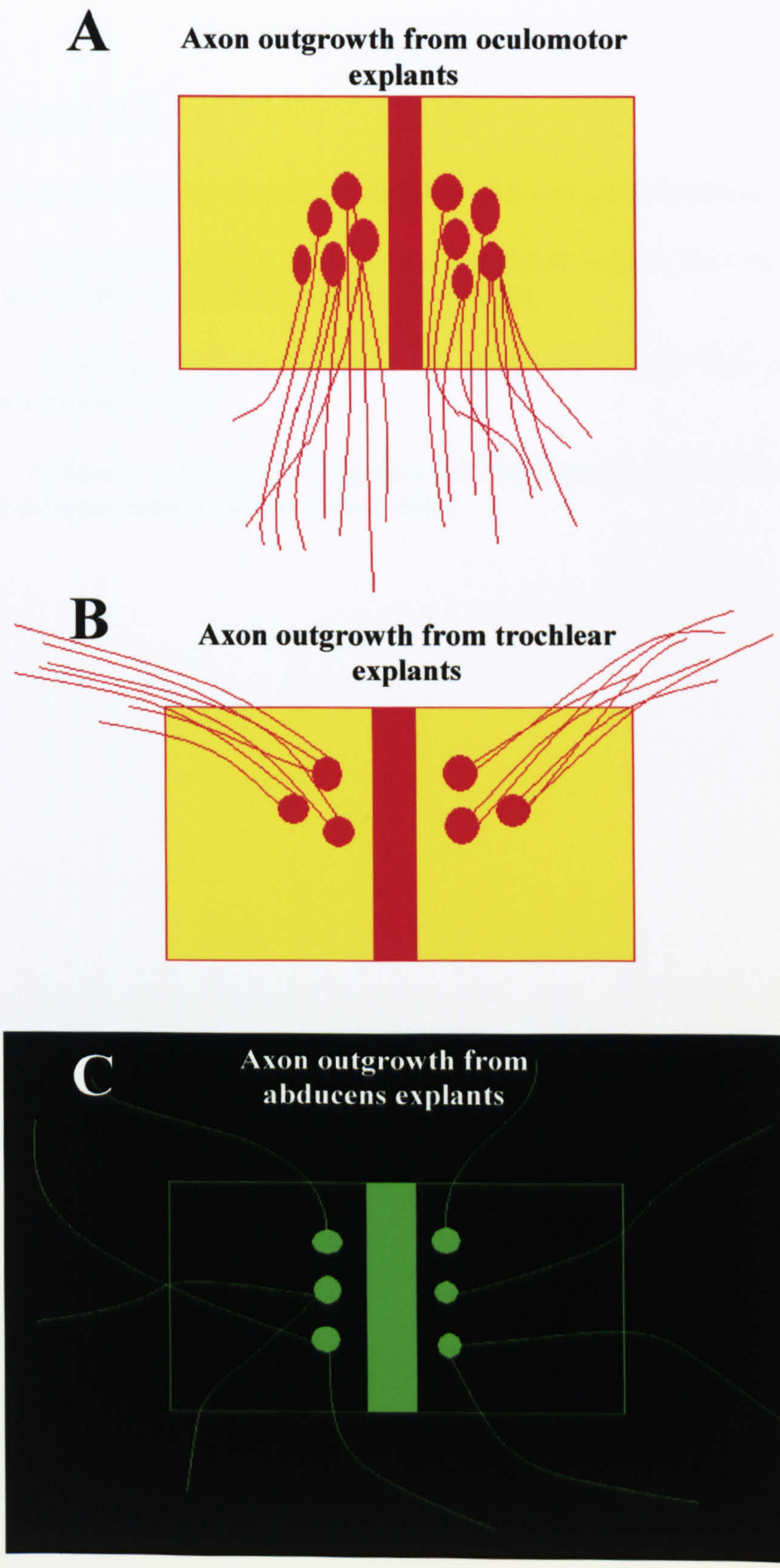
A
Axon outgrowth from oculomotor explants
B
Axon outgrowth from trochlear explants
C
Axon outgrowth from abducens explants

Figure 2.2

Figure 2.2

Outgrowth from oculomotor, trochlear and abducens explants

A – Oculomotor explant. Motor axon outgrowth occurs from the caudal edge in two broad bundles extending parallel to the midline

B – Trochlear explant. Motor axon outgrowth occurs from lateral edges in two fasciculated bundles.

C – Abducens explant. FITC-dextran labelled motor axons exit ventrally and extend in the collagen independently of each other.

Figure 2.3

Figure 2.3

Outgrowth scores for oculomotor and trochlear explants using the semi-quantitative index

In many cases outgrowth from oculomotor and trochlear explants was assessed using the 0-5 semi-quantitative scale. 0 indicates no outgrowth and 5 the most prolific outgrowth seen, as based on the number and length of axons. This figure indicates the typical amount seen for oculomotor (left column) and trochlear (right column) explants attaining each score (1 at the top, 5 at the bottom).

In some experiments the overall explant score was taken (a composite score of the two bundles). In experiments in which explants were cultured with cell clusters or beads, outgrowth from the half facing the cluster and the half facing away from the cluster were scored separately using the same index. The difference between outgrowth from the proximal half score and the distal half score made up the net explant score.

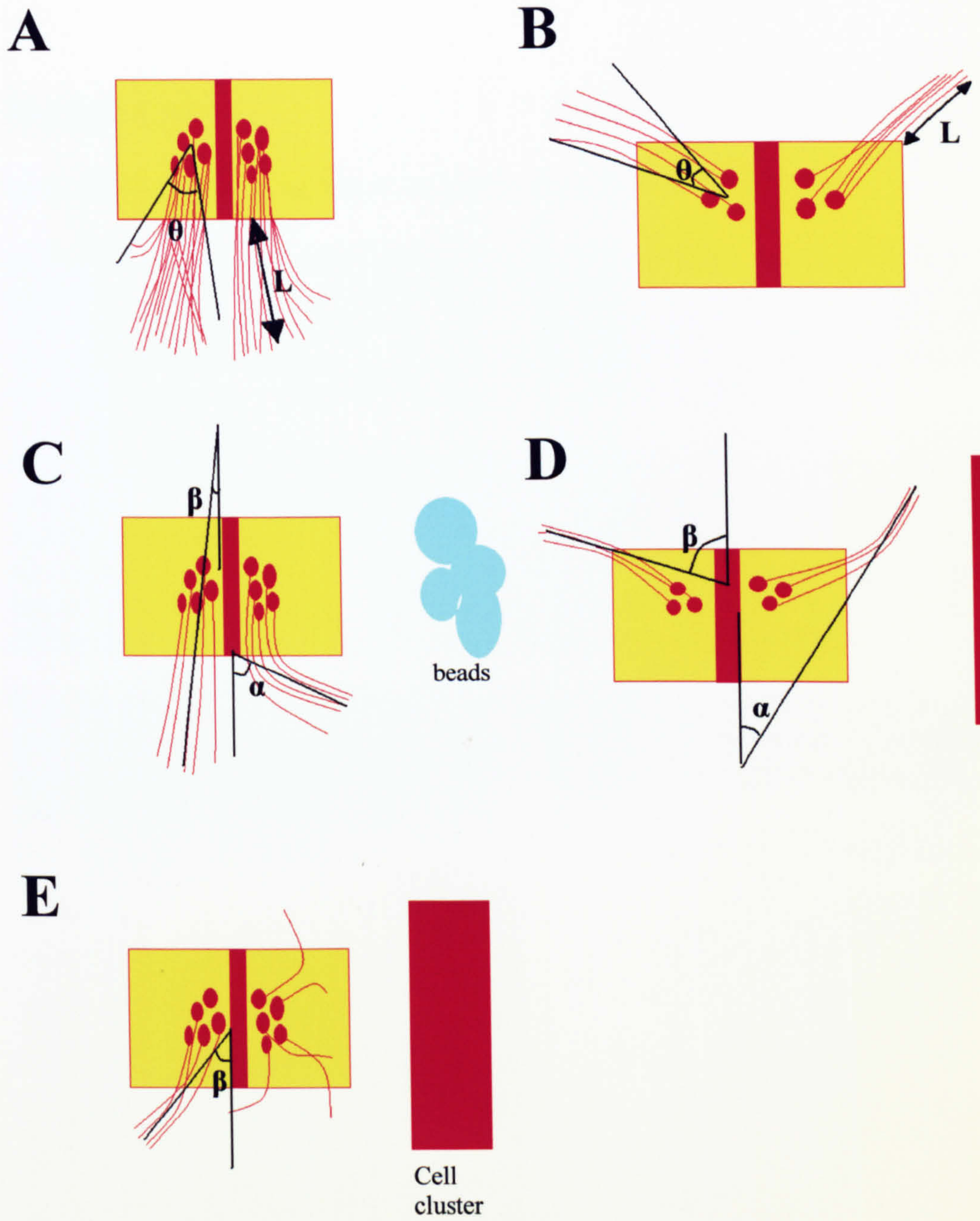

Figure 2.4

Figure 2.4

Quantitative measurements on oculomotor and trochlear explants

A, B Measurements of length of bundles (L), shown on the right in each case, and the angle of spread θ, shown on the left in each case. L is the length of the line drawn along the middle of the bundle from the centre of the exit point to the end of the bundle. Θ is the angle of spread of axons, measured from the centre of the nucleus and encompassing the entire bundle. **A** - oculomotor explant, **B** - trochlear explant

C, D Measurement of the angle of deflection. Angle of deflection is equal to (α-β), where α is the angle between the line through the middle of the proximal bundle and the midline, and β is the angle between the line through the middle of the distal bundle and the midline. A positive angle of deflection indicates attraction of axons towards the cluster of cells or beads, and a negative angle indicates repulsion of axons away from the cluster of cells or beads. **C** - oculomotor explant. **D** - trochlear explant.

E In the case of oculomotor explants cultured with Sema3F-secreting clusters, the angle of deflection refers to the angle that a line drawn through the middle of the distal bundle makes with the midline (β) because there was insufficient outgrowth from the proximal side in most cases to measure the angle.

Chapter 3: Analysis of Expression Patterns of Candidate Guidance Cues in the Chick Extraocular Muscles, Using *In Situ* Hybridisation

3.1 INTRODUCTION

The question that I address in this thesis is what mechanisms govern the guidance of motor axons to the extraocular muscles, and the innervation of each muscle by axons from the appropriate nerve. To restate the problem briefly: the six extraocular muscles are in close spatial proximity to each other and are still migrating when axons reach them; nevertheless motor axons are able to accurately distinguish the cognate target and innervate the appropriate muscle, whilst ignoring and extending past other extraocular muscles. Indeed, the oculomotor nerve grows past without sending any branches, not only the lateral rectus, which is the cognate target for the abducens nerve, but also three other muscles (ventral rectus, medial rectus, dorsal rectus), which are its appropriate targets; it will only innervate them once the axons have made contact with the furthest muscle, the ventral oblique. It follows from this that extraocular muscles cannot rely on secreting generic attractants to secure innervation from the appropriate population of motor axons; each muscle has to express certain signalling molecules to attract the specific motor axons and/or exclude the inappropriate ones. There are a number of ways in which this exquisite control can be exercised. For example, the late formation of oculomotor branches to some of its targets could be due to one of the following. Firstly, DR, VR and MR may express a repulsive cue for oculomotor axons, which is only downregulated after the pioneer axons have extended past these muscles. Alternatively, these muscles may activate the expression of an attractant for oculomotor axons at this late stage. Secondly, different subpopulations of oculomotor neurons may be sensitive to different cues, which would govern what muscle they are destined to innervate; the delayed innervation of some targets could then be due to a later emergence of these axonal subpopulations. Thirdly, some form of retrograde signal from the ventral oblique

may be required to initiate branch formation to the other oculomotor targets. Similarly, the lateral rectus may express cues which either attract abducens axons, and to which oculomotor axons are insensitive, or which repel oculomotor axons and have no effect on abducens axons. The dorsal oblique, in turn, has to express a specific attractant for trochlear axons and/or repellents for other axons.

The hypothesis centred on the possible roles of five different guidance cues in the establishment of the specificity of innervation. Three secreted (class III) semaphorins (Sema3A, Sema3C, Sema3F) were chosen on the basis of the expression pattern of neuropilins in motor nuclei and the disruption of cranial nerves observed in *Sema* and *NPN* mutants (Chilton and Guthrie 2003, 2004, Chen et al 2000, Giger et al 2000, Sahay et al 2003). Semaphorins were hypothesized to act as repellents in this system. Cues that were selected as putative attractants in this system were HGF and SDF-1, based on their effects on other populations of cranial motor axons and reported expression in the periocular mesenchyme (Caton et al 2000, Lieberam et al 2005, Eickholt – personal communication)

The first step in testing the proposed hypotheses is to identify the spatiotemporal pattern of expression of the candidate guidance cues. The method chosen to achieve this objective was to identify the presence of the mRNA of the gene in question by hybridising it with fragments of complementary anti-sense RNA. This was done on 20μm-thick cryosections, either in a transverse or parasagittal orientation, because this method allows greater resolution of the precise location of an area of expression than whole-mount *in situ* hybridisation. In addition, indirect immunofluorescence was used to identify muscle, axons or motor neuron nuclei concurrently, which enables precise spatial identification of a region of expression in relation to the position of the target muscle or the developing nerve. Generally speaking, the identification of which embryonic features regions of expression correspond to was done with reference to gross anatomical landmarks such as ventricles, different appearance in brightfield microscopy of neuroepithelium and mesenchyme, the position of nerve tracts identified by neurofilament immunostaining, the position of muscles identified by mf20

immunostaining (which binds to the myosin light chain) or the position of motor neuron nuclei identified by islet immunostaining (which binds to a motor neuron specific transcription factor), depending on experiment.

The experiments were carried out at different developmental stages, which were of relevance to a particular event in the development of this system. At HH stage 18/19, abducens axons have exited the neuroepithelium and the pioneer axons are making first contacts with the lateral rectus primordium; at the same stage oculomotor axons are exiting the neural tube. At HH stage 21 trochlear axons are exiting into the periphery and at HH stage 26 oculomotor and trochlear nerves are making first contacts with their targets. At HH stage 28 the oculomotor nerve is forming branches into its other targets.

The expression of *Sema3A*, *Sema3C*, *Sema3F*, *SDF-1* and *HGF* was investigated at HH stage 26-8 when oculomotor and trochlear nerve are making contacts with their targets and oculomotor branches are starting to form, to determine whether these ligands could play a part in target selection. In addition, expression of *Sema3A* and *Sema3C* at HH stage 19 was studied to see if these cues may be relevant to abducens axon guidance. Expression of *SDF-1* was also assessed at HH stages 18 and 21 when oculomotor and trochlear axons respectively are exiting the neural tube, since SDF-1 has been implicated in promoting axonal exit from the neural tube for spinal motor neurons and hindbrain somatic motor neurons (Lieberam et al 2005). Expression of the receptor for SDF-1, *CXCR4*, was also assessed, as it had previously been found to be expressed transiently on other motor neurons (Lieberam et al 2005), and it was therefore important to ascertain if and when it is present on oculomotor and trochlear motor neurons, and subsequently at which stages of axon growth SDF-1 is likely to play a part.

3.2 RESULTS

3.2.1 Expression of class III semaphorins

3.2.1.1 Sema3F

Analysis of expression of *Sema3F* was carried out at HH stage 25 (when oculomotor and trochlear axons are extending towards their targets) and 28 (when trochlear axons have made contact with the dorsal oblique and oculomotor axons have innervated the ventral oblique and are starting to form branches into the other targets). Expression patterns in the head were found to be largely identical at these developmental stages. *Sema3F* expression at HH stage 28 is shown in figure 3.1.

Four regions of *Sema3F* expression were identified in the developing chick head (see figure 3.1 A, B). Two areas of *Sema3F* expression were within the neural tube – in the caudal midbrain (marked with 1, figure 3.1A, B), and in the dorsal part of rhombomere 1 (marked with 2, figure 3.1A, B). These areas of expression correlate to similar regions of expression reported in the mouse by Giger et al (2000). In that paper the authors argued that the expression of *Sema3F* in the dorsal neural tube, interrupted at the level of the trochlear nerve's exit point, formed a corridor of surround repulsion which enabled trochlear axons to exit correctly. In the *NPN-2* mutant trochlear axons failed to fasciculate and exit appropriately and the trochlear nerve was not formed (Giger et al 2000). The midbrain expression of *Sema3F* was also reported by Watanabe et al (2004), similarly, they postulated that the presence of this cue is necessary to direct trochlear axons along their correct trajectory, since adding a soluble NPN-2 receptor to sequester Sema3F resulted in trochlear axons invading the midbrain. The expression pattern of *Sema3F* within the neural tube is also consistent with a previous report of *Sema3F* expression within the neural tube of the chick (Chilton and Guthrie 2003).

The cranial phenotype in *Sema3F* and *NPN-2* mutant mice also included the defasciculation of the oculomotor nerve (Giger et al 2000, Chen et al 2000, Sahay et al

2003). This might suggest that *Sema3F* is normally present around the trajectory of the oculomotor nerve to maintain its fasciculation. In fact, this is not the case in the chick. Outside the CNS there are two areas of *Sema3F* expression – one in the mesoderm dorsal to the nasal cavity (4, figure 3.1A, E, F), which lies anterior to the ventral oblique muscle (the farthest target of the oculomotor nerve); Sema3F secreted from this region may act as a repellent to prevent oculomotor axons overshooting the ventral oblique. Another region of *Sema3F* expression is located between four of the extraocular muscles, dorsal to the developing ventral rectus/medial rectus (marked with 3, figure 3.1B, E, F). This region may correspond to the optic nerve exit point judging from anatomical landmarks and the position of muscles and major nerve tracks identified by immunohistochemistry. Since the oculomotor nerve trajectory lies ventral to the ventral rectus/medial rectus (marked with black arrowheads figure 3.1E, F), Sema3F may be acting to prevent the oculomotor axons from entering a more dorsal territory. None of the extraocular muscles express *Sema3F* (figure 3.1E, F, G, H), so Sema3F is unlikely to function as a repellent that prevents the innervation of inappropriate muscle targets.

3.2.1.2 Sema3C

Analysis of expression of *Sema3C* was carried out at HH stage 19 (when abducens axons are making first contacts with the lateral rectus muscle (Wahl et al 1994)), HH stage 25 (when oculomotor and trochlear axons are extending towards their targets (Chilton and Guthrie 2004) and 28 (when trochlear axons have made contact with the dorsal oblique and oculomotor axons have innervated the ventral oblique and are starting to form branches into the other targets (Chilton and Guthrie 2004)).

At HH stage 19 (figure 3.2) high levels of *Sema3C* expression were detected in oculomotor neurons (figure 3.2D), the developing lateral rectus muscle (figure 3.2A, E), the pharyngeal endoderm (figure 3.2B-E) and the mantle layer of the caudal neural tube (which is the region where motor neurons reside) starting from rhombomere 5 (figure 3.2D). Abducens neurons, resident in r5 and r6, express medium levels of *Sema3C*. Other tissues expressing medium levels of *Sema3C* include the trigeminal ganglion

(figure 3.2A), the ventral telencephalon (figure 3.2A, D) and the anterior tectum (figure 3.2D). *Sema3C* is also weakly expressed in the paraxial mesoderm surrounding the notochord (figure 3.2B, C) – the region through which abducens neurons extend their axons en route to their target. The strong expression of *Sema3C* in the lateral rectus muscle, which is the target of the abducens nerve, and weak *Sema3C* expression along the trajectory of the nerve at the HH stage when the muscle is being innervated by abducens axons raises the possibility of it acting as an attractant for abducens axons.

At HH stage 28 when all the extraocular muscles can be identified by immunohistochemistry for the mf20 antigen, strong *Sema3C* expression is maintained in the lateral rectus muscle (figure 3.3E, F), but at this stage it is confined to the posteriolateral part of the muscle. Although by this stage more than 48hrs have passed since the pioneer abducens axons had made first contact with the muscle (Wahl et al 1994), it is still worth noting that the nerve enters the anteromedial corner of the muscle and turns laterally towards the area of *Sema3C* expression, since the later populations of abducens axons may still be growing towards the muscle. *Sema3C* is expressed more weakly in other extraocular muscles (figure 3.3) and this expression doesn't extend throughout the muscle, rather it is confined to cells at the margin of the muscle and adjacent to it. These $Sema3C^{+}$ cells adjacent to the muscles (as identified by mf20 immunostaining) may be neural crest cells that are forming the muscle sheath (Noden 1983b, Koentges and Lumsden 1996) or they may be myoblasts that haven't yet switched on the expression of mf20.

Figure 3.4 shows the overall pattern of *Sema3C* expression in the head at HH stage 28. As well as the lateral rectus, *Sema3C* expression is maintained in the floor plate (figure 3.4A,B), ventral telencephalon (figure 3.4B) and the trigeminal ganglion (although like in the lateral rectus *Sema3C* expression becomes more restricted – in this case confined to the part of the ganglion nearest the neural tube) (figure 3.4A). *Sema3C* expression is also found in the mesenchyme adjacent to the dorsal and to the ventral edge of the eye, in a stream of mesenchymal cells between the rostral neural tube and the retina (figure 3.4A) – which is adjacent to and parallel to the trajectory of the trochlear nerve. *Sema3C*

expression is also found in the ventricular zone of the ventral diencephalon (where *Sema3C* expression has also been reported in the mouse (Puschel et al 1996)), and other parts of the forebrain (figure 3.4A, B).

3.2.1.3 Sema3A

Analysis of expression of *Sema3A* was carried out at HH stage 19 (when abducens axons are making first contacts with the lateral rectus muscle (Wahl et al 1994)), HH stage 25 (when oculomotor and trochlear axons are extending towards their targets (Chilton and Guthrie 2004) and 28 (when trochlear axons have made contact with the dorsal oblique and oculomotor axons have innervated the ventral oblique and are starting to form branches into the other targets (Chilton and Guthrie 2004)).

At HH stage 19 *Sema3A* expression is fairly ubiquitous in the head but with varying intensity, ranging from very strong expression in the lens (figure 3.5F), to strong expression in the ventral diencephalon and ventromedial head mesoderm (figure 3.5D), medium levels of expression in the periocular mesenchyme (figure 3.5E, F) to areas of little or no expression such as the rostral telencephalon or the midbrain (3.5D). *Sema3A* is also expressed in the ventral mandibular arch, in the notochord and in motor neurons including abducens motor neurons (figure 3.5B, C, E).

These data are in accordance with other published reports of *Sema3A* expression in the chick embryo, which also documented *Sema3A* expression in the notochord (Anderson et al 2003) and the eye lens (Chilton and Guthrie 2003). The ubiquity of *Sema3A* expression in the cranial mesenchyme may be to do with the fact that most of this mesenchyme is derived form neural crest cells and will go on to form cartilage and skeletal tissue; condensing cartilage has been shown to express *Sema3A* and is a tissue avoided by motor nerves – a notable phenotype in the *Sema3A* knockout mice was an invasion of cartilage by spinal and cranial motor axons (Taniguchi et al 1997).

Sema3A expression is notable by its absence from the path of the abducens nerve. Figure 3.5E shows a parasagittal section through the plane of the abducens path. The paraxial mesoderm through which the abducens nerve extends is free of *Sema3A* expression. A more medial parasagittal section (figure 3.5D) and a more lateral section (figure 3.5F) both show strong *Sema3A* expression at that level. This pattern can also be seen on a transverse section at the level of the abducens nerve exit from the neuroepithelium, where *Sema3A* is strongly expressed in the notochord and the lateral mesoderm, and more weakly in the more medial mesoderm, with the region surrounding the notochord – where the abducens axons will extend through, free from *Sema3A* expression (figure 3.5B, C). At a more rostral level where the target muscle is located, there is no expression in the region that corresponds to the lateral rectus primordium, but it is surrounded by *Sema3A* expression (figure 3.5A).

This can also be seen at HH stage 28, when the lateral rectus muscle is *Sema3A*$^-$ but is encased in a sheath of *Sema3A* expression (figure 3.6 E, F). This is similar for the pattern observed for all the other extraocular muscles, which are surrounded by *Sema3A* expressing mesenchymal cells. This expression sometimes extends into a part of, but not the whole muscle (figure 3.6). This expression pattern is similar to that of *Sema3C* at the same stage. Again it is unclear whether the cells surrounding the extraocular muscles are neural crest-derived connective tissue-forming cells, or whether they are muscle cells that are yet to activate the expression of mf20. Overall expression of *Sema3A* in the head at this stage is widespread (figure 3.7). It is particularly strong in the mesenchyme surrounding the eye, especially at the ventral oblique level (figure 3.7C), in the pial layer of the ventral diencephalon (figure 3.7A) and the ventricular layer of the hindbrain neural tube (figure 3.7A).

3.2.2 Expression of HGF

HGF is a good candidate as an attractant for both oculomotor and trochlear nerve, for which no target-derived attractants have been identified so far. Immunostaining for the mf20 antigen to identify muscle and neurofilament heavy chain to identify axon tracts

aided the positioning of these nerves and extraocular muscle in relation to areas of *HGF* expression. The experiment was carried out at HH stage 26-7, at which point the first trochlear axons have contacted the dorsal oblique, and the first oculomotor axons are about to contact the ventral oblique. Oculomotor branches into the dorsal rectus and ventral rectus/medial rectus are yet to form.

HGF is expressed in the dorsal periocular mesenchyme in a region flanked by the dorsal surface of the developing eye and the lateral midbrain and diencephalon on the other side. Trochlear axons extend through this region on the approach to the dorsal oblique muscle. This region of *HGF* expression encompasses the antero-dorsal part of the developing dorsal oblique muscle, but some mf20^{+} fibres within the dorsal oblique do not express *HGF* (figure 3.8A, B). *HGF* is also strongly expressed in a region of periocular mesenchyme adjacent to the ventral edge of the eye. This region of strong *HGF* expression surrounds the ventral oblique muscle (but *HGF* is not expressed in the mf20^{+} muscle fibres) (figure 3.8I, J) and lies medial to the developing ventral rectus/medial rectus (figure 3.8G, H).

The observed expression patterns are in agreement with Caton et al (2000), who reported *HGF* expression in two mesenchymal stripes ventral and dorsal to the eye at HH stage 21. The technique of performing *in situ* hybridisation on cryosections with concurrent immunohistochemistry to identify muscle and nerves, which was employed here, enabled a greater resolution of these regions of *HGF* expression in relation to the position of extraocular muscles and the surrounding neural crest mesenchyme. Caton et al (2000) attributed these regions of *HGF* expression to two extraocular muscles, we can clarify that the expression is largely confined to the neural crest mesenchyme with some expression in the dorsal oblique muscle, but not in the ventral extraocular muscles, at least not in the fibres that have activated the expression of mf20. It is also possible that expression within the muscles has been downregulated by HH stage 26. Either way, this expression pattern is nonetheless consistent with the hypothesis of HGF acting as an attractant for oculomotor and trochlear axons. It is expressed both in the target muscle and along the trajectory of trochlear axons. It is also expressed in the region along the

latter part of the oculomotor trajectory, between the ciliary ganglion and the ventral oblique muscle. Oculomotor axons extend ventrally from the midbrain to the ciliary ganglion where the axons of the parasympathetic component of the nerve synapse, and the somatic motor axons turn rostrally towards the ventral oblique (see figure 1.1). It is possible that HGF expressed in this ventral mesenchymal region induces the rostral tum of the oculomotor axons, although HGF may also act as a permissive or a growth-promoting cue for oculomotor axons in the final part of their trajectory.

Other extraocular muscles, namely the dorsal rectus and the lateral rectus, do not express *HGF* at HH stage 26 (figure 3.8C, D, G, H). However, axon guidance to the lateral rectus occurs at an earlier stage (HH st19) and branching into the dorsal rectus occurs at HH stage 28. To exclude the involvement of HGF in abducens axon guidance to the lateral rectus or in branching of the oculomotor nerve into the dorsal rectus, expression of *HGF* needs to be analysed at those stages.

3.2.3 Expression of *SDF-1* and *CXCR4*

CXCR4 is the only known receptor for SDF-1, so in order for axons to be capable of responding to SDF-1 signalling, CXCR4 needs to be present on the growth cones. In the mouse spinal cord, SDF-CXCR4 signalling has been shown to play an important part in the ventral exit of spinal motor neurons. *CXCR4* expression is first detected in motor neurons at E9.5, concurrently with the activation of Islet-1, is then restricted to newly generated neurons at E10 and is completely downregulated by E10.5, by which point the motor axons have reached the base of the limb (Lieberam et al 2005). In the chick, oculomotor neurons are generated between HH stages 14-25; their axons exit the neural tube starting from HH stage 16 and make initial contacts with the extraocular muscle targets from HH stage 27. Trochlear neurons are generated between HH stages 17-25, their axons exit the neural tube form HH stage 21 onwards and make initial contacts with the dorsal oblique muscle at HH stage 25.

Expression of the receptor in motor neurons was investigated using *in situ* hybridisation with a *CXCR4* probe in combination with immunohistochemistry with antibodies recognising Islet1/2 to identify the position of the motor neuron nuclei, and neurofilament heavy chain to identify axon tracts. Expression was examined at HH stages 18 (when oculomotor neurons are emerging into the periphery), HH stage 21 (when trochlear axons are exiting the neural tube) and HH stage 25 (when trochlear axons have made initial contacts with their target muscle, and oculomotor axons have reached the ciliary ganglion and are growing towards the ventral oblique muscle). At HH stage 18 many, but not all, oculomotor neurons express *CXCR4*. The *CXCR4*$^{+}$ and *CXCR4*$^{-}$ populations are not segregated but rather intermingle (figure 3.9A, B, C). This situation is maintained at HH stage 21 (figure 3.9D, E, F), where the *CXCR4* expressing motor neurons intermingle with the *CXCR4*$^{-}$ population. The expression of the receptor is notably stronger in the progenitor cells of the ventricular zone than in the islet^{+} differentiated motor neurons at both these stages. It must be noted that the method used in the *in situ* hybridisation experiments involved a deposition of a large quantity of precipitate particularly in areas of high expression. Therefore the co-localisation of islet and neurofilament expression (as identified by immunohistochemistry) with CXCR4 expression needs to be interpreted with caution because the precipitate could be masking the antigen, therefore making areas of high *CXCR4* expression appear to be islet or neurofilament negative, which is not necessarily the case. Expression of *CXCR4* is maintained in oculomotor neurons at HH stage 25 (figure 3.9G, H). In the trochlear motor neurons *CXCR4* is expressed at HH stage 18 (when their axons are extending dorsally within the neural tube), but is downregulated by HH stage 21 with the expression almost exclusively confined to the ventricular zone and the floor plate (<10% of islet^{+} cells express CXCR4) (figure 3.9I-N). This raises the question of whether SDF-1 signalling is relevant for the latter part of the trochlear axon pathfinding, although the expression of the receptor at the protein level probably persists some time after it is extinguished at the mRNA level. Figure 3.9i shows the same sections as figure 3.9 at higher magnification to more clearly illustrate the overlap between *CXCR4* and islet expression.

SDF-1 expression is ubiquitous in the head mesenchyme at HH stage 18, particularly at rostral levels and in regions flanking the forebrain (figure 3.10A-C). This expression becomes progressively restricted: at HH stage 21 mesenchymal regions directly adjacent to the neuroepithelium, which go on to form the brain-forming meninges, maintain high levels of expression, but elsewhere it is downregulated (figure 3.10D-F); and at HH stage 26/7 expression is confined to smaller mesenchymal regions notably one between the rostral edge of the eye and the telencephalon and a region of periocular mesenchyme flanking the dorsal edge of the eye (figure 3.10G-I). Interestingly, high levels of *SDF-1* expression are seen in the region adjacent to the oculomotor nerve's exit point from the neural tube at HH stage 18 (figure 3.11A,B), and this is maintained at HH stage 21 (figure 3.11C,D). In fact, at this stage the expression appears to be enriched at the exact point where oculomotor axons are exiting into the periphery. By HH stage 26/7 the expression of *SDF-1* in this region has been turned off (figure 3.11E, F). Therefore, the expression of *SDF-1* in the mesenchyme adjoining the oculomotor nucleus correlates exactly with the time when the majority of oculomotor axons are exiting into the periphery. The mesenchyme overlying the roof plate at the midbrain-hindbrain boundary level (the point where trochlear axons exit the neural tube) shows weak expression at HH stage 18 (about 12hrs before the axons begin to emerge), has increased levels of expression at HH stage 21 (when the axons have started to exit) and maintains expression at HH stage 26/7, albeit at reduced levels, by which point most trochlear axons have left the neural tube, and the pioneers have made contact with the dorsal oblique (fig 3.11G-L).

At HH stage 26/7 *SDF-1* expression is confined to more restricted regions, such as an area of mesenchyme between the antero-dorsal part of the eye and the telencephalon which surrounds the dorsal oblique (figure 3.10H, figure 3.12A, B). *SDF-1* expression is also activated at this stage in two extraocular muscles: the ventral oblique muscle, in a region confined to the centre of the muscle (figure 3.12I, J), and in a similar region in the centre of the dorsal rectus muscle (figure 3.12C, D). Oculomotor axons make contact with the ventral oblique muscle at HH stage 27 and send branches into the dorsal rectus from HH stage 28. The expression of *SDF-1* presages these events raising the possibility

that SDF-1 acts as a signal to promote the innervation of these muscles. There is no *SDF-1* expression in the lateral rectus or the ventral rectus/medial rectus at this stage (figure 3.12E-H). Therefore, if SDF-1 promotes branch formation into the dorsal rectus, oculomotor axon innervation of ventral rectus and medial rectus is activated by another mechanism.

3.3 DISCUSSION

3.3.1 Semaphorins

The starting hypothesis in relation to the semaphorins was that they are likely to function as repellents. However, the expression patterns of *Sema3A* and *Sema3C* at HH stage 19, when abducens axons are making initial contacts with their target muscle (Wahl et al 1994), suggest a different possibility in relation to abducens nerve pathfinding. The expression of the two ligands is largely complementary. *Sema3C* is expressed at high levels in the target muscle of the abducens and at low levels along the trajectory of the nerve. *Sema3A* on the other hand is expressed around the trajectory of the abducens nerve in a graded fashion, with strong expression in the lateral mesoderm which fades nearer the pathway of the nerve; and strong expression in the notochord medially to the course of the nerve. *Sema3A* expression is also found around the developing lateral rectus muscle. This suggests that Sema3A may act as a repellent for abducens axons preventing their inappropriate entry into regions adjacent to their normal trajectory, and/or overshooting their target. Indeed, this is consistent with Varela-Echavarria et al (1997) findings that abducens axonal growth is inhibited by Sema3A *in vitro*. The generally high levels of *Sema3A* expression in the cranial mesenchyme could argue against a proposed role for Sema3A as a repellent as it could diffuse throughout the head and create a hostile environment for growing axons; however, it has been questioned whether Sema3A is capable of long distance diffusion because its highly basic carboxy-terminal tail would render it liable to adhesion to cell-surfaces and the extracellular

matrix (Raper 2000).Thus the lack of Sema3A expression along the trajectory of the abducens nerve might make that territory a permissive growth substrate for abducens axons.

Sema3C, on the other hand, could be hypothesized to act as an attractant for abducens axons, promoting growth towards their target, based on its expression in the target muscle and along the trajectory at HH stage 19. The combinatorial expression pattern of *Sema3A* and *Sema3C* in the region of the lateral rectus persists until HH stage 27/8 when the muscle's precise position can be determined using immunostaining. *Sema3C* is expressed in the muscle, albeit restricted to the lateral part and the abducens nerve is observed turning towards this area of *Sema3C* expression. *Sema3A* on the other hand is expressed by the cells surrounding the muscle, consistent with the idea that it serves to prevent overshooting by abducens axons. By this stage the pioneer axons have already innervated the lateral rectus muscle, but semaphorin signalling may still influence the pathfinding of the later cohorts of abducens axons. The effect of the semaphorins *in vitro* on abducens outgrowth will be investigated in the next chapter. It must be noted that only neuropilin-1 (NPN-1) is expressed on abducens neurons (Chilton and Guthrie 2003), which argues against Sema3A and Sema3C having different effects on abducens axons, since they would need to be transduced into the cell by the same receptor. Another important feature of the semaphorins' expression patterns at this stage is that both *Sema3A* and *Sema3C* are expressed at high levels in the abducens neurons themselves. If the ligands are secreted at the growth cone, it may reduce the axons' sensitivity to them or indeed render them entirely insensitive, in a similar manner to ephrin-As that, when co-expressed with EphA receptors, reduce the sensitivity of those receptors to exogenous ephrin-As (Hornberger et al 1999).

The disruption of oculomotor and trochlear nerves in *Sema3F* and *NPN-2* mouse mutants (Giger et al 2000, Chen et al 2000, Sahay et al 2003) demonstrates the importance of Sema3F signalling for extraocular muscle innervation *in vivo*. The analysis of Sema3F expression was carried out to further elucidate the precise role Sema3F plays in oculomotor axon guidance and to identify further possible roles for

Sema3F in trochlear axon guidance. Sema3F has already been hypothesized to play an important part in the guidance of trochlear axons within the neural tube by Giger et al (2000) who proposed that Sema3F forms a surround corridor of repulsion around the trochlear exit point, which accounts for the failure of trochlear axons to exit the neural tube in the *NPN-2* mutant; and by Watanabe et al (2004) who reported trochlear axons invading the midbrain, when soluble NPN-2 was used to sequester Sema3F expressed in the caudal midbrain. A possible role for Sema3F in the peripheral guidance of trochlear axons was hypothesised in addition to its function within the neural tube. However, at HH stages 25/6 and 27/8, when innervation of the muscles is taking place, there is little expression of *Sema3F* in the periphery and none in the proximity of the trochlear nerve's trajectory, arguing against this ligand playing a major role in the later stages of trochlear axon guidance. The lack of Sema3F expression in the vicinity of the oculomotor nerve was a surprise, given the defasciculation of the nerve reported in mouse mutants for *Sema3F* and *NPN2* (Giger et al 2000, Chen et al 2000, Sahay et al 2003). It is possible that the fasciculation of the oculomotor nerve is maintained by Sema3D, which has been shown to be expressed in the periocular mesenchyme (Chilton and Guthrie 2003), or the discrepancy could be a result of species difference between mouse and chick. Sema3F could play a part in the latter stages of the pathfinding of oculomotor axons, however, since it is expressed in the mesenchyme adjacent to the optic nerve exit point from the retina, which lies dorsal to the developing ventral rectus/medial rectus and in between the developing dorsal rectus and ventral oblique. The oculomotor nerve takes a course ventral to these muscles, sending branches dorsally between HH stages 28-31 to innervate these targets. The expression of *Sema3F* in this region could prevent oculomotor axons following a more dorsal trajectory, if it is acting as a repellent for this population of axons.

Since oculomotor and trochlear neurons express both *NPN-1* and *NPN-2*, their axons may be sensitive to the action of Sema3A and Sema3C as well as Sema3F. *Sema3A* expression in particular surrounds each extraocular muscle between HH stages 26 and 28, with particularly high levels of expression found in the mesenchyme surrounding the ventral oblique, dorsal to the dorsal rectus and anterior to the dorsal oblique. Thus, if

Sema3A is repulsive or growth-inhibitory for trochlear and oculomotor axons, it may be expressed in these regions to prevent axons overshooting their targets. *Sema3C* expression is quite weak in the oculomotor target muscles but it can be seen in cells at the interface between developing muscle and the surrounding crest-derived mesenchyme of the ventral rectus/medial rectus, ventral oblique and dorsal oblique. Therefore, if repulsive to oculomotor axons it may act to prevent target overshooting also. *Sema3C* is also expressed around the dorsal oblique, where it may prevent trochlear axons overshooting, and in a stream of cells between the forebrain and the retina, parallel to the course of the trochlear nerve where it may act as a repulsive barrier to prevent trochlear axons from straying off course.

3.3.2 HGF, SDF-1 and CXCR4

HGF has been hypothesized as a possible attractant for oculomotor and trochlear axons. The expression pattern identified here is consistent with this hypothesis. The trochlear nerve, once it has exited the neuroepithelium at the dorsal surface, crosses the midline, extends around the neural tube at the level of the midbrain-hindbrain boundary, then grows towards the dorso-posterior edge of the eye and the extends parallel to the dorsal edge of the eye, dipping ventrally prior to make contact with the dorsal oblique. At HH stage 26, just prior to trochlear axons making first contacts with the target, *HGF* is expressed in a stripe at the level of and parallel to the dorsal edge of the eye, corresponding to the path of the trochlear nerve, which widens into a region of *HGF* expression in the mesenchyme surrounding the anterodorsal part of the eye, which overlaps with the dorsal oblique primordium. Thus it is feasible that HGF functions as an attractant for trochlear axons. There is no *HGF* expression in the region of the initial oculomotor projection, from the midbrain to the ciliary ganglion; however, *HGF* is expressed in a region of mesenchyme around the ventral edge of the eye that encompasses the latter part of the oculomotor projection, borders the developing ventral rectus/medial rectus primordium and surrounds the developing ventral oblique. At HH stage 26, oculomotor axons are extending through this territory towards the ventral

oblique. Therefore, this expression pattern is consistent with the possibility of HGF acting as an attractant for oculomotor axons, also.

The expression of *CXCR4* is maintained in oculomotor neurons over the period of axonal growth towards their targets; therefore SDF-1 signalling may be relevant at all stages of axon guidance. In the case of the trochlear neurons *CXCR4* expression is on at HH stage 18 (not long after trochlear neurons have started to differentiate) but is turned off in most neurons by HH stage 21, when axons begin to exit the neural tube. It seems likely that SDF-CXCR4 signalling can only play a part in the early stages of trochlear axon guidance, as the axons extend dorsally through the neuroepithelium and exit through the roof plate. *SDF-1* is expressed in the region of mesenchyme surrounding the dorsal oblique, and therefore may be hypothesized to act as a guidance signal for trochlear axons, but only if the CXCR4 protein persists on the trochlear growth cones for the ~36hrs which elapse between the downregulation of *CXCR4* expression and trochlear axons making contact with the dorsal oblique. It is more likely that SDF-1 plays a part in directing trochlear axons' exit from the neural tube. Lieberam et al (2005) describe how ventrally-projecting spinal and hindbrain motor neurons express *CXCR4* transiently prior to axon outgrowth, whilst *SDF-1* is expressed in the mesenchyme overlying their ventral exit point; in mice mutant for either the *CXCR4* or the *SDF-1* gene some these axons fail to exit ventrally and project dorsally instead. It may be that a similar but topographically reversed mechanism is occurring in the case of the trochlear axons: *CXCR4* is expressed transiently in the motor neurons a few hours prior to them exiting through the roof plate; in the meantime *SDF-1* is already weakly expressed in the mesenchyme overlying the roof plate at HH stage 18, this expression is upregulated at HH stage 21 (when trochlear axons are beginning to exit) and is maintained at a lower level up to HH stage 26/7, when all the axons have exited the neural tube. Thus, *SDF-1* expression may be necessary to direct trochlear axons dorsally and/or enable them to exit the neural tube.

SDF-1 is also expressed in the mesenchyme adjoining the oculomotor nerve exit point. This expression is found throughout the rostral head mesenchyme at HH stage 18, is

maintained at HH stage 21 and in fact appears to be concentrated at points where oculomotor axons are emerging into the periphery. By HH stage 26/7 the expression of *SDF-1* around the oculomotor exit point has been downregulated. This expression pattern is consistent with the hypothesis that SDF-1 facilitates the exit of oculomotor axons from the neural tube. In addition, at HH stage 26/7 (which is just prior to oculomotor axons contacting the ventral oblique and sending branches into the dorsal rectus) *SDF-1* is expressed in dorsal rectus and ventral oblique muscles in a highly localized fashion, raising the possibility that it acts as an attractive signal for oculomotor axons, directing them to these muscles.

Another interesting feature of the expression patterns identified is the co-expression of some of these ligands in certain regions. This raises the possibility that some of these ligands act cooperatively to influence the outcome of axon pathfinding. For example, the region surrounding the dorsal oblique expresses *SDF-1*, *HGF*, *Sema3C* and *Sema3A* at the stage when trochlear axons are making contacts with the dorsal oblique muscle. *SDF-1* and *Sema3F* are co-expressed in the region dorsal to the ventral rectus/medial rectus. *HGF* and Sema3A are co-expressed in the region surrounding the ventral oblique, whilst *SDF-1* is expressed within that muscle, at the stage when oculomotor axons are contacting the muscle. The effects of some of the combinations of ligands on oculomotor and trochlear outgrowth *in vitro* will be tested in the next chapter.

3.3.3 Conclusions

In summary, the expression results are consistent with some aspects of the hypothesis stated at the beginning of this chapter, inconsistent with other aspects, and also highlight some new possibilities. The strong expression of *Sema3C* in the lateral rectus is consistent with the idea that it acts to prevent LR innervation by oculomotor axons if these axons are sensitive to Sema3C-mediated repulsion. However, as this expression is present at early stages (before oculomotor axons have reached the region) it also raises the possibility that Sema3C may act as an attractant for abducens axons. With the exception of the lateral rectus innervation, the hypothesis that different semaphorins

function in target selection for different populations of axons seems less likely. *Sema3F* is not expressed in any of the extraocular muscles, and *Sema3A* and *Sema3C* are only expressed in cells at the margins of the muscles. The semaphorins may, however, function to prevent oculomotor and trochlear axons from entering inappropriate territory, since *Sema3A* and *Sema3C* are expressed around the extraocular muscle targets they may be acting to prevent overshooting of the target and Sema3F by being secreted from a region dorsal to the developing ventral rectus/medial rectus may be directing oculomotor axons along a more ventral trajectory.

The idea that HGF and SDF-1 function as attractants for oculomotor and trochlear axons is also plausible. In particular *HGF* is expressed along the trajectory of the trochlear nerve and in the target; it is also expressed along the latter part of the oculomotor trajectory and the extraocular muscles it innervates (with the exception of the dorsal rectus). Even more intriguingly *SDF-1* expression is highly localised in the centre of two of the oculomotor targets (dorsal rectus and ventral oblique) at a stage just prior to these muscles being contacted by oculomotor axons. *SDF-1* is also expressed around the dorsal oblique, but is less likely to be involved in directing the latter stages of trochlear axon guidance because the expression of the receptor is extinguished at HH stage 21. It may, however, play a part in guiding trochlear axons out of the neural tube. SDF-1 may also perform this role for oculomotor axons as it is expressed in the mesenchyme underlying the oculomotor exit point at the appropriate stage.

However, the expression data merely demonstrates the *possibility* that a guidance cue is involved in a particular step of the innervation process because it is present in the right place at the right time. In order to further substantiate the hypotheses stated at the beginning of this chapter it is necessary to examine the effects that these guidance cues have on the behaviour of these populations *in vitro*. This will be addressed in the next chapter.

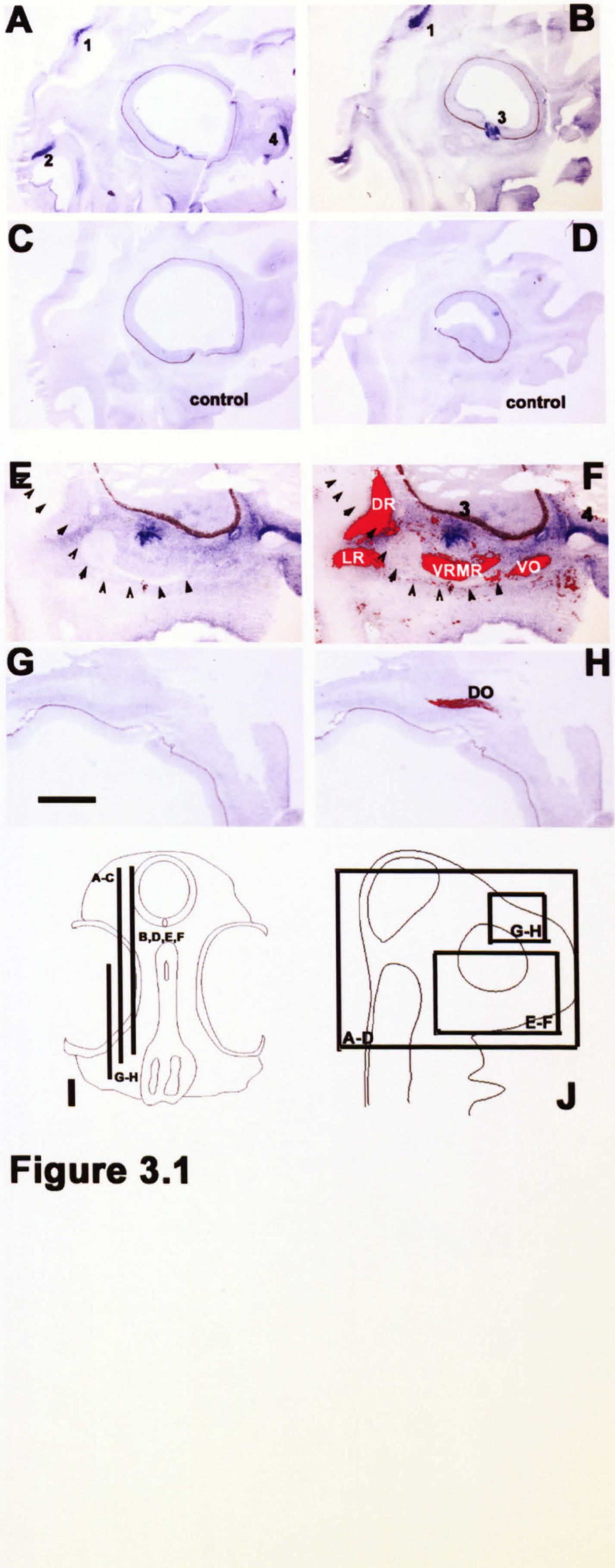
A
1
2
4
control
B
1
3
C
control
D
E
F
DR
3
4
LR
VRMR
VO
G
H
DO
A-C
B,D,E,F
G-H
I
G-H
E-F
A-D
J

Figure 3.1

Figure 3.1

Expression of *Sema3F* on chick parasagittal sections at HH stage 28

Four regions of *Sema3F* expression were identified (marked on the figure with numbers 1-4, 1 – *Sema3F* expression in the caudal midbrain, 2 – *Sema3F* expression in the dorsal part of rhombomere1, 3 – *Sema3F* expression in the periocular mesenchyme adjacent to the optic nerve exit point, 4 – *Sema3F* expression in the mesoderm dorsal to the nasal cavity)

A – Lateral section through the head
B – More medial section through the head.
C, D – Control sections (hybridized with sense probe) at positions equivalent to A and B
E, F – A higher power view of the region containing the oculomotor target muscles and lateral rectus. E shows *Sema3F* expression, F is the same image superimposed with mf20 staining (in red), which identifies muscle positions. Black arrowheads point to the course of the oculomotor nerve.
G, H – A higher power view of the region containing the dorsal oblique. G shows *Sema3F* expression, H is the same image with mf20 staining superimposed (in red).
I, J – Schematic sketches of the chick head in transverse and sagittal section showing the positions of the sections shown in panels A-H.

Abbreviations: DO – dorsal oblique, DR – dorsal rectus, VRMR – ventral rectus/medial rectus, VO – ventral oblique, LR – lateral rectus

Scale bar (G) – 640μm (A-D)
360μm (E, F)
180μm (G, H)

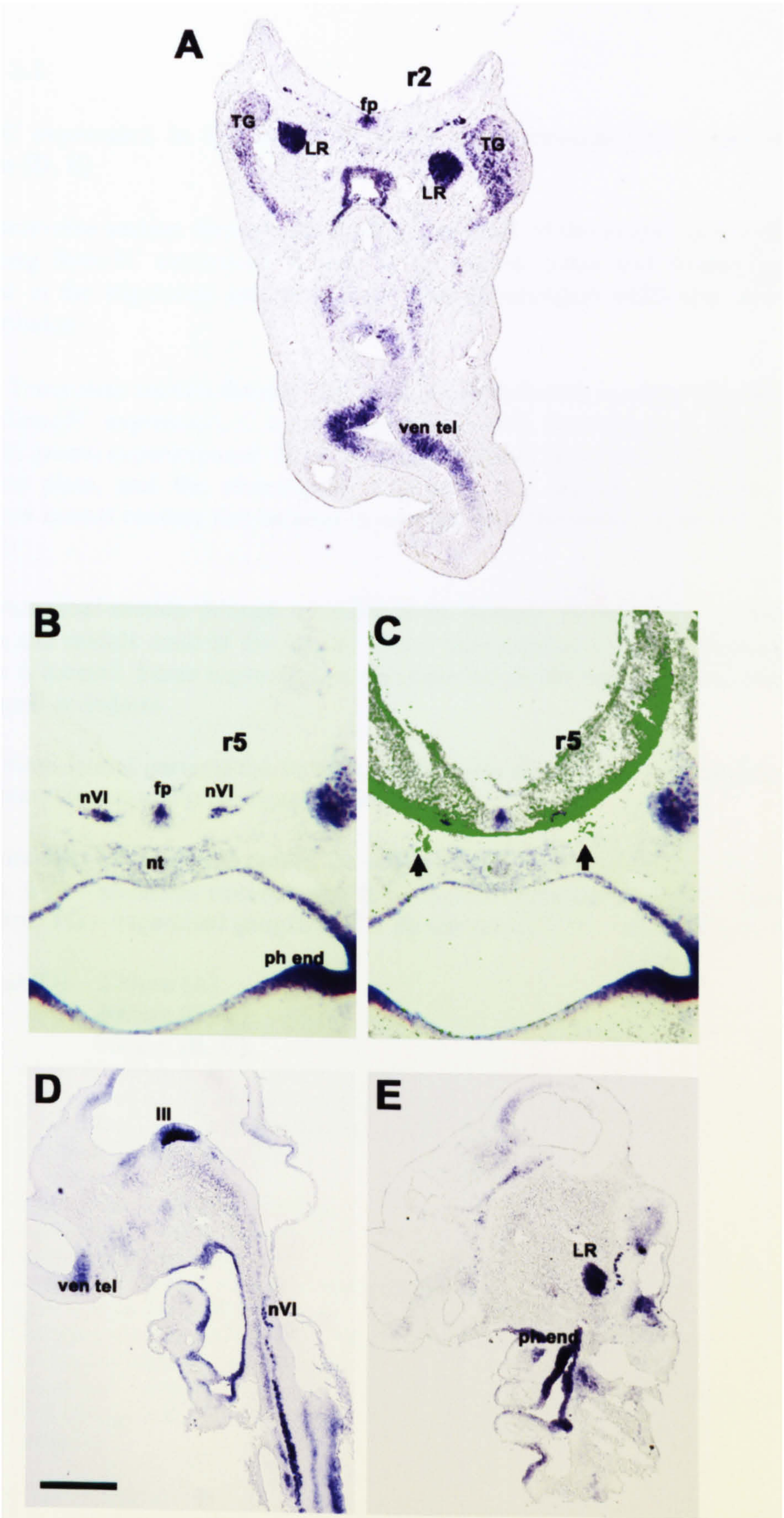
A
r2
fp
TG
LR
TG
LR
ven tel
B
r5
nVI
fp
nVI
nt
ph end
C
r5
D
III
ven tel
nVI
E
LR
ph end

Figure 3.2

Figure 3.2

***Sema3C* expression in HH stage 19 chick on transverse (A-C) and parasagittal sections (D, E)**

A – Transverse section through the head at the level of the lateral rectus (rhombomere 2). Strong *Sema3C* expression is seen in the lateral rectus and weaker expression is detected in the trigeminal ganglion, floor plate, pharyngeal endoderm and the ventral telencephalon.

B, C – Transverse section through the level of the abducens nucleus (rhombomere 5). B shows *Sema3C* expression, C is the same image with neurofilament staining (showing axons, in green) superimposed. *Sema3C* is expressed at high levels in abducens neurons, the floor plate, and the pharyngeal endoderm; and weakly around the notochord. Abducens axonal rootlets can be seen to emerge from the neural tube in C (marked with arrows).

D – Parasagittal section through a medial level. *Sema3C* is expressed in the oculomotor nucleus and mantle zone of the caudal neural tube starting from r5 where the abducens nucleus is located. Some expression is also detected in the ventral telencephalon and the pharyngeal endoderm.

E – A more lateral parasagittal section. High levels of *Sema3C* expression are detected in the lateral rectus and pharyngeal endoderm.

Abbreviations: LR – lateral rectus, ph end – pharyngeal endoderm, nIII – oculomotor nucleus, nVI – abducens nucleus, ven tel – ventral telencephalon, fp – floor plate, nt – notochord, TG – trigeminal ganglion, r2 – rhombomere 2, r5 – rhombomere 5

Scale bar (D) – 270μm (A)
400μm (D, E)
160μm (B, C)

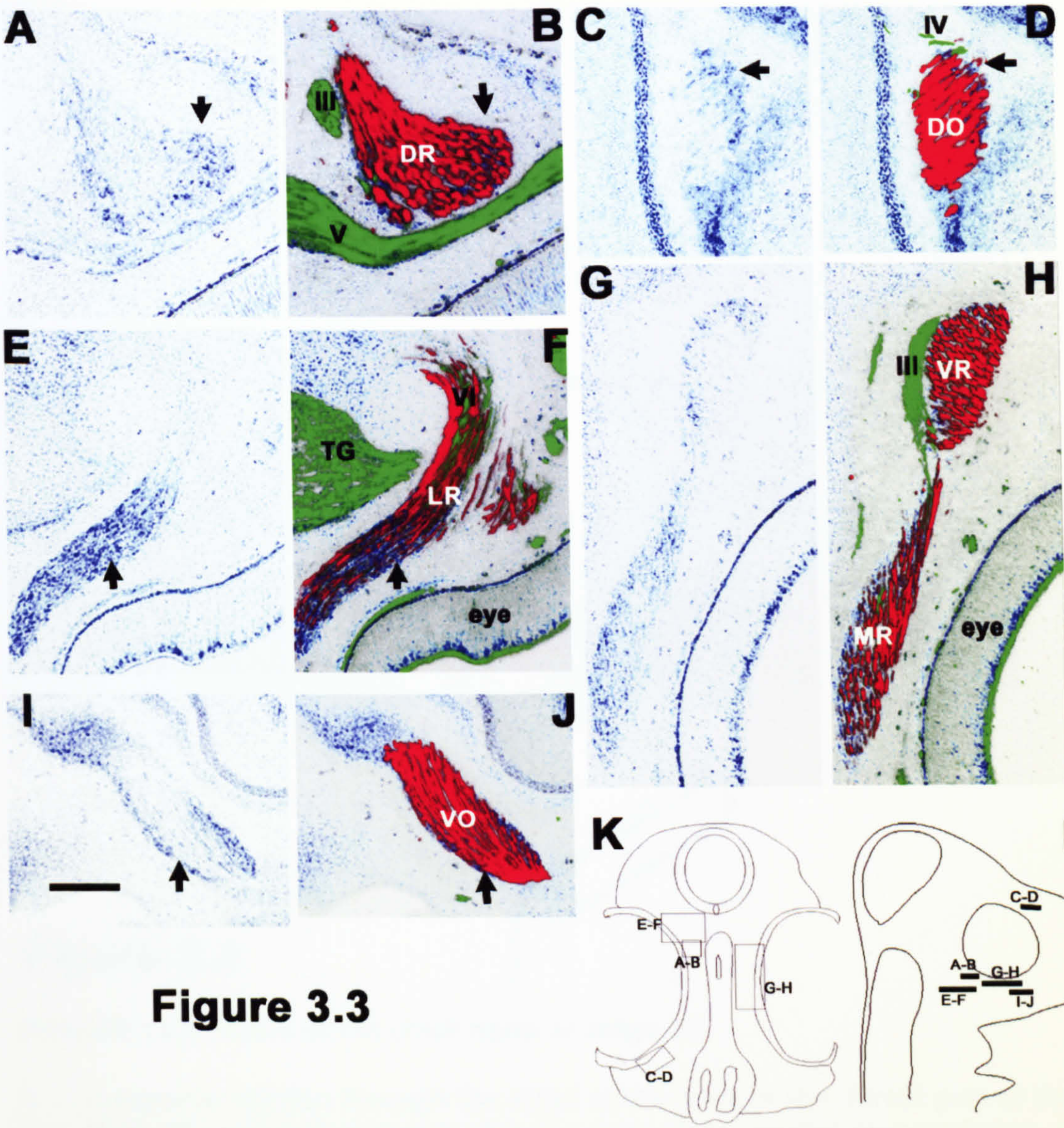

Figure 3.3

Sema3C expression in the extraocular muscles at stage 28 (transverse sections)

Panels on the left (A, C, E, G, I) show the expression of *Sema3C*, the corresponding panel on the right is the same image with immunostaining for mf20 to show muscle (red) and neurofilament to show axons (green) superimposed. Arrows point to an area of expression in both sets of panels to show a corresponding spot.

A, B – Region around the dorsal rectus.
C, D – Region around the dorsal oblique.
E, F – Region around the lateral rectus.
G, H – Region around the ventral rectus/medial rectus.
I, J – Region around the ventral oblique.
K,L – Schematic sketches of the chick head in transverse and sagittal section showing the positions of the sections shown in panels A-J.
Abbreviations: DO – dorsal oblique, DR – dorsal rectus, VRMR – ventral rectus/medial rectus, VO – ventral oblique, LR – lateral rectus, III – oculomotor nerve, V – trigeminal nerve, TG – trigeminal ganglion

Scale bar (J) – 80μm (C, D, I, J)
100μm (G,H)
130μm (A, B, E, F)

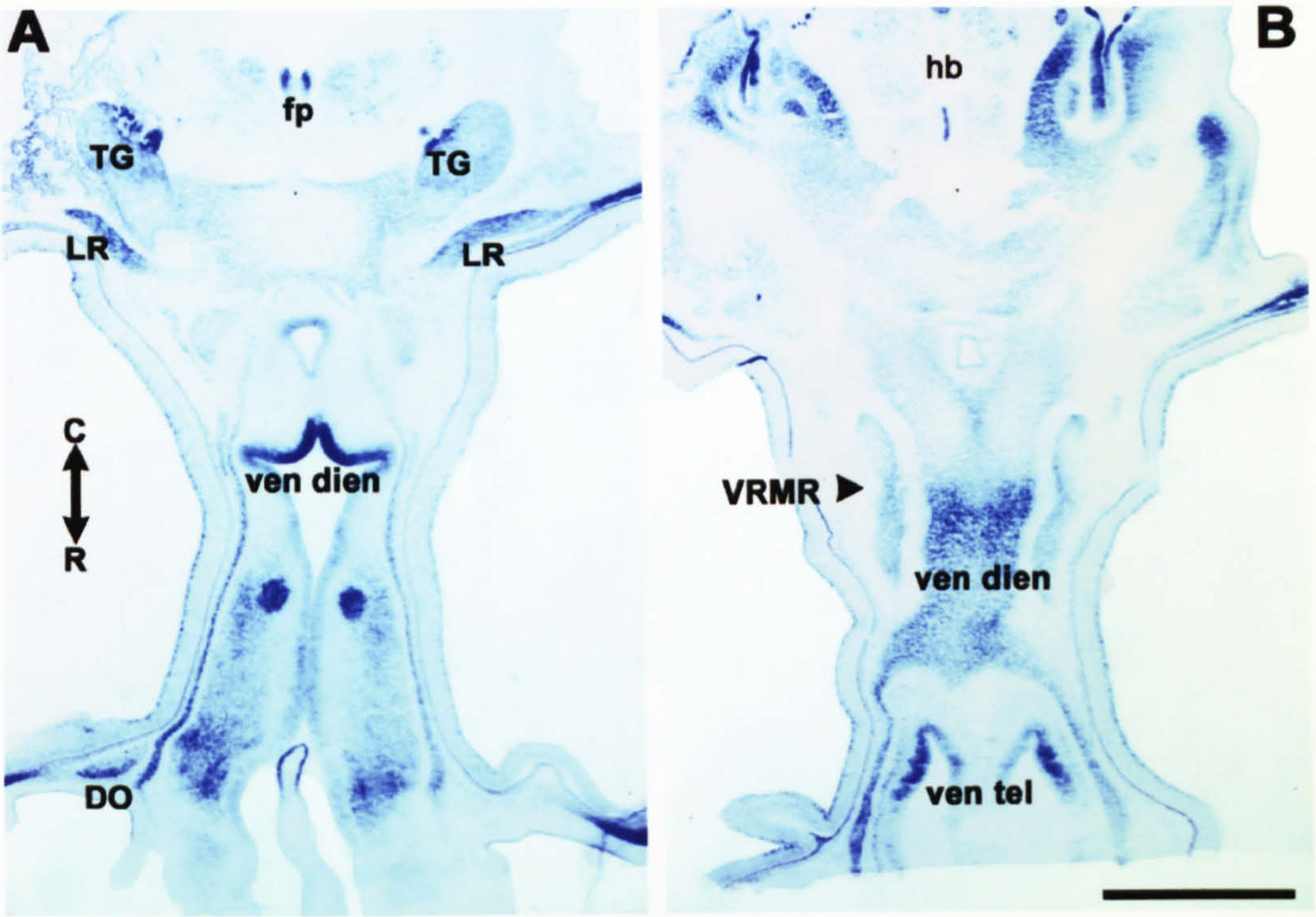

Figure 3.4

Sema3C expression in the chick head at stage 28

A – Transverse section through the head at the level of the dorsal part of the eye. *Sema3C* expression detected in the floor plate, ventral diencephalon, trigeminal ganglion, lateral rectus, dorsal oblique, a stream of mesenchymal cells between the retina and the forebrain and parts of the telencephalon
B – Transverse section through the head at the level of the ventral part of the eye. *Sema3C* expression detected in the ventral diencephalon, ventral telencephalon and mesodermal tissues laterally adjoining the hindbrain
C – Schematic sketch of the chick head in a sagittal orientation showing the position of sections A and B.

Abbreviations: LR – lateral rectus, TG – trigeminal ganglion, VRMR – ventral rectus/medial rectus, DO – dorsal oblique, fp – floor plate, hb – hindbrain, ven tel – ventral telencephalon, ven dien – ventral diencephalon, C –caudal, R – rostral.

Scale bar – 1mm

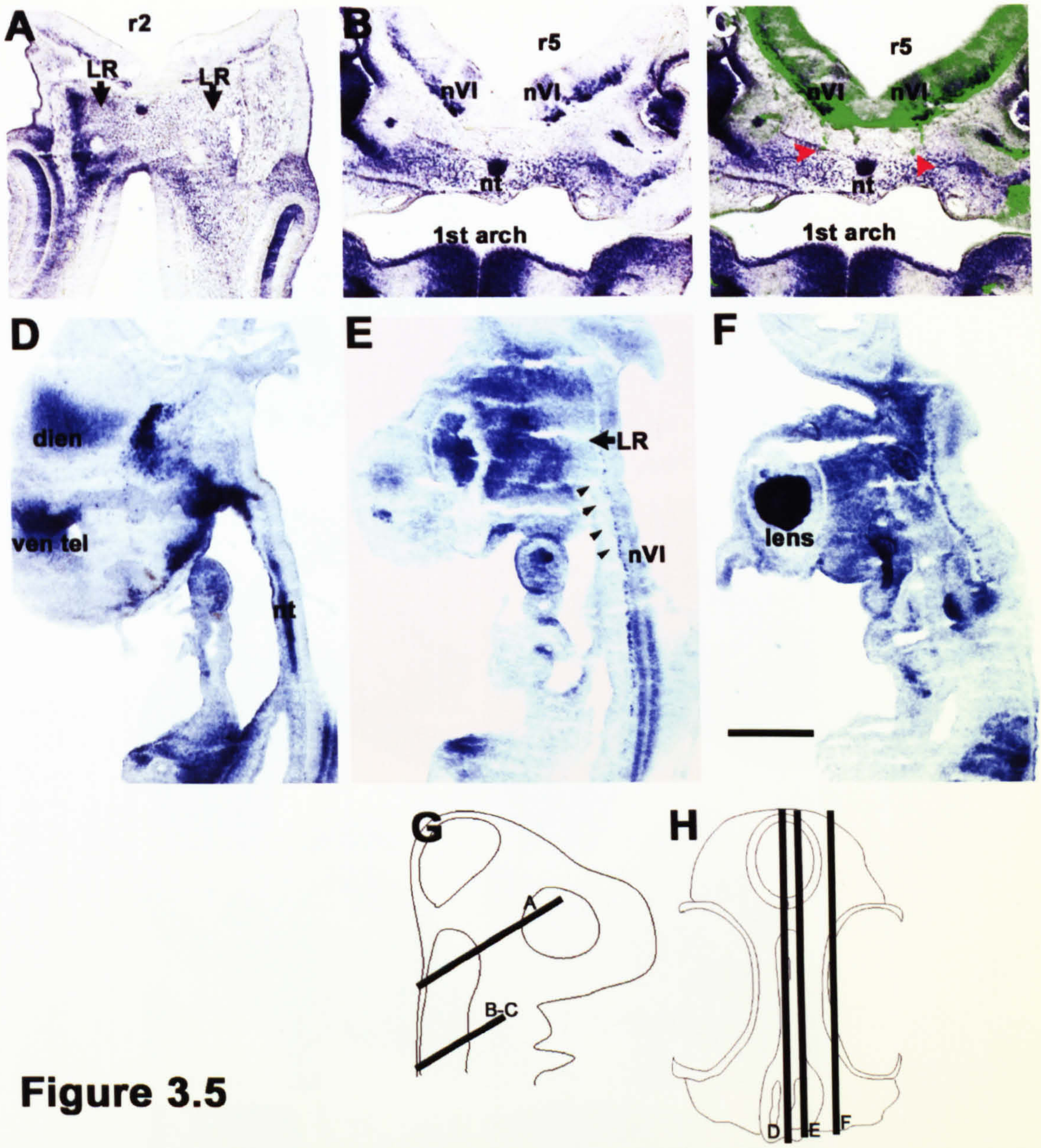

Figure 3.5

Sema3A expression at stage 19 in the chick on transverse and parasagittal sections

A – *Sema3A* expression at the level of the lateral rectus (transverse section).
B,C – *Sema3A* expression at the level of the abducens nucleus. Panel C shows the same image as B, with neurofilament staining superimposed (in green). Abducens neurons (nVI) show high levels of Sema3A expression, as does the notochord, lateral mesoderm and the medial part of first arch mesoderm. In C abducens axonal rootlets can be seen emerging into the mesoderm (indicated with red arrows).
D, E, F – *Sema3A* expression on parasagittal sections. Panel E shows a section through the level corresponding to the path of the abducens nerve. The trajectory of the nerve is indicated with black arrowheads. Panel D shows a more medial section, and panel F shows a more lateral section.
G, H – Schematic sketches of the chick head in transverse and sagittal section showing the positions of the sections shown in panels A-F.
Abbreviations: LR – lateral rectus, nVI – abducens nucleus, nt – notochord, ven tel –ventral telencephalon, ven dien - ventral diencephalon, r2 – rhombomere 2, r5 – rhombomere 5

Scale bar (F) - 400μm (A, D-F)
275μm (B, C)

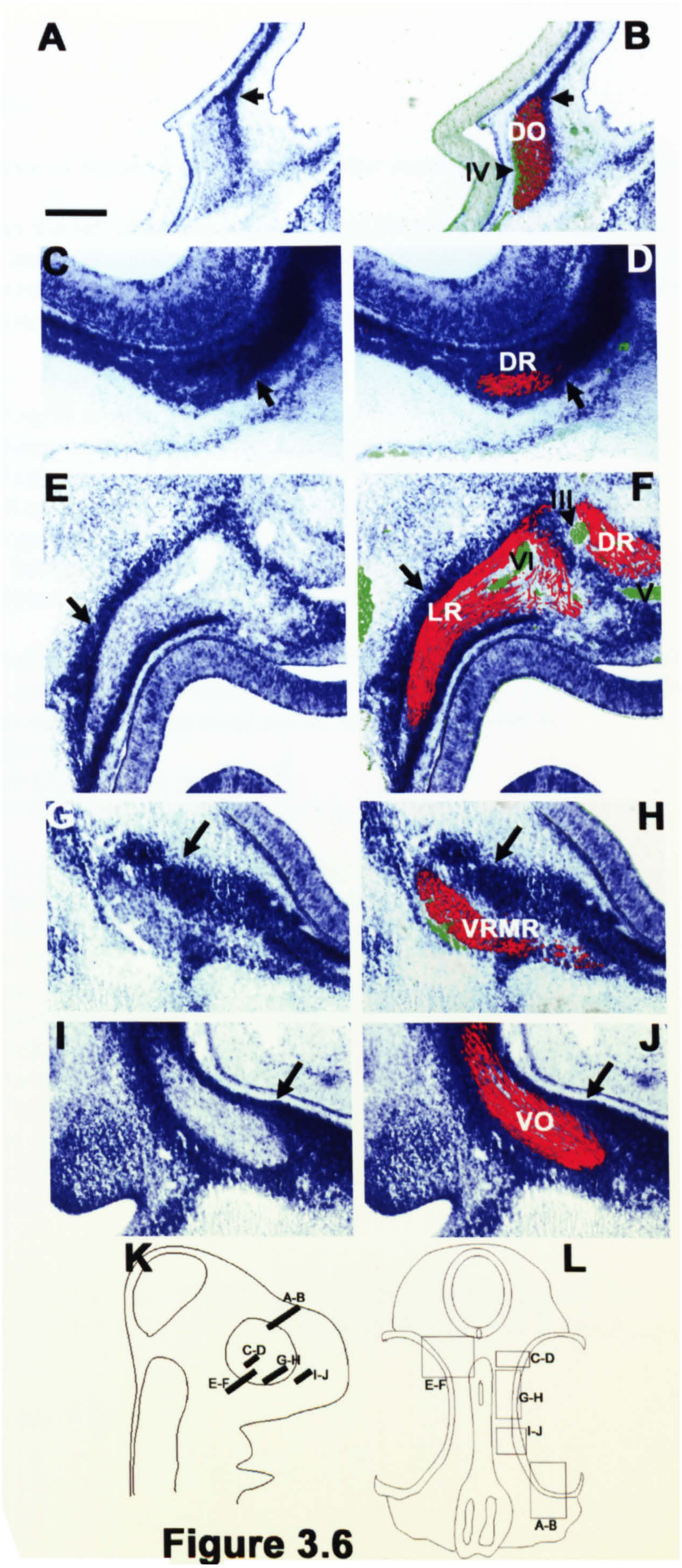
A
B
DO
IV
C
D
DR
E
F
III
DR
VI
V
LR
G
H
VRMR
I
J
VO
K
A-B
C-D
E-F
G-H
I-J
L
C-D
E-F
G-H
I-J
A-B

Figure 3.6

Figure 3.6

Expression of *Sema3A* in the extraocular muscles at stage 28 (transverse sections)

Panels on the left show the expression of *Sema3A*, the corresponding panel on the right is the same image with immunostaining for mf20 to show muscle (red) and neurofilament to show axons (green) superimposed. Arrows point to an area of expression in both sets of panels to show a corresponding spot.

A, B – Region around the dorsal oblique
C, D – Region around the dorsal rectus
E, F – Region around the lateral rectus
G, H – Region around the ventral rectus/medial rectus
I, J – Region around the ventral oblique
K, L – Schematic sketches of the chick head in transverse and sagittal section showing the positions of the sections shown in panels A-J.

Abbreviations: DO – dorsal oblique, DR – dorsal rectus, LR – lateral rectus, VRMR – ventral rectus/medial rectus, VO – ventral oblique, III – oculomotor nerve, IV – trochlear nerve, V – trigeminal nerve, VI – abducens nerve.

Scale bar (A) - 225μm (A, B, E-J)
185μm (C, D)

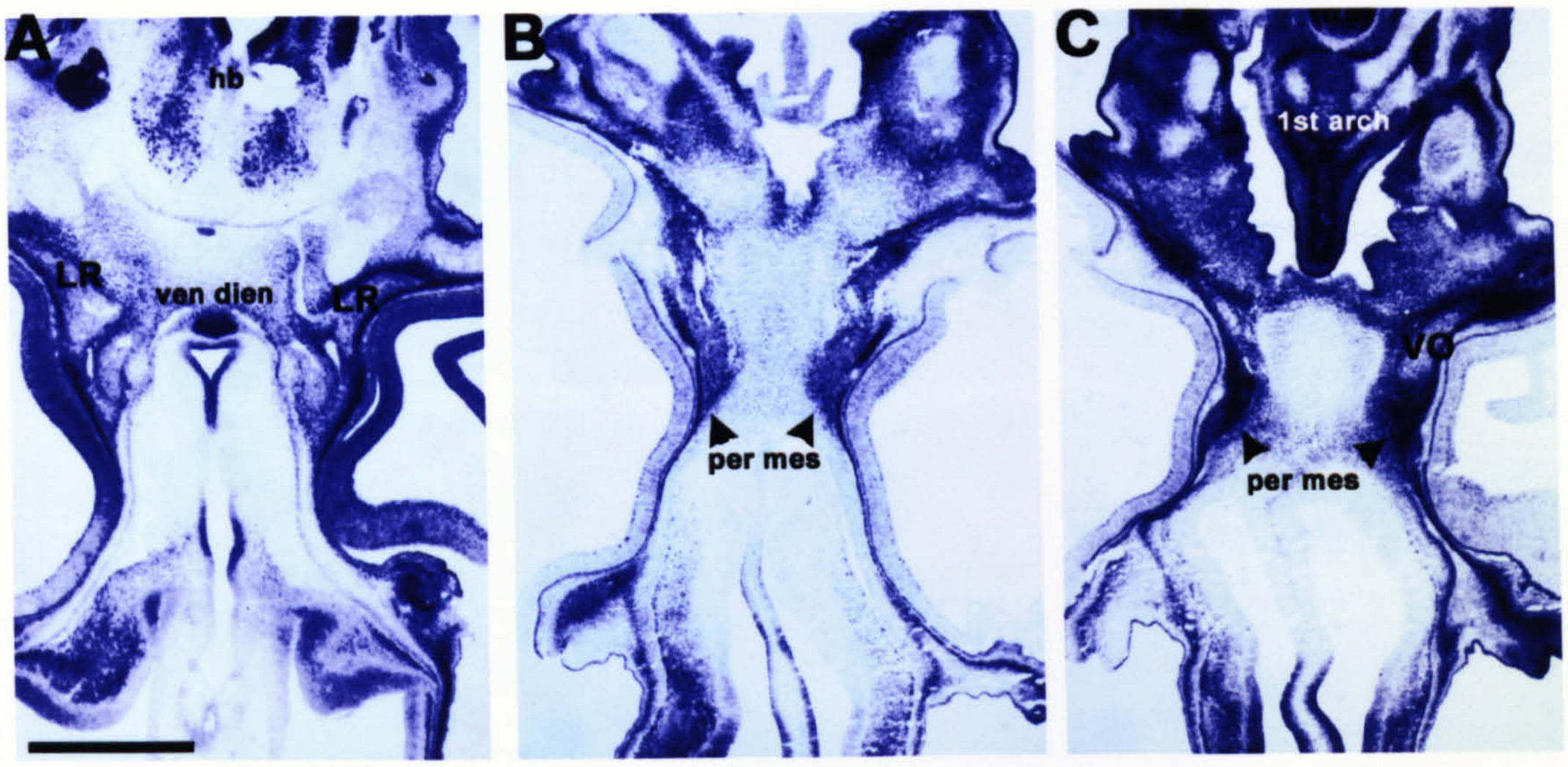

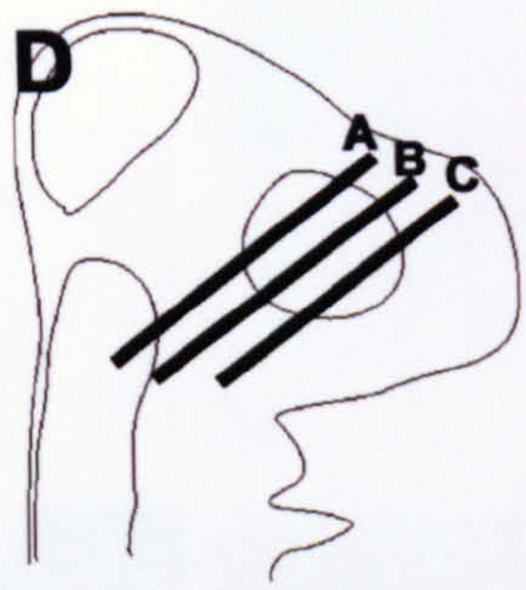

Figure 3.7

***Sema3A* expression in the chick head at stage 28**

A – Transverse section through the head at the level of the dorsal part of the eye. Particularly strong *Sema3A* expression detected in the ventricular layer of the hindbrain, pial layer of the diencephalon and parts of the periocular mesenchyme.
B – Transverse section through the head at the level of the middle part of the eye. *Sema3A* expression detected in the periocular mesenchyme and in the first arch.
C – Transverse section through the head at the level of the ventral part of the eye. Particularly strong *Sema3A* expression detected in the periocular mesenchyme and the first arch.
D - Schematic sketch of the chick head in a sagittal orientation showing the position of sections A-C.

Abbreviations: hb – hindbrain, LR – lateral rectus, ven dien – ventral diencephalon, per mes –periocular mesenchyme, VO – ventral oblique

Scale bar – 1mm

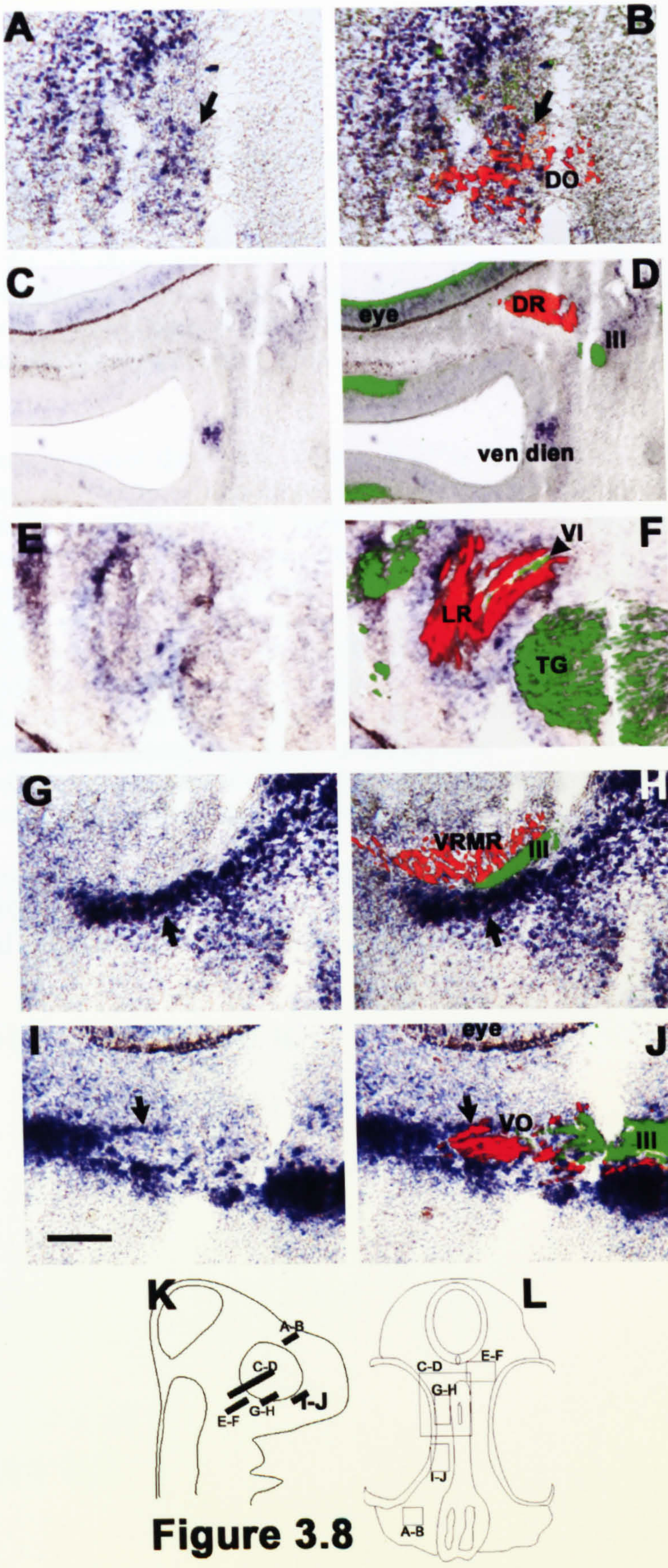
A
B
DO
C
D
eye
DR
III
ven dien
E
F
VI
LR
TG
G
H
VRMR
III
I
eye
J
VO
III
K
A-B
C-D
E-F
G-H
I-J
L
C-D
E-F
G-H
I-J
A-B

Figure 3.8

Figure 3.8

Expression of *HGF* in the extraocular muscles at HH stage 26/7 (transverse sections)

Panels on the left show the expression of *HGF*, the corresponding panel on the right is the same image with immunostaining for mf20 to show muscle (red) and neurofilament to show axons (green) superimposed. Arrows point to an area of expression in both sets of panels to show a corresponding spot.

A, B – Region around the dorsal oblique. *HGF* is expressed in the anterior part of the section with the region of expression encompassing part of the dorsal oblique muscle and adjoining mesenchyme. The posterio-ventral part of the dorsal oblique and the adjacent mesenchyme do not express *HGF*.
C, D – Region around the dorsal rectus
E, F – Region around the lateral rectus
G, H – Region around the ventral rectus/medial rectus. *HGF* is expressed in the mesenchyme flanking the muscle on the medial side
I, J – Region around the ventral oblique. *HGF* is expressed in the surrounding mesenchyme but is absent from $mf20^{+}$ muscle fibres.
K, L – Schematic sketches of the chick head in transverse and sagittal section showing the positions of the sections shown in panels A-J.

Abbreviations: DO – dorsal oblique, DR – dorsal rectus, VRMR – ventral rectus/medial rectus, VO – ventral oblique, LR – lateral rectus, III – oculomotor nerve, TG – trigeminal ganglion, ven dien – ventral diencephalon

Scale bar (A) - 240μm (A, B, G, H)
120μm (E, F)
100μm (C, D, I-L)

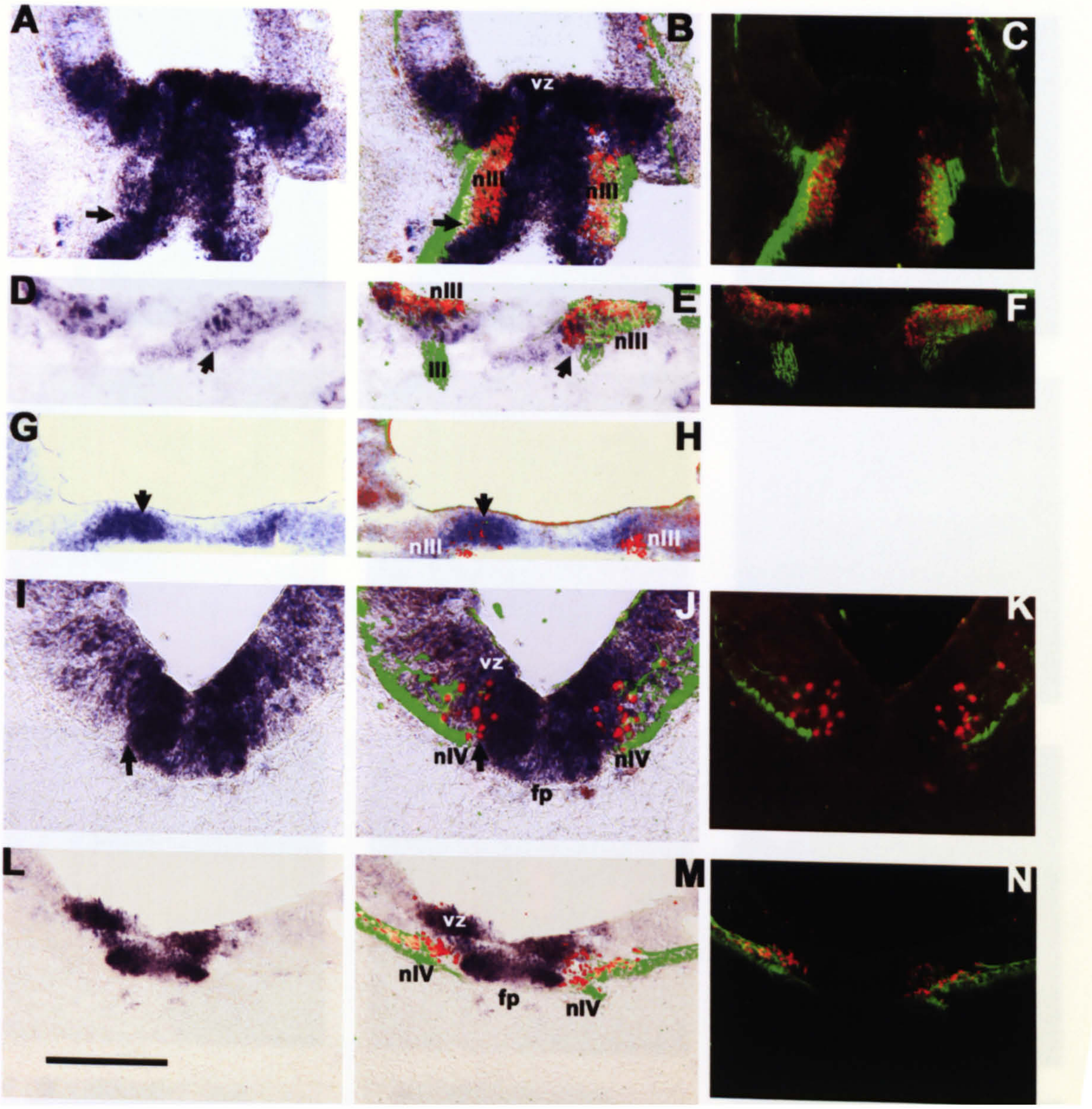
A
B
vz
nIII
nIII
C
D
nIII
E
nIII
III
F
G
H
nIII
nIII
I
J
vz
nIV
nIV
fp
K
L
M
vz
nIV
fp
nIV
N

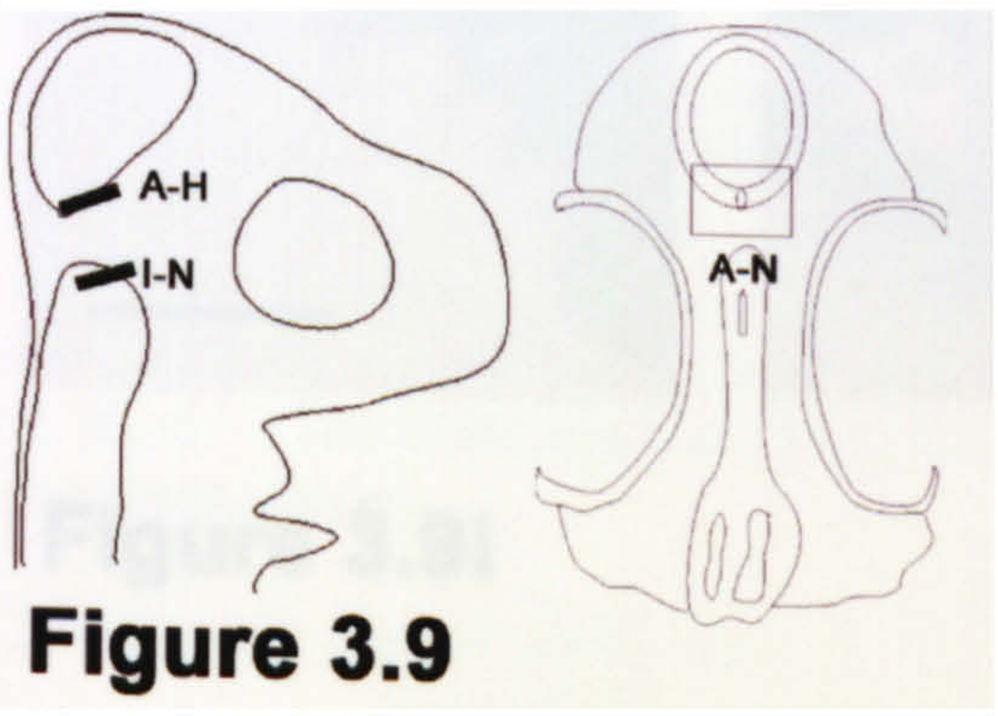
A-H
I-N
A-N

Figure 3.9

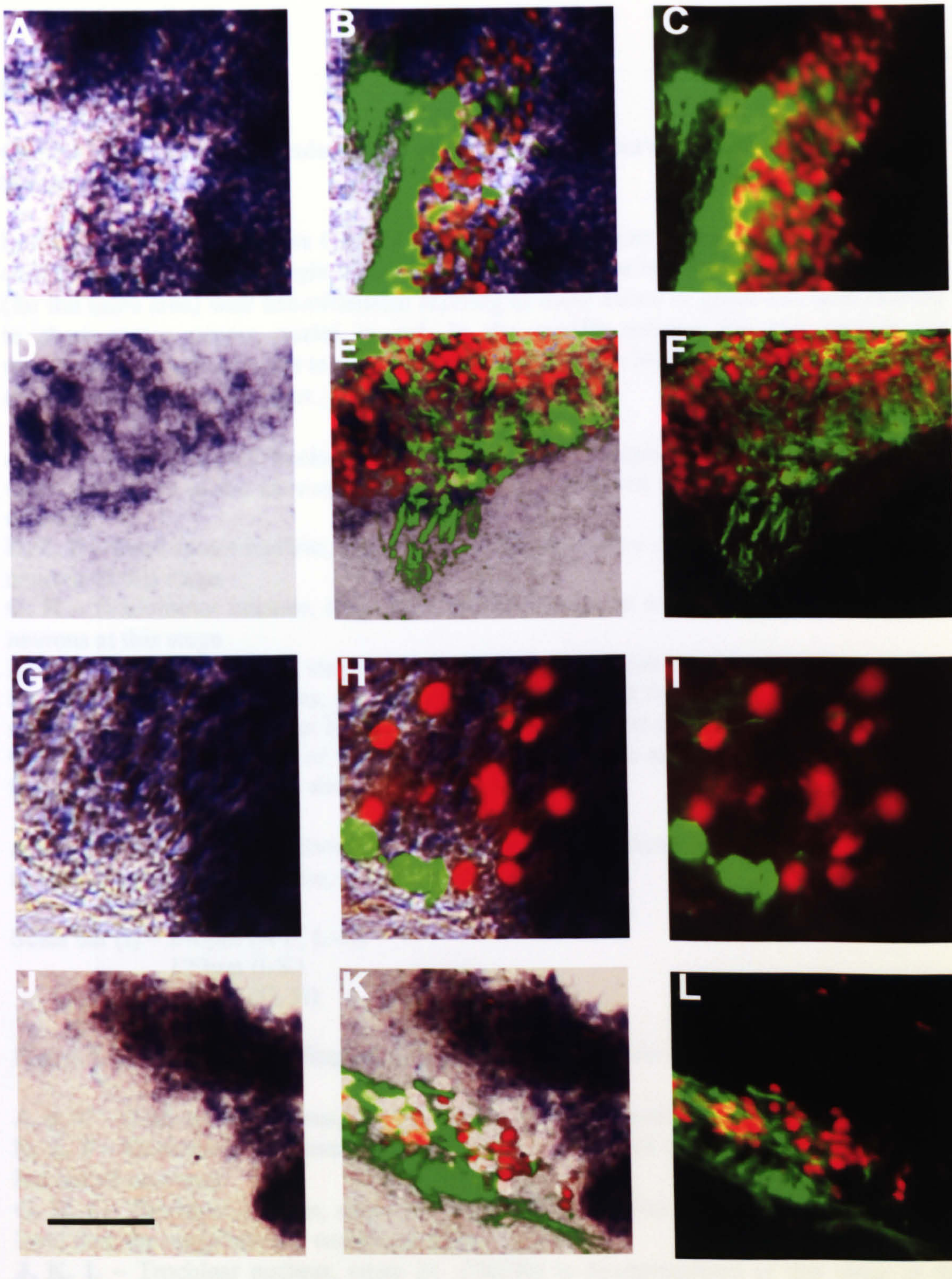

Figure 3.9i

Figure 3.9 & 3.9i

***CXCR4* expression in oculomotor and trochlear neurons at HH stages 18-26 (transverse sections)**

Left column of panels shows *CXCR4* expression on sections at the level of oculomotor and trochlear cell bodies. Right column of panels shows the immunofluorescence images (for the same area) with neurofilament staining to show axons in green and islet staining to show motor neuron nuclei in red. In the middle column the two images are superimposed. Arrows point to an area of expression in the left and middle sets of panels to show a corresponding spot.

A, B, C – Oculomotor nucleus, stage 18. *CXCR4* is expressed at high levels in the ventricular zone of the neuroepithelium and at lower levels in the differentiated motor neurons.
D, E, F – Oculomotor nucleus, stage 21. *CXCR4* expression is maintained in oculomotor neurons at this stage.
G, H – Oculomotor nucleus, stage 26. *CXCR4* expression is maintained in oculomotor neurons at this stage.
I, J, K – Trochlear nucleus, stage 18. Some trochlear neurons express *CXCR4*
L, M, N – Trochlear nucleus, stage 21. Expression of *CXCR4* in postmitotic neurons is switched off at this stage, but is maintained in the floor plate and ventricular zone
O, P – Schematic sketches of the chick head in transverse and sagittal section showing the positions of the sections shown in panels A-J.

Abbreviations: nIII – oculomotor nucleus, III – oculomotor nerve, nIV – trochlear nucleus, vz – ventricular zone, fp – floor plate

Scale bar (I) – 240μm (A-F, L-N)
120μm (I-K)
320μm (G, H)

Figure 3.9i – Higher magnification images of sections shown in figure 3.9

A, B, C – Oculomotor nucleus, stage 18. Most neurons express *CXCR4*.
D, E, F – Oculomotor nucleus, stage 21. Patchy expression of *CXCR4* (present in some but not all neurons)
G, H, I – Trochlear nucleus, stage 18. Most neurons express *CXCR4*, albeit at a lower level than the neighbouring ventricular zone.
J, K, L – Trochlear nucleus, stage 21. CXCR4 is downregulated at this stage in the trochlear neurons.

Scale bar (I) – 60μm (A-F, J- L)
30μm (G-I)

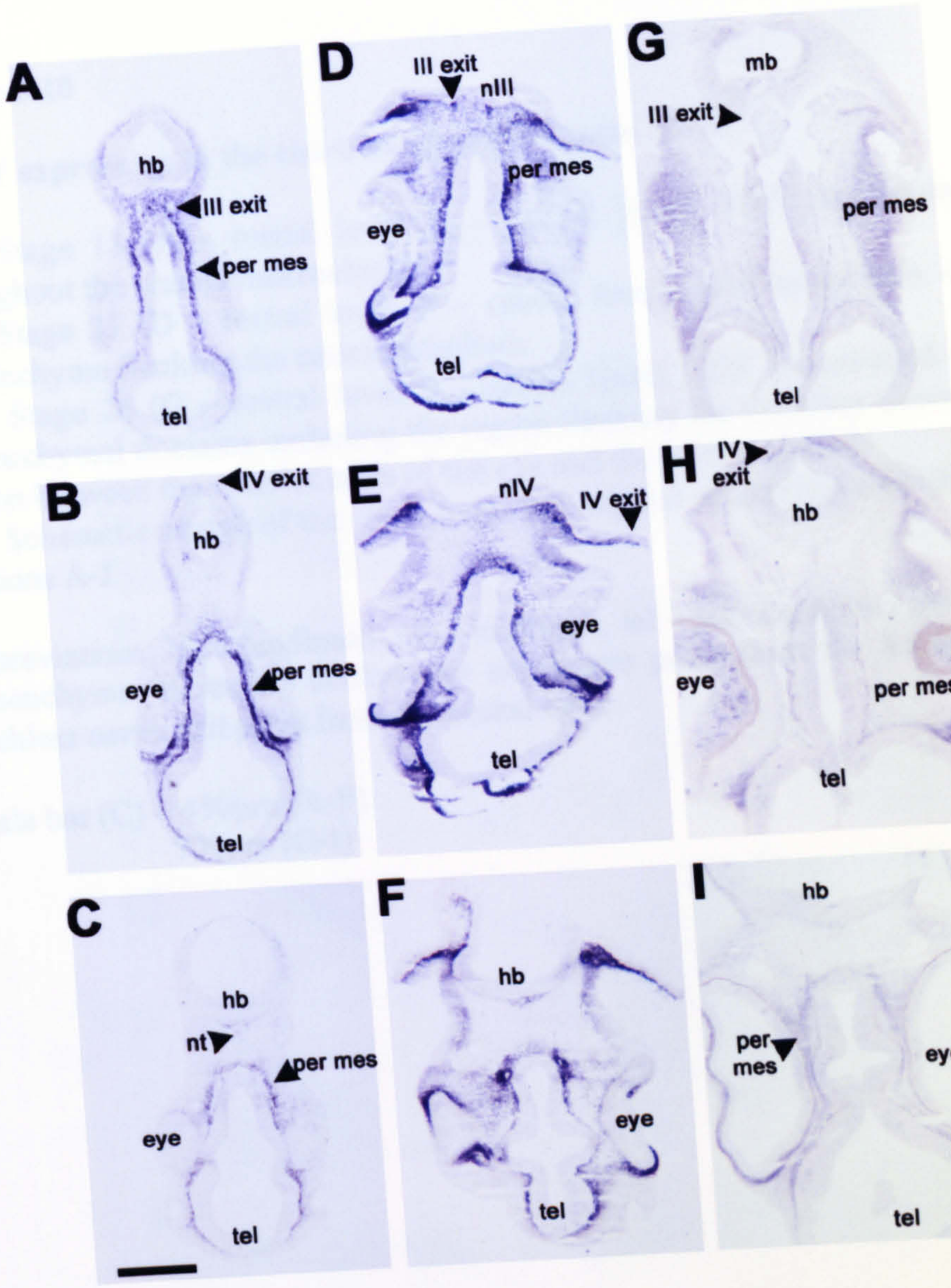
A
hb
III exit
per mes
tel
D
III exit
nIII
per mes
eye
tel
G
mb
III exit
per mes
tel
B
IV exit
hb
eye
per mes
tel
E
nIV
IV exit
eye
tel
H
IV exit
hb
eye
per mes
tel
C
hb
nt
per mes
eye
tel
F
hb
eye
tel
I
per mes
eye
tel

Figure 3.10

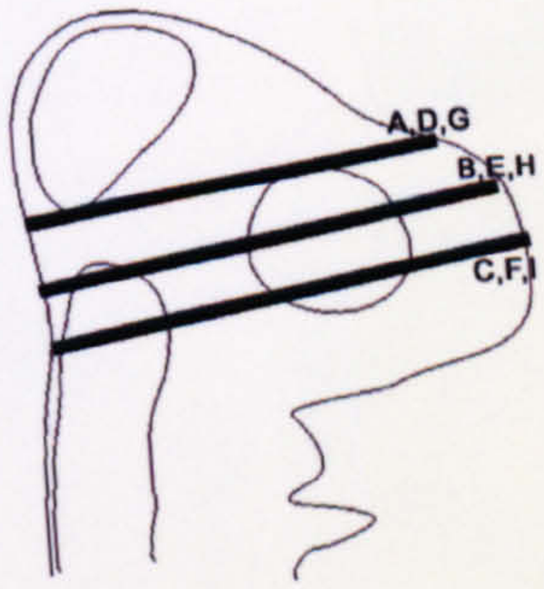
A,D,G
B,E,H
C,F,I

Figure 3.10

***SDF-1* expression in the chick head at HH stages 18-26**

A-C Stage 18 (A – rostral level, C – caudal level). *SDF* expression is widespread throughout the cranial mesenchyme.
D-F Stage 21 (D – rostral level, F – caudal level). *SDF* expression is maintained in mesenchyme flanking the neuroepithelium.
G-I Stage 26 (G – rostral level, I – caudal level). *SDF* is restricted further to a few mesenchymal domains including the region flanking the trochlear nerve exit point and a region between the anterior edge of the eye and the telencephalon.
K – Schematic sketch of the chick head in a sagittal orientation showing the position of sections A-J.

Abbreviations: hb – hindbrain, mb - midbrain, tel – telencephalon, per mes – periocular mesenchyme, III exit – oculomotor nerve exit point from the neural tube, IV exit – trochlear nerve exit point from the neural tube.

Scale bar (C) – 450μm (A-F)
700μm (G-I)

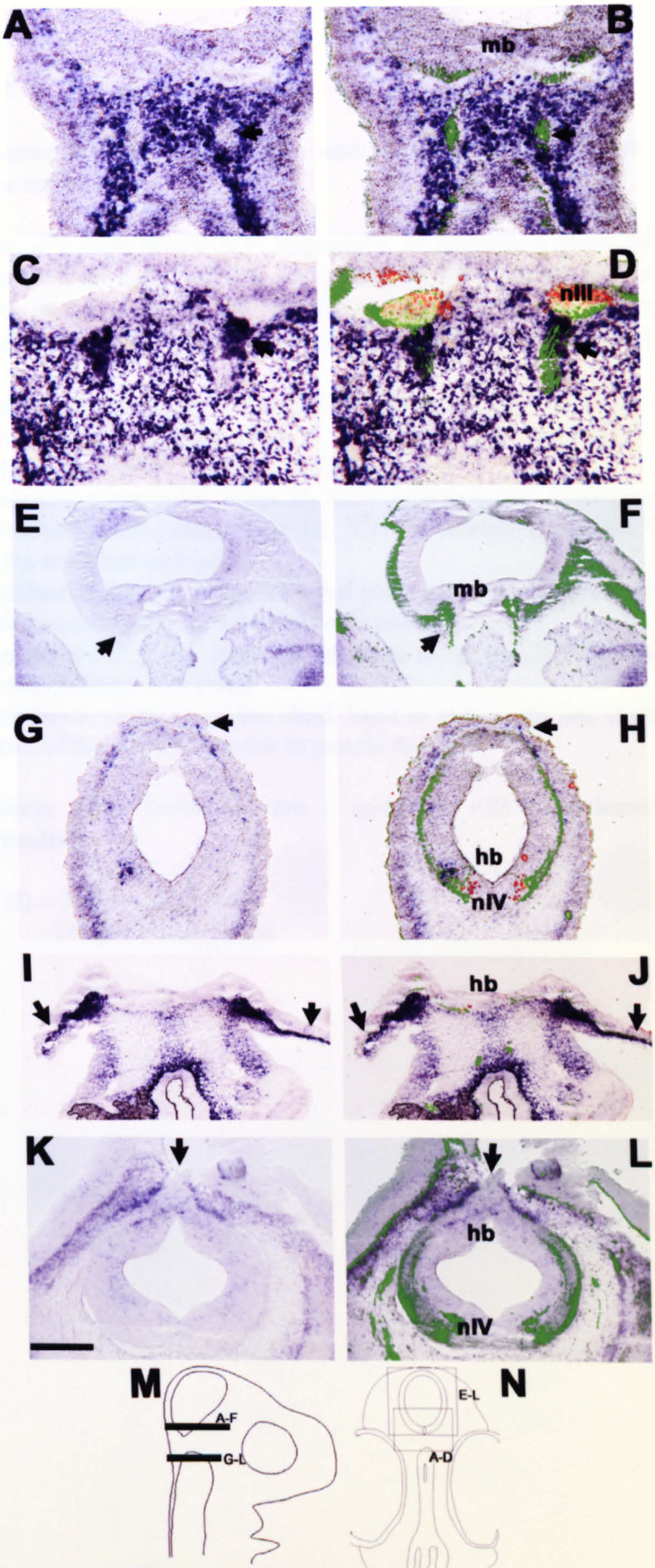

Figure 3.11

Figure 3.11

***SDF-1* expression at oculomotor and trochlear exit points at stages 18-26 (transverse sections)**

Left column of panels shows *SDF* expression on sections at three different stages at the level of oculomotor and trochlear cell bodies. Right column of panels shows the same images with immunostaining for neurofilament to show axons (green) and islet to show motor neuron nuclei (red) superimposed. Arrows indicate the exit point.

A,B – Oculomotor exit point, stage18. *SDF* expression surrounds the emerging axons
C, D – Oculomotor exit point, stage 21. *SDF* expression is enriched in the mesenchyme directly adjacent to the oculomotor cell bodies
E, F – Oculomotor exit point, stage 26. *SDF* expression has been downregulated
G, H – Trochlear exit point, stage 18. *SDF* is weakly expressed in the mesenchyme adjoining the trochlear exit point.
I, J – Trochlear exit point, stage 21 (roof plate opened). High levels of *SDF* expression in mesenchyme adjoining the trochlear exit point
K, L – Trochlear exit point, stage 26. Medium levels of *SDF* expression in mesenchyme adjoining the trochlear exit point
M, N - Schematic sketches of the chick head in transverse and sagittal section showing the positions of the sections shown in panels A-L.

Abbreviations: hb – hindbrain, mb – midbrain, nIII – oculomotor nucleus, nIV – trochlear nucleus

Scale bar (I) – 250μm (E, F, I-L)
100μm (A-D, G, H)

Figure 3.12

Expression of *SDF-1* in the extraocular muscles at stage 26/7 (transverse sections)

Panels on the left show the expression of SDF, the corresponding panel on the right is the same image with immunostaining for mf20 to show muscle (red) and neurofilament to show axons (green) superimposed. Arrows point to an area of expression in both sets of panels to show a corresponding spot.

A, B – Image shows region around the dorsal oblique. *SDF* is expressed in the mesenchyme flanking the muscle antero-medial side
C, D – Image shows region around the dorsal rectus. *SDF* is expressed in the centre of the muscle.
E, F – Image shows the region around the lateral rectus
G, H – Image shows the region around the ventral rectus/medial rectus
I, J – Image shows the region around the ventral oblique. *SDF* is expressed in the centre of the muscle.

Abbreviations: DO – dorsal oblique, DR – dorsal rectus, LR – lateral rectus, VR – ventral rectus, MR – medial rectus, VO – ventral oblique, III – oculomotor nerve, V – trigeminal nerve, VI – abducens nerve, dien - diencephalon.

Scale bar (A) - 250μm (A, B, E, F)
170μm (C, D, I, J)
400μm (G, H)

Chapter 4: Response of Oculomotor, Trochlear and Abducens Axons to Candidate Guidance Cues *In Vitro*

4.1 INTRODUCTION

The aims of this project were to identify the mechanisms that control the process of axon growth to the extraocular muscles. Of the six extraocular muscles, four are innervated by the oculomotor nerve, whose cell bodies are located in the caudal midbrain. Oculomotor axons exit the neural tube close to the ventral midline and grow ventrally towards the ciliary ganglion, where a subset of oculomotor axons synapses. After reaching this intermediate target the somatic oculomotor axons extend rostrally towards the ventral oblique, which is the farthest target, and subsequent to making contact with the ventral oblique, the oculomotor nerve forms branches to the remaining targets: the ventral rectus, the medial rectus and the dorsal rectus (Chilton and Guthrie 2004). The trochlear nerve originates in the rostral part of rhombomere1; its axons extend dorsally within the neural tube, exit in the roof plate, where they decussate and project contralaterally to the dorsal oblique muscle (Irving et al 2002). The abducens nerve originates in rhombomeres 5 and 6; its axons exit the neural tube ventrally and extend rostrally to innervate the lateral rectus muscle (Wahl et al 1994).

The accurate selection of the appropriate target for innervation, the specific and reproducible choice of trajectory and the stereotyped timing of the innervation imply a strict control of the axon guidance process. This is thought to be accomplished by the action of axon guidance cues, both secreted and cell-surface bound, which either attract axons towards or repel them away from areas where these cues are expressed. Each population of axons responds to different cues or to the same cues in a different manner depending on the complement of receptors the axons express on their growth cones and which downstream signal transduction components they possess. Thus specificity of

target selection can be conferred by a differential response of different axonal populations to guidance cues expressed in the targets.

To investigate the control of axon guidance in this system, five axon guidance cues were chosen. The secreted class III semaphorins (Sema3A, Sema3C and Sema3F), HGF and SDF-1 are implicated in the control of cranial motor axon guidance by a number of lines of evidence, as discussed in section (1.5). Expression patterns of the five candidate cues in the chick head at the developmental stages when axon growth to the extraocular muscles occurs, which were described in chapter 3, provided additional evidence to elaborate the hypotheses with respect to the roles that these ligands might play in the control of innervation of extraocular muscles (see section 2.3). The hypotheses regarding the roles of the various guidance cues in the control of extraocular muscle innervation, which are based on previously published data and the expression results needed to be tested further by assessing the responsiveness of the different populations of axons to these cues *in vitro*.

In order to investigate the *in vitro* response of the oculomotor, trochlear and abducens axons to different guidance cues, the collagen co-culture system was chosen, which has been extensively used to address similar questions (Lumsden and Davies 83, Guthrie and Pini '95, Varela-Echavarria et al '97, Hammond et al '05). A bilateral segment of the neuroepithelium containing the motor nucleus of interest is dissected out and grown in a three dimensional collagen matrix. Collagen is a permissive cue for most axonal populations and allows the axons to exit the explanted neuroepithelium. The explants are exposed to the action of a candidate guidance molecule, which can either be added to the culture medium to assess its impact on the overall outgrowth of axons, or presented from a focal source (from a cluster of cells or beads) to judge whether it can re-orient axons towards or away from the source of the cue. Adding protein to the culture medium enabled the assessment of axonal outgrowth from explants compared to control explants cultured in medium alone and determine whether the addition of the cue promoted axonal outgrowth, inhibited it or had no effect. A growth-promoting effect observed *in vitro* suggests that the cue acting as an attractant for that population of axons *in vivo*,

while a growth-inhibiting effect suggests that the cue acting as a repellent *in vivo*, although a more convincing demonstration of a chemoattractive or chemorepulsive effect is axons turning to align along the gradient of a guidance cue. Culturing explants with a cluster of cells or beads secreting cue means that the axons growing out of the explant are exposed to a gradient of that cue, and growth cones have been shown to respond to gradients by turning up the gradient of attractive cues or down the gradient of repulsive cues (Rosoff et al 2004). Therefore, as well as measuring the effect on total outgrowth, this assay enables to measure a potential chemoattractive or chemorepulsive effect by measuring the angle axons emerging into the collagen make with the midline. Deviation towards the source of the cue would indicate a chemoattractive effect and deviation away from the source of the cue would indicate a chemorepulsive effect.

The explants were dissected from E12 rat embryos. Cranial motor axon outgrowth *in vitro* is at its most prolific in the rat at this stage (Varela-Echavarria et al 1997) and consists of a combination of *de novo* and regenerating outgrowth; much less outgrowth occurs in younger (E11) or older (E13) embryos (personal observations). The rat was chosen in preference to the chick as the model organism in this assay because chick cranial motor axons grow very poorly in rat collagen gels (S. Guthrie – personal communication).

Oculomotor neurons are found in the caudal midbrain. Oculomotor explants consisted of the ventral third of the caudal midbrain neuroepithelium. The axonal outgrowth was visualised by staining with the F84.1 antibody, which recognises the SC1 antigen that is present on oculomotor axons and cell bodies at this axial level as well as floor plate cells (Prince et al 1992). SC1-positive axons exited the explant exclusively from the caudal edge in two thick, "brush-like" bundles either side of the midline (Varela-Echavarria et al 1997). Clusters of semaphorin-secreting cells were positioned either parallel to the caudal edge at a distance of approximately 500μm, to assess their effect on outgrowth, or orthogonally next to the lateral edge to compare the outgrowth on the proximal and distal sides of the explant and assess the direction of axonal outgrowth relative to the gradient of the guidance cue. The anticipated effects of semaphorins on oculomotor

outgrowth was repulsive, which would result in fewer axons emerging from the proximal side of the explant and axons turning away from the cluster, or no effect, in which case outgrowth from experimental explants would be similar to controls. HGF and SDF-1 were added directly to the medium and their effect on axonal outgrowth was compared to explants cultured in the control medium. SDF-1 was also presented on beads as a focal source to measure its ability to redirect oculomotor axons. Here the expectation was a growth-promoting effect and possibly a chemoattractive effect.

Trochlear motor neurons are found in the rostral part of rhombomere 1. The cell bodies localise ventrally, so the ventral third of r1 neuroepithelium was cultured. Trochlear axons grow towards a dorsal exit point *in vivo*, so when a ventral fragment of the neural tube is explanted the axons exit laterally in a fasciculated bundle. They can be distinguished by F84.1 staining. In order to investigate the effects of secreted semaphorins, clusters of Sema-secreting cells were positioned orthogonally to the lateral edge of the explant at a distance of approximately 300μm; and outgrowth from the distal and proximal sides of the explant was compared. HGF and SDF-1 were added directly to the medium and their effect on axonal outgrowth was compared to explants cultured in the control medium. SDF-1 was also presented on beads as a focal source to measure its ability to redirect trochlear axons.

Abducens motor neurons are located in rhombomere 5 in the rat. There is no antibody to distinguish abducens axons from other axonal populations found in this rhombomere, so the axons were visualised by retrogradely labelling them before using FITC-conjugated dextran amine tracers. Explants consisted of the ventral third of the neuroepithelium. Abducens axons do not fasciculate together in culture, but rather exit ventrally and grow independently through the collagen. Semaphorin-secreting cell clusters were positioned approximately 300μm away from the lateral edge of the explant and the axonal outgrowth from the distal half of the explant was compared to the outgrowth from the proximal half.

4.2 RESULTS

4.2.1 Effect of secreted semaphorins on abducens outgrowth

At HH stage 19 the lateral rectus muscle expresses high levels of Sema3C (see figure 3.2). At this developmental stage abducens axons are making their first contacts with the lateral rectus primordium (Wahl et al 1994), therefore it is possible that Sema3C is functioning as an attractant for abducens axons. The effect of Sema3C was examined by culturing r5 rat explants, containing fluorescently-labelled abducens neurons together with clusters of cells stably expressing Sema3C. The cluster was positioned opposite one of the lateral edges of the explant. Over the 42hrs of culture the secretion of Sema3C from the cluster establishes a gradient of this guidance cue, and the axons exiting the proximal half of the explant are exposed to a higher concentration of Sema3C than the axons exiting from the distal half. If Sema3C exerts a growth promoting effect on abducens axons, one would expect more and/or longer axons to emerge from the proximal half of the explant. If Sema3C is a chemoattractant, axons would be expected to turn towards the source of the cue. On the other hand explants cultured with control clusters, which do not secrete Sema3C, would be expected to display more or less symmetrical outgrowth from both halves.

Following 42 hours of culture abducens outgrowth was recorded by confocal microscopy and presented as a flattened z-stack (see figure 4.1). Relative outgrowth from the proximal and distal explant halves was measured by counting pixels on both sides using Scion Image software and presenting the amount of outgrowth from the half facing the cluster as a percentage of total outgrowth. A score of 50% indicates symmetrical outgrowth, more than 50% indicates greater outgrowth on the side facing the cluster and a score of less than 50% indicates greater outgrowth on the side away from the cluster. The mean score for abducens explants cultured with Sema3C clusters (n=20) was 59%, whereas the mean score for abducens explants cultured with control clusters (n=23) was 47%. The increase in outgrowth from the side facing the cluster in the presence of Sema3C was statistically significant ($p=0.0127$ calculated using

Student's two-tailed t-test). Therefore, Sema3C exerts a growth-promoting effect on abducens axons *in vitro* (Figure 4.4). The enhancement of outgrowth induced by Sema3C manifested itself both in more axons growing towards the cluster (e.g. figure 4.1B) and in longer axons growing towards the Sema3C-secreting cluster (e.g. figure 4.1A)

The question of whether Sema3C acts as a chemoattractant is harder to answer. Because abducens axons exit ventrally into the collagen and do not fasciculate together the pattern of outgrowth appears haphazard, with axons often changing direction of growth a number of times. Many axons do turn towards the cluster, in some cases making 180° turns (see figure 4.1B), but others turn away from it, and there is no systematic alignment along the gradient.

This result is consistent with Sema3C expression being observed in the target of the abducens nerve, but is surprising in the context of an earlier finding that Sema3A inhibited the outgrowth of abducens axons (Varela-Echavarria et al '97). Surprising, because class III secreted semaphorins require the presence of a neuropilin receptor and abducens neurons only express neuropilin-1 (NPN-1) and not neuropilin-2 (NPN-2) (Chilton and Guthrie 2003). This implies that the two ligands, Sema3A and Sema3C, both bind to the same receptor but exert opposite effects on axonal behaviour. Therefore, the effects of Sema3A on abducens outgrowth were re-examined, especially since the earlier study relied on a small sample and a less quantitative measure of outgrowth.

The experiment was conducted in the same way as described above, with clusters of cells stably expressing Sema3A providing a focal source of the guidance cue. Quantitation of pixels representing outgrowth from each half of the explant was carried out, with outgrowth from the side facing the cluster expressed as a percentage of total outgrowth; hence scores of >50% indicating an increase in outgrowth in the presence of elevated Sema3A, and scores of <50% indicating a reduction in outgrowth in the presence of Sema3A. The mean score for explants cultured with Sema3A-secreting clusters (n=22) was 31%. The mean score for control explants (n=22) was 45%. The

reduction in outgrowth in the presence of Sema3A was statistically significant (p=0.00369, Student's t-test, figure 4.4), therefore this data is in agreement with the previously published result. However, little evidence of chemorepulsive activity of Sema3A was observed, as defined by the ability to induce axonal turning away from the source of the guidance cue. Instead the action of Sema3A appears to be inhibitory, the reduction of outgrowth on the side proximal to the cluster is due to fewer axons being able to exit the cluster, and those that do possessing on average a shorter length (see figure 4.2).

So, despite the presence of only one neuropilin on abducens neurons, the two semaphorins that were tested induce a diametrically opposite response in these axons. As discussed in the introduction chapter, this phenomenon, although unusual, is not unprecedented. For example Sema3B attracts anterior commissure axons and Sema3F repels them, both signal through NPN-2. The mechanism responsible for this effect was not investigated any further, but there are a number of possible explanations, which will be discussed in more detail in section 4.3.1.

It is also interesting to note that control clusters in themselves cause a slight inhibition of abducens outgrowth. A possible explanation is that the 293 cells secrete an unknown substance(s) which inhibits abducens axons. This could explain why the growth promoting effect of Sema3C appears less dramatic, because it is partially masked by the inhibitory effect of 293 cells.

The combination of *in vitro* effects of Sema3A and Sema3C on abducens axons and the expression pattern of these guidance cues around the trajectory of this nerve suggests a possible mechanism in which the two cues co-operate to direct the guidance of abducens axons. Sema3C is strongly expressed in the target muscle and weakly along the trajectory of the nerve (see figure 3.2). Sema3A expression, on the other hand, surrounds the lateral rectus and the pathway of the abducens nerve (see figure 3.5). It is possible, therefore, that the two ligands co-operate in the guidance of abducens axons *in vivo*. The response of abducens axons to both semaphorins *in vitro* was tested by placing a cluster

of Sema3A-secreting cells opposite one side of an abducens explant and a cluster of Sema3C-secreting cells opposite the other side. The control experiment was to place two clusters of 293 cells either side of an abducens explant. The outgrowth from explants sandwiched between two control clusters was fairly symmetrical The observed response of abducens axons presented with opposing gradients of Sema3A and Sema3C was stronger than when presented with an individual cluster; outgrowth towards the Sema3C-secreting cluster was quite prolific, whilst little outgrowth occurred towards the Sema3A-secreting cluster (figure 4.3). The outgrowth was again measured by quantitatively. The mean percentage of outgrowth was 23% from the side facing the Sema3A cluster and 77% from the side facing the Sema3C cluster (n=10, p=0.00764). The effect of the two semaphorins appears to be additive, outgrowth towards Sema3C clusters is enhanced quite dramatically in some cases (e.g. figure 4.3B), whilst the percentage of outgrowth towards Sema3A clusters is even lower than when explants are cultured with Sema3A clusters alone (figure 4.4). However, there was no sign of a systematic alignment of abducens axons up the Sema3C gradient and down the Sema3A gradient, which would have been the expected outcome if Sema3A and Sema3C were acting co-operatively as a repellent and an attractant.

4.2.2 Effect of secreted semaphorins on oculomotor outgrowth

NPN-1 and NPN-2 are initially expressed throughout the oculomotor nucleus, but between HH stages 25 and 31 in the chick, NPN-1 becomes restricted to the ventral subnuclei and NPN-2 expression becomes enriched in the dorsal subnuclei (Chilton and Guthrie 2004). This should render oculomotor neurons susceptible to the action of different secreted semaphorins. Indeed, both NPN-2 and Sema3F mutant mice exhibit an abnormal defasciculation of the oculomotor nerve (Chen et al 2000, Giger et al 2000, Sahay et al 2003). Furthermore, Sema3C and Sema3A are expressed in and around the oculomotor targets, and Sema3F is expressed in an area between four of the extraocular muscles in proximity to the path of the extraocular nerve. Therefore, the effects of secreted semaphorins on oculomotor outgrowth were tested *in vitro*.

In initial experiments, clusters of semaphorin-secreting or control cells were positioned opposite the caudal edge of the explants, from which all $SC1^+$ outgrowth occurs. The explants were cultured for 42hrs, fixed and stained with the F84.1 antibody against SC1. Outgrowth was assessed by assigning a score of 0-5 to each explant, with 0 indicating no outgrowth and 5 the most prolific outgrowth seen. The scoring was carried out blind (i.e. without knowledge of whether the explant is a control or an experimental one) to avoid introducing observer bias. The distribution of scores for control and experimental samples was evaluated using the non-parametric Mann-Whitney U-test, which assesses the probability of two samples belonging to the same population when the values for members of a sample are grouped into discrete sets. The resulting probability is the p value. When $p<0.05$, the difference between experimental and control groups is taken to be statistically significant.

When oculomotor explants were cultured with Sema3A-secreting clusters (n=30), no significant difference in outgrowth was observed, compared to explants cultured with control clusters (n=29, p=0.83; see figures 4.5 and 4.7). Similarly, no effect was seen when oculomotor explants were cultured with Sema3C-secreting clusters (n=35); overall outgrowth was similar to that seen with control explants (n=16, p=0.67, see figures 4.5 and 4.7).

In contrast, co-culture with Sema3F-secreting clusters resulted in a substantial reduction in outgrowth from oculomotor explants (n=27), compared to controls (n=28, p=0.00421, see figure 4.7). In most cases fewer axons were observed to emerge from the explant and they tended to be shorter and less fasciculated. Also, unlike axons growing out of control explants, which extended caudally as two broad 'brush-like' bundles, axons from explants cultured with Sema3F did not grow caudally, but spread in different directions often turning laterally parallel to the cluster (figure 4.5).

In order to assess whether Sema3F can induce turning of oculomotor growth cones, the assay was performed with Sema3F-secreting clusters placed lateral to the explant. If Sema3F exercises a chemorepulsive effect on oculomotor axons, they would be

expected to turn away from the cluster since the gradient of Sema3F is at a right angle to their normal course of growth. Indeed, Sema3F appears to exercise both a growth-inhibiting and a chemorepulsive effect. Unlike control explants, where two caudally-extending bundles growing parallel to the cluster are observed (figure 4.6C, D), explants cultured with Sema3F display inhibition of outgrowth from the proximal half of the explant, with axons sometimes turning around inside the explant and emerging rostrolaterally (figure 4.6B), whilst outgrowth from the distal half is repelled with axons deviating from their normal caudal course by, in some cases 90° or more (figure 4.6 A, B). Outgrowth from the two halves of the bilateral explant can be scored separately, allowing a different measure of the inhibitory effect of Sema3F. The outgrowth score of the distal half of the explant can be subtracted from the score of the proximal half of the explant; this results in an overall score between -5 and 5, with -5 indicating strong repulsion and +5 strong attraction. The scores for control explants would be expected to cluster around 0 with the distribution assuming a shape similar to a normal distribution; the distribution of scores for explants co-cultured with Sema3F clusters would shift to the left, indicating a greater reduction of outgrowth on the proximal half of the explant, which is exposed to a higher concentration of Sema3F. Indeed, this is the situation observed (figure 4.8A); 36% of explants cultured with Sema3F-secreting clusters (n=33) have a score of -2 or less, compared with 12% of control explants (n=25). The difference in distribution is statistically significant (p=0.0112, Mann-Whitney U test). This orientation of explants also allowed for a measure of repulsion. For each explant, a line was drawn from the centre of the oculomotor nucleus in the distal half of the explant along the middle of the bundle (for diagram, see figure 2.4E) and the angle to the midline was measured. If axons are repelled by the gradient of Sema3F emanating from the cluster the angle would be expected to increase as the axons are forced to turn away from their normal course. Indeed, this commonly happens, in the two examples shown in figure 4.7, oculomotor axons turn perpendicular to the midline and exit the explant laterally. The angle measurement confirms this; in control explants the average angle to the midline was 46°, and in the presence of Sema3F, the average angle increased to 65° (figure 4.8B). This difference was statistically significant (p=0.0411, Student's t-test).

In summary, neither Sema3A nor Sema3C exerted any effect on oculomotor axons *in vitro*, whilst Sema3F both inhibited oculomotor outgrowth and repelled oculomotor axons away from a focal source. Thus the Sema3F^{+} region dorsal to the developing medial rectus/ventral rectus (figure 3.1) may play a role in directing the growth of the oculomotor nerve ventrally of these muscles. The absence of an effect of Sema3A on oculomotor axons is consistent with a previous report (Varela-Echavarria et al '97). It seems unlikely that the expression of Sema3A and Sema3C in the extraocular muscles that are innervated by the oculomotor nerve plays an important part in axon guidance to these muscles, unless there are mechanistic differences between the chick and the rat in this instance.

4.2.3 Effect of secreted semaphorins on trochlear outgrowth

Trochlear neurons express NPN-1 and NPN-2 at high levels during the stages when nerve outgrowth and innervation of the target muscle is occurring (HH stage 21-27 in the chick). This should, in theory, enable them to respond to all three semaphorins in question because different combinations of NPN-1 and NPN-2 in the receptor complex are thought to transduce signals from Sema3A, Sema3C and Sema3F. The response of trochlear axons to secreted semaphorins *in vitro* has been examined previously (Varela-Echavarria et al 1997, Giger et al 2000), but these studies used unilateral explants, relied on small samples and reported conflicting results. Varela-Echavarria and colleagues found that trochlear axons were repelled by Sema3A. Giger et al observed no effect of Sema3A or Sema3C, but found that Sema3F repelled trochlear axons in culture. The finding that Sema3A and Sema3C are expressed in and around the dorsal oblique highlights the possibility of their function in trochlear axon guidance, possibly to prevent overshooting of the target by trochlear axons.

When grown in collagen, trochlear axons emerge from the lateral edges of the explant as a fasciculated bundle on each side. The amount of outgrowth and the degree of fasciculation is highly variable, requiring relatively large samples to obtain a reliable result. Explants were cultured with the semaphorin-secreting cluster placed opposite the

lateral edge of the explant at a distance of 300-500μm. After 42 hours of culture the collagen gels were fixed and stained with the F84.1 antibody to visualise trochlear axons. Outgrowth from each side was scored on the 0-5 scale. Subtracting the outgrowth score on the distal side from the outgrowth score on the proximal side gave a relative measure of outgrowth, with a negative score indicating inhibitory effect and a positive score indicating a growth-promoting effect.

When trochlear explants were cultured with Sema3F, little outgrowth was seen on the side facing the cluster. In very few cases a laterally protruding fasciculated bundle of axons was observed; in most cases outgrowth was suppressed altogether, or a few axons grew out in random directions (see figure 4.9A, B). The graph showing the difference in outgrowth scores (figure 4.10) indicates a shift towards repulsion for explants cultured with Sema3F-secreting clusters (47% of explants have negative scores, n=58), compared to control explants (35% of explants have negative scores, n=69). However, this difference is not statistically significant ($p=0.127$, Mann-Whitney U test). This is most likely due to the growth-inhibiting effect of Sema3F being sufficiently strong to inhibit outgrowth from the distal half of the explant, as well (see for example 4.9B). When outgrowth scores from the proximal half are compared between Sema3F and control explants a drastic reduction in outgrowth is observed (median=1 for explants cultured in the presence of Sema3F, median=3 for control explants, $p<0.01$, see figure 4.10B). These data are broadly in agreement with the findings of Giger et al (2000), who also reported an inhibitory effect of Sema3F on trochlear axons in co-culture. However, the authors report observing a chemorepulsive effect of Sema3F, with trochlear axons turning away from the source of the ligand, in some cases by as much as a 180° to the normal direction of growth and extending past the floor plate. This was never seen in the much larger sample used in this study. In the few cases in which a bundle of trochlear axons emerged from the side facing the Sema3F-secreting cluster, the axons grew towards the cluster rather than turning down the gradient. In other cases where a few individual axons extended from the explant they grew in a random, disorganized pattern and did not exhibit systematic turning away from the source of Sema3F. It is possible that the bilateral explants used in this study experienced a stronger repulsion from the

midline and therefore trochlear explants hemmed in between two strong repulsive gradients largely failed to grow, or grew haphazardly. However, the only conclusion I can draw from this study is that Sema3F has a growth-inhibiting effect on trochlear axons; chemorepulsion has not been demonstrated.

Sema3C had no effect on trochlear outgrowth. Explants co-cultured with Sema3C secreting clusters (n=65) exhibited a similar distribution in outgrowth to control explants (n=51, p=0.701). Similarly, culturing trochlear explants in the presence of Sema3A (n=42), did not alter their outgrowth score distribution significantly compared to control explants (n=43, p=0.738). This is in agreement with the result reported by Giger et al (2000), but contradicts the findings of Varela-Echavarria and colleagues (1997), who saw a repulsive effect of Sema3A on trochlear axons. It is conceivable that Sema3A exerts an effect on trochlear axons by repelling them away from the cluster without inhibiting outgrowth from the proximal side. In order to test this, the angle of deflection was measured in all explants with a discernable bundle on both sides (score of $\geq$2 on each side). The angle of deflection is the difference between the angle the distal bundle makes with the midline and the angle the proximal bundle makes with the midline. A negative angle indicates the bundle facing the cluster being deflected away and thus repelled by the cluster; whereas a positive angle indicates the proximal bundle being deflected towards the cluster and thus signifies attraction. In the presence of Sema3A the mean angle of deflection is -6°, whereas for control explants it is -7°. Therefore there is no evidence of Sema3A repelling trochlear axons.

In summary, this study concurs with Giger and colleagues (2000) that trochlear axons are unaffected by Sema3A and Sema3C *in vitro*, and are inhibited by Sema3F; although a chemorepulsive effect has not been confirmed. This study disagrees with Varela-Echavarria et al (1997) who found that Sema3A inhibited trochlear outgrowth. In relation to the expression patterns of semaphorins along the route of the trochlear nerve, previous studies (Watanabe et al 2004, Giger et al 2000) highlighted the importance of Sema3F in guiding trochlear axons within the neural tube and enabling their exit into the periphery. This study didn't identify any regions of Sema3F expression in peripheral

regions in the vicinity of the trochlear nerve trajectory, so it is unlikely that it plays a role in peripheral trochlear axon guidance. Although *Sema3A* and *Sema3C* expression was seen in and around the dorsal oblique muscle at the stages when it is receiving innervation from the trochlear nerve, the fact that neither Sema3A nor Sema3C influences trochlear outgrowth *in vitro* implies that this expression may not play a role in trochlear axon guidance and is likely to serve another purpose, such as playing part in the migration or differentiation of muscle and connective tissue developing in that region. Another possibility is that semaphorins influence trochlear axon guidance indirectly, through interaction with other cues such as HGF and SDF-1. This possibility will be examined in section 4.2.6

4.2.4 Effect of HGF and SDF-1 on trochlear outgrowth

The only guidance cue thus far identified as an attractant for trochlear axons is FGF8, which is involved in guiding trochlear axons within the neural tube (Irving et al 2002). Little is known about which signals direct its growth towards the dorsal oblique. A reasonable candidate to test is the hepatocyte growth factor (HGF), since it has been shown to attract other cranial motor axons and was reported to be expressed in the periocular mesenchyme (Caton et al 2000). This study has confirmed its expression in the region of interest in particular in the developing dorsal oblique and along the trajectory of the trochlear nerve (figure 3.8).

The effect of HGF on trochlear outgrowth was tested by culturing the explants in collagen for 42hrs as usual, but with HGF added to the growth medium at a concentration of 10ng/ml (the concentration determined to be effective in previous studies (Caton et al 2000, Naeem et al 2002)). The results were dramatic; HGF induced a vast increase in the number of axons emerging into the collagen, a substantial increase in their length and a defasciculation from a compact bundle to a radial spread of axons (figure 4.11). Outgrowth was initially measured by blind scoring on the 0-5 scale and comparing control explants with ones cultured with HGF. As expected, it produced a highly significant result (see figure 4.12A, $p<0.001$, $n=40$(HGF), $n=35$(controls)).

However, this measurement is less meaningful in this instance, partly because the vast majority of HGF explants scored 5, having far more prolific outgrowth than that seen in any control explant, and partly because any notion of blind scoring was moot, since it was generally obvious when an explant had been cultured with HGF. Two additional measurements were used to quantify the effects of HGF. One was to measure the axonal length (at the midpoint of the bundle); another was to measure the angle of the spread of axons (see methods chapter for detailed explanation). The average length was 203μm in control explants and that had more than doubled to 418μm in the presence of HGF ($p<0.001$) (figure 4.12C), demonstrating the strong growth promoting effect that HGF has on trochlear axons. In addition, the angle of spread also more than doubled from 34° to 77° ($p<0.001$)(figure 4.12B). This is a result of greater defasciculation of axons and the increase in number of axons. The increase in the apparent number of axons could be a result of several different phenomena: an increase in the number of axons that exit the explant, an increase in branching of those or a proliferation of trochlear neurons. It is difficult to measure the relative contribution of these factors, but I believe that all three play a part. Axons appear more branched, and all seem to exit the explant (unlike control explants were axons often grow within the explant but fail to emerge into the collagen), and there appear to be more trochlear neurons judging by F84 immunostaining of trochlear cell bodies. The proliferation of trochlear neurons is unlikely to be the key factor though because although HGF is known to function as a neurotrophic factor (Ebens et al 1996), at E12 trochlear neurons are not yet trophic factor-dependent (Hatton and von Bartheld 1999).

Stromal cell-derived factor 1 (SDF-1) is a cytokine, which has recently been implicated in axon guidance (Xiang et al 2002, Chalasani et al 2003, Li et al 2005, Lieberam et al 2005). The receptor for SDF-1, CXCR4, is expressed in the trochlear neurons at the time when their axons are extending (see figure 3.9). Furthermore, SDF-1 is expressed around the developing dorsal oblique, suggesting a possible role for SDF-1 in trochlear axon guidance. Therefore the effect of SDF-1 on trochlear outgrowth was tested in vitro, by adding SDF-1 protein to the growth medium of trochlear explants being cultured in collagen. The outgrowth was scored on the 0-5 scale, and outgrowth from control

explants (n=20) was compared to outgrowth from explants cultured in the presence of SDF-1 (n=16). The outgrowth was significantly increased ($p<0.001$, Mann Whitney U test, see figure 4.14A). The effect of SDF-1 on outgrowth manifested itself in longer and denser bundles of axons (see figure 4.13), but did not result in a radial spread of axons as seen with HGF. The length of axonal bundles and the angle of spread of axons in the presence of SDF-1 were measured, in the same way as was done for explants cultured with HGF. The average length increased from 172μm to 311μm ($p<0.001$) in the presence of SDF-1. The angle of spread also increased slightly, but was not statistically significant (figure 4.14B, C).

The growth promoting effect of SDF-1 on trochlear axons having been demonstrated it would be interesting to see whether a gradient of SDF-1 can redirect trochlear axons towards the focal source of the cue. This was tested by soaking heparin-coated beads in SDF-1, and placing a cluster of SDF-soaked beads laterally to the explant. Axonal outgrowth in these explants was comparable to the controls, which were cultured with a cluster of PBS-soaked beads (figure 4.15). Outgrowth from each side was scored on the 0-5 scale and the difference in the score between the proximal side and the distal side was compared for control explants (n=30) and explants cultured with SDF-soaked beads (n=24). There was no significant difference between the score distributions of the two samples (see figure 4.16A, $p=0.304$, Mann Whitney U test). In addition the angle between the axonal bundle and the midline was measured on each side of the explant. Subtracting the angle on the distal side from the angle on the proximal side gives the measure by which axons are deflected, a positive value indicates chemoattraction and a negative value indicates chemorepulsion. The angle difference for explants cultured with SDF-soaked beads was -1(±10)° and for control explants it was 7(±7)° (figure 4.16C); therefore SDF-1 was unable to deflect trochlear axons. The average relative length of axonal bundles (length of proximal bundle – length of distal bundle) was slightly increased in the presence of SDF-1 (an example can be seen in 4.15B), but it was not a statistically significant increase (figure 4.16B). So, SDF-1 secreted from beads had no effect on trochlear outgrowth, nor was it able to chemoattract them. It is possible that insufficient protein was released from the beads into the collagen, which could explain

the discrepancy with the finding that SDF-1 had a strong growth-promoting effect when added to the culture medium.

In summary, the addition of HGF and SDF-1 to the culture medium increased trochlear outgrowth in collagen gels in both cases. SDF-1 increased the length and density of axonal bundles, whereas HGF increased axonal length and the number of axons emerging from the explant and also promoted the defasciculation of trochlear axons. Given the expression patterns of the two ligands in the developing embryo, it is possible that they function as attractants for trochlear axons *in vivo*, although SDF-1 failed to chemoattract trochlear axons *in vitro* when presented from a focal source. Another possibility for a follow-on experiment is to express SDF-1 in cells, and culture trochlear explants with SDF-secreting cells. This method would release more protein into the collagen gel and would generate a more stable gradient of SDF-1 and is therefore more likely to induce an effect. It would also be interesting to see if HGF secreted from a focal source is capable of chemoattracting trochlear axons.

4.2.5 Effect of HGF and SDF-1 on oculomotor outgrowth

HGF is also expressed along the latter trajectory of the oculomotor nerve and around some of the targets (see figure 4.8). Hence its effect on oculomotor outgrowth *in vitro* was tested by the addition of the protein to the culture medium, at 10ng/ml. HGF promoted axonal outgrowth from oculomotor explants although not as strongly as from trochlear explants (see figure 4.17). Outgrowth from control explants (n=31) and explants cultured with HGF (n=33) was scored on the 0-5 scale and comparison of the distribution of scores showed a statistically significant increase (see figure 4.18A, p= 0.0432, Mann Whitney U test). Length of axonal bundles and angle of spread of axons were also measured, as for the trochlear explants (see materials and methods for diagram). Average length of axons increased from 290μm in the controls to 350μm in the presence of HGF, a statistically significant increase (p=0.0171), and the average angle of spread increased slightly from 61° to 68° (p=0.0465). Therefore, HGF stimulates outgrowth from oculomotor explants.

The receptor for SDF-1, CXCR4 is expressed in the oculomotor neurons at the stages when axon guidance to the extraocular muscles is occurring (figure 3.9). SDF-1 is expressed strongly in the mesenchyme adjacent to the oculomotor nerve exit point at the stages when oculomotor axons are emerging from the neural tube (figure 3.11), and it is expressed in a localized fashion in the extraocular muscles at the time when they are in the process of being innervated (figure 3.12). Thus it is possible that SDF-1 acts to facilitate the exit of oculomotor axons from the neural tube and/or chemoattracts oculomotor axons to their muscle targets. To ascertain whether SDF-1 is capable of acting in the hypothesized manner, its effect on oculomotor outgrowth was tested *in vitro*.

Addition of SDF-1 to the culture medium at 100ng/ml results in a dramatic proliferation of axonal outgrowth, with an increase in the density and the length of axonal bundles (see figure 4.19). Outgrowth was measured on the 0-5 scale, and the distribution of scores was compared for control explants (n=21) and explants cultured with SDF-1 (n=15). The increase in outgrowth was statistically significant (p=0.00429, Mann Whitney U test) (figure 4.20A). The length of axonal bundles was also measured, as described before, and was found to be significantly increased from 355μm to 405μm (p=0.021, Student's t-test) (figure 4.20B). The angle of spread of axons also increased slightly from 69 to 71 degrees, but was not statistically significant (p=0.498, Student's t-test) (figure 4.20C). In addition 4 out of 15 explants cultured with SDF-1 exhibited a rostral exit of a fasciculated bundle of stained axons (for an example see figure 4.19B), a situation never observed in control explants (in fact, something that was never seen in any of the hundreds of oculomotor explants cultured in this study under different conditions). Given the expression of SDF-1 in the mesenchyme abutting the oculomotor exit point from the neural tube, and the recent finding by Lieberam et al (2005) that SDF-1 is involved in directing the ventral exit of spinal motor axons, it is possible that SDF-1 plays a role in enabling oculomotor axon exit from the neuroepithelium. Thus presence of SDF-1 in the culture medium may override whatever non-permissive cues

are found rostrally to the oculomotor nucleus allowing axons to exit from the rostral edge of the explant.

Since SDF-1 is also expressed in the oculomotor target muscles at the time of innervation, it is also possible that it is functioning as an attractant for oculomotor axons. To test this possibility, oculomotor explants were cultured adjacent to clusters of SDF-soaked beads, and their ability to re-orient oculomotor axons was assessed. Outgrowth from the caudal edge of the explant was similar to that observed in controls (figure 4.21). There was nothing like the prolific outgrowth witnessed when SDF-1 is added to the medium, perhaps because insufficient protein was released from the beads. However, in six out of 25 explants cultured with SDF beads, as opposed to one out of 15 controls, some oculomotor axons exited laterally rather than from the caudal edge of the explant and grew towards the beads. In one case, this phenotype was quite striking – a fasciculated bundle exiting from the middle of the lateral edge and growing a considerable distance, contacting one bead, and changing direction to grow further yet and contact another bead (figure 4.21A). To quantify the effect of SDF beads three measures were used. The net score, where outgrowth each half of the explant is scored on the 0-5 scale and the difference between the proximal half and the distal half is taken, is shown in figure 4.22A. No significant difference in the distribution of scores for control and experimental explants was found ($p=0.576$). Measuring the difference in length between the proximal and the distal bundle also yielded little difference between experimental and control explants (figure 4.22C). However, measuring the angle of deflection (the difference in the angle the proximal and the distal bundle make to the midline) showed that oculomotor axons were deflected slightly towards SDF beads (by 15° rather than the 3° seen in controls), indicating that SDF-1 might be chemoattractive for these axons. However, this effect fell short of statistical significance ($p=0.0778$). Further experiments are needed, in particular culturing oculomotor explants with cell clusters expressing SDF-1, which may give a stronger effect due to the cells' ability to release larger quantities of protein into the collagen.

In summary both HGF and SDF-1 are able to promote outgrowth from oculomotor explants, when added to the culture medium. The effect of HGF on oculomotor axons is less dramatic than that on trochlear axons, however it is significant, and, coupled with the expression of HGF along the oculomotor trajectory, increases the likelihood that HGF acts as a chemoattractant for oculomotor axons. Its ability to redirect oculomotor axons *in vitro* needs to be tested by presenting HGF from a focal source, such as a cluster of beads or cells transfected to express HGF. SDF-1 exerts a stronger effect on oculomotor outgrowth and is in addition able to facilitate rostral exit from the explant. When presented on beads it induces some axons to exit laterally and grow towards the beads, and it can cause some re-orientation of caudally exiting axons towards the beads, although more evidence is required to support this preliminary result. Taken together, the results of the expression analysis and *in vitro* experiments involving SDF-1 point to two possible roles for this molecule; one is facilitating oculomotor axon exit from the neural tube, and another possibility is that it acts as a chemoattractant to guide oculomotor axons to their targets.

4.2.6 Effect of combinations of guidance cues on oculomotor and trochlear axons

Although Sema3A was unable to influence oculomotor or trochlear axon outgrowth *in vitro*, its expression in the extraocular muscles raises the possibility that it influences the guidance of these axons indirectly, through interaction with other guidance cues. SDF-1 has been shown to modify the effects of other guidance cues including semaphorins and slits (Chalasani et al 2003). SDF-1 is co-expressed with Sema3A in the mesenchyme adjoining the dorsal oblique muscle and the two ligands are co-expressed in the ventral oblique and the dorsal rectus, two targets of the oculomotor nerve (see figures 3.6 and 3.13). It is possible that SDF-1 converts the absence of response of oculomotor and trochlear axons to Sema3A into attraction. The logic behind this hypothesis was that since SDF-1 abolishes the repulsive effect of Sema3A on dorsal root ganglion axons, through elevation of intracellular cAMP (Chalasani et al 2003), it may convert the absence of an effect by Sema3A into attraction by the same mechanism. This possibility

was tested by adding SDF-1 to the culture medium of oculomotor and trochlear explants cultured with either Sema3A-secreting or control clusters.

Oculomotor explants cultured with Sema3A clusters and ones cultured with control clusters both exhibited less outgrowth from the half facing the cluster in the presence of SDF-1 (figure 4.23), but the inhibition was more marked in explants cultured with Sema3A. Comparing the experimental and control groups using the semi-quantitative net explant score index bears this observation out – control explants have a median score of -1, but explants cultured with Sema3A have a median score of -2, with >40% of explants scoring -3 or less compared to 7% of control ones (figure 4.24A). The length of the axonal bundle on the side facing the cluster is reduced by an average of 300μm in the presence of Sema3A compared with a 50μm average reduction in length in control explants (figure 4.24B). This difference was statistically significant ($p=0.0164$, Student's t-test). No deflection of axons away from Sema3A clusters was observed, with the net angle of deflection comparable between the oculomotor and control groups (figure 4.24C). This result was a surprise since the expectation was that SDF-1 may convert Sema3A into an attractive cue for oculomotor axons. However, the opposite occurs – in the presence of SDF-1, Sema3A is able to exert a growth-inhibiting action on oculomotor axons. Given the co-expression of *Sema3A* and *SDF-1* in the ventral oblique muscle and the surrounding mesenchyme, the inhibitory effect of Sema3A in the presence of SDF-1 on oculomotor axons may function as a stop signal, to prevent oculomotor axons from overshooting their target. Similarly, in the dorsal rectus which expresses *SDF-1* in the centre of the muscle at HH stage 27, just prior to oculomotor branch formation into this muscle, and *Sema3A* is expressed in cells at the margins of the muscle, the interaction between the two cues may prevent oculomotor axons from overshooting the target.

Trochlear explants cultured with Sema3A or control clusters in the presence of SDF-1 display the abundant outgrowth normally witnessed when SDF-1 is added to the culture medium, but the outgrowth is symmetrical from both sides of the explant in both experimental and control groups (figure 4.25). The distribution of net explant scores for

the experimental and control explants is not significantly different and the relative bundle length is not affected by Sema3A. Nor is there a significant change in the angle of deflection in the presence of Sema3A (figure 4.26). Therefore, SDF-1 does not alter the response of trochlear axons to Sema3A.

Sema3A is co-expressed with HGF in the dorsal oblique and in some of the oculomotor targets such as the ventral oblique (see figures 3.6 and 3.8). The HGF receptor Met is known to interact with class IV semaphorin signalling directly at the receptor level (Giordano et al 2002). It is possible that Sema3A and HGF signalling interact at some intracellular level. The possibility that this plays a role in oculomotor and trochlear axon guidance was tested by culturing oculomotor and trochlear explants with Sema3A or control clusters and HGF added directly to the medium.

Oculomotor outgrowth was enhanced, as expected, by the addition of HGF to the medium. The purpose of the experiment, though, was to establish whether Sema3A is now able to alter the outgrowth compared to controls or redirect oculomotor axons. The outgrowth in the presence of Sema3A appears symmetric and similar to that in control explants (figure 4.27). The measures used to quantify any possible effect were the net explant score, the relative length of the proximal and distal bundles, and the angle of deflection in the presence of Sema3A compared to controls. Figure 4.24 charts the comparison. The addition of HGF does not influence the outcome, as Sema3A still exerts no effect on oculomotor outgrowth. The distribution of net scores is for experimental explants is shifted to the left somewhat (figure 4.28A), but the inhibition of outgrowth is not statistically significant compared to control explants. There is a slight reduction in the relative length of bundles in the presence of Sema3A, but again it is not significant (figure 4.28B). The angle of deflection for control and experimental explants is very similar (and very close to 0, representing a symmetric situation) (figure 4.28C).

Similar results were obtained with trochlear explants. The enlarged bundles of longer axons normally seen after culture with HGF were present. Outgrowth was fairly symmetrical; the bundle from the half facing the cluster was generally more fasciculated,

but this was true both for control and Sema3A clusters. The axons often extended some distance into the cluster, again irrespective of whether the cluster was secreting Sema3A or a control (figure 4.29). The results are quantified in figure 4.30. Again, the relative length and the angle of deflection were similar for control and experimental samples. The distribution of net scores was slightly shifted towards repulsion for experimental explants, but the difference was not statistically significant.

In summary, combinations of Sema3A secreted from clusters with SDF-1 or HGF added to the medium did not result in novel effects on trochlear axonal growth. The explants displayed the prolific outgrowth normally seen in the presence of SDF-1 or HGF, but the Sema3A clusters did not redirect trochlear axons, nor did they alter trochlear outgrowth compared to control clusters – which is the same result as was obtained when trochlear explants were cultured with Sema3A clusters without other molecules being added to the medium. Similarly, HGF in combination with Sema3A clusters produced no novel effect on oculomotor outgrowth. However, when oculomotor explants were cultured with Sema3A clusters in the presence of SDF-1, Sem3A was able to inhibit oculomotor outgrowth from the proximal side of the cluster at the same time as overall outgrowth was enhanced by SDF-1. This result was contrary to expectation, since SDF-1 had previously been shown to reduce the growth cone-collapsing effects of repulsive cues (Chalasani et al 2003), not to potentiate the repulsive effect of cues to which axons had previously been unresponsive. This result indicates that guidance cues in this system are capable of exerting combinatorial effects in which one cue enables another cue, to which axons had previously been unresponsive, to exert an effect. Other combinations of cues which could be tested in the *in vitro* system include SDF-1 and Sema3F, which are co-expressed in the region of the optic nerve exit point, which lies immediately dorsal to the developing ventral rectus/medial rectus, and HGF and Sema3C, which are co-expressed in the mesenchyme around the dorsal oblique muscle.

4.3 DISCUSSION

4.3.1 Abducens axon growth *in vitro*

The behaviour of abducens axons in culture in response to different guidance cues has received relatively little attention to date. It has been reported that abducens axons are inhibited by Sema3A *in vitro* (Varela-Echavarria et al 1997) and are unresponsive to Slits (Hammond et al 2005). The results presented here show that Sema3C promotes abducens axonal outgrowth and Sema3A inhibits it. When an explant is faced with opposing gradients of these two semaphorins, the effects are magnified.

The finding that Sema3A is inhibitory to abducens axonal growth is not a surprise, given that it concurs with the previous report. However, it is difficult to reconcile the fact that Sema3A and Sema3C exert opposing actions on abducens axons with the fact that only NPN-1 and not NPN-2 are expressed on abducens axons (Chilton and Guthrie 2003) and therefore the same receptor has to transduce signals which evoke opposing responses in the cell. There are several scenarios that can account for these observations. Firstly there maybe another, as yet undiscovered, neuropilin present on abducens neurons that transduces either the Sema3A or the Sema3C signal, although I regard this possibility as unlikely. A more credible explanation is that NPN-1 forms different holoreceptor complexes with other components such as plexins, which preferentially bind one or the other semaphorin to evoke a different intracellular response. The receptor combination that binds Sema3C would thus promote growth cone extension, and the receptor combination that binds Sema3A would promote growth cone collapse. A third possibility is that one of the semaphorins is not evoking a functional response but merely acting as a competitive inhibitor. Abducens neurons themselves express both Sema3A and Sema3C (Chilton and Guthrie 2003), if these semaphorins are secreted at the growth cone, then the axons are exposed to a certain endogenous level of each semaphorin. Thus if Sema3A binding increases the probability of growth cone collapse, an increase in the level of Sema3C in the environment reduces the binding of endogenous Sema3A by competing for the same receptor sites, therefore promoting axonal growth.

Conversely, Sema3C could be acting as a competitive inhibitor for Sema3A. I find this explanation less likely, because I would expect a fairly mild effect if a ligand was enhancing outgrowth merely by competitively inhibiting an endogenous growth suppressor (or vice versa), however the enhancement of outgrowth seen in the presence of Sema3C can be very substantial (in particular where an explant had been placed between a Sema3A and Sema3C cluster – see figure 4.3A,B); and likewise a considerable inhibition of outgrowth was seen in the presence of Sema3A (figure 4.2A). This mechanism can not be ruled out, however. But even if true, it doesn't necessarily mean that the result is not physiologically relevant, since it is conceivable that Sema3C, for example, can act as an attractant *in vivo* by enhancing the propensity of abducens axons to extend by lifting the growth inhibition imposed by Sema3A, expressed and possibly secreted by the neurons themselves and thus increasing the probability of axons growing in a direction towards higher Sema3C concentration, therefore acting as an apparent attractant. Further research is needed to establish the exact mechanism by which the two semaphorins evoke the different responses and to distinguish between the different possibilities outlined here. Analogous examples were discussed in the introduction chapter, where Sema3B and Sema3F produce opposing responses in anterior commissure neurons, which only express NPN-2 (Falk et al 2005). Similarly, in olfactory bulb axons, Sema3F and Sema3B evoke opposing responses *in vitro*, presumably through signalling to NPN-2 (del Castro et al 1999). The mechanisms which govern this behaviour have not been elucidated, but probably warrant further attention.

Seen in the context of the expression of these semaphorins in the developing embryo at the time of abducens nerve growth, the *in vitro* response of abducens axons to Sema3A and Sema3C appears plausible. Sema3C is expressed at high levels in the lateral rectus primordium prior to being contacted by the abducens nerve and at lower levels along the path of the nerve (figure 3.2), which is consistent with it functioning as an attractant for this population of axons. Sema3A in contrast is expressed around the trajectory of the nerve and beyond the target (figure 3.5), which is consistent with it acting as a non-permissive cue, restricting the axons to their appropriate route and preventing overshooting of the target. Further confirmation of the physiological relevance of

semaphorin signalling to abducens axon guidance is required from *in vivo* experiments. One possibility is to analyse the pattern of abducens growth in mice lacking these semaphorin genes and comparing it to wild type mice; defects in projection pattern in the mutants would indicate a crucial role for the semaphorins. Another possibility is to disrupt the normal signalling by *in ovo* misexpression of semaphorins or neuropilins and analyzing the outcome with respect to abducens innervation. Both of these approaches will be addressed in the next chapter.

4.3.2 Oculomotor and trochlear axon growth *in vitro*

One of the fundamental questions in addressing the issue of axon guidance to the extraocular muscles is what distinguishes the three nerves that innervate them in terms of their sensitivity and responsiveness to different guidance cues, since the nerves are able to identify the correct targets and complete innervation in a highly stereotyped manner, whilst avoiding inappropriate targets, despite their spatial proximity and continued migration during the period of innervation. One way in which their guidance cue receptor profile differs, as already established by previous research, is in their differential expression of neuropilin receptors. Abducens neurons express *NPN-1*, trochlear neurons express *NPN-1* and *NPN-2*, whilst oculomotor neurons initially express both neuropilins throughout the nucleus but subsequently restrict *NPN-1* expression to the ventral subnuclei before innervation of extraocular muscles is complete. Given that different class III semaphorins are expressed in specific patterns in and around several of the extraocular muscles (see chapter 3) it is pertinent to suppose that they may play a major role in guiding the nerves to their appropriate targets.

The results obtained indicate that Sema3F is an important guidance cue for both oculomotor and trochlear neurons. Sema3F had already been implicated as a repellent for trochlear axons in previous research (Giger et al 2000). It has also been suspected to be involved in oculomotor axon guidance, given that both *NPN-2* and *Sema3F* mutants display a defasciculation of the oculomotor nerve. The data here confirm that Sema3F is a chemorepellent for oculomotor axons *in vitro*. In so far as its relevance to the

pathfinding of the oculomotor nerve in the periphery is concerned, the area of *Sema3F* expression located dorsally to the developing ventral rectus/medial rectus could be important in ensuring the axons take their course ventrally to these muscles and do not invade the more dorsal regions. With regard to the trochlear nerve, Giger and colleagues (2000) have already identified a circumferential region of *Sema3F* expression around the trochlear nerve's exit point from the neural tube, which has been implicated in the failure of trochlear axons to exit the neuroepithelium in NPN-2 mutants. There are no regions of *Sema3F* expression along the peripheral part of the trochlear trajectory; therefore Sema3F is unlikely to play a major part in the guidance of trochlear axons once they have exited the neural tube.

Another point of note is the nature of the *in vitro* responses of oculomotor and trochlear axons to Sema3F. Oculomotor axons were repelled by this ligand, as manifested by the deflection of axons away from their normal course and alignment down the Sema3F gradient, as well as being inhibited in their growth. Trochlear axons on the other hand were subject to a substantial growth inhibition in the presence of Sema3F, often failing to exit the explant altogether, but the axons didn't reorient away from the source of the cue, as they would be expected to if they were subject to chemorepulsion by Sema3F. This maybe due to the precise experimental conditions, since Giger et al (2000) report observing chemorepulsion in a similar assay, however it may represent a different mechanistic response of the two populations of axons to this cue. The area of *Sema3F* expression at the trochlear exit point forms a surround corridor of repulsion, and it maybe that its function is to prevent trochlear axons from entering that zone and to ensure fasciculation of the nerve at the exit point, for which role a strong growth inhibiting effect would be sufficient. The ability of Sema3F to deflect oculomotor axons *in vitro*, on the other hand, may mean that its role is in the more long range guidance of oculomotor axons, re-directing them along their course. These are fairly speculative assumptions though, not fully borne out by the evidence, and further experiments would be required to substantiate them.

Hepatocyte growth factor was found to promote the outgrowth of both oculomotor and trochlear axons. These effects are consistent with its hypothesised role as an attractant for these axons; a hypothesis which stemmed from its known function as an attractant for other cranial motor neurons (Caton et al 2000), and its expression in the targets and along the trajectories of the oculomotor and trochlear nerves. There are two points of note, with regard to the action of HGF. Firstly, its effects on oculomotor and trochlear axons are different. Oculomotor axons experienced a 15% increase in length and slight increase in the semi-quantitative score, when HGF was added to the culture medium. Trochlear axons on the other hand, double in length, spread over a much larger area when they exit the explant and are less fasciculated in the presence of HGF. The weaker effects of HGF on oculomotor axons may indicate that more different attractants are necessary for the guidance of oculomotor axons, or that not all oculomotor subpopulations are sensitive to HGF. The vastly increased number of axons that exit trochlear explants in the presence of HGF could also be due to neurotrophic effects of the ligand as well as its axon growth-promoting effects. The defasciculation seen in the presence of HGF, coupled with its stronger expression within the dorsal oblique, may indicate that HGF promotes the branching of the nerve once the target is reached to innervate the different components of the muscle. Again, these are speculative suggestions which require further substantiation. The second point is that so far only a growth-promoting effect of HGF has been demonstrated. To further advance the hypothesis of its role as a chemoattractant to these populations of axons, it would be desirable to demonstrate its ability to reorient axons when presented from a graded source, such as a cluster of beads or HGF-secreting cells. Also, to support the physiological significance of its action, *in vivo* evidence would be desirable. This would include analysis of oculomotor and trochlear projections in *HGF* or *Met* mutants to see if the disruption of HGF signalling actually prevents the correct pathfinding of these nerves.

During the relatively short period of time that SDF-1 has been investigated as an axon guidance molecule, quite a number of different modes of action have been attributed to it. It has been implicated as an axonal repellent (Xiang et al 2002), an axonal attractant

(Li et al 2005), a modulator of other guidance cues (Chalasani et al 2003), or as influencing exit point selection in motor axons (Lieberam et al 2005).

The effects of SDF-1 on oculomotor and trochlear axons *in vitro*, described here, highlight several possibilities. The increase in axonal length and density of axons exhibited by both oculomotor and trochlear axons indicates that SDF-1 acts as a growth-promoting cue. For the oculomotor axons there is some indication that SDF-1 can act as a chemoattractant, since it is able to deflect axons to some degree towards the graded source of the cue. This correlates well with its expression in the oculomotor targets at the stages when they are receiving innervation. However, since the effect is not statistically significant, further investigation is needed. In addition, SDF-1 is able to induce oculomotor axon exit from the rostral and lateral edges of the explant, a situation that doesn't normally occur. Since SDF-1 is strongly expressed in the region of oculomotor exit point at stages when its axons are emerging from the neural tube, and in the light of Lieberam and colleagues' (2005) findings that SDF-1 influences exit point choice of spinal motor neurons, it is likely that it also promotes oculomotor axon exit into the periphery. Further experiments that would be necessary to demonstrate its function as a chemoattractant could include using SDF-secreting cell clusters as a graded source, since their ability to secret greater quantities of the protein into the collagen is more likely to generate an effect. Analysis of *CXCL12* (SDF-1) or *CXCR4* mutants would yield greater insights about the function of SDF-1 signalling in this system *in vivo*.

In experiments using combinations of guidance cues *in vitro*, the addition of HGF to the medium did not alter the response of oculomotor or trochlear axons to Sema3A, i.e. Sema3A still had no effect on their outgrowth. Nor did the addition of SDF-1 alter the response of trochlear axons to Sema3A. However, the addition of SDF-1 to oculomotor explants cultured with Sema3A, resulted in Sema3A exerting a growth-inhibiting effect on oculomotor axons, whereas Sema3A on its own did not alter oculomotor outgrowth. SDF-1 had previously been shown to modulate the effects of other cues (Chalasani et al 2003), however the action of SDF-1 described in that paper consisted of reducing the

repulsive effects of cues such as Sema3A (on DRG axons) and slits (on retinal ganglion axons) through elevation of intracellular cAMP. Therefore, the expectation in this experiment was that, since Sema3A had no effect on oculomotor axons alone, in combination with SDF-1 it may exert a chemoattractive or growth-promoting effect as a result of an increase in intracellular cAMP. In fact, the opposite occurs and SDF-1 endows Sema3A with a growth-inhibiting faculty it did not previously possess with respect to this population of axons. However, this is perhaps not so surprising since in the brief period of time that SDF-1 has been in the spotlight as an axon guidance cue, a number of different modes of action have been ascribed to it. Cerebellar axons are repelled by SDF-1 (Xiang et al 2002), while the cell bodies of the same neurons are attracted by SDF-1 *in vitro* (Zhu et al 2002), fish retinal axons are chemoattracted by SDF-1 *in vivo* (Li et al 2005) and SDF-1 facilitates the ventral exit of spinal motor axons in vivo either through direct chemoattraction, or by shielding these axons from the action of midline chemorepellents (Lieberam et al 2005). Furthermore, SDF-1 has been shown to signal through a number of intracellular signalling pathways to effect these diverse outcomes including two distinct Rho-dependent pathways (Arakawa et al 2003), two phospholipase C-dependent pathways (Xiang et al 2002), as well as by elevating cAMP (Chalasani et al 2003).

The expression of *SDF-1* in oculomotor target muscles, such as the ventral oblique and the dorsal rectus, shortly prior to innervation suggests that SDF-1 may be attracting oculomotor axons to these targets. However, Sema3A is also expressed in these targets in the fibres at the margin of the muscle and in the surrounding mesenchyme, and SDF-1 converts Sema3A into a repellent for oculomotor axons. How can the opposing actions be reconciled? One factor to consider is that the highly basic tail of Sema3A may severely limit its ability to diffuse by rendering it liable to stick to cell surface and extracellular matrix components (Raper 2000). Indeed given the widespread expression of Sema3A in the head (figures 3.5, 3.6, 3.7) and its repulsive effects on a number of cranial motor axon populations (Varela-Echavarria et al 1997), it would be surprising if it could diffuse very far, since it would make motor axon growth in the head rather challenging. Therefore, SDF-1 could be acting as a longer-range attractant, while in

close proximity of the target Sema3A (in combination with SDF-1) might inhibit the further growth of oculomotor axons to prevent overshooting of the target.

4.3.3 Conclusions

In summary, the co-culture data presented here have identified several prospective chemoattractants and chemorepellents for each of the three nerves studied. For the abducens nerve Sema3C has been identified as a putative attractant and Sema3A as a putative repellent. For the trochlear nerve Sema3F was found to inhibit axonal outgrowth and HGF and SDF-1 enhanced it. Similarly for the trochlear nerve, HGF and SDF-1 had growth promoting effects, whilst Sema3F was chemorepulsive.

There are a number of interesting observations that arise from these findings. One is the substantiation of the idea that different semaphorins can act co-operatively to guide the same population of axons by exerting opposing effects on them. It has already been demonstrated that Sema3F is a chemorepellent for olfactory bulb axons *in vitro* while Sema3B attracts them and both semaphorins are thought to signal through NPN-2, and the expression patterns of Sema3F and Sema3B are consistent with this proposed mode of action (de Castro et al 1999). Similarly, anterior commissure axons are attracted by Sema3B and repelled by Sema3F, both acting through NPN-2 (Falk et al 2005). The results described here support the idea that Sema3C and Sema3A, both signalling through a NPN-1 containing complex, can, likewise, exert opposing effects on abducens axons and co-operate in their guidance to the target. Another idea stemming from these results is that Sema3C might be a ligand that determines which nerve innervates the lateral rectus muscle. Sema3C is expressed at high levels in the lateral rectus and the lateral rectus is innervated by the abducens nerve, whose axons are chemoattracted by Sema3C. The oculomotor nerve, on the other hand, which passes in close proximity to the lateral rectus muscle, does not innervate it possibly because its axons are not sensitive to Sema3C. Another idea stemming from these results is that HGF is a general target-derived chemoattractant for cranial motor axons. It has already been shown to be expressed in the branchial arches and chemoattract branchiomotor axons *in vitro* (Caton

et al 2000), and the results here indicate it may perform the same function for both oculomotor and trochlear axons. The role of SDF-1 in axon guidance to the extraocular muscles appears the most complex. The results here suggest three points during the whole process at which the action of SDF-1 could be important. Firstly, exit from the neural tube – *SDF-1* is expressed in the mesenchyme adjoining the exit point of both oculomotor axons (near the ventral midline) and trochlear axons (overlying the dorsal roof plate), and the presence of SDF-1 in oculomotor explant cultures can induce axons to exit from inappropriate points in the explant. Trochlear explants exhibit enhanced outgrowth in the presence of SDF-1, which may be at least partially due to more axons being able to exit the explant. Secondly, the expression of SDF-1 in oculomotor target muscles and the growth promoting effect of SDF-1 on oculomotor axons in culture, suggest that it could act as a target-derived attractant, promoting growth of oculomotor axons towards these muscles or branch formation. Thirdly, the conversion of Sema3A to a repulsive cue for oculomotor axons in the presence of SDF-1 highlights the possibility of SDF-1 acting as a modulator of other guidance cues. It is important to stress this last point because it is highly unlikely that individual attractants or repellents determine the pathfinding choices of a population of axons. As discussed in the introduction, there is multitude of axon guidance cues expressed throughout the developing embryo and most axonal populations are sensitive to a wide range of them, therefore the pathfinding choices made by a growth cone at each stage of axonal growth, and the resulting trajectory of the nerve, depend on the integration of a number of signals.

The next step in the investigation, addressed in the following chapter, is to analyse the projections of the nerves *in vivo*, following the disruption of the signalling of one of the above guidance cues, to lend further credence to the physiological significance of their action.

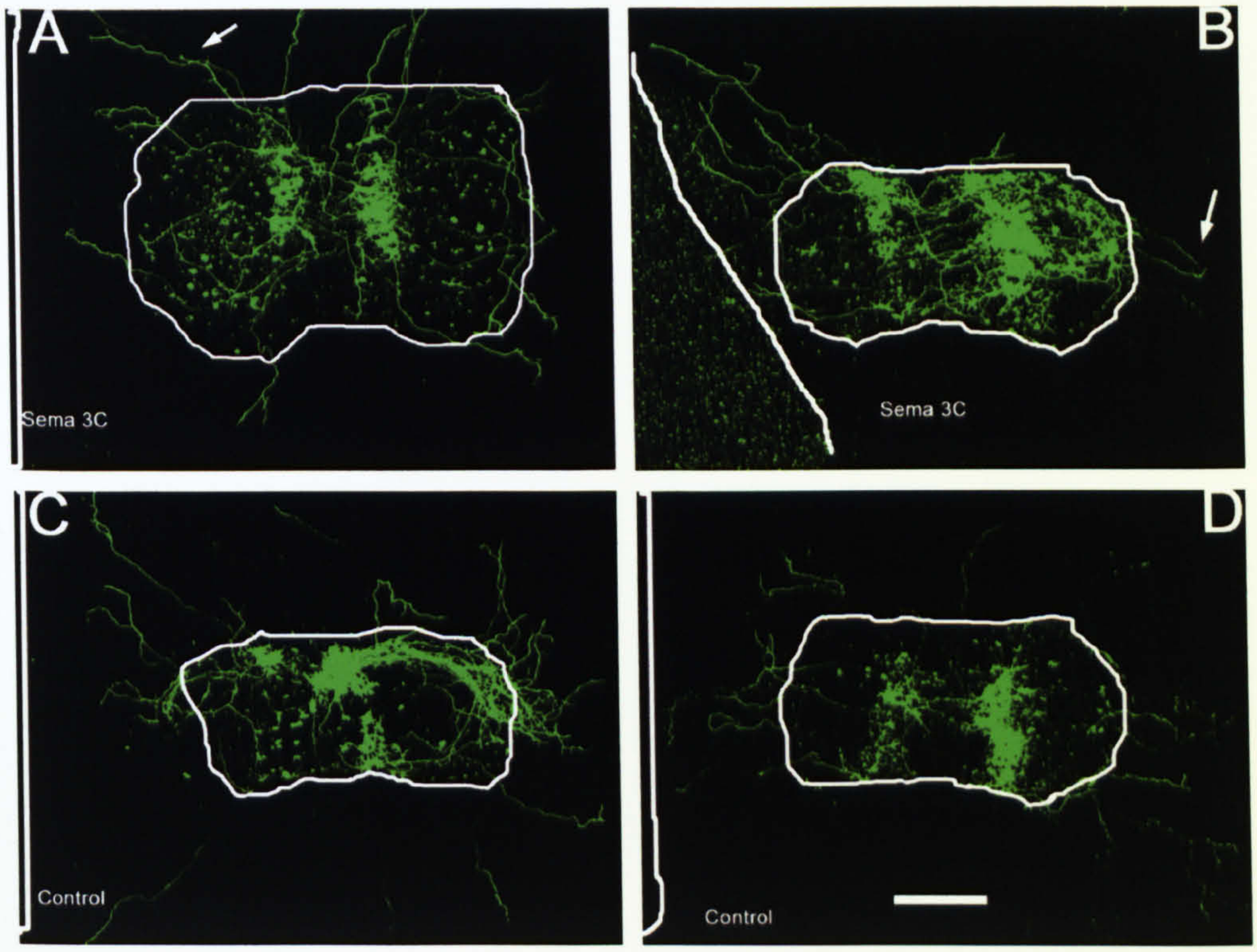

Figure 4.1

Effect of Sema3C on abducens outgrowth

Abducens (r5) explants cultured with Sema3C-secreting clusters (A, B) exhibit greater outgrowth towards the cluster than away from the cluster. whereas abducens explants cultured with control explants (C, D) show a more or less symmetrical outgrowth. Some axons in (A, B) are seen to turn towards the cluster (shown with white arrows). Clusters positioned on the left in each case and explant edges are outlined in white.
Scale bar (D) = 0.15mm

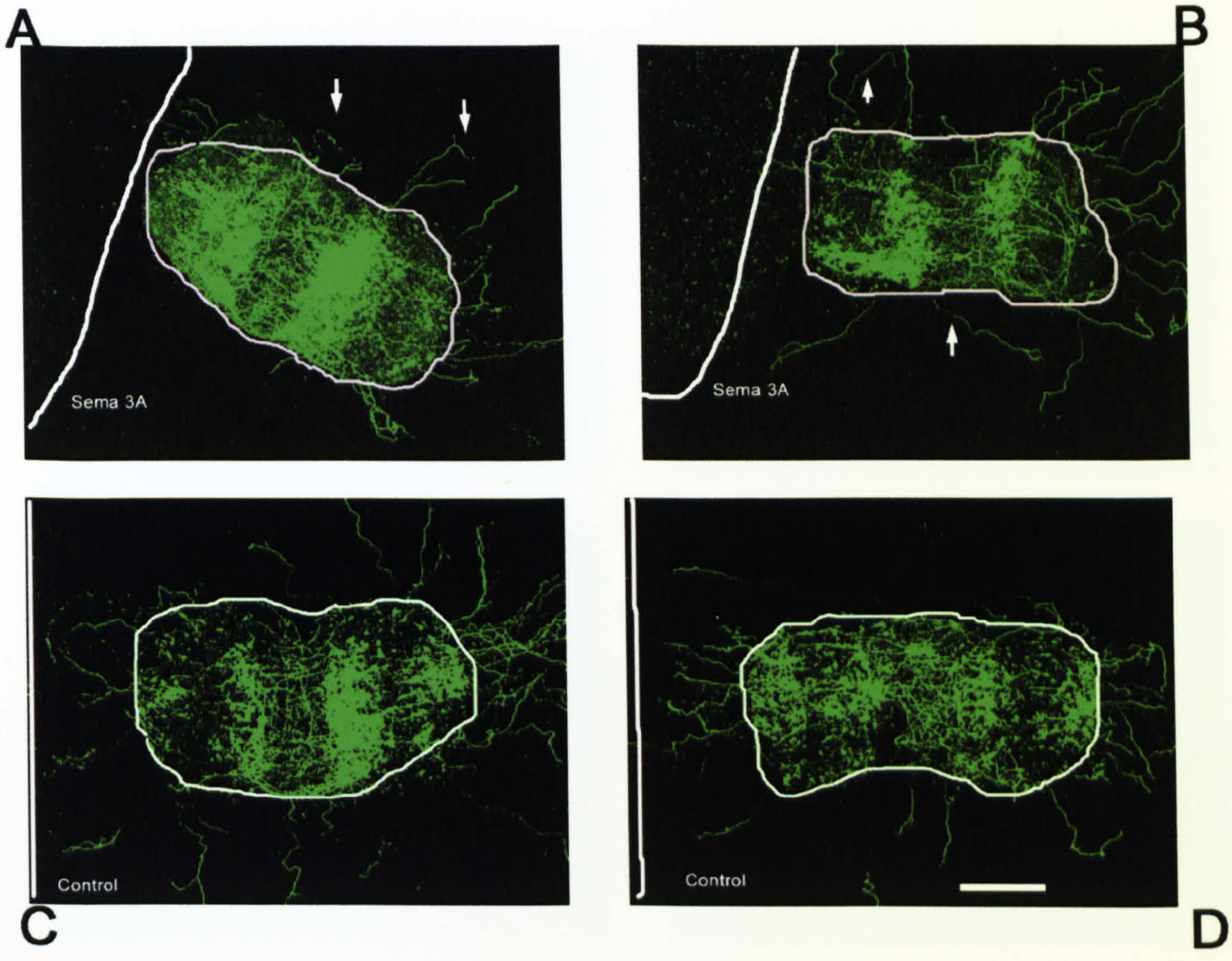

Figure 4.2

Effect of Sema3A on abducens outgrowth

Abducens (r5) explants cultured with Sema3A-secreting clusters (A,B) or control clusters (C, D). In A and B outgrowth towards the cluster is inhibited and some axons are seen to turn away from the cluster (marked with white arrows). In C and D outgrowth is largely symmetrical. Cluster is on the left in all cases and edge of explant is outlined in white. Scale bar (D) = 0.15mm

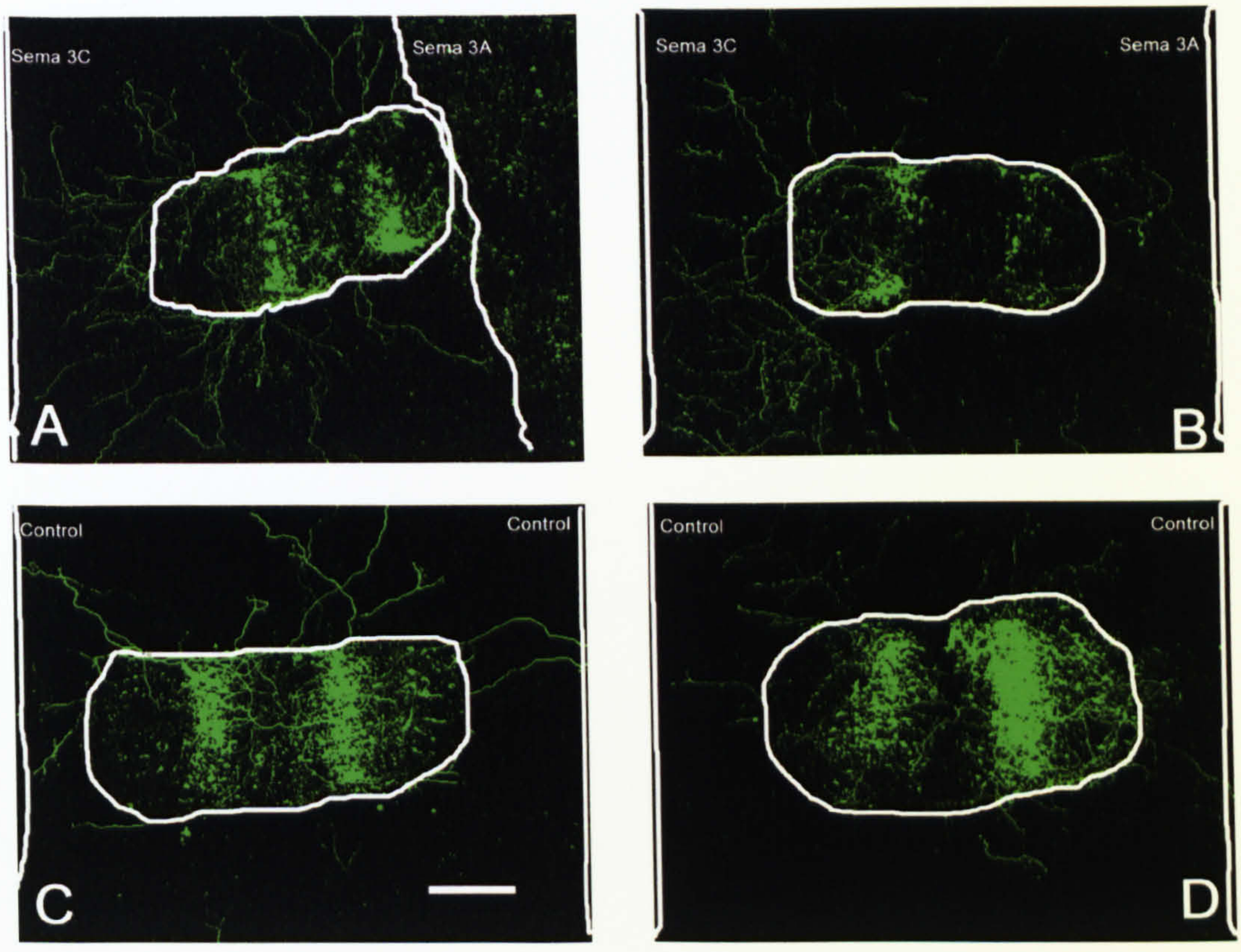

Figure 4.3

Effect of Sema3C and Sema3A combined on abducens outgrowth

Abducens (r5) explants cultured between a Sema3C-secreting cluster (on the left) and a Sema3A-secreting cluster on the right (A, B); or between two control clusters (C, D). In control explants the outgrowth is largely symmetrical, in experimental explants most outgrowth occurs towards the Sema3C cluster. Explant edges are outlined in white. Scale bar = 0.15mm

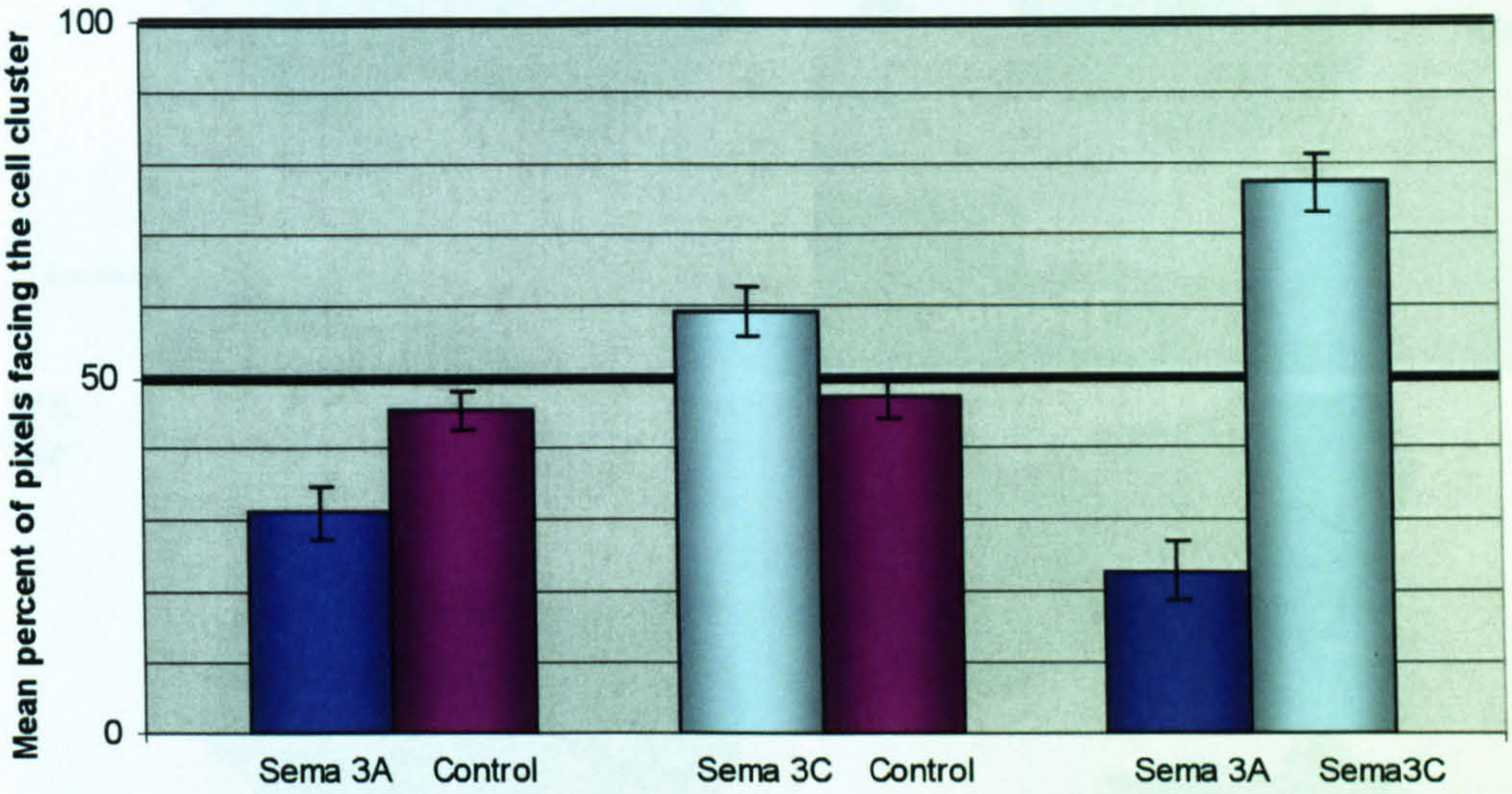

Figure 4.4

Graph comparing outgrowth from the two halves of abducens explants using pixel counting. On the left outgrowth towards Sema3A clusters (shown in blue) is compared to outgrowth towards control clusters (shown in purple). Significantly less outgrowth occurs towards Sema3A clusters than control clusters. In the middle outgrowth towards a Sema3C cluster (turquoise) is compared to outgrowth towards a control cluster (purple). Significantly more outgrowth occurs towards Sema3C clusters than Sema3A clusters. On the right outgrowth from two sides of abducens explants sandwiched between a Sema3A and a Sema3C cluster is compared. Error bars show the estimated standard error.

	Percentage of pixels facing the Sema3A/ control cluster	Percentage of pixels facing the Sema3C/ control cluster	p (Student's t-test)
Sema3A (n=22)	31		0.00369
Control (n=22)	45		
Sema3C (n=20)		59	0.0127
Control (n=23)		47	
Sema3A/Sema3C (n=10)	23	77	0.00764
Control/control (n=10)	43	57	

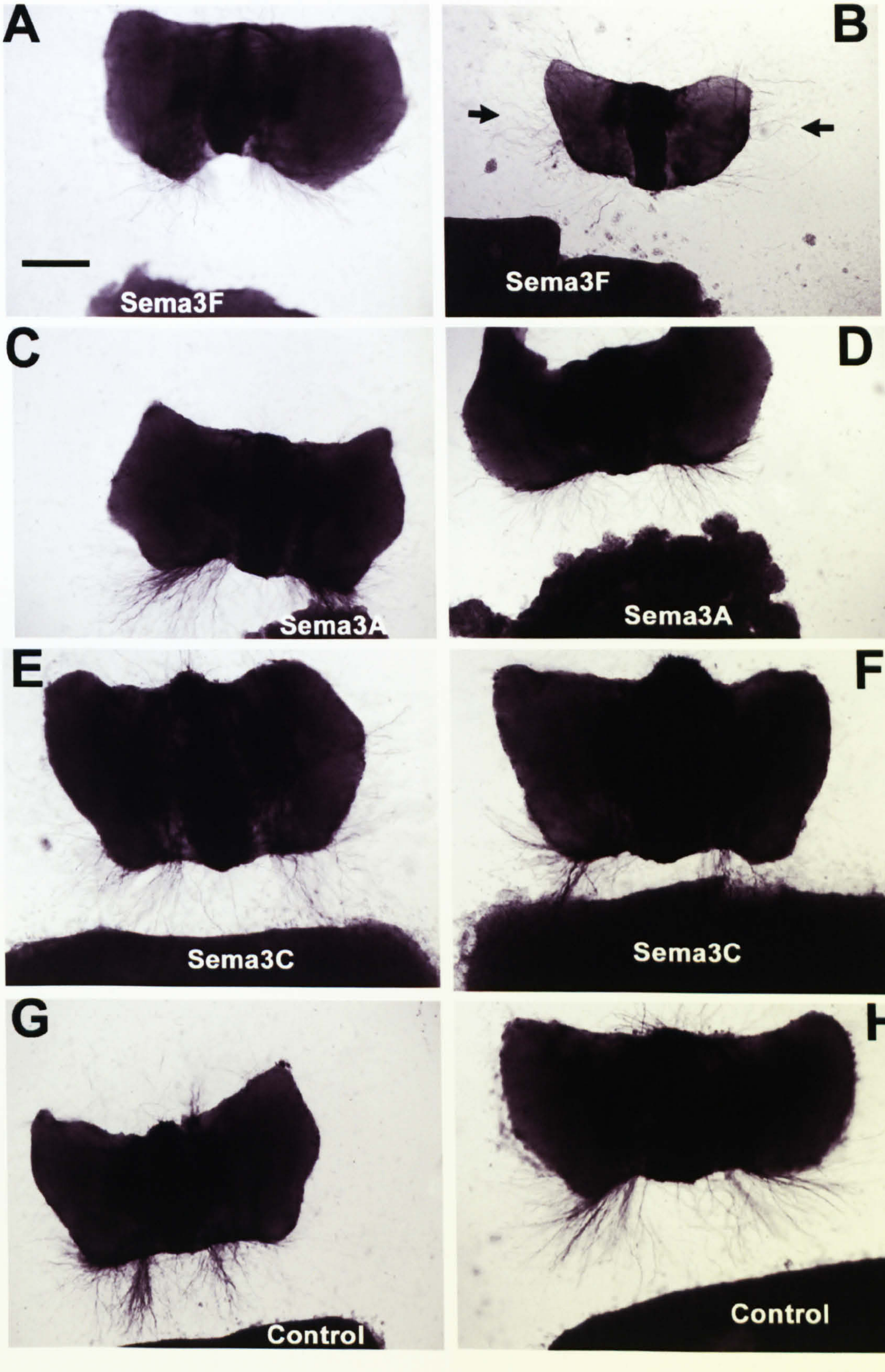
A
Sema3F
B
Sema3F
C
Sema3A
D
Sema3A
E
Sema3C
F
Sema3C
G
Control
H
Control

Figure 4.5

Figure 4.5

Oculomotor explants cultured with clusters secreting different semaphorins or control clusters.

In this and all subsequent figures:
- the caudal edge of the explant is at the bottom and the rostral edge is at the top.
- axons, cell bodies and floor plate are visualised with F84.1 antibody (see section 2.2.6).

(A, B) Oculomotor explants cultured with Sema3F-secreting clusters. Much less outgrowth is observed from the caudal edge of the explants, than is the case in controls (G, H). In some cases (eg B) outgrowth is disorganized with axons turning away from the cluster (marked with arrows).

(C, D) Oculomotor explants cultured opposite Sema3A-secreting clusters. Outgrowth from the caudal edge is similar to that observed in controls.

(E, F) Oculomotor explants cultured opposite Sema3C-secreting clusters. Outgrowth from the caudal edge is similar to that observed in controls.

(G, H) Oculomotor explants cultured opposite control explants. Stained outgrowth occurs from the caudal edge in two broad bundles.

Scale bar (A) – 0.35mm (A, B, C, D, G, H)
0.25mm (E, F)

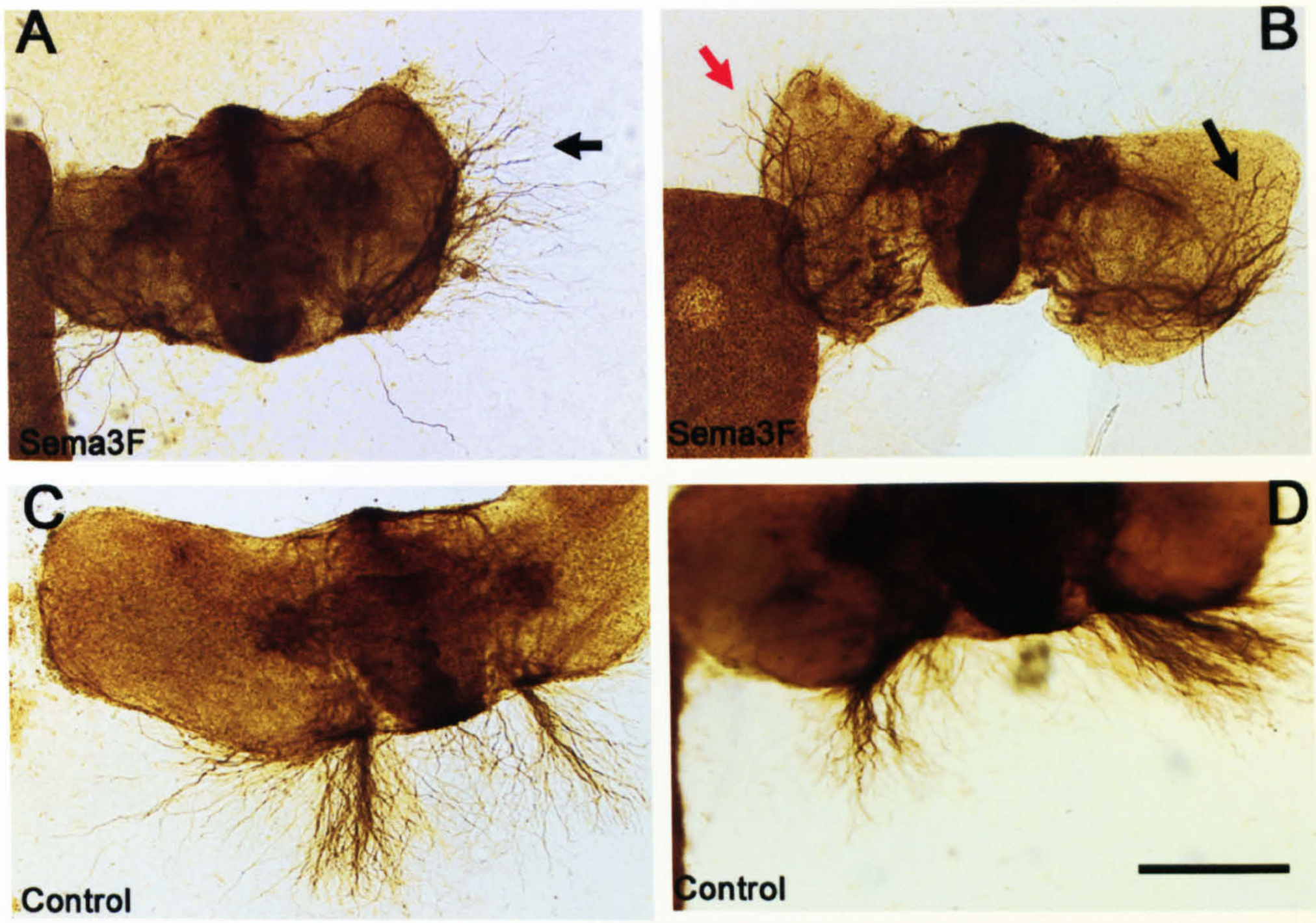

Figure 4.6

Oculomotor (caudal midbrain) explants cultured with Sema3F-secreting clusters (A.B) or control clusters (C, D). Cluster on the left in each case. Outgrowth from the side facing the cluster is normal in control explants (C, D) but inhibited in experimental explants (A, B). In (B) axons on the proximal side reverse direction of growth and emerge from the lateral side above the cluster (red arrow). Outgrowth from the far side is normal in control explants (C, D), but in (A) axons are growing laterally away from the cluster. In (B) axons fail to exit the explant on the far side, but can be seen to be extending laterally within the explant (black arrow). Scale bar (D) is 0.35mm.

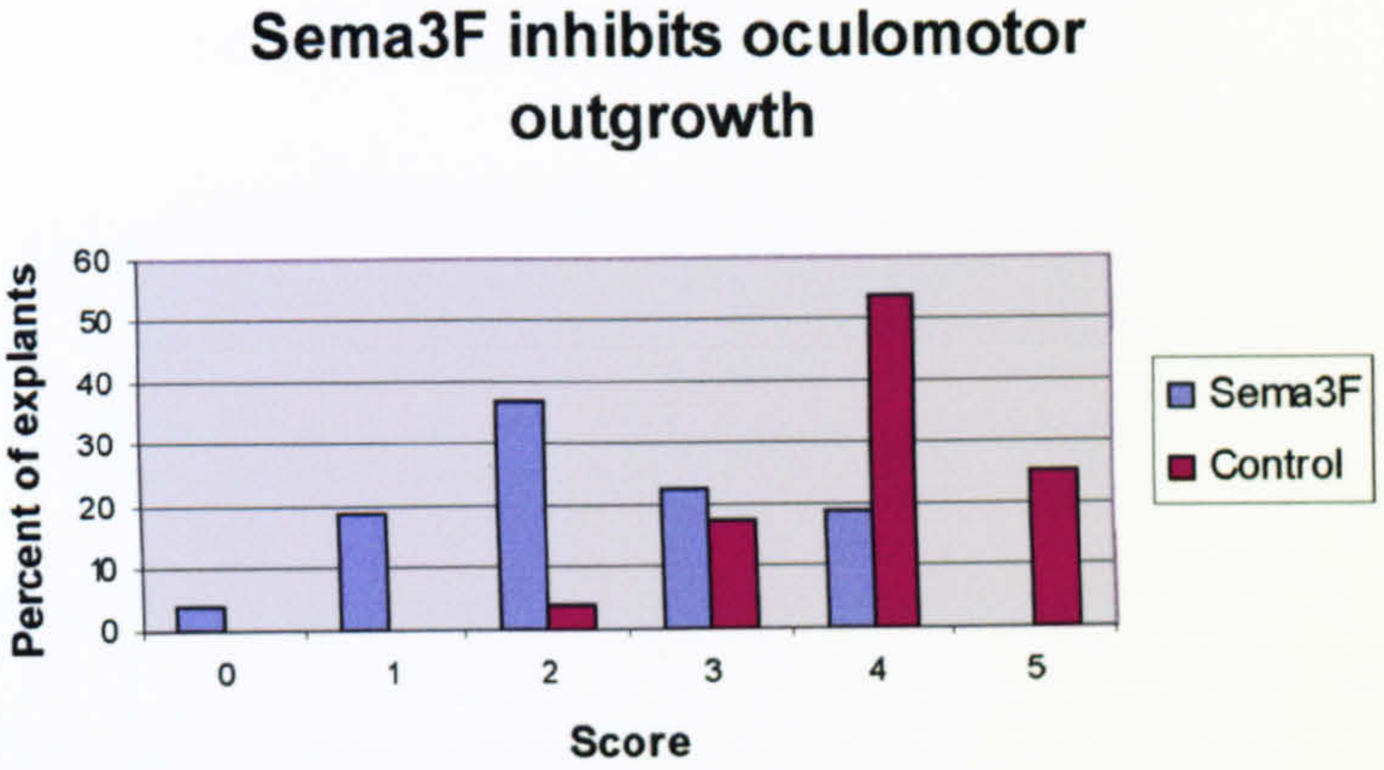

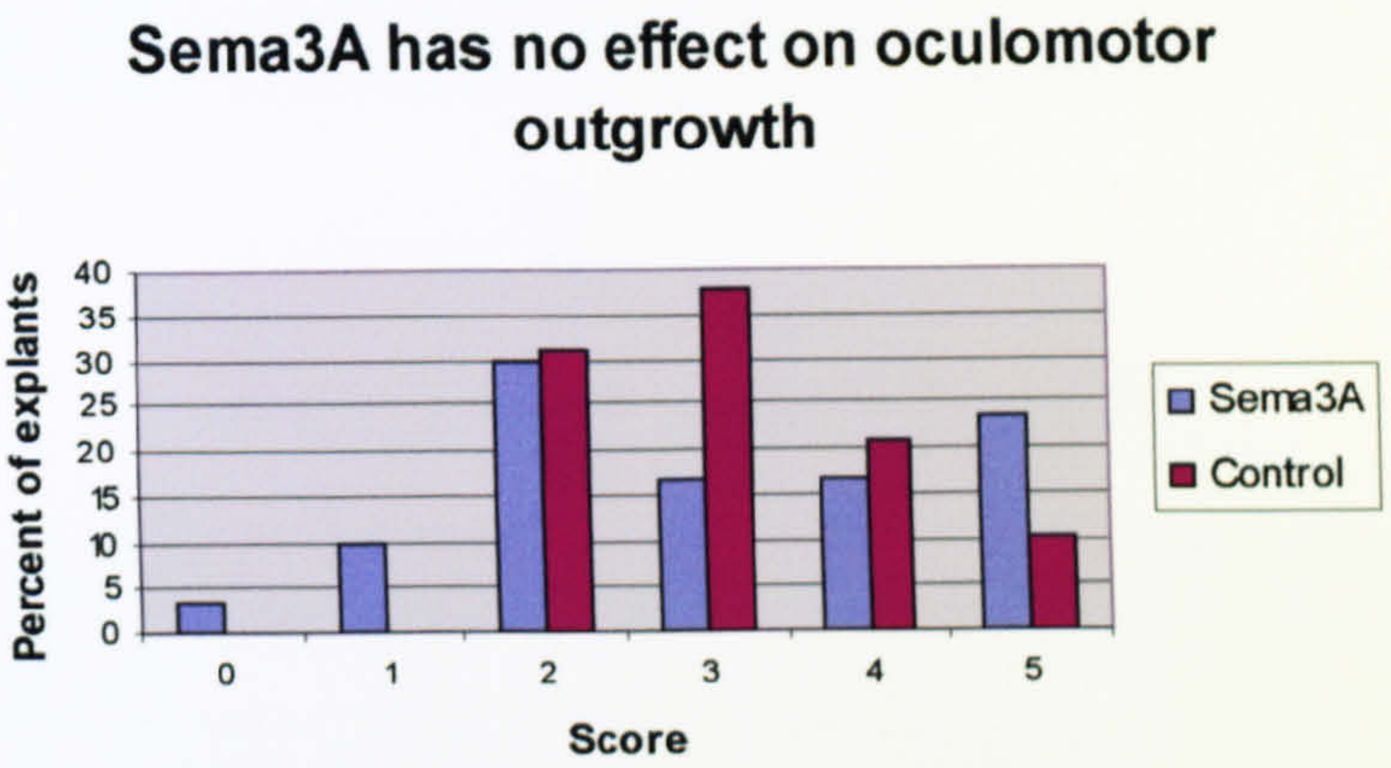

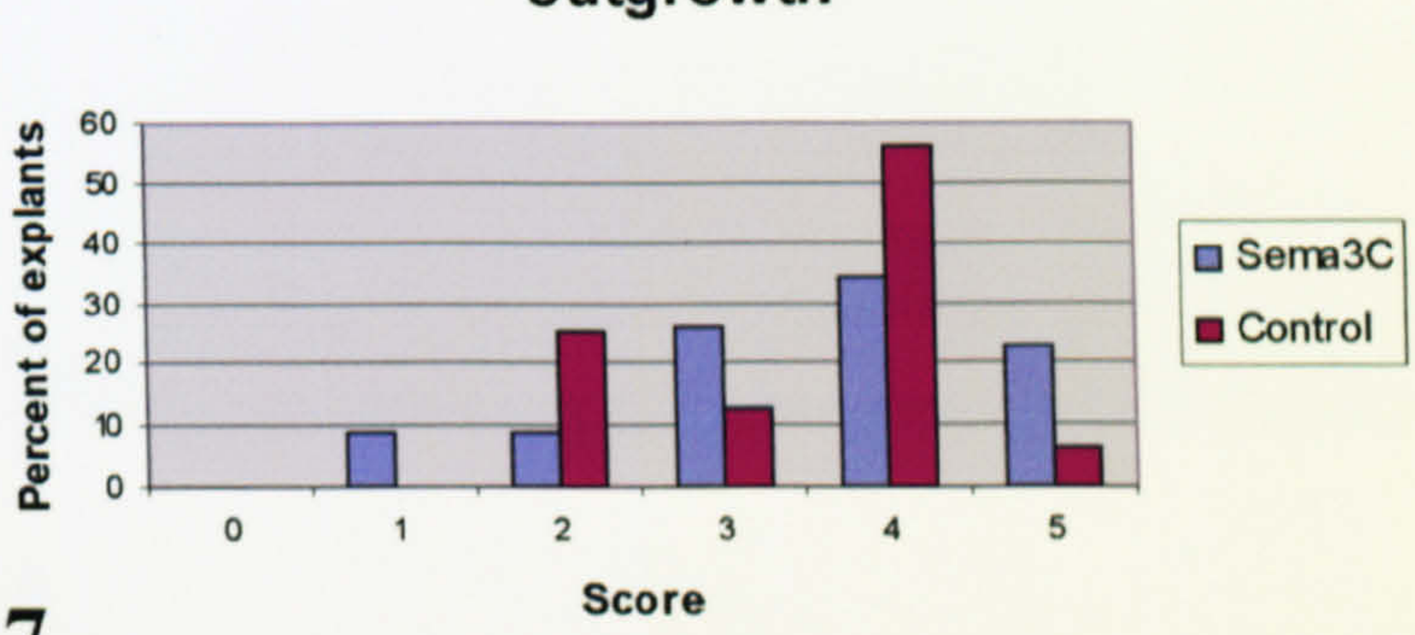

Figure 4.7

The graphs show the distributions of scores for experimental (blue) and control (brown) explants, as assessed on the 0-5 semi-quantitative scale. Sema3F (top graph) inhibits oculomotor outgrowth as evidenced by the shift of the distribution to the left. Sema3A (middle graph) and Sema3C (bottom graph) have no effect.

	Sema 3F	Sema3A	Sema3C
n (experimental)	27	30	35
n (control)	28	29	16
p (Mann Whitney U test)	0.00421	0.83	0.67

A

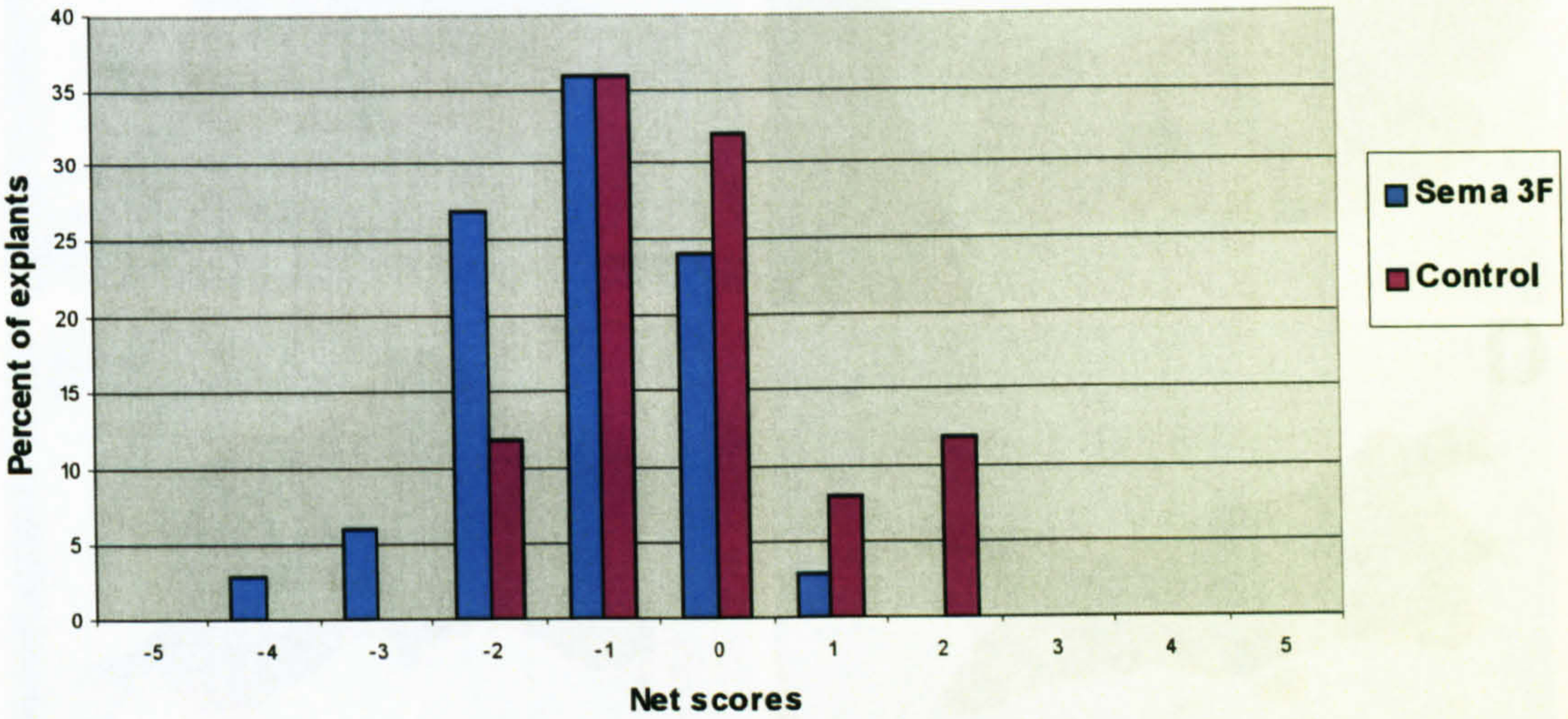

B

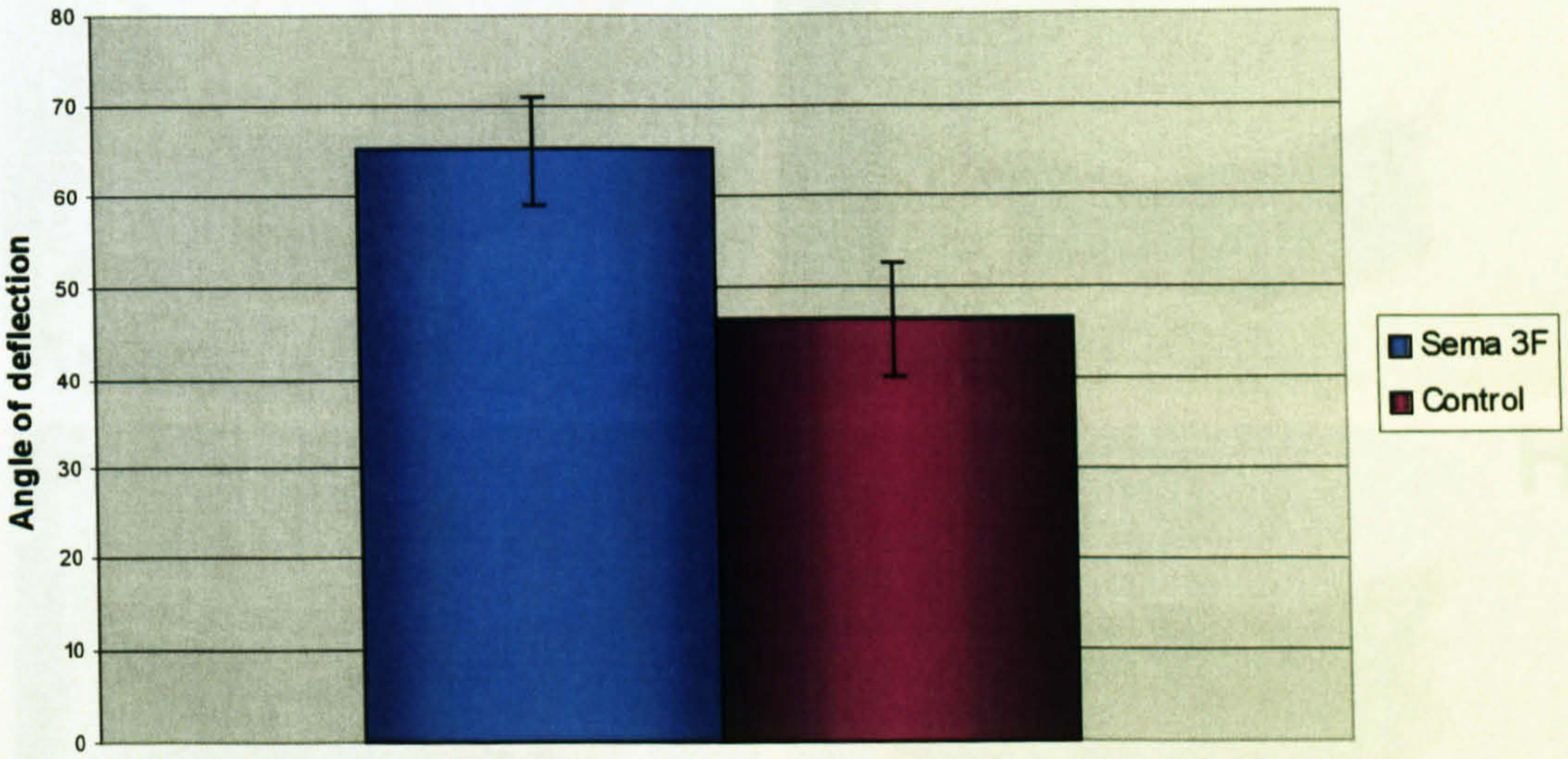

Figure 4.8

The top graph (A) shows the distribution of net outgrowth scores for oculomotor explants in the presence of Sema3F (blue) and controls (brown). The shift to the left for the blue bars indicates an inhibitory effect of Sema3F on oculomotor outgrowth (more explants have negative scores in the presence of Sema3F). This effect is statistically significant ($p=0.012$, Mann Whitney U test). When the angle between the midline and the direction of axonal outgrowth on the distal side of the explant was measured (B), a statistically significant increase was found in the presence of Sema3F compared to control explants ($p=0.0411$), which indicates that oculomotor axons are repelled by Sema 3F. Error bars in (B) indicate the estimated standard error.

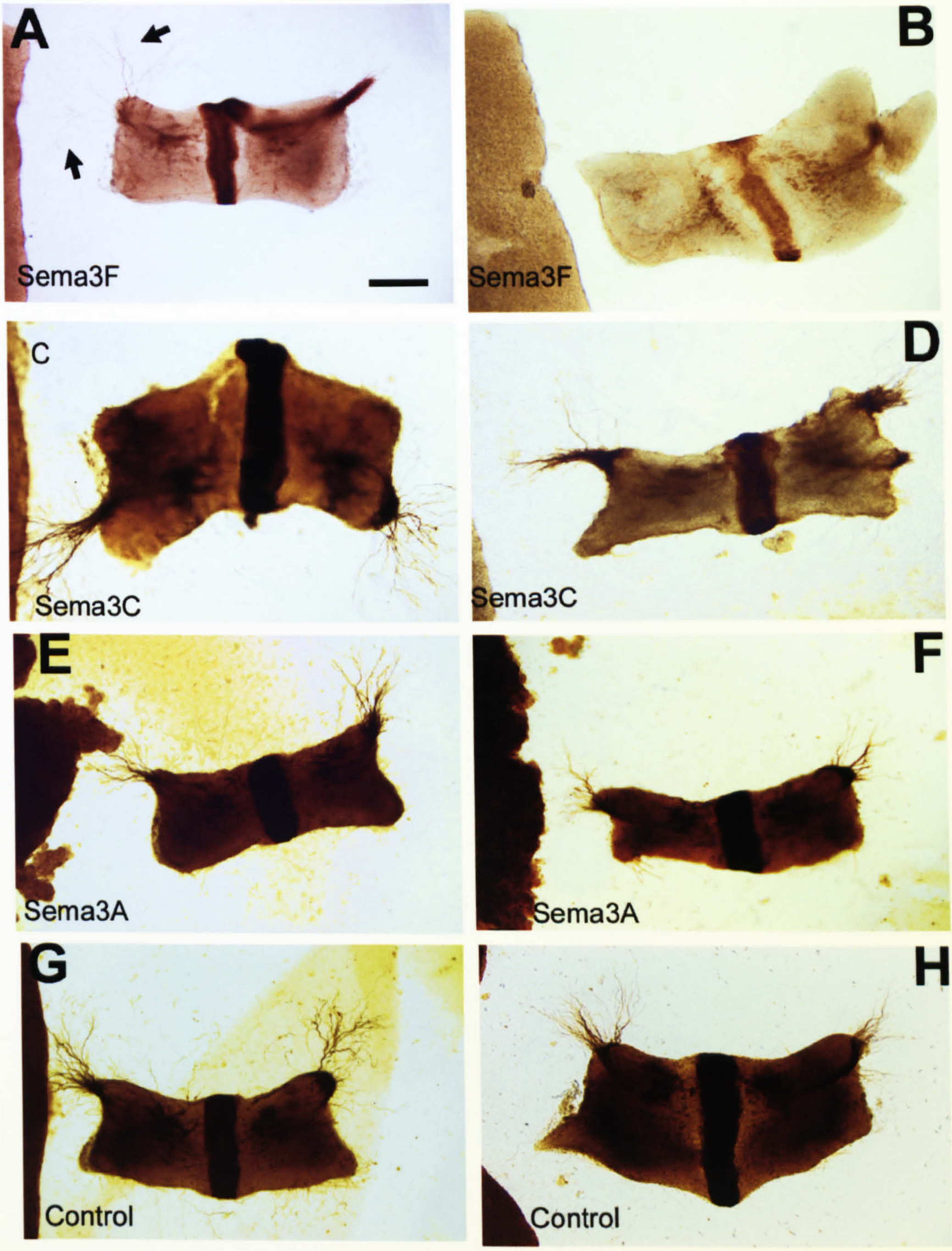
A
Sema3F
B
Sema3F
C
Sema3C
D
Sema3C
E
Sema3A
F
Sema3A
G
Control
H
Control

Figure 4.9

Figure 4.9

Trochlear explants cultured with clusters secreting different semaphorins or control clusters.

(A, B) Trochlear explants cultured with Sema3F-secreting clusters. Very little outgrowth is observed from the half facing the Sema3F cluster. In some cases it consists of a few disorganized axons (A, marked with arrows), and often it is suppressed altogether (B). Outgrowth is sometimes suppressed from the distal half also (B).

(C, D) Trochlear explants cultured with Sema3C-secreting clusters. Outgrowth from the side facing the cluster is similar to outgrowth from the distal side and is similar to outgrowth seen in controls.

(E, F) Trochlear explants cultured with Sema3A-secreting clusters. Outgrowth from the side facing the cluster is similar to outgrowth from the distal side and is similar to outgrowth seen in controls.

(G, H) Trochlear explants cultured with control explants. Outgrowth is in two bundles, one from the lateral edge of the side facing the cluster and one from the lateral edge away from the cluster and is fairly symmetrical.

Scale bar (A) – 0.3mm (A, D, E, F, G,)
0.22mm (B, C, H)

A

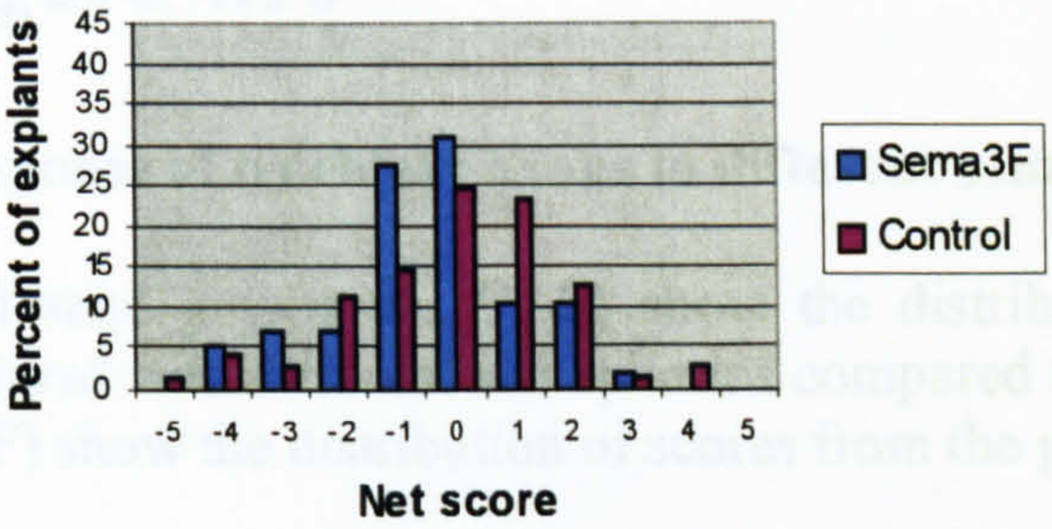

B

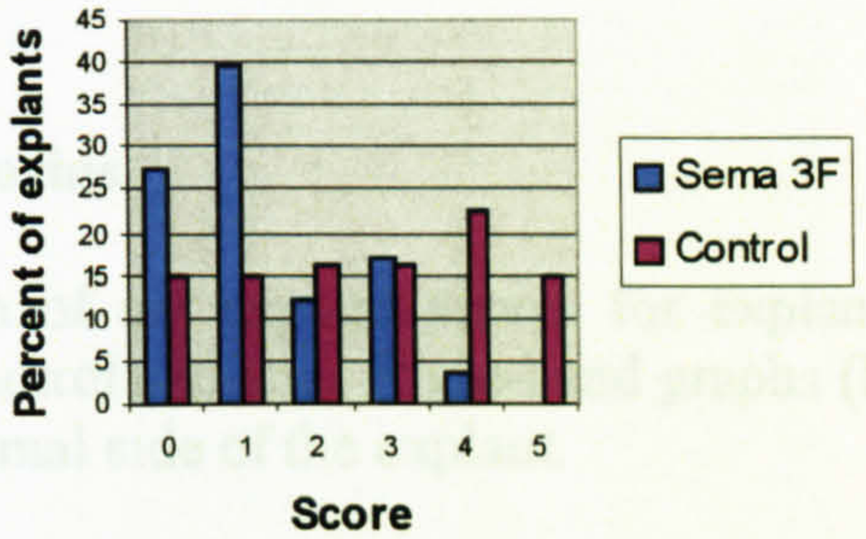

C

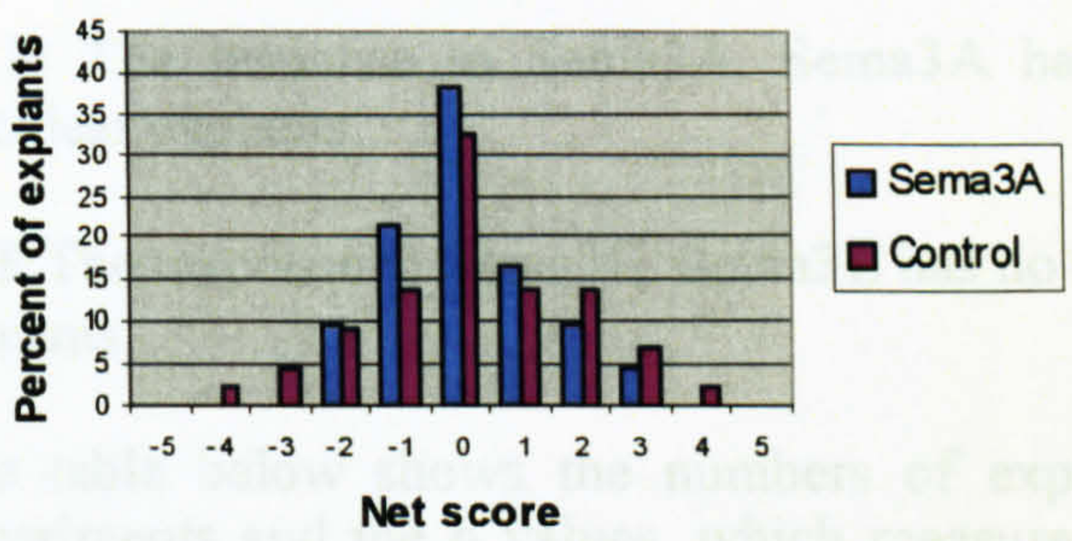

D

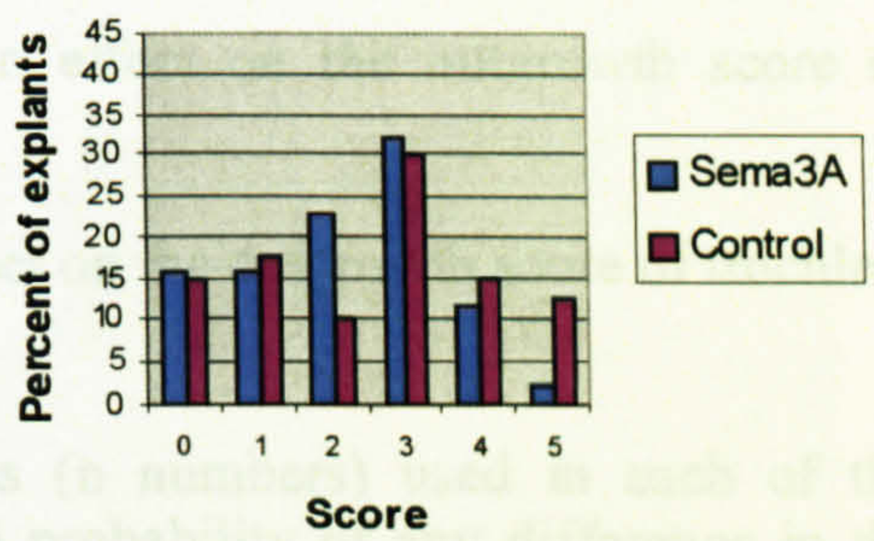

E

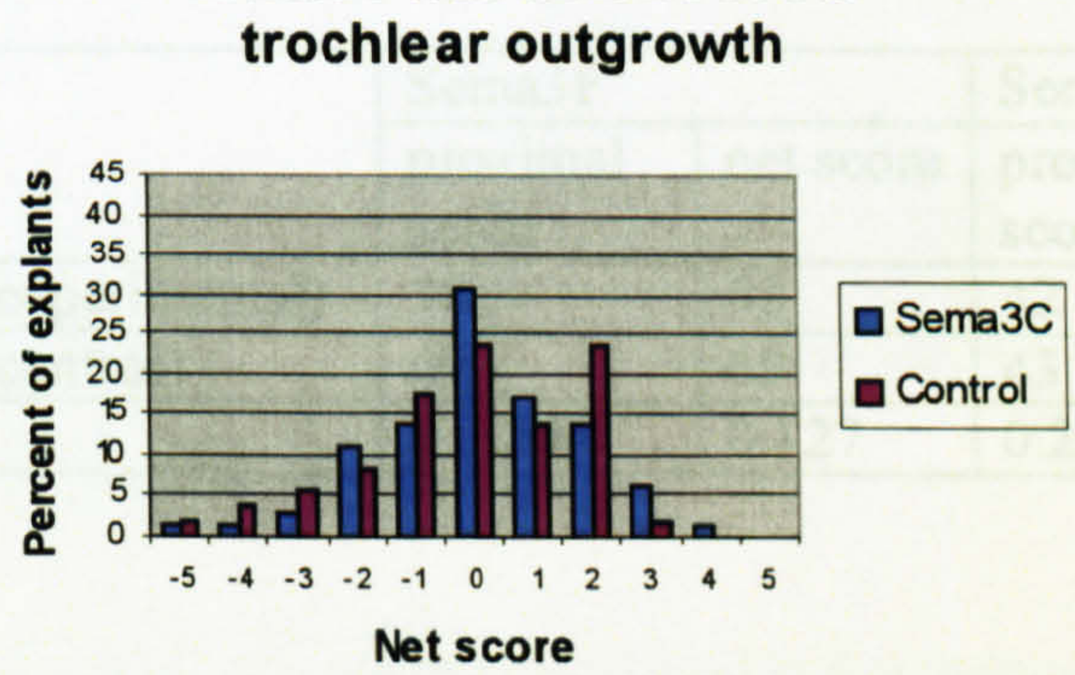

F

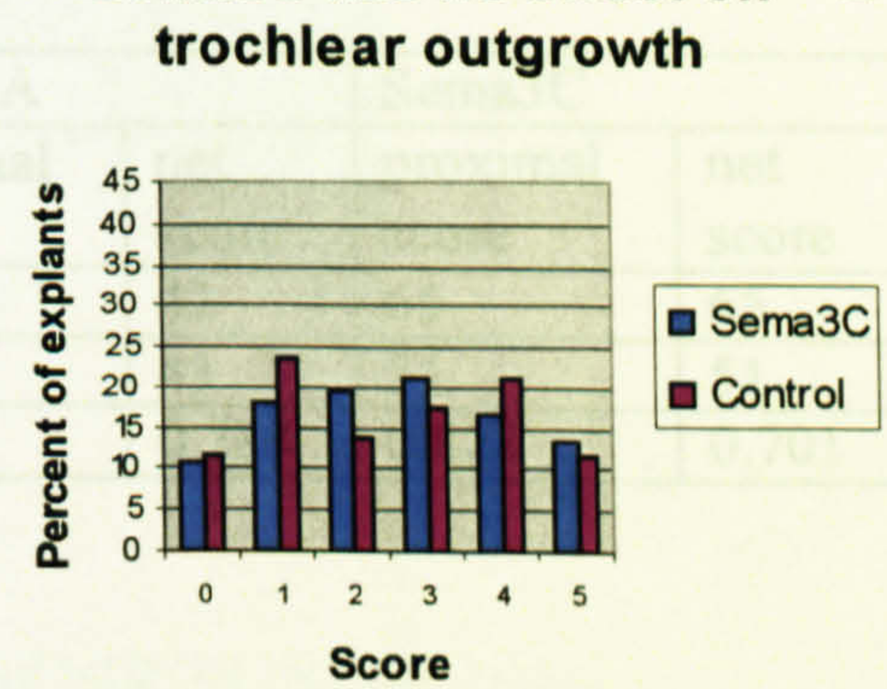

Figure 4.10.

Figure 4.10

Response of trochlear axons to different semaphorins

Left-hand graphs (A, C, E) show the distribution of net explant scores for explants cultured with different semaphorins compared to control explants. Right-hand graphs (B, D, F) show the distribution of scores from the proximal side of the explant.

A, B The response to Sema3F. Outgrowth from the proximal side (B) is dramatically inhibited in the presence of Sema3F. The net score (A), however, is only slightly reduced in the presence of Sema3F, probably because it inhibits outgrowth from the distal side also.

C, D The response to Sema3A. Sema3A has no effect on the outgrowth score of trochlear explants.

E, F The response to Sema3C. Sema3C has no effect on the outgrowth score of trochlear explants.

The table below shows the numbers of explants (n numbers) used in each of the experiments and the p values, which measure the probability of any difference in the scores distribution between the control and experimental groups having arisen by chance. A p value of less than 0.05 indicates a statistically significant effect.

	Sema3F		Sema3A		Sema3C	
	proximal score	net score	proximal score	net score	proximal score	net score
n (experimental)	58	58	42	42	65	65
n (control)	69	69	43	43	51	51
p	0.00984	0.127	0.27	0.738	0.822	0.701

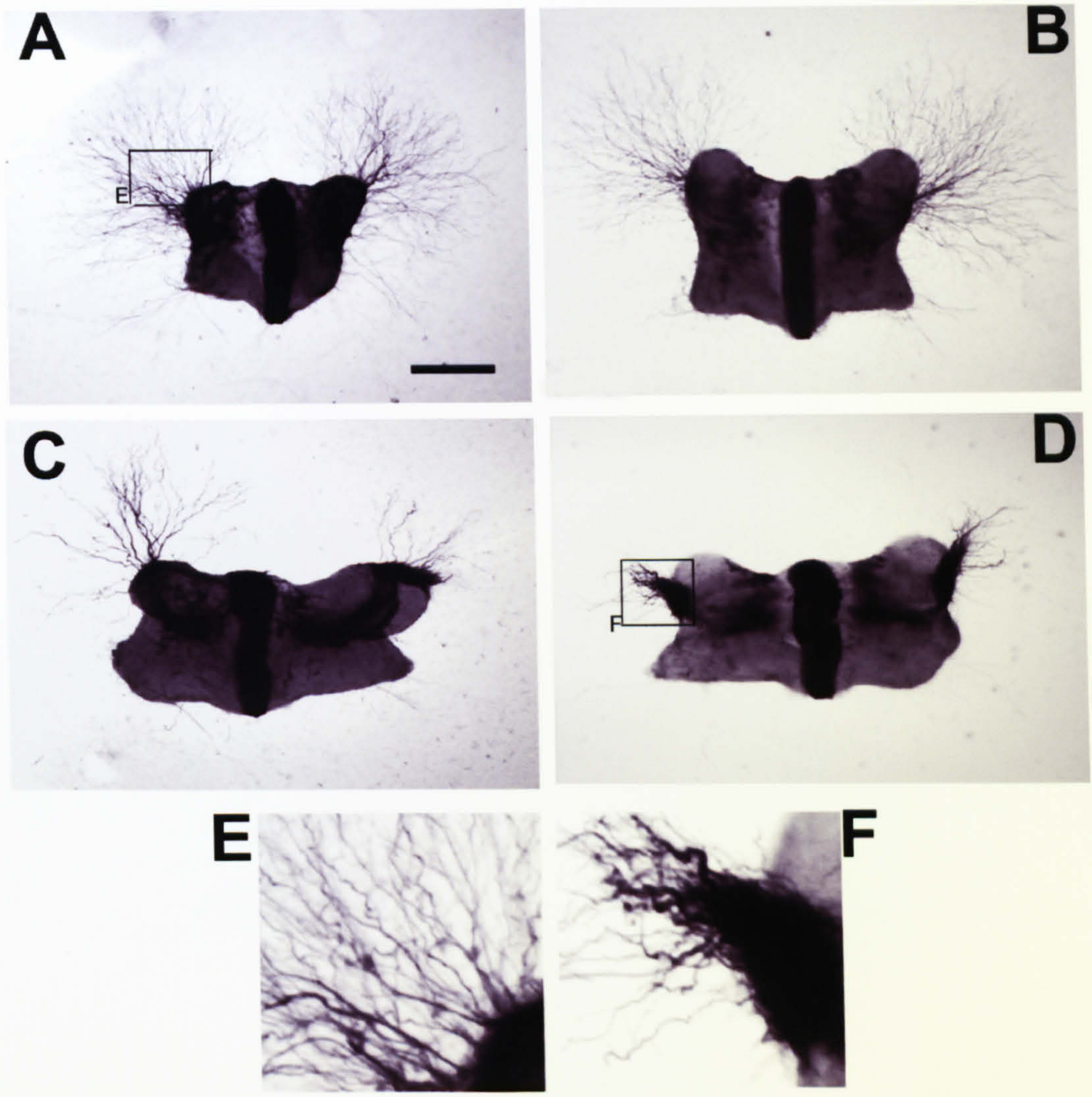

Figure 4.11

Trochlear (r1) explants cultured in the presence of HGF (A, B) and in the absence of HGF (C,D).In control explants (C,D) two stained axonal bundles are seen to exit the lateral side of the explant exhibiting a greater (D) or lesser (C) degree of fasciculation. In experimental explants (A, B) a drastic increase in axonal outgrowth is observed, with an increase in the number of axons, their length, and the area over which they are spread. The axons also appear on the whole less fasciculated than in control explants. Panel (E) shows a higher power image of trochlear axons cultured with HGF (magnified from (A) - see box) and panel (F) shows a higher power image of trochlear axons in a control explant (magnified from (D) - see box)
Scale bar (A) = 0.3mm (A - D)
75µm (E - F)

A

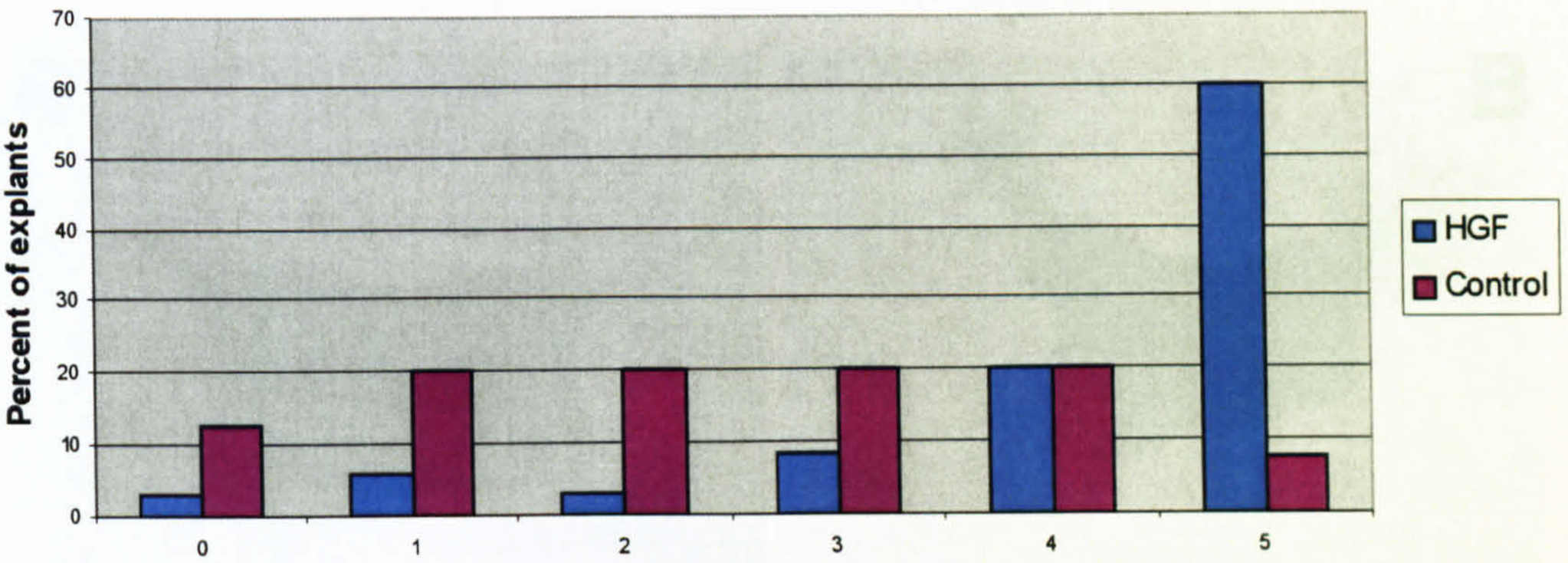

B

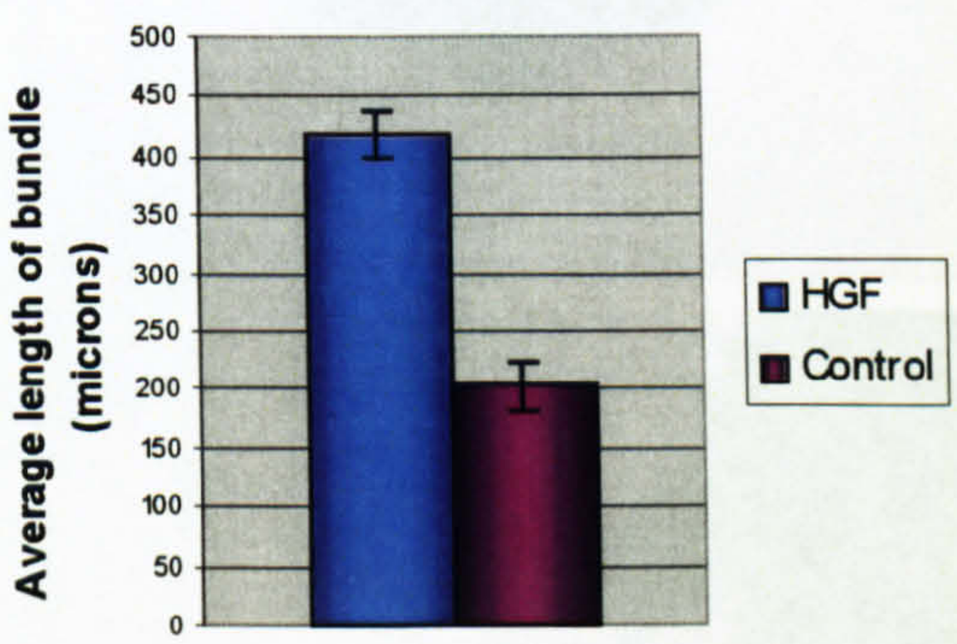

C

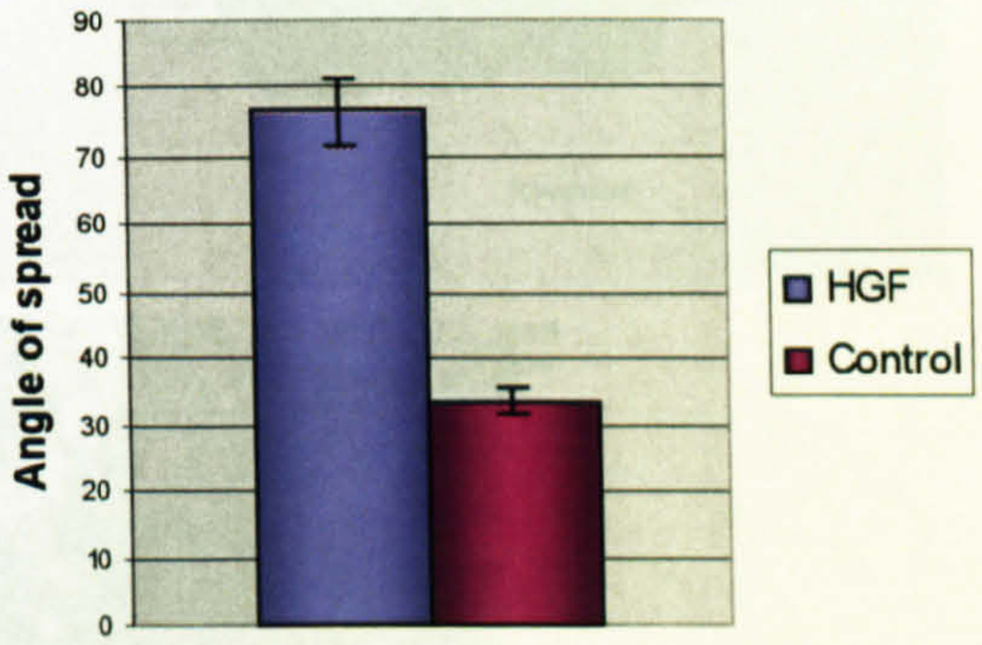

Figure 4.12

The distribution in the top graph (A) clearly shows a dramatic increase in trochlear outgrowth in the presence of HGF with 60% of explants scoring the maximum value, compared with 8% of control explants. Graph B shows the average angle over which the bundle of trochlear axons is spread, this more than doubles from 34° to 77° in the presence of HGF. Average length of axonal bundles (C) also doubles from 203 to 418 micrometers in the presence of HGF. Error bars in (B) and (C) indicate the estimated standard error.

	Score (median)	Angle of spread (mean)	Average length (mean)
HGF (n=35)	5	77°	203μm
Control (n=40)	2	34°	418μm
p	0.00392 (Mann Whitney U test)	1.11×10^{-6} (Student's t-test)	1.33×10^{-5} (Student's t-test)

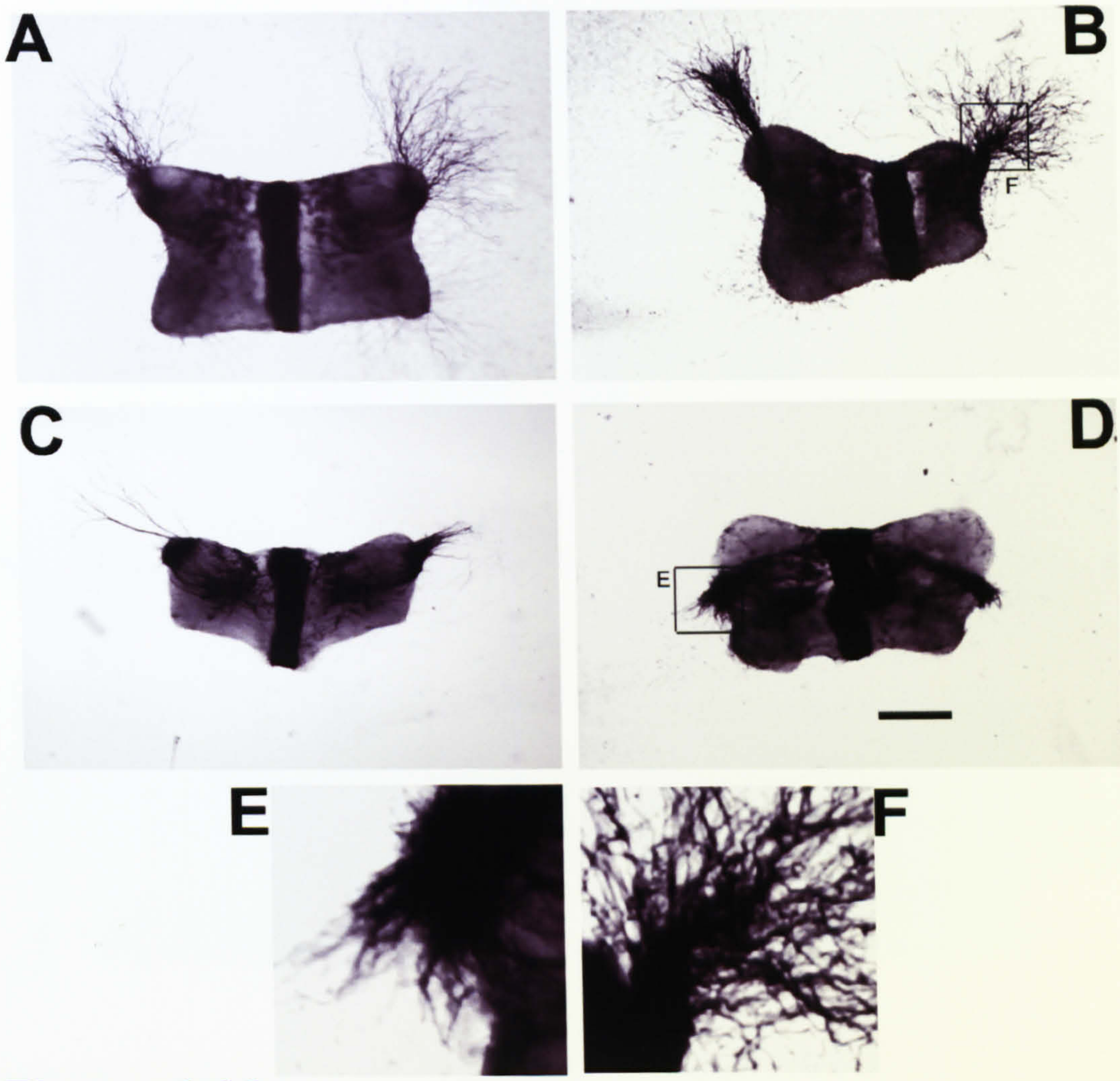

Figure 4.13

Trochlear (r1) explants cultured in the presence of SDF-1 (A, B) or in the absence of SDF-1 (C,D). SDF markedly increasesoutgrowth with longer and denser bundles observed (A, B) compared to controls (C, D). The fasciculation of trochlear axons in the presence of SDF-1 is comparable to the controls - see higher power images of trochlear axons with SDF-1(F) and without SDF-1 (E).
Scale bar (D) = 0.3mm (A - D)
75µm (E, F)

A

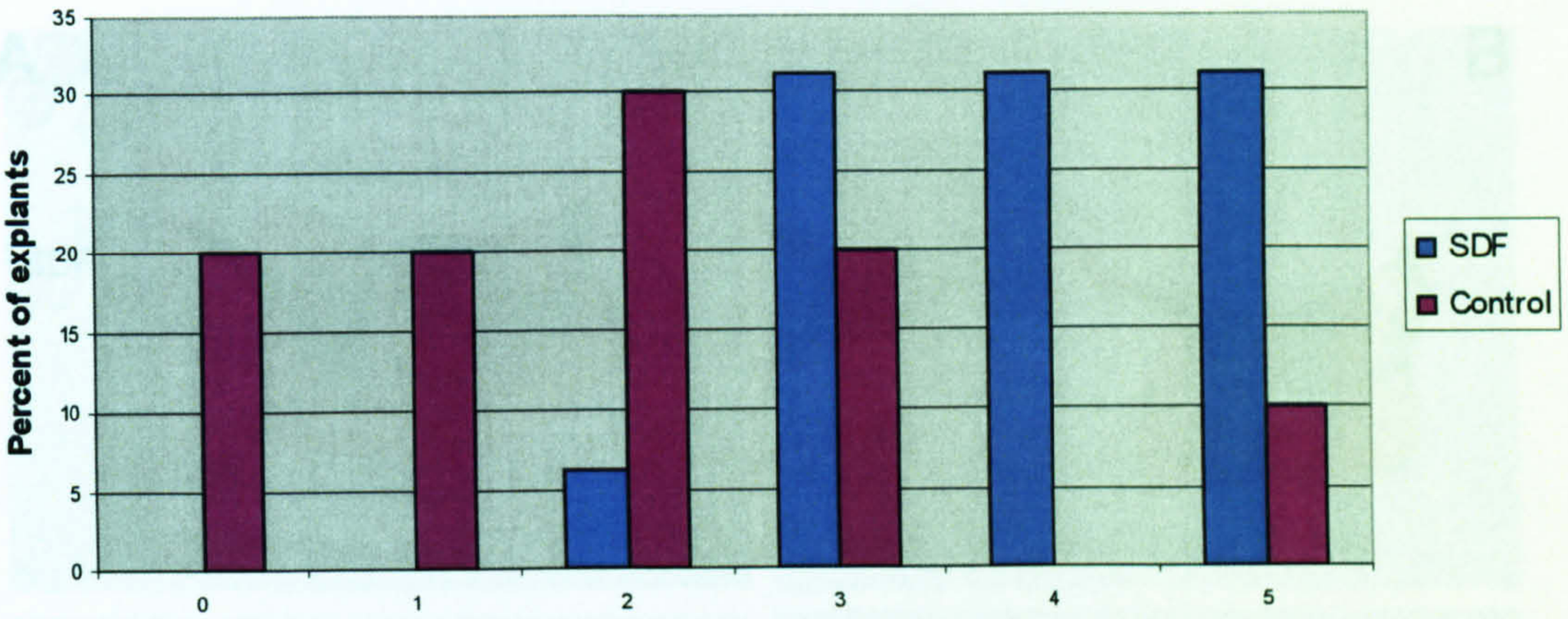

B

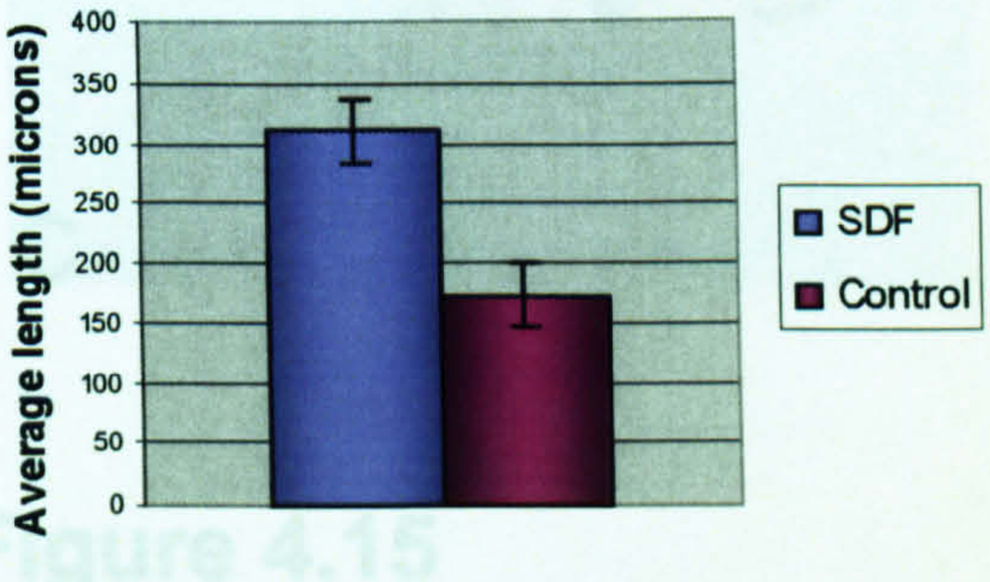

C

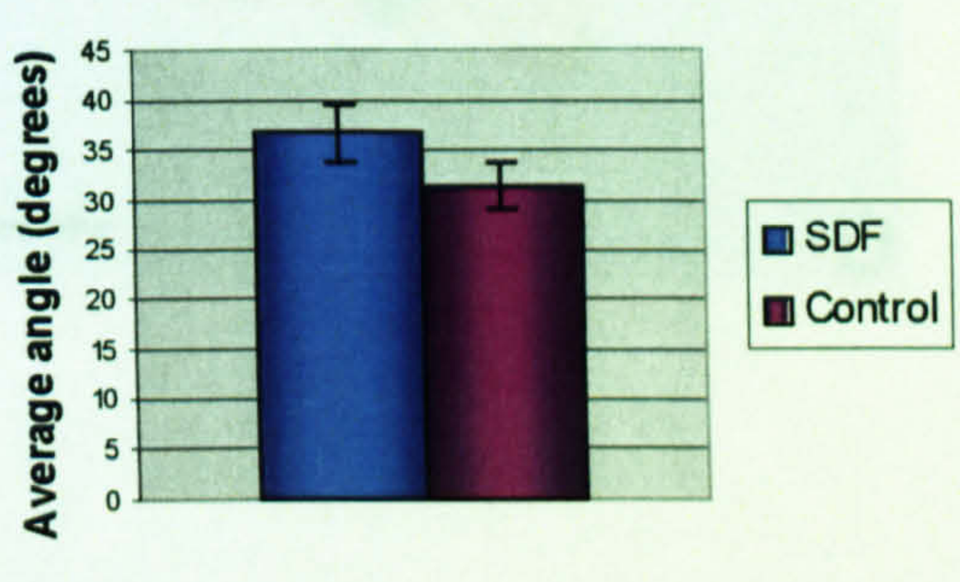

Figure 4.14

The top graph (A) shows the distribution of outgrowth scores for trochlear explants in the presence and absence of SDF. SDF clearly promotes trochlear outgrowth as can be seen from the change in distribution, with 94% of explants having a score of 3 or above in the presence of SDF, compared to 30% of controls. Graph B demonstrates that the average length of the trochlear bundle increase significantly in the presence of SDF, from 172 micrometers to 311 micrometers. Average angle of spread of the trochlear bundle, however, isn't significantly altered (31° in controls, 37° in the presence of SDF — (C)).

	Explant score (median)	Average length (mean)	Average angle (mean)
SDF (n=16)	4	311μm	31°
Control (n=20)	2	172μm	37°
p	2.22×10^{-4}	6.48×10^{-4}	0.155

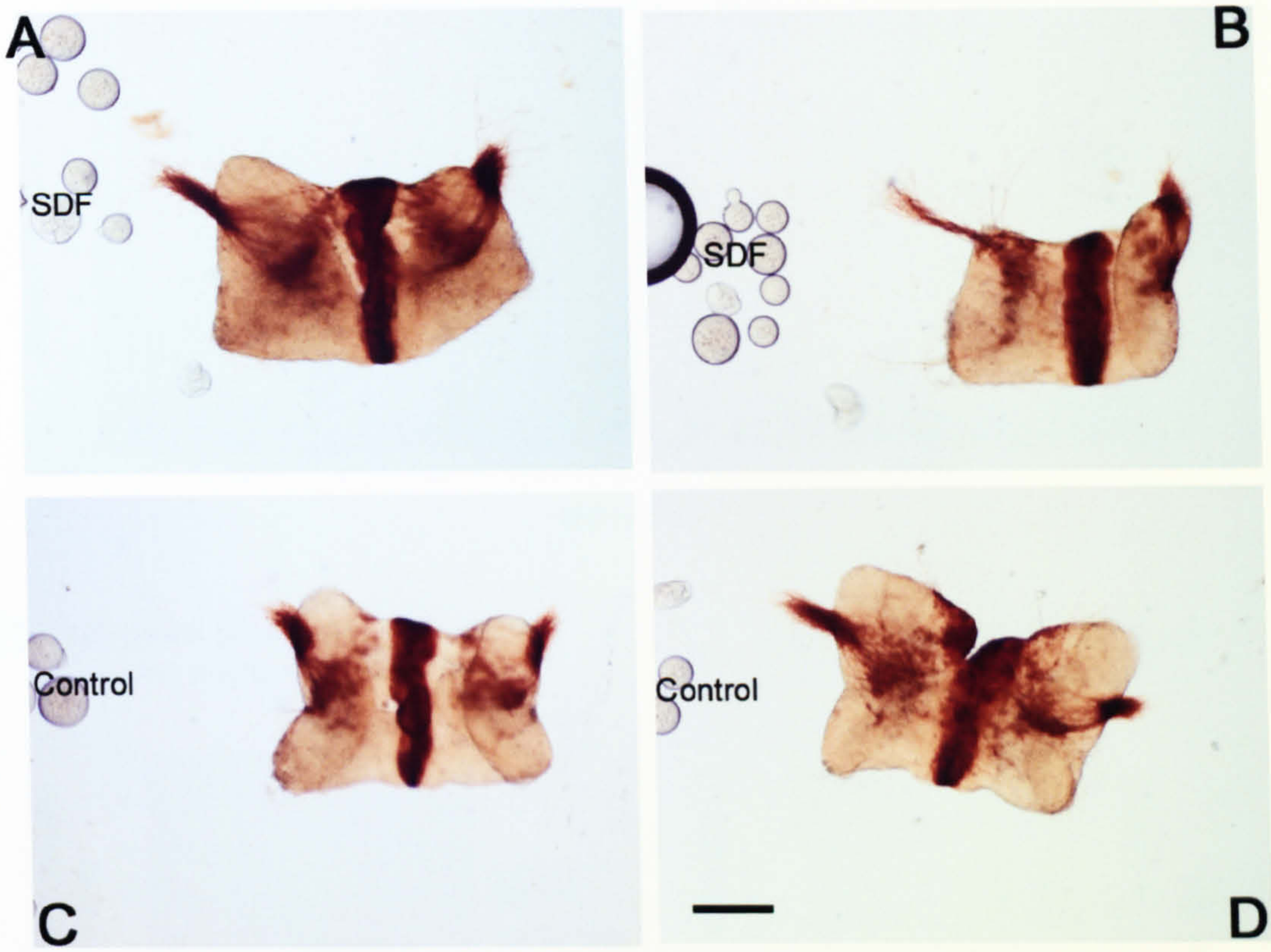

Figure 4.15

Trochlear (r1) explants cultured opposite a cluster of heparin-coated beads pre-soaked with SDF-1 protein (A, B) and explants cultured with PBS-soaked heparin beads (C, D). Outgrowth towards SDF-soaked beads appears enhanced comparedto the outgrowth towards control beads, and compared to outgrowth from the distal side of the explant. However, the increase in axonal length is not statistically significant (see figure 4.16).
Scale bar (D) = 0.3mm.

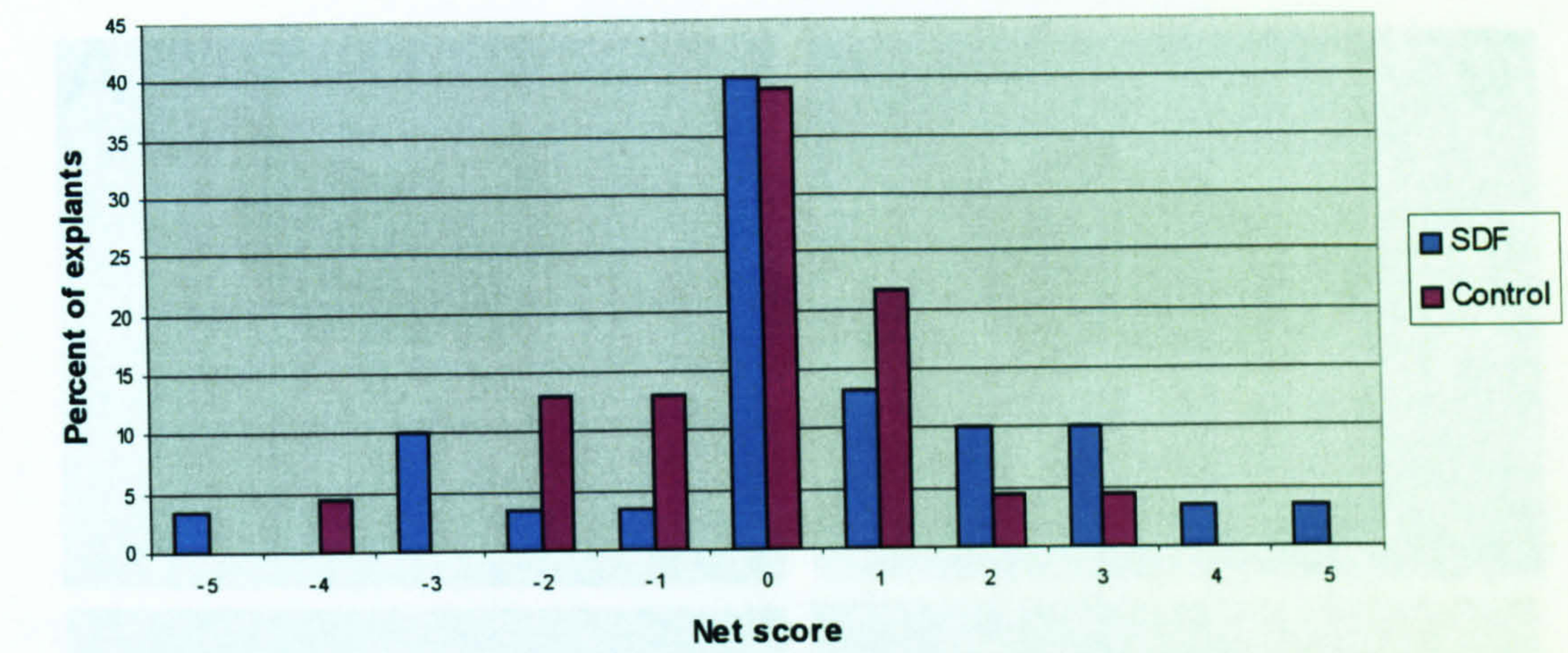

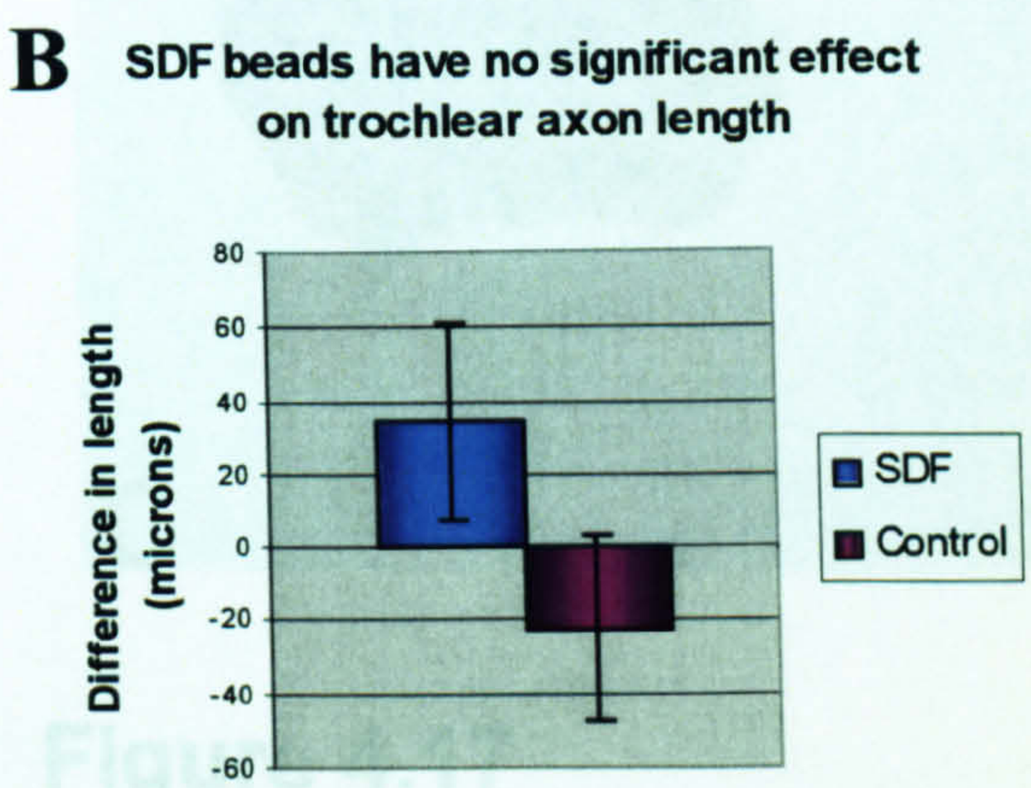

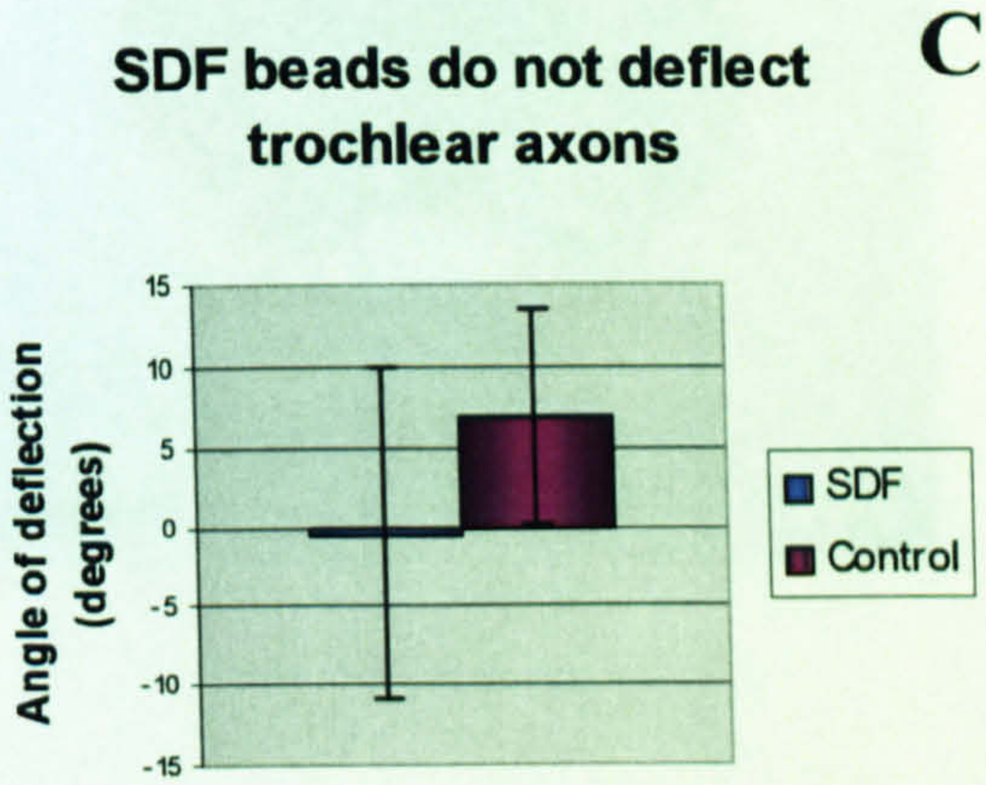

Figure 4.16

SDF released from beads has no effect on trochlear axons. Graph A shows the distribution of net scores for explants that have been cultured opposite SDF beads compared to explants cultured opposite control beads. No significant difference in the distribution of scores is observed. There is a slight increase in the average length of axonal bundles facing the SDF beads compared to bundles facing away from the beads (B) , but this increase is not statistically significant relative to the situation observed in the controls. Graph C shows the angle of deflection towards the beads, and again there is no effect. Error bars in (B) and (C) indicate the estimated standard error.

	Net score (median)	Difference in length (mean)	Angle of deflection (mean)
SDF (n=30)	0	35μm	-0.5°
Controls (n=23)	0	-22μm	7°
p	0.304 (Mann Whitney U test)	0.138 (Student's t-test)	0.536 (Student's t-test)

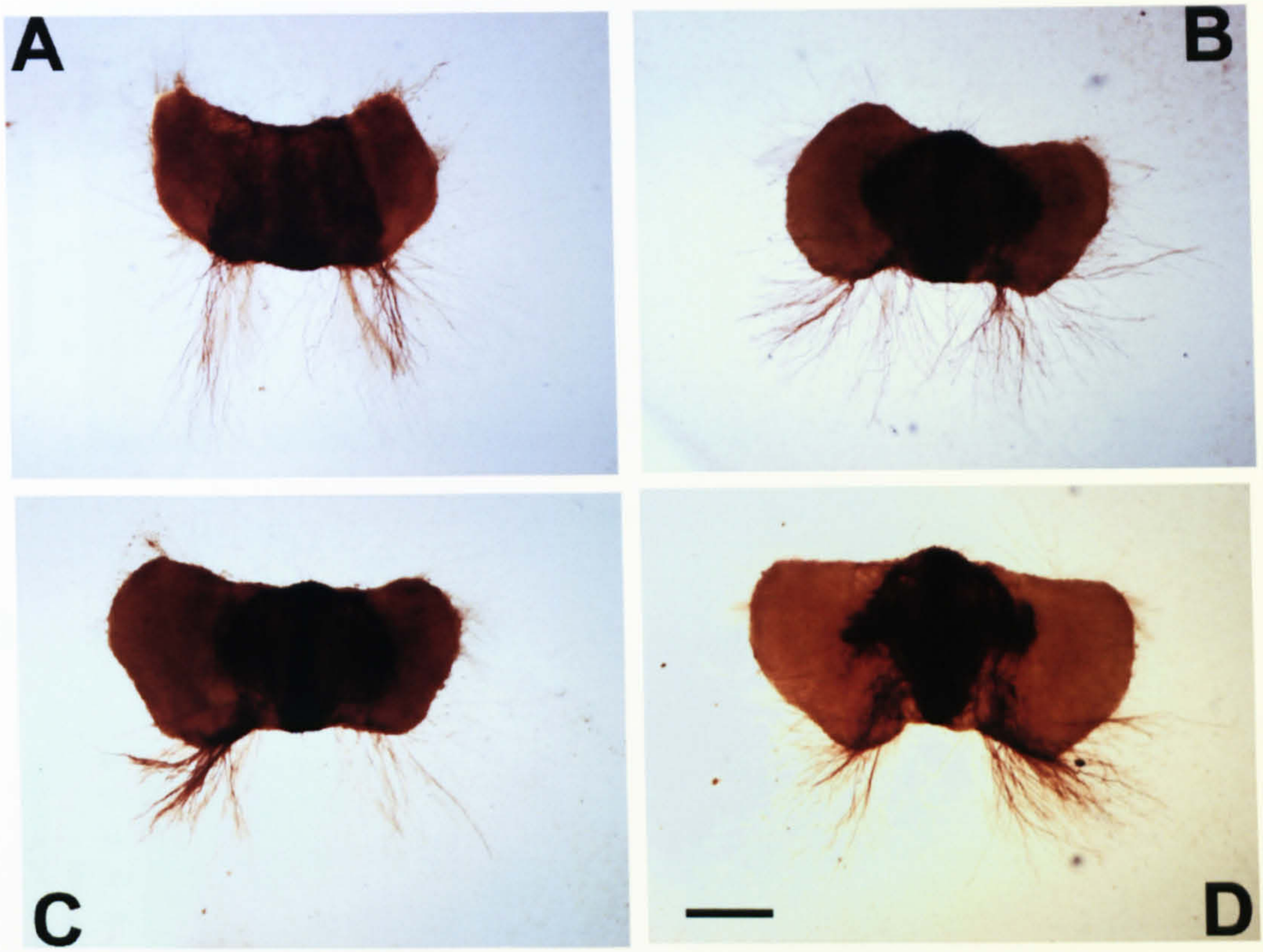

Figure 4.17

Oculomotor explants cultured in the presence (A, B) and in the absence (C, D) of HGF. Addition of HGF to the growth medium increases motor axon outgrowth from the caudal edge of the explants
Scale bar (D) = 0.3mm

A

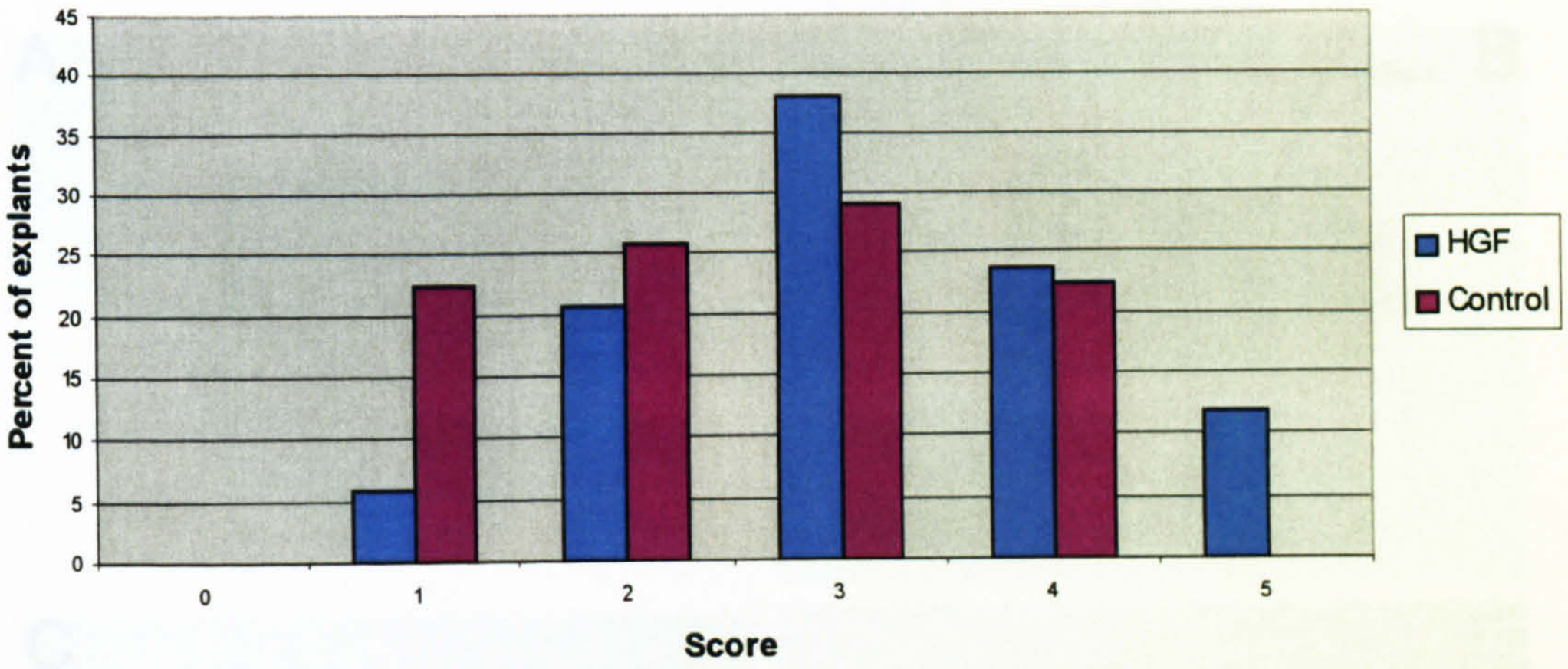

B

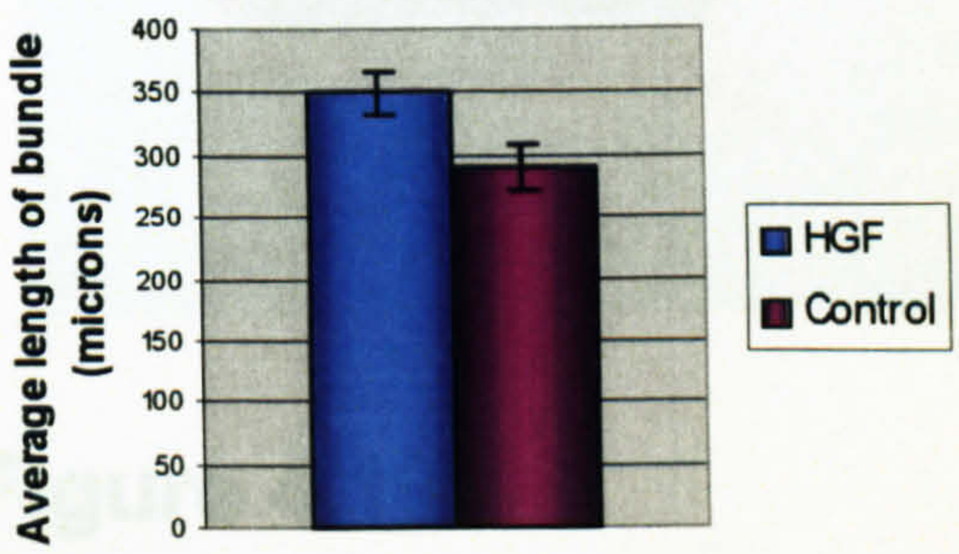

C

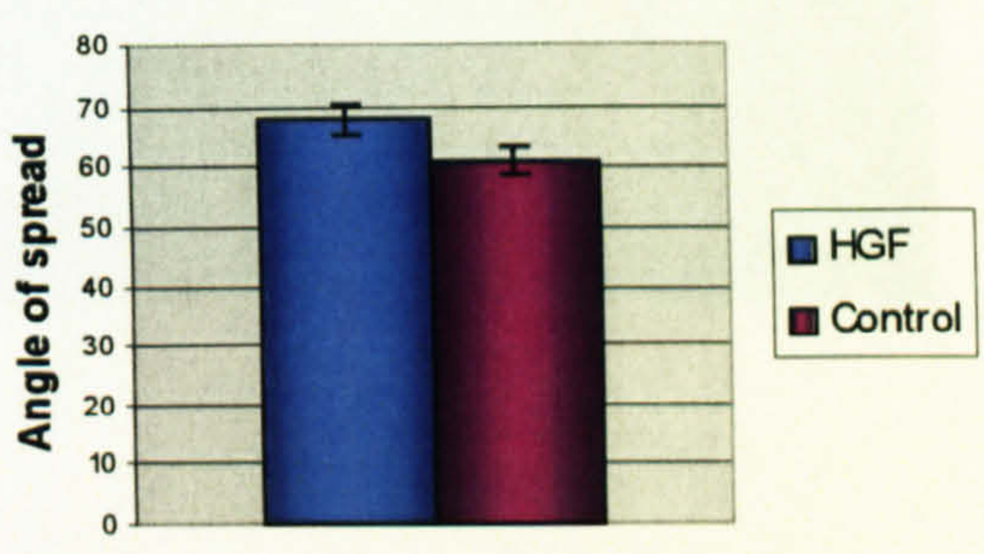

Figure 4.18

The top graph (A) shows the distribution of scores for oculomotor explants cultured in the presence of HGF and in the absence of HGF. HGF increases oculomotor outgrowth as evidenced by the rightward shift in the scores distribution for the experimental explants (48% of control explants score 2 or less, compared to 26% of experimental explants). Graph B shows the average length of axonal bundles, where there is a small but significant increase in the presence of HGF (from 290 to 350 micrometers). Similarly graph C shows that there is a small but significant increase in the angle of spread of oculomotor axons (from 61° to 67°). Error bars in (B, C) indicate the estimated standard error.

	Explant score (median)	Average length (mean)	Average angle of spread (mean)
HGF (n=34)	3	350μm	61°
Control (n=31)	3	290μm	67°
p	0.0424 (Mann Whitney U test)	0.0171 (Student's t-test)	0.0465 (Student's t-test)

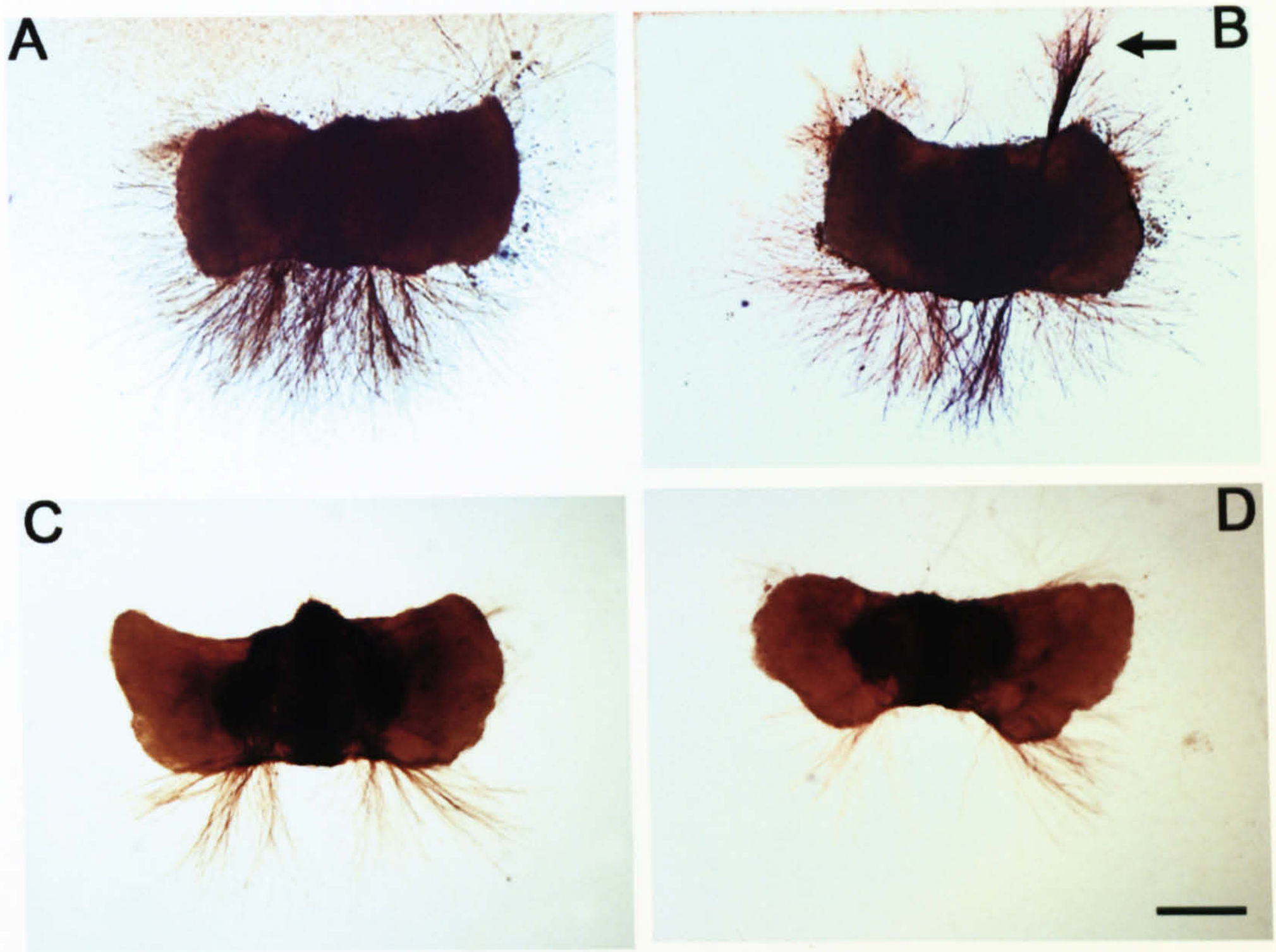

Figure 4.19

Oculomotor explants cultured in the presence (A, B) or absence (C,D) of SDF. Motor axon outgrowth occurs from the caudal edge of the explants. In the presence of SDF outgrowth was markedly increased, with denser and longer bundles of axons observed (A, B). In some cases bundles of stained axons emerged from the rostral edge of the explant (B - marked with arrow), a situation never observed in control explants.
Scale bar (D) = 0.3mm

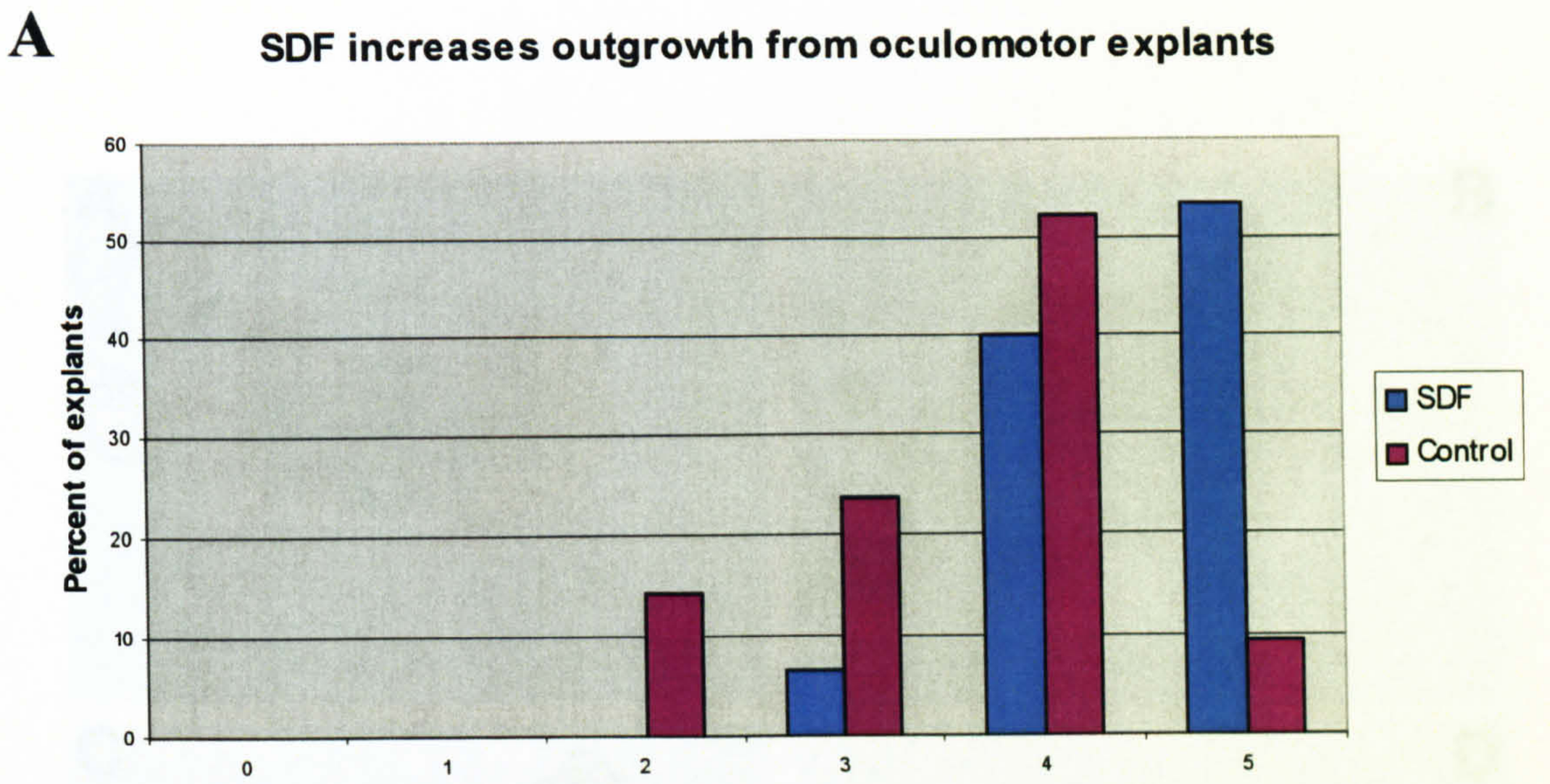

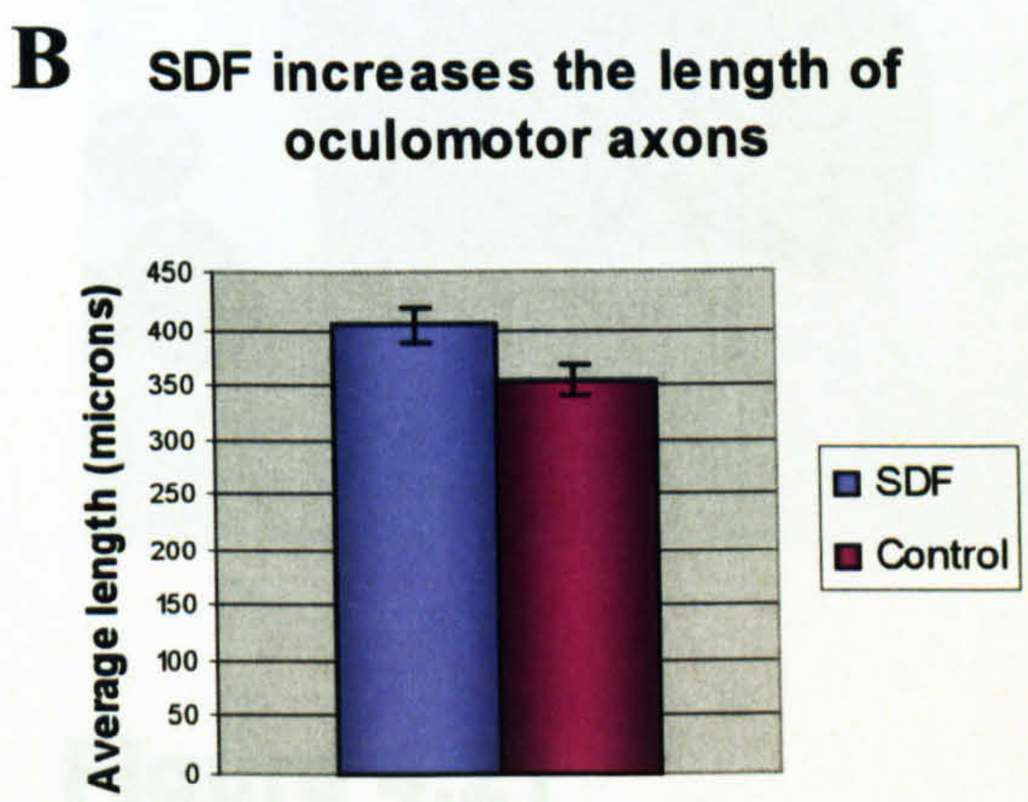

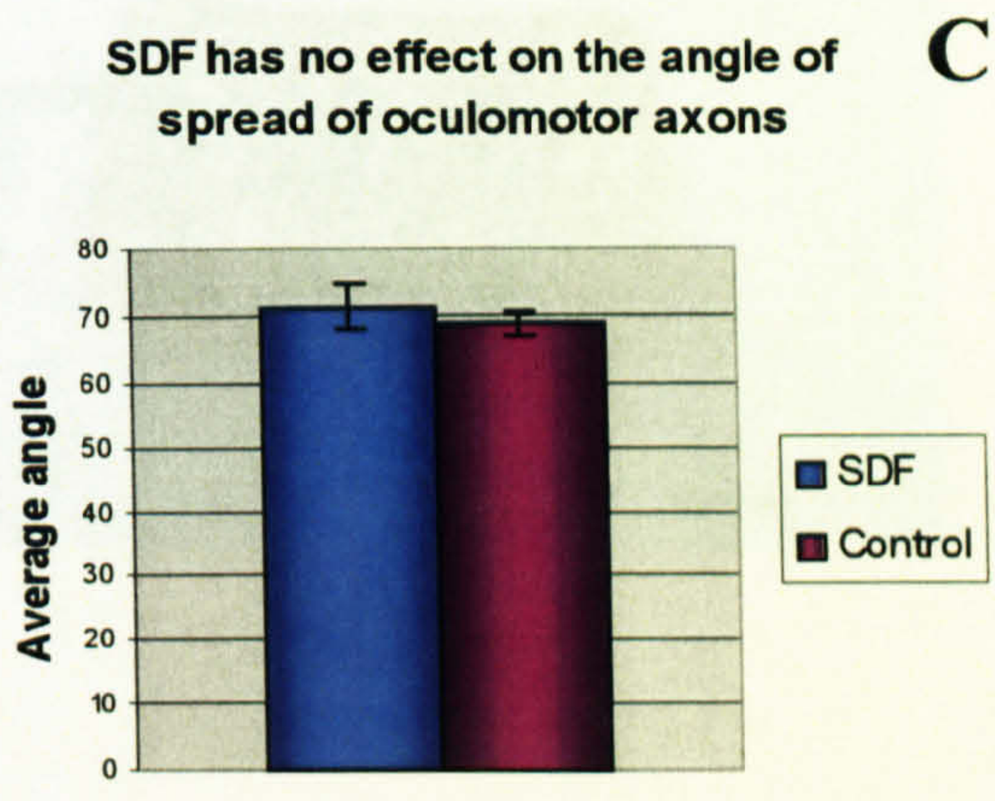

Figure 4.20

The top graph (A) shows the distribution of scores for oculomotor explants cultured in the presence and absence of SDF. There is a shift to the right in the distribution of scores for explants cultured with SDF, indicating that SDF is promoting oculomotor outgrowth. (B) shows that the average length of oculomotor axons increases in the presence of SDF. (C) shows that the angle of spread of oculomotor axons is not significantly altered in the presence of HGF.

	Explant score (median)	Average length (mean)	Angle of spread (mean)
SDF (n=15)	5	405	71°
Control (n=21)	4	355	69°
p	0.00429 (Mann Whitney U test)	0.021 (Student's t-test)	0.498 (Student's t-test)

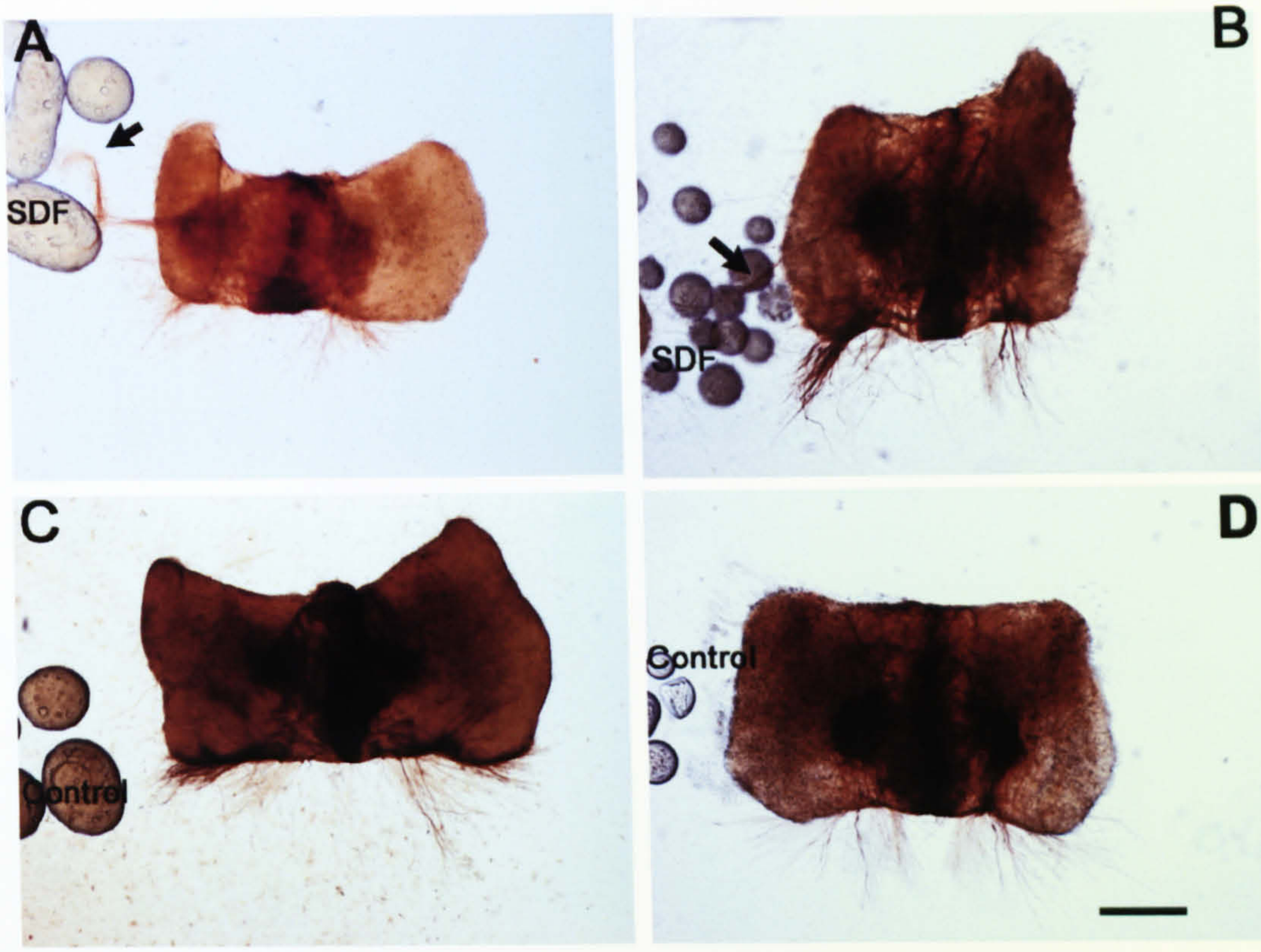

Figure 4.21

Oculomotor explants cultured next to a cluster of beads pre-soaked in SDF (A, B) or next a cluster of PBS-soaked beads (C, D). SDF does not notably alter the outgrowth from the caudal edge of the explant, although there is some deflection towards the beads. In several explants oculomotor axons also aberrantly exited from the lateral edge of the explant and grew towards the beads (marked with arrows).
Scale bar (D) = 0.3mm

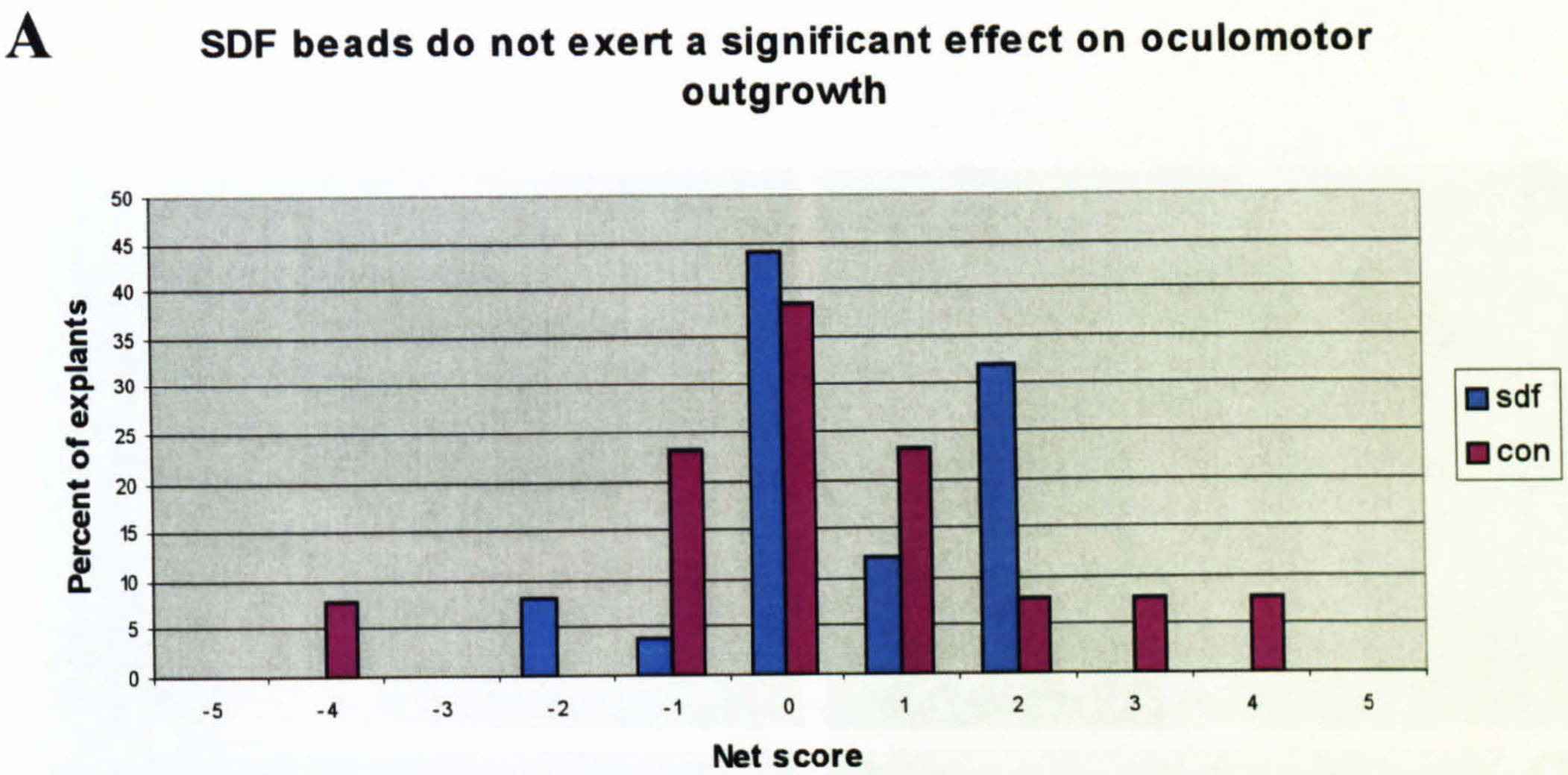

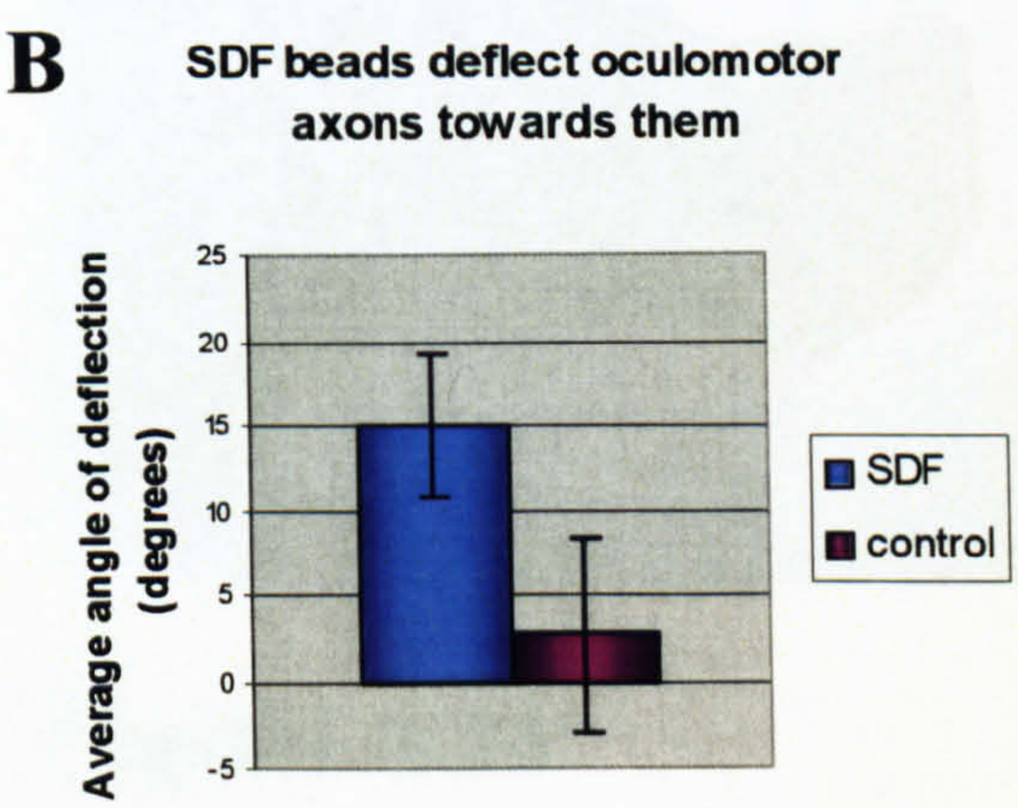

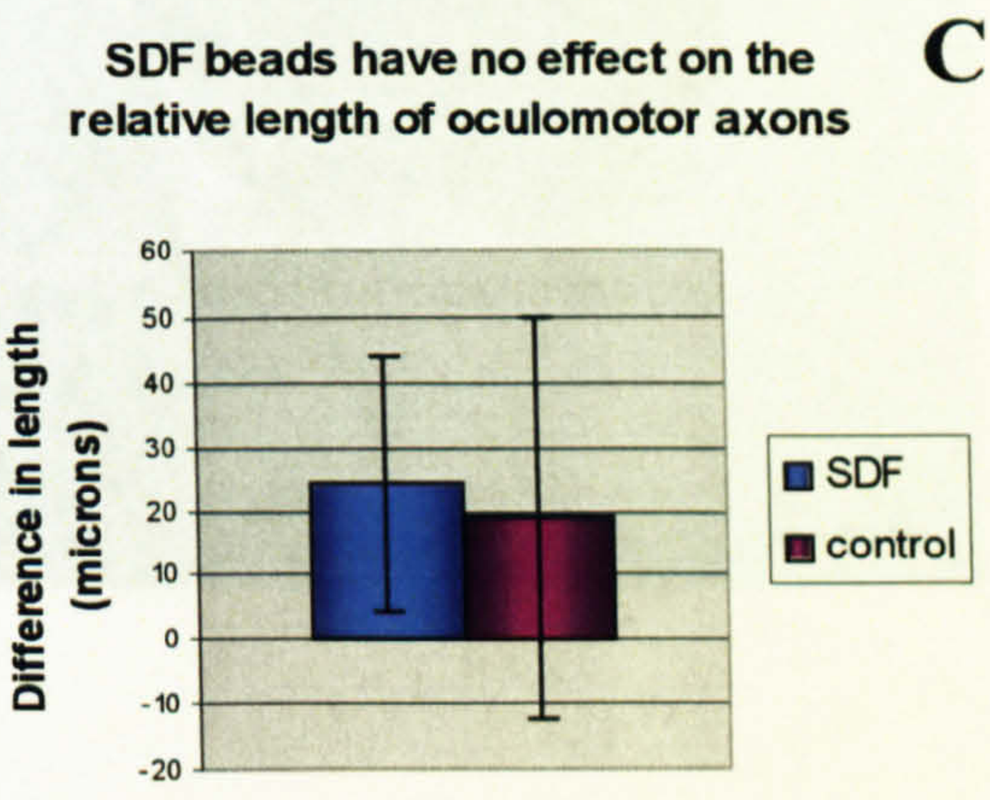

Figure 4.22

(A) shows the distribution of net scores for oculomotor explants cultured with SDF-soaked beads and controlled beads. SDF beads do not have a significant effect on oculomotor outgrowth. (B) shows the angle of deflection of oculomotor axons towards the beads. Oculomotor axons do exhibit a slight attraction towards SDF beads, as the average angle of deflection is 15°, compared to 3° for controls. However, this effect falls short of statistical significance ($p=0.0778$). The length of the proximal bundle relative to the length of the distal bundle of axons is unaffected by SDF (C). Error bars in (B) and (C) indicate the estimated standard error.

	Explant net score (median)	Angle of deflection (mean)	Difference in length (mean)
SDF beads (n=25)	0	15°	24μm
PBS beads (n=15)	0	3°	19μm
p	0.576	0.0778 (Student's t-test)	0.677 (Student's t-test)

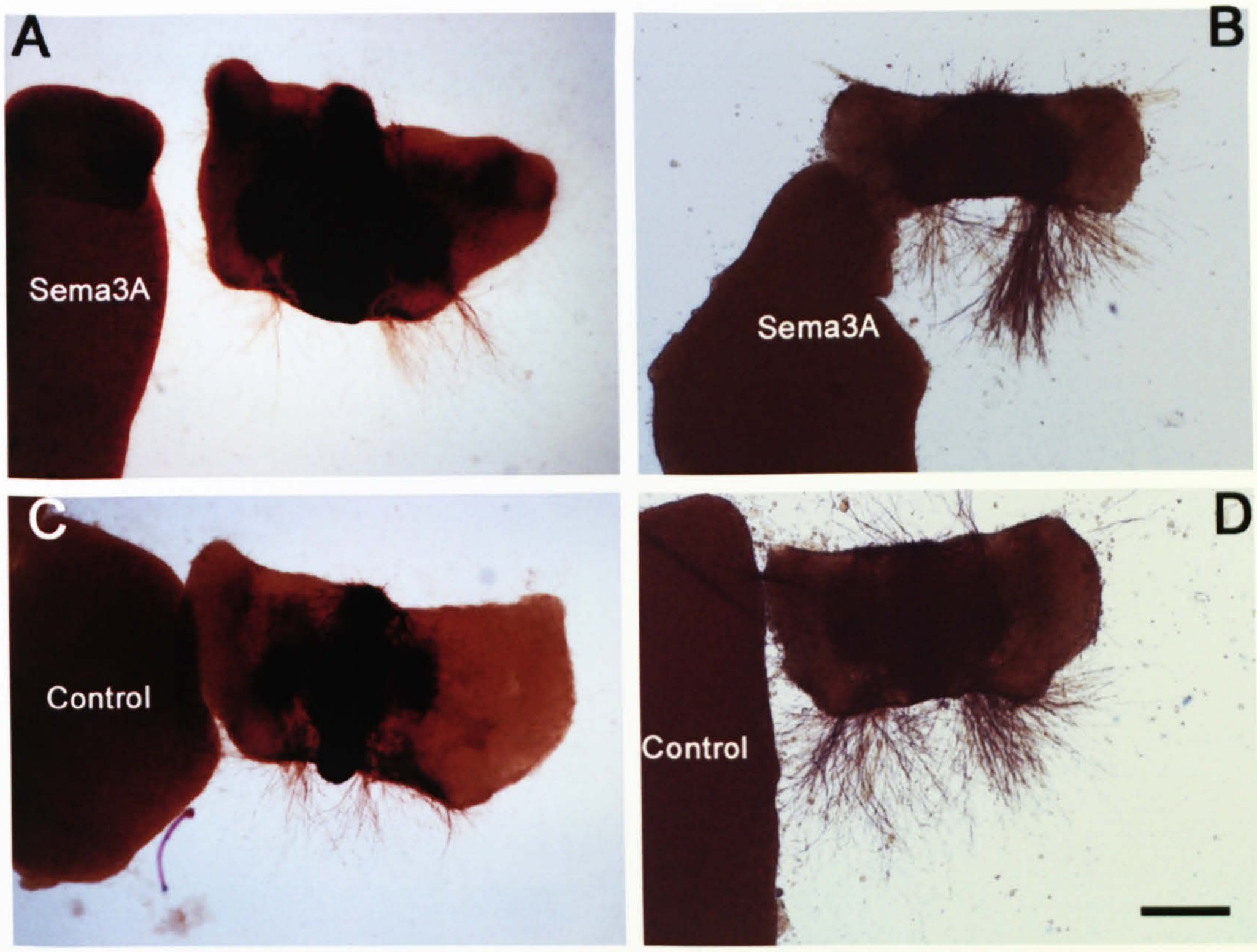

Figure 4.23

Oculomotor explants cultured in the presence of SDF and next to Sema3A secreting clusters (A, B) or control clusters (C, D). Axonal outgrowth from the side facing the cluster is reduced compared to outgrowth from the side facing away in explants cultured with Sema3A clusters and SDF but not in explants cultured with control clusters and SDF. Scale bar (D) = 0.3mm

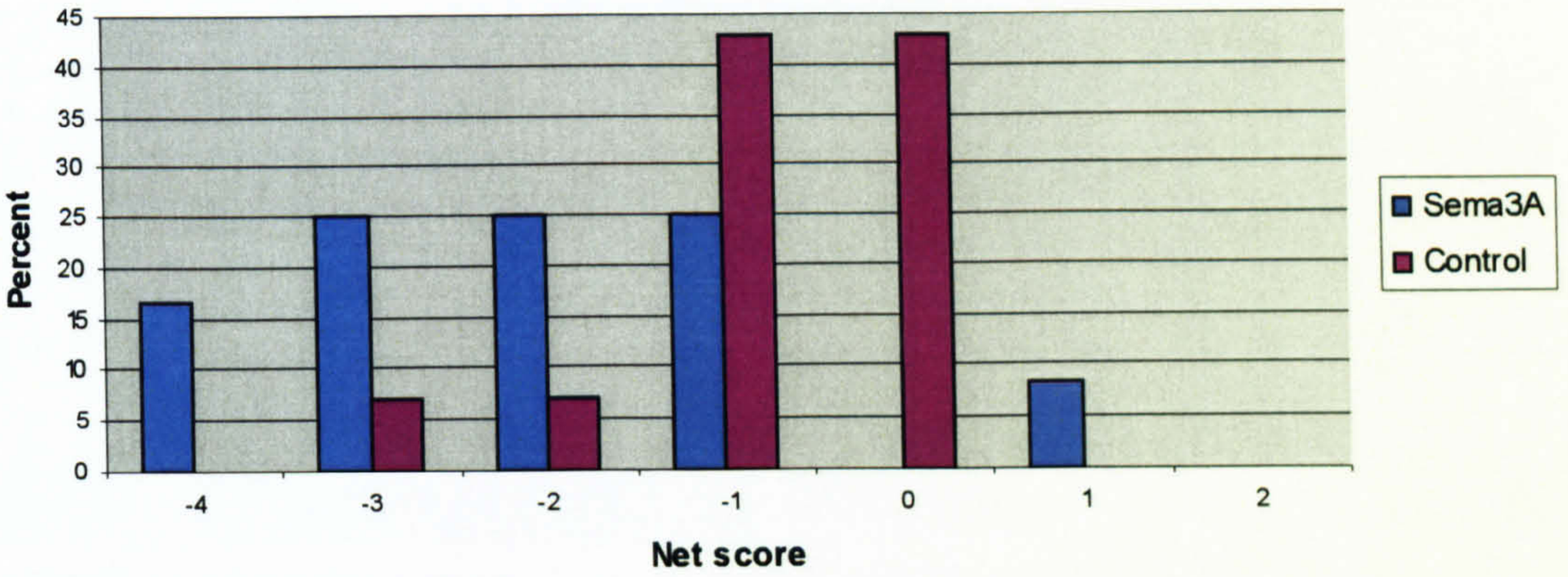

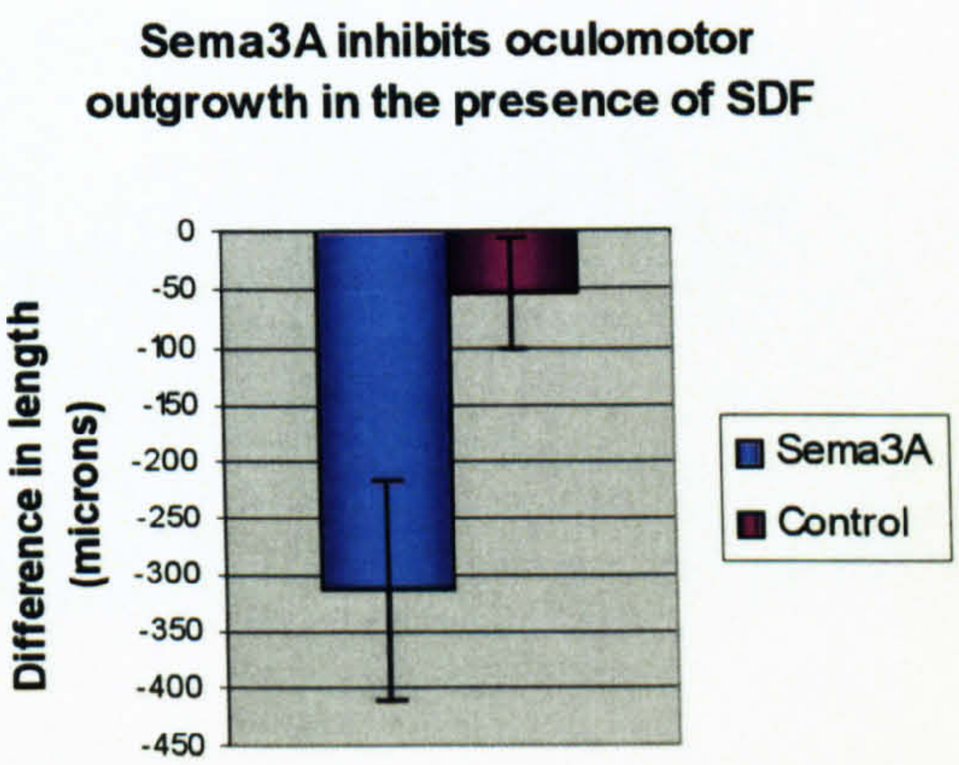

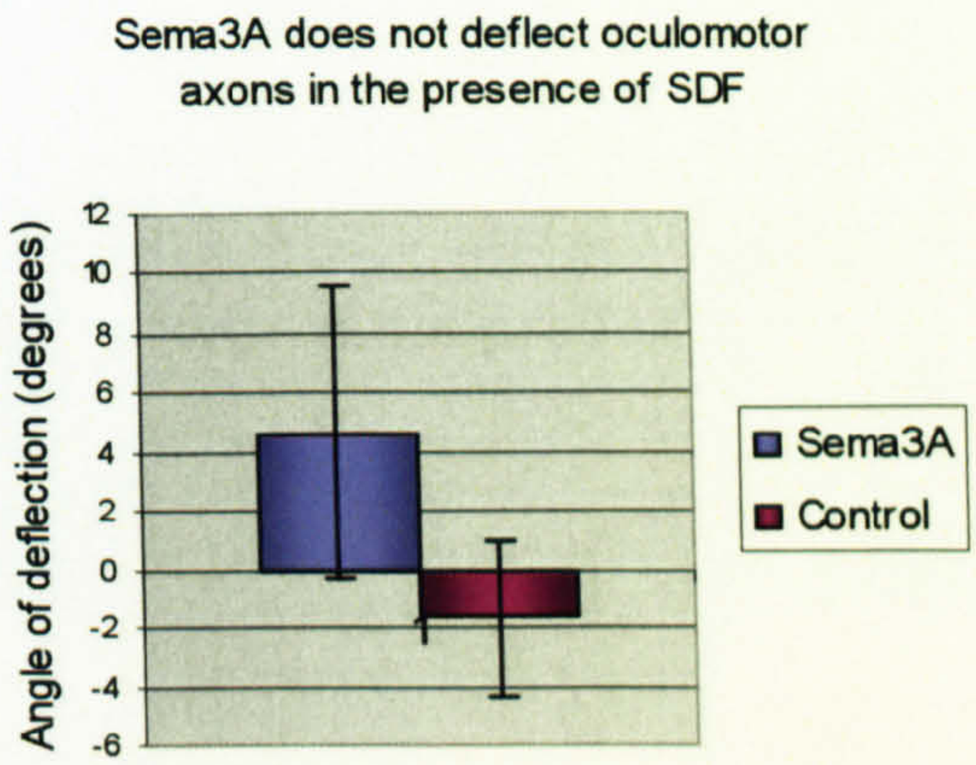

Figure 4.24

Graph (A) shows the distribution of net scores for oculomotor explants cultured with Sema3A clusters or control clusters, in the presence of SDF. Sema3A inhibits outgrowth as evidenced by the distribution of scores being shifted to the left for the experimental group. The inhibition evoked by Sema3A is also demonstrated by the reduction in axonal length from the side facing the cluster in experimental explants (B). However, there is no change in the angle of deflection in the presence of Sema3A (C). Error bars in (B) and (C) denote estimated standard error.

	Explant net score (median)	Difference in length (mean)	Angle of deflection (mean)
Sema3A clusters (n=12)	-1	-313μm	5°
Control clusters (n=14)	-2	-54μm	-2°
p	0.00117 (Mann Whitney U-test)	0.0164 (Student's t-test)	0.257 (Student's t-test)

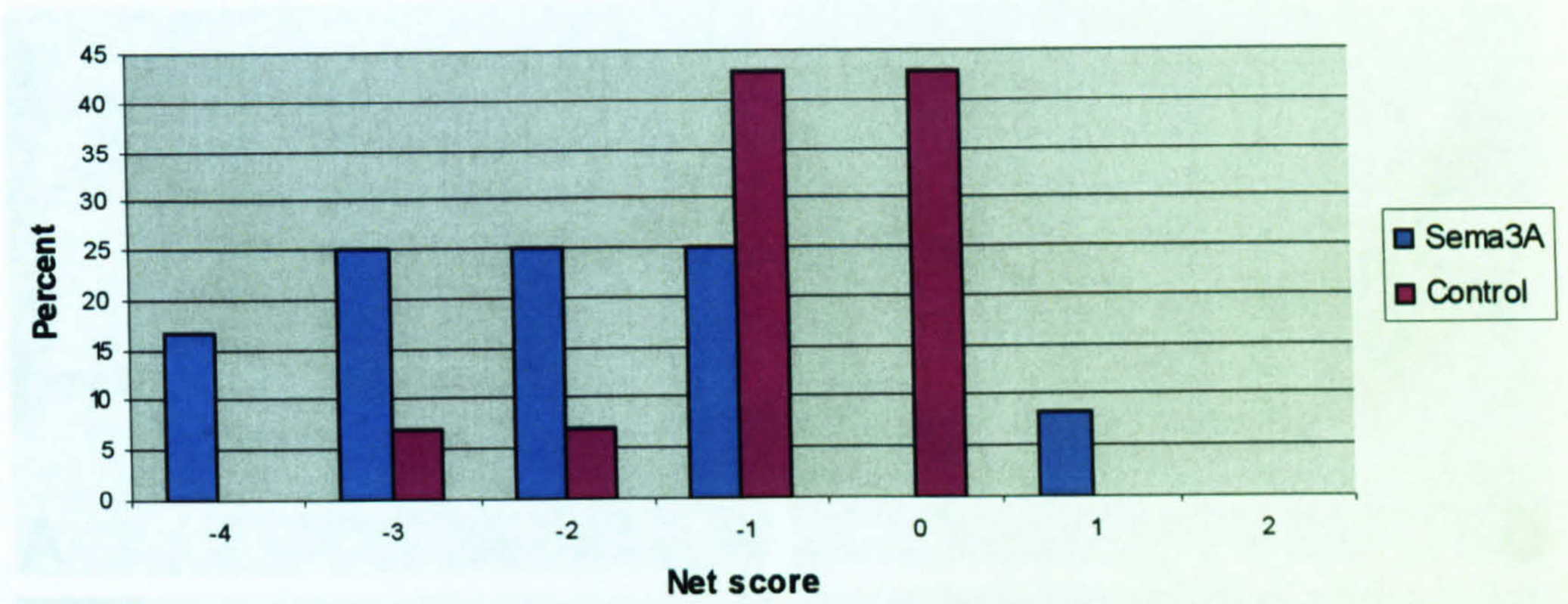

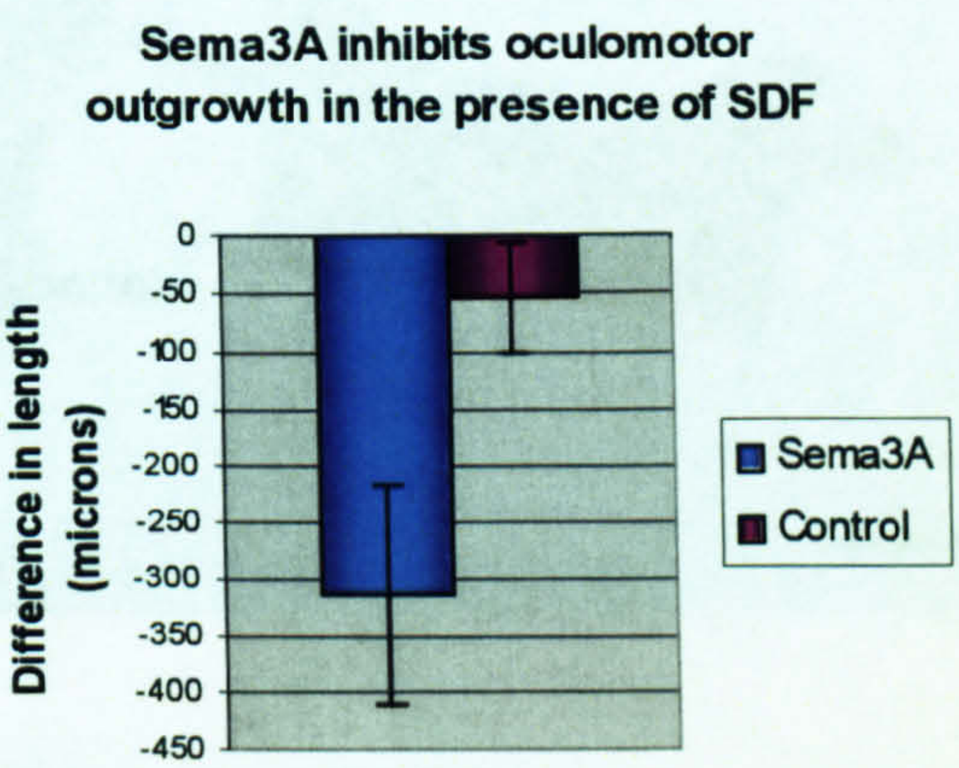

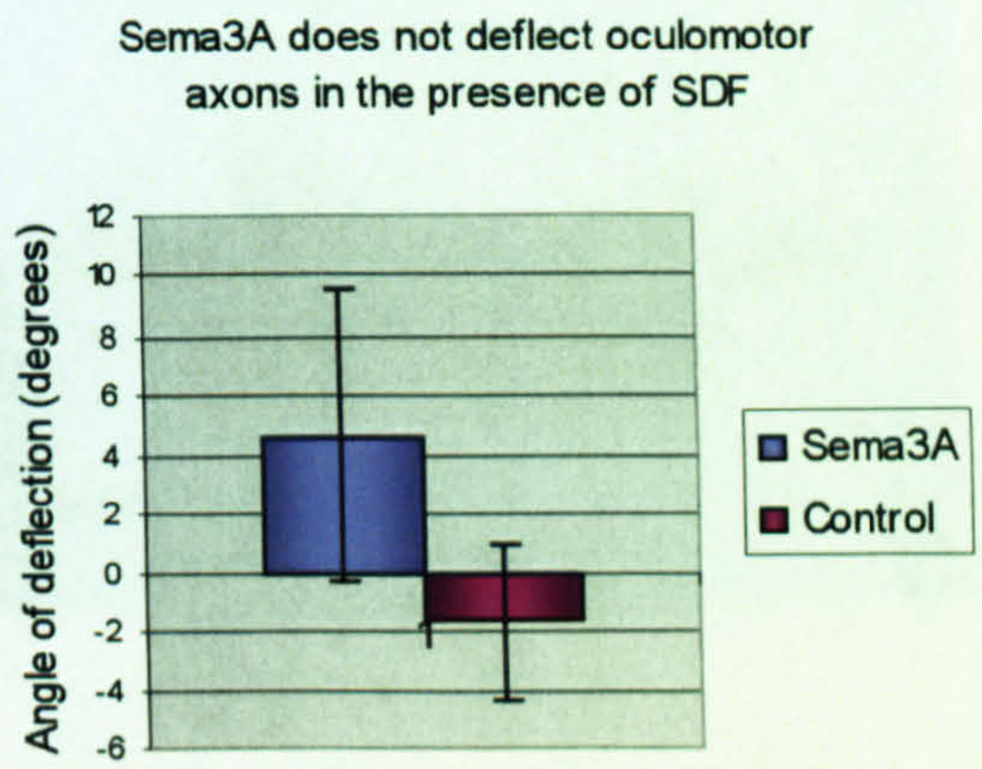

Figure 4.24

Graph (A) shows the distribution of net scores for oculomotor explants cultured with Sema3A clusters or control clusters, in the presence of SDF. Sema3A inhibits outgrowth as evidenced by the distribution of scores being shifted to the left for the experimental group. The inhibition evoked by Sema3A is also demonstrated by the reduction in axonal length from the side facing the cluster in experimental explants (B). However, there is no change in the angle of deflection in the presence of Sema3A (C). Error bars in (B) and (C) denote estimated standard error.

	Explant net score (median)	Difference in length (mean)	Angle of deflection (mean)
Sema3A clusters (n=12)	-1	-313μm	5°
Control clusters (n=14)	-2	-54μm	-2°
p	0.00117 (Mann Whitney U-test)	0.0164 (Student's t-test)	0.257 (Student's t-test)

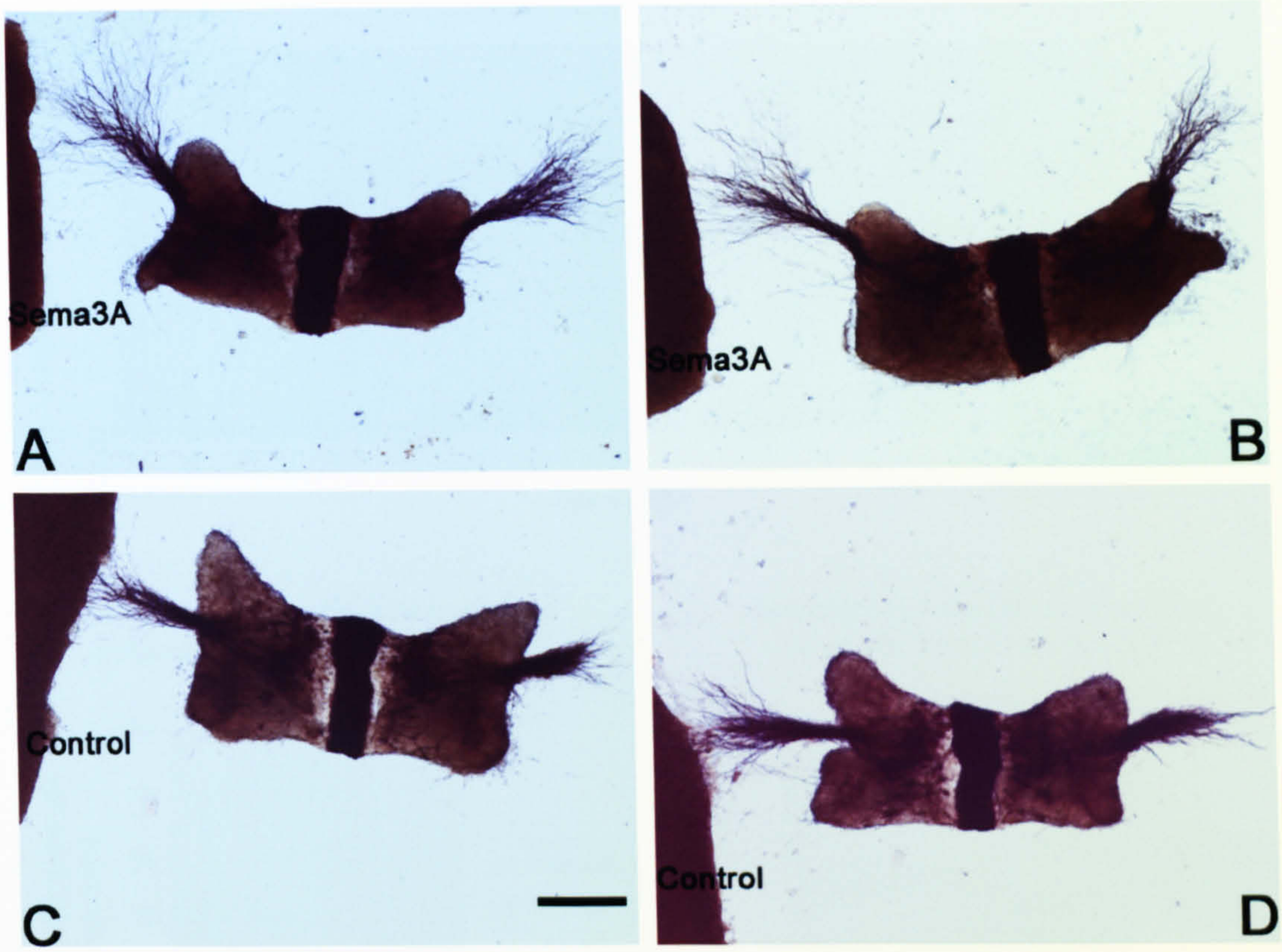

Figure 4.25

Trochlear explants cultured in the presence of SDF with Sema3A clusters (A, B) and control clusters (C, D). There is no difference between control and experimental explants, outgrowth is symmetrical in both groups. Scale bar = 0.3mm

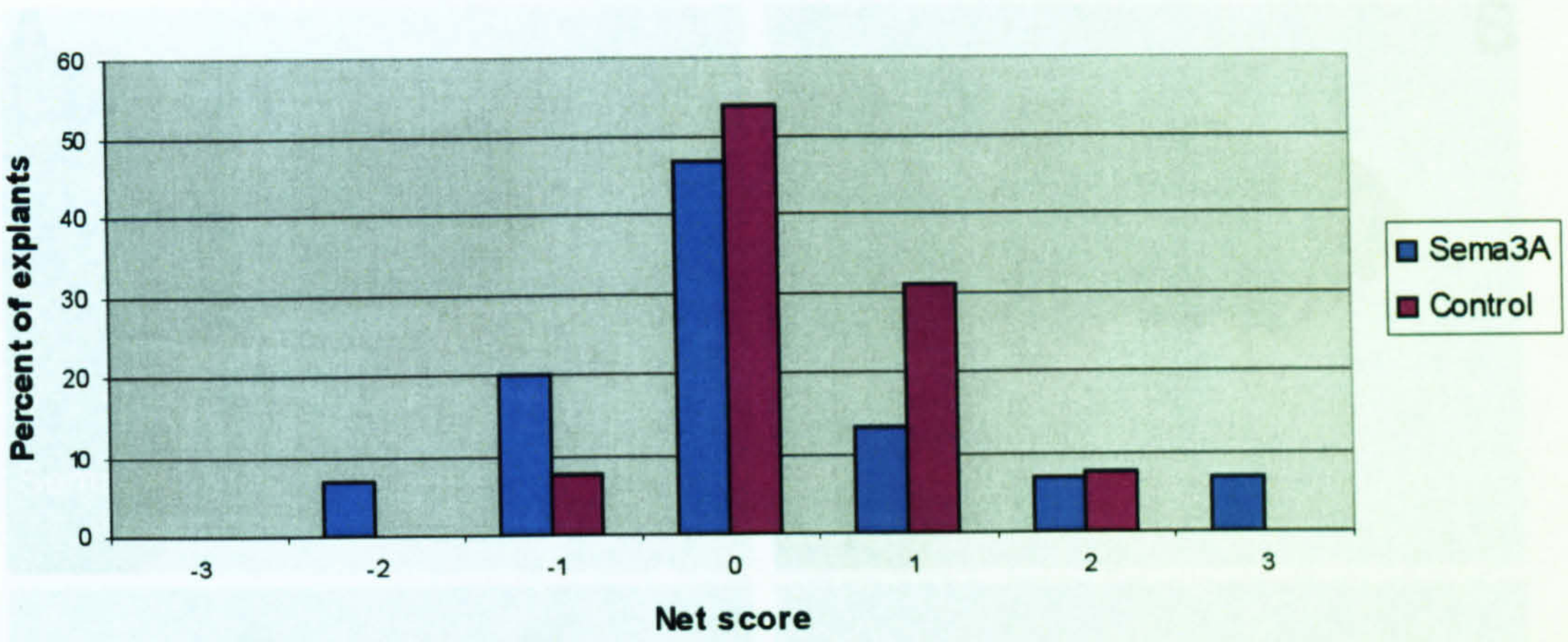

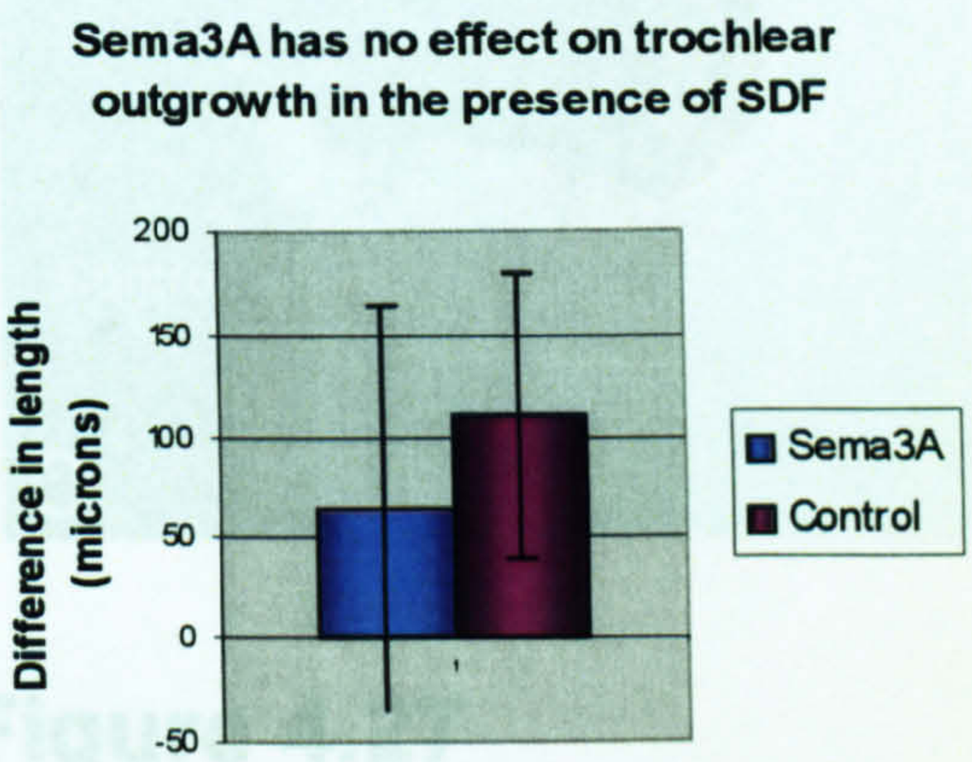

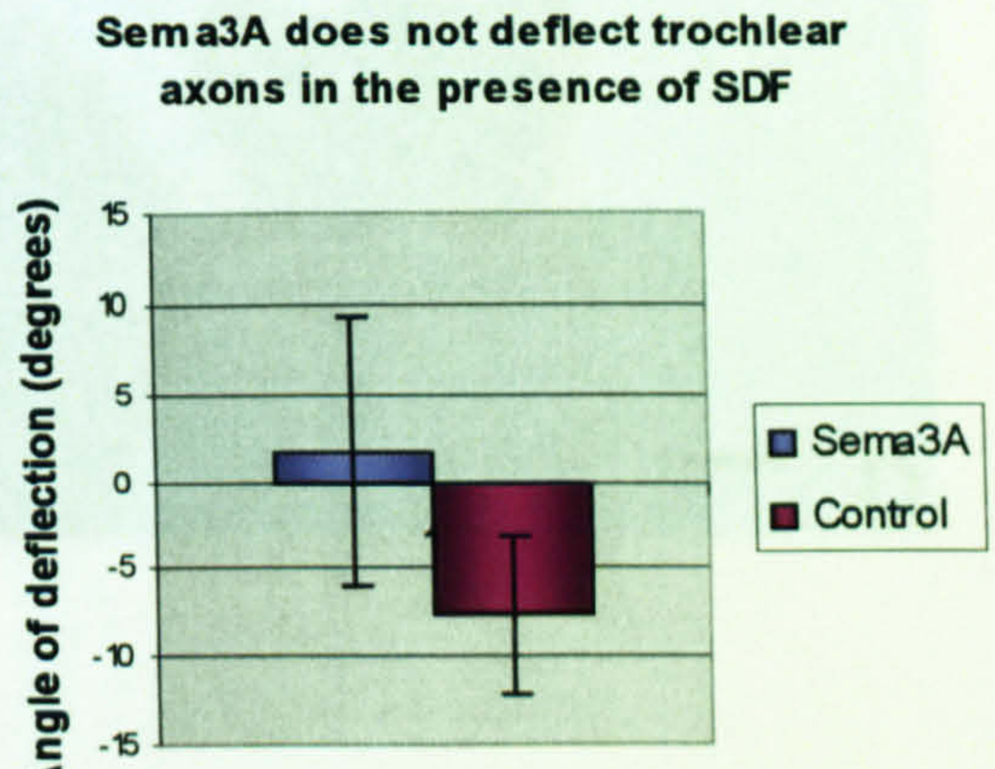

Figure 4.26

Graph (A) shows the distribution of net scores for trochlear explants in the presence of SDF when cultured opposite a Sema3A-secreting cluster or opposite a control cluster. There is no significant difference in outgrowth in the presence of Sema3A. Graph (B) shows the average difference in length between the proximal and the distal bundle, and there is no significant difference on this measure between experimental and control explants. Graph (C) shows the average angle of deflection and again there is no significant difference between explants cultured with control clusters and Sema3A clusters. Error bars in (B) and (C) denote estimated standard error.

	Explant net score (median)	Difference in length (mean)	Angle of deflection (mean)
Sema3A clusters (n=15)	0	65μm	2°
Control clusters (n=13)	0	110μm	-7°
p	0.381 (Mann Whitney U test)	0.718 (Student's t-test)	0.341 (Student's t-test)

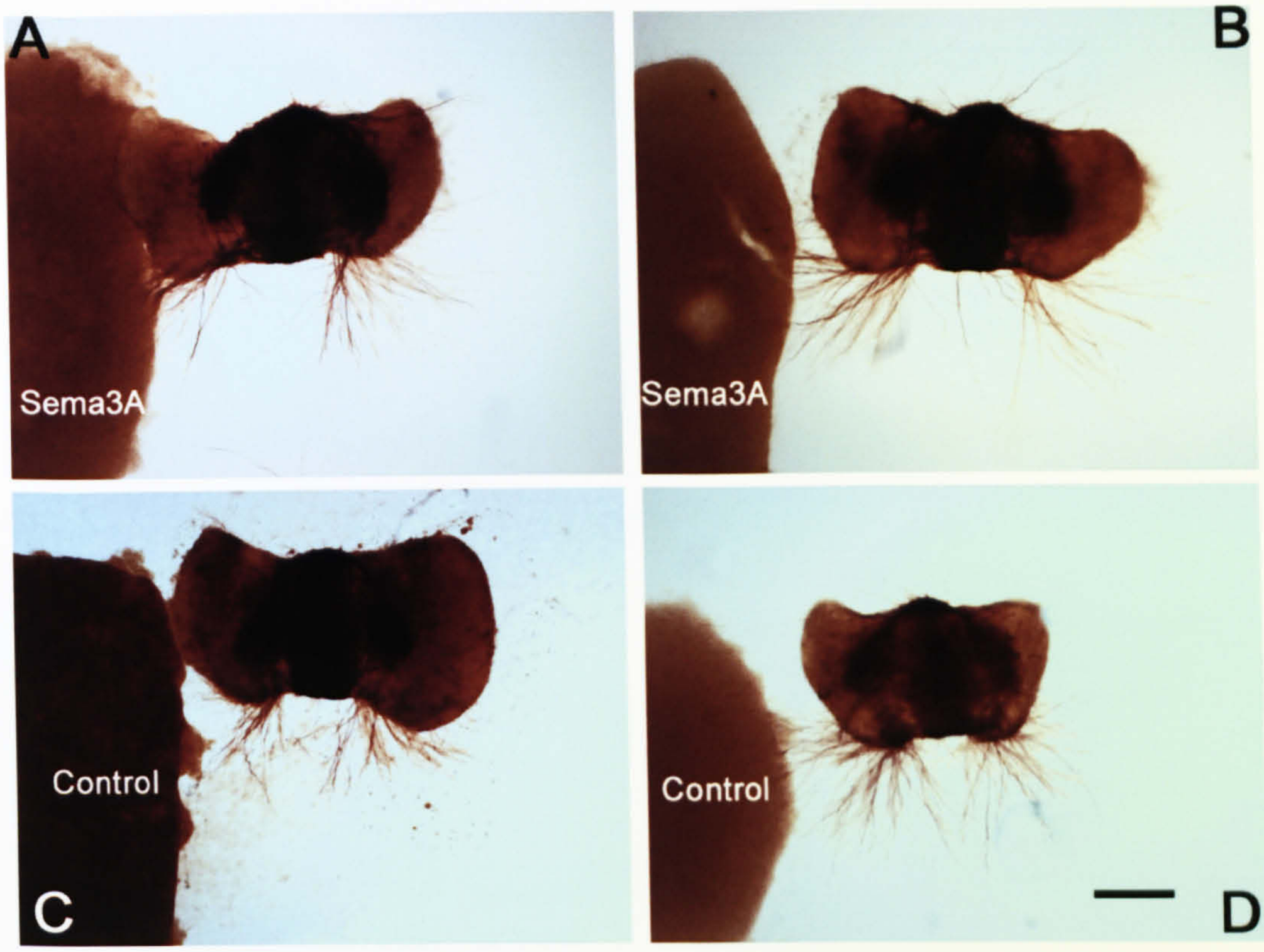

Figure 4.27

Oculomotor explants cultured in the presence of HGF and next to either Sema3A-secreting clusters (A, B) or control clusters (C, D). Axonal outgrowth on the proximal side is not affected by Sema3A relative to the outgrowth on the distal side, compared to controls.
Scale bar (D) = 0.3mm

A

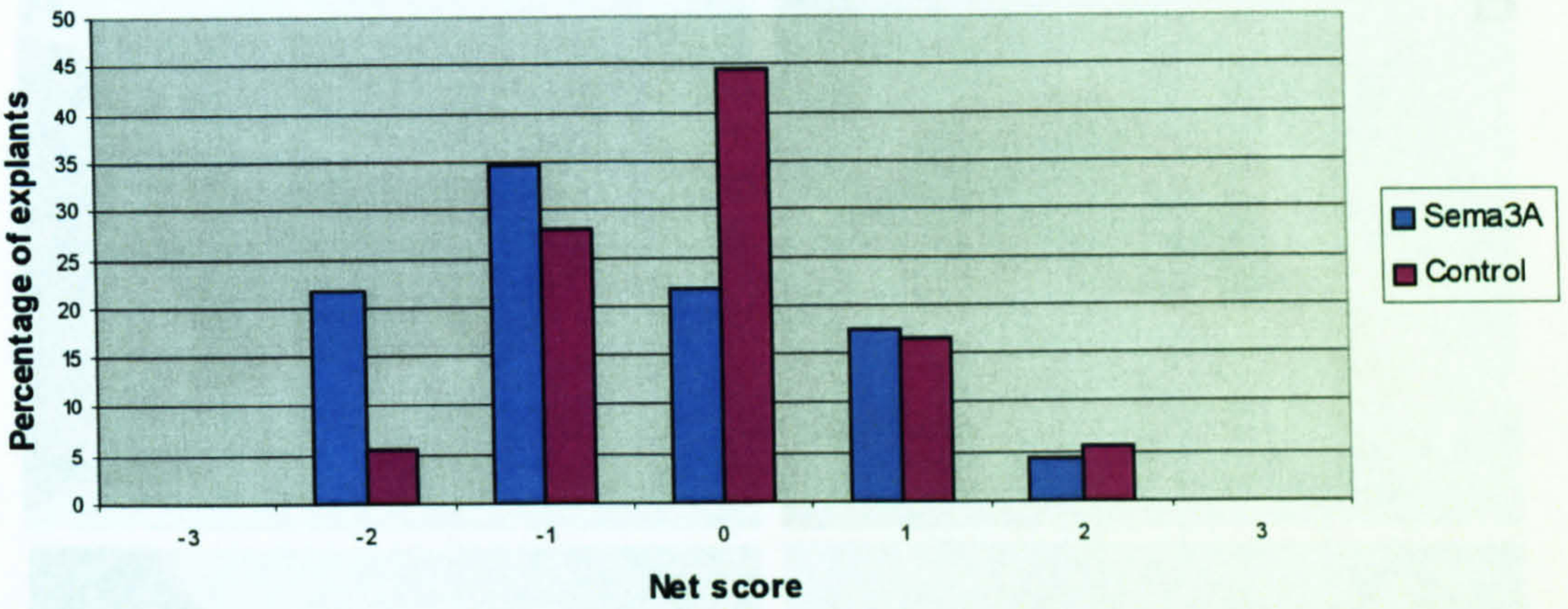

B

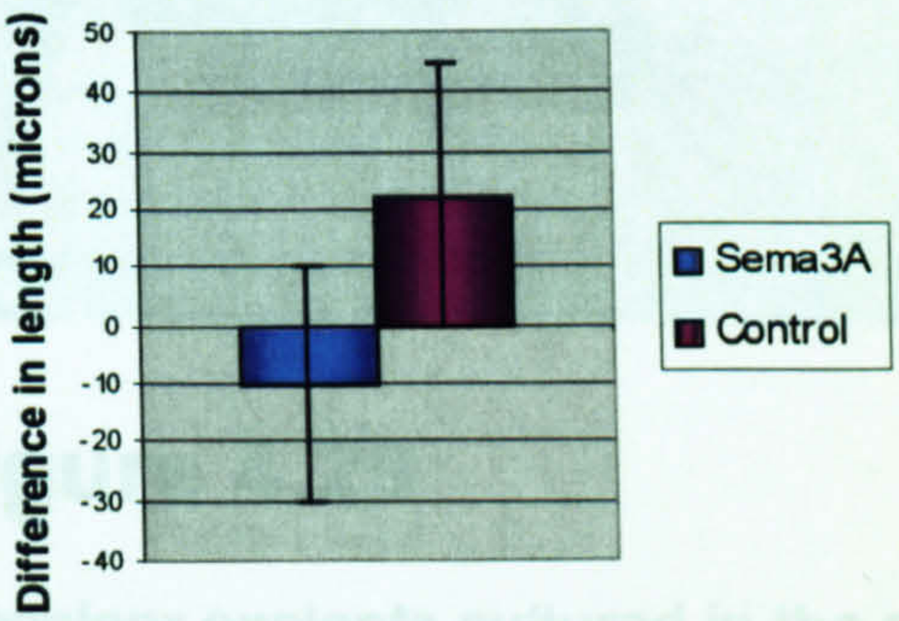

C

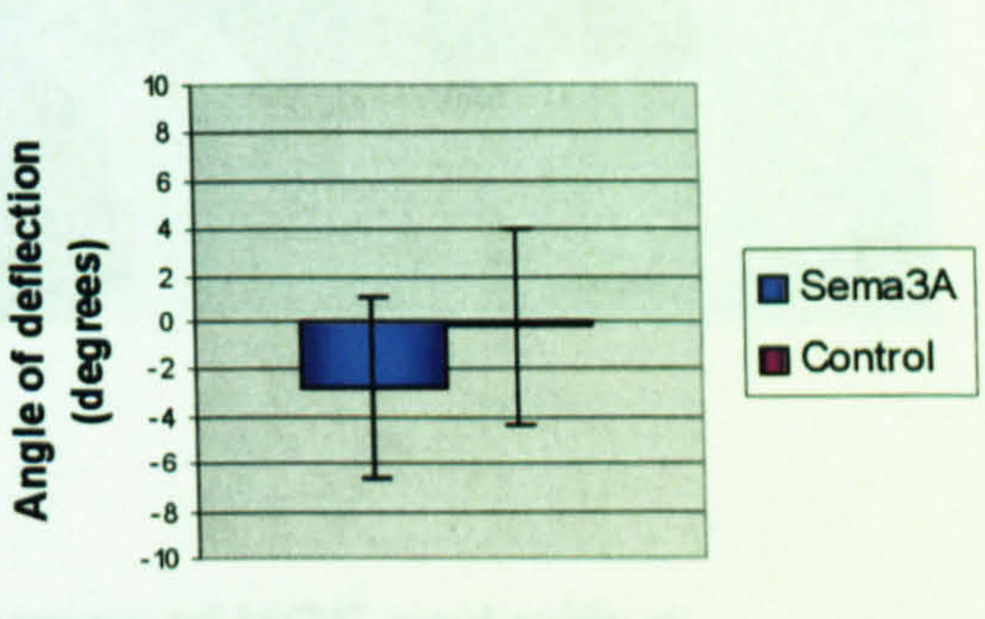

Figure 4.28

(A) shows the distribution of net scores for oculomotor explants cultured in the presence of HGF either opposite a Sema3A-secreting cluster or opposite a control cluster. Although there is a slight leftward shift in the distribution of scores for explants cultured with Sema3A clusters, there is no significant change in oculomotor outgrowth in the presence of Sema3A compared to controls. (B) shows the average difference in length between the proximal and the distal bundle in experimental and control explants, there is no significant effect of Sema3A. (C) shows the average angle of deflection towards the cluster in experimental and control explants; again there is no significant difference. Error bars in (B) and (C) indicate estimated standard error.

	Explant net score (median)	Difference in length (mean)	Angle of deflection (mean)
HGF/Sema3A (n=23)	-1	-10μm	-3°
HGF/Control (n=18)	0	22μm	0°
p	0.217 (Mann Whitney U test)	0.289 (Student's t-test)	0.645 (Student's t-test)

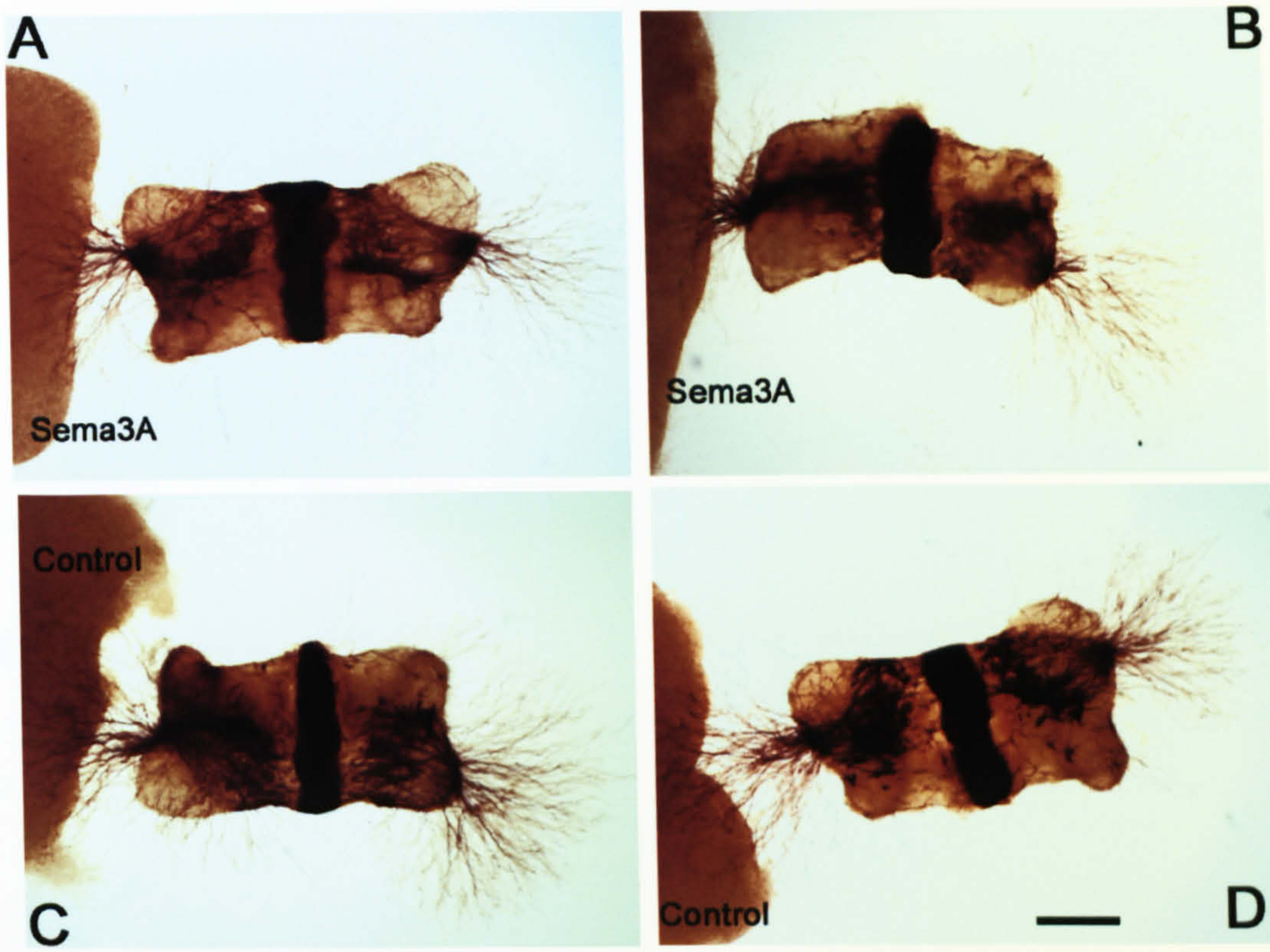

Figure 4.29

Trochlear explants cultured in the presence of HGF and with a Sema3A-secreting cluster (A, B) or a control cluster (C, D). All explants display the abundant axonal outgrowth induced by the presence of HGF in the medium. Axons growing from the side facing the cluster are more fasciculated than axons growing from the opposite side. However, there is no difference in the pattern of outgrowth between explants cultured with Sema3A clusters and explants cultured with control clusters. Scale bar (D) = 0.3mm

A

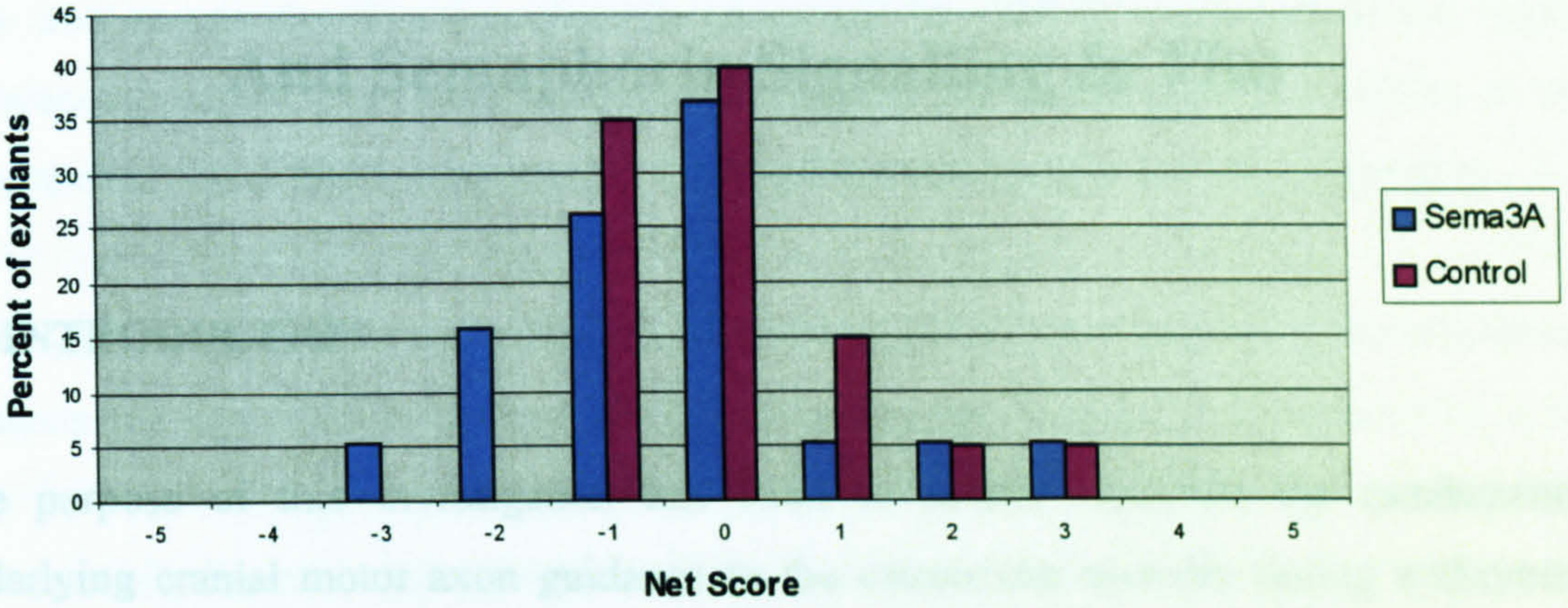

B

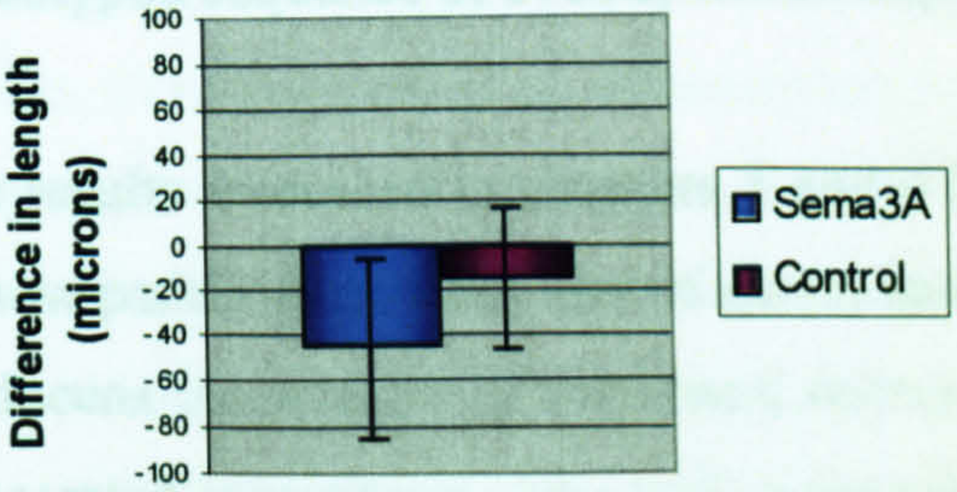

C

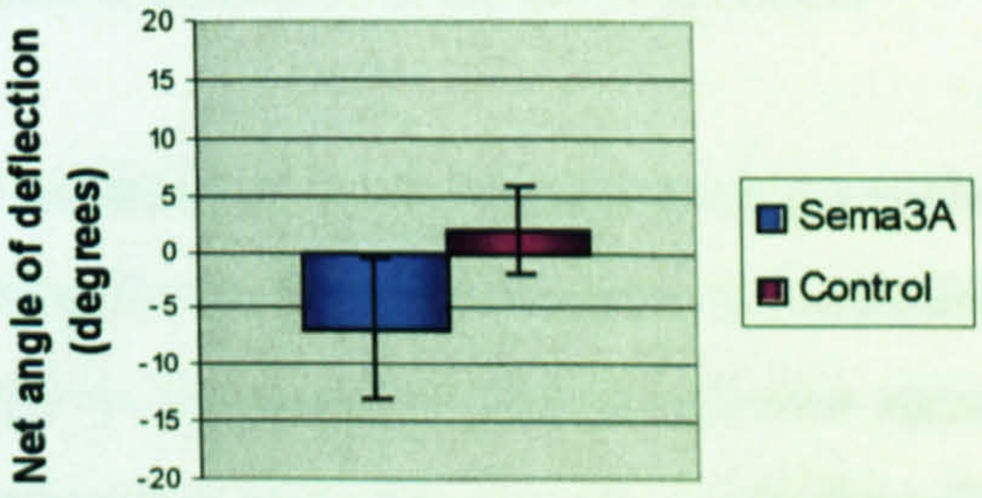

Figure 4.30

(A) shows the distribution of net scores for trochlear explants in the presence of HGF when cultured opposite a Sema3A-secreting cluster or opposite a control cluster. There is no significant difference in outgrowth in the presence of Sema3A. (B) shows the average difference in length between the proximal and the distal bundle, and there is no significant difference on this measure between experimental and control explants. (C) shows the average angle of deflection and again there is no significant difference between explants cultured with control clusters and Sema3A clusters. Error bars in (B) and (C) denote estimated standard error.

	Explant net score (median)	Average difference in length (mean)	Average angle of deflection (mean)
HGF/Sema3A (n=19)	0	-45μm	-7°
HGF/Control (n=20)	0	-15μm	2°
p	0.249 (Mann Whitney U test)	0.551 (Student's t-test)	0.226 (Student's t-test)

Chapter 5: Analysis Of The Perturbation Of SDF-1 And Semaphorin Signalling *In Vivo*

5.1 INTRODUCTION

The purpose of this investigation has been to further elucidate the mechanisms underlying cranial motor axon guidance to the extraocular muscles during embryonic development. Three cranial nerves send their axons to innervate six muscles, which are found in close proximity to each other and are still in the process of translocation at the point of initial contact by pioneer axons. The axon growth proceeds through a highly stereotyped sequence of events, which implies that the process is strictly regulated.

The results discussed in chapters 3 and 4 have enabled us to start constructing a model of how pathfinding behaviour of axons innervating the extraocular muscles is controlled. Abducens innervation of the lateral rectus might be regulated by the co-ordinate action of secreted semaphorins. Sema3C promoted abducens outgrowth in vitro, while Sema3A was inhibitory; the expression pattern of these two ligands at the stage when abducens growth is occurring also supports this hypothesis, since Sema3C is expressed in the target muscle and Sema3A is expressed around the trajectory of the abducens nerve. Oculomotor axon pathfinding is influenced by three ligands *in vitro*. SDF-1 and HGF are growth-promoting *in vitro*, whilst Sema3F repels oculomotor axons. Combining this information with the expression patterns produces the following model: oculomotor exit from the neuroepithelium is promoted by the action of SDF-1, which is expressed in the adjacent mesenchyme at the HH stage 18-21; growth to the muscle targets is driven by the attractive action of HGF, which is expressed in the ventral periocular mesenchyme; the ventral course of the nerve past the ciliary ganglion is partly determined by the repulsive action of Sema3F, which is expressed dorsal to the developing ventral rectus/medial rectus; and branch formation into its targets is facilitated by the action of SDF-1 whose expression is activated at the HH stage 27, in a highly localized fashion in

two of the oculomotor target muscles. Trochlear axon growth dorsally within the neural tube and exit in the dorsal midline is promoted by SDF-1, expressed in the region adjacent to the exit point, and axon growth towards the dorsal oblique is driven by the attractive action of HGF, expressed in the target muscle and the surrounding region.

The conclusions summarised above are derived from the interpretation of the expression analysis and data from *in vitro* assays. However, it is by no means certain that this is the way in which the processes are actually controlled in the developing embryo. The presence of a ligand in the right place at the right time enables it to be implicated in the involvement in the process of interest. However, further evidence is needed since the expression of a particular molecule could serve a different purpose than the one ascribed to it, e.g. it may be involved in controlling cellular migration or differentiation, or in the guidance of a different population of axons, which also navigate through the same region. Confirmation of an effect on axon growth *in vitro* lends stronger credence to the proposed role of the candidate guidance cue, but these experiments also have their limitations. It is difficult to ascertain the physiologically relevant concentration of a guidance cue (even if it were possible to accurately determine the *in vivo* concentration of a ligand, it is much more difficult to know its actual effective concentration since it can bind to cells and components of the extracellular matrix) hence the concentration used in culture may be too high and yield a significant effect, which is not physiologically relevant. Secondly, even if the result of an *in vitro* experiment is indeed correct and the guidance cue in question does exercise a significant effect on a given population of axons, it says nothing about how important the contribution of this particular cue is *in vivo*. Since axons are likely to integrate signals from a large number of sources to make correct pathfinding choices, the effect of any given cue may not be crucial and could be easily compensated by other guidance signals present in the environment. In order to more convincingly substantiate the conclusions derived from *in vitro* experiments and expression studies, it is desirable to demonstrate that disrupting the signalling from a particular cue *in vivo* results in axon pathfinding.

Two methods used to investigate the *in vivo* relevance of the proposed mechanisms. Firstly, mice with null mutations in genes coding for the guidance cues in question or their receptors were examined for abnormalities in the projection patterns of the oculomotor, trochlear or abducens nerves. Specifically, immunohistochemistry was performed on wholemount Sema3C and Sema3A/Sema3C mutant mice to identify potential abnormalities in the abducens nerve pathfinding, and on sections of CXCR4 mutant mice to examine oculomotor and trochlear nerve's projections. Secondly, *in ovo* electroporation of a dominant negative NPN-1 construct into abducens motor neurons was carried out to disrupt their responses to semaphorin signalling and thus to examine the consequent effects on their axonal projections.

5.2 RESULTS

5.2.1 *CXCR4* mutant mice

Lieberam et al (2005) have described a number of motor axon pathfinding errors that occur in mice lacking *SDF-1* or its receptor, *CXCR4*. The phenotypes of these mutants were identical, strongly indicating that SDF-1 signals through CXCR4. The abnormalities that were observed affected axon guidance of somatic motor neurons including spinal motor axons, abducens and hypoglossal motor axons, which normally exit the neural tube ventrally. The errors included axons aberrantly projecting dorsally within the neural tube, and at axial levels were dorsally-exiting axons were also found, some of these axons also exited through the dorsal exit point. Some somatic motor axons were observed to aberrantly extend across the floor plate within the neural tube, and far fewer somatic motor axons exited the neural tube ventrally compared to wild-type mice (Lieberam et al 2005)

The method used by the authors involved crossing the *CXCR4* or *SDF-1* mutants with mice expressing GFP under the control of the HB9 promoter. *HB9* is expressed by most ventrally-projecting but not dorsally-projecting motor neurons, which meant that GFP

selectively labelled ventrally-projecting motor neurons, and it was therefore possible to identify when their axons aberrantly followed a dorsal trajectory. The authors also reported expression of *CXCR4* in oculomotor, but not trochlear neurons, however, because oculomotor neurons do not express *HB9*, the fate of their axons in these mutants was not investigated (I Lieberam – personal communication).

A litter of E12.5 *CXCR4* mutant mouse embryos was obtained from Dr I Lieberam and Prof T Jessell. The litter contained three homozygous mutants, two heterozygotes and one wild-type embryo. The embryos were frozen in OCT according to the protocol described in the materials and methods chapter, either in a transverse or a sagittal orientation. Immunohistochemistry was carried out with anti-neurofilament and anti-Islet antibodies to identify the position of the motor nuclei and the projection patterns of their axons.

Comparison of the homozygotes with their heterozygous or wild-type littermates revealed an alteration in the oculomotor axonal projection in the absence of CXCR4, shown in figure 5.1. Normal oculomotor axonal trajectory involves a ventral exit of the axons (figure 5.1B) at a level just rostral to the midbrain-hindbrain boundary followed by caudal extension towards the developing ciliary ganglion (figure 5.1D, F). In embryos lacking *CXCR4* the majority of axons fail to exit the neural tube in the appropriate ventral position and instead project rostro-dorsally within the neural tube (figure 5.1A). A small subset of oculomotor axons in the mutant exit correctly and form a nerve, which is substantially reduced in size relative to controls, as seen both in transverse section (figure 5.1C) and sagittal section (figure 5.1E). In addition some oculomotor axons are seen to aberrantly project towards the floor plate within the neural tube (figure 5.1A,C). From these data it appears that SDF-CXCR4 signalling is indeed crucial for correct oculomotor axon exit into the periphery, as hypothesized. It is more difficult to determine whether the projections to the extraocular muscles are affected by the absence of CXCR4 since far fewer oculomotor axons reach the target region as a result of their failure to exit. In any case, the method used doesn't allow to accurately determine what happens to oculomotor axons in the latter part of their projection

because the latter part of the oculomotor projection lies close to the much larger trigeminal nerve, which is also positive for the neurofilament antigen, and it is difficult to assign the oculomotor nerve.

Trochlear axons project dorsally within the hindbrain the roof plate, at the level of the midbrain-hindbrain boundary, where they exit and project contralaterally (figure 5.2A). In transverse section, the trochlear projection in the mutant embryo appears identical to the projection in a heterozygous littermate (figure 5.2A,B). One difference was noted : in the heterozygote some axons project towards the ventricle within the neural tube, however in the mutant, this phenotype is more pronounced with fascicles of axons projecting to the ventricle. The nerve also looks similar in sagittal section in the mutant and wild-type (figure 5.2E,F). Overall, three mutant embryos, two heterozygous and one wild-type embryos were examined. There was some variability in the diameter and the degree of fasciculation of the trochlear nerve within the control group of embryos, and the appearance of the nerve in mutant embryos did not fall outside the normal range of variability observed in the controls. Thus it would appear that the absence of CXCR4 does not produce major abnormalities in the trochlear projection.

It should be noted that a normal appearance of the trochlear nerve identified with neurofilament immunostaining does not necessarily mean that all trochlear axons project correctly. A small subset of trochlear axons may project aberrantly within the neural tube, indeed the fascicles of axons projecting towards the ventricle may be ectopic trochlear axons, although they cannot be unambigously assigned as such using neurofilament immunostaining. The previous study of SDF-1 in motor axon guidance (Lieberam et al 2005) identified errors in abducens axon guidance including dorsal misprojections by abducens axons because the trajectory of all abducens axons could be easily traced, as they expressed GFP under the control of the *HB9* promoter. However, I could not identify these abnormalities using neurofilament immunostaining because abducens axons could not be easily traced within the neural tube where many other neurofilament^{+} axon tracks are present. In CXCR4 mutant embryos the appearance of the abducens nerve in the periphery is comparable to that in control mice (figure

5.3C,D). The nerve projects rostrally at an acute angle to the edge of the neural tube, both in wild-type and in mutant mice, it extends as far as rhombomere 2 in both and displays a similar diameter and degree of fasciculation (figure 5.3C,D). One defect was identified in the abducens pathfinding in CXCR4 mutants, which was not reported by Lieberam et al (2005), namely abducens axons projecting towards the midline after having exited the neural tube ventrally (figure 5.3A).

In summary, the absence of CXCR4 results in defects in oculomotor axon guidance which closely resemble those reported for spinal and hindbrain somatic motor axons (Lieberam et al 2005). Few oculomotor axons exit ventrally resulting in a reduced diameter of the oculomotor nerve compared to controls, a number of oculomotor axons aberrantly project dorsally within the neural tube and some oculomotor axons extend towards the floor plate. No abnormalities in the trochlear nerve projection were observed, with the exception of possible misrouting of some axons towards the ventricle. In the case of the abducens nerve, previously reported axon guidance defects such as dorsal misprojection within the neural tube and crossing the floor plate could not be detected using neurofilament immunohistochemistry, however, a previously unreported defect in abducens axon pathfinding was identified, namely abducens axons projecting towards the midline after having exited the neural tube ventrally.

5.2.2 *In ovo* electroporation of a dominant negative NPN-1 (dnNPN-1) construct into the ventral hindbrain.

Renzi and colleagues (1999) had generated a dnNPN-1 construct by deleting part of the extracellular domain of the protein. This modified protein exerts a dominant negative effect by sequestering the wild-type neuropilin into inactive complexes and abolishes semaphorin signalling to cells expressing the construct. Its action has been verified *in vivo* by misexpression in olfactory sensory neurons, which causes their axons to overshoot the olfactory bulb because of loss of sensitivity to Sema3A expressed in the telencephalon (Renzi et al 2000).

This construct was misexpressed together with a tauGFP expression construct (Guidato et al 2003) in the ventral neuroepithelium of the chick hindbrain (including rhombomeres 5 and 6, where abducens cell bodies are located) by *in ovo* electroporation. Since the hypothesis is that abducens axons are guided to their target by semaphorin signalling (attractive signals from Sema3C and inhibitory signals from Sema3A), misexpression of a dominant-negative neuropilin-1 construct should abolish semaphorin signalling and therefore result in pathfinding errors by abducens axons. However, results from this experiment were inconclusive.

Expression of the construct was detected using GFP fluorescence and indirect immunofluorescence using an antibody against the myc tag in the dnNPN-1 construct. GFP fluorescence and myc immunofluorescence correlated exactly, indicating that the plasmids were taken up and expressed in the same cells, but the expression was confined largely to the cell bodies with little expression seen in the axons and the growth cones

The construct was expressed in the cell bodies in the appropriate region, as detected by indirect immunofluorescence, but little expression was seen in the axons or growth cones. In the vast majority of cases (42/44) the projection of the abducens nerve on the electroporated side was normal and comparable to that on the control side (figure 5.4A,B). In two cases the abducens projection was disrupted on the electroporated side (figure 5.4C,D). It is difficult to say whether the lack of phenotype in most electroporated embryos was due to insufficient mutant neuropilin found on axons and growth cones or because disruption of semaphorin signalling does not significantly alter the ability of abducens axons to pathfind correctly *in vivo*. Conversely, the two examples in which abducens pathfinding was disrupted are insufficient in number to confirm the importance of semaphorin signalling *in vivo*.

5.2.3 *Sema3C* mutant mice

Sema3C mutant mice have been reported to display severe cardiovascular abnormalities, which result in death shortly after birth (Feiner et al 2001). However, the projection of the abducens nerve and any potential abnormalities in abducens axonal pathfinding had not been previously investigated.

A litter of 14 E10.5 Sema3C mutant mice was obtained from Dr F. Mann. Two of the embryos were homozygous mutants, the rest were heterozygotes or wild-type. Abducens projections in these mice were analysed by immunohistochemistry on whole embryos bisected in the sagittal plane. Anti-neurofilament immunohistochemistry was used to visualise axon tracts and anti-Islet1/2 immunohistochemistry to localise motor neuron nuclei. As Sema3C has been postulated to provide an attractive signal from the target for abducens axons, the expectation was that abducens axons will fail to extend rostrally in their usual manner in the mutant. However, comparison of abducens projection in the homozygote and the wild-type mouse shows little difference (figure 5.5). Nine heterozygous and wild-type mice were analysed, there was some variation in the diameter, length and degree of fasciculation of the abducens nerve even within the same embryo – as can be seen in figure 5.5 (A, B). The axons project parallel to the neural tube and reach the level of rhombomere 2, medial to the trigeminal ganglion, where the lateral rectus primordium is located at this stage (Mootoosamy and Dietrich 2002). In the mutant embryos abducens axons exit ventrally at the level of rhombomere 5 and project rostrally in a fasciculated nerve parallel to the neuroepithelium, reaching the level of rhombomere 2 (figure 5.5C,D). Any differences in the appearance of the abducens nerve are within the normal range of variability observed in wild-type and heterozygous embryos.

5.2.4 *Sema3A/Sema3C* mutant mice

A litter of 13 E10.5 Sema3A/Sema3C compound mutant mice was obtained from Dr F. Mann. Two of the embryos were homozygous mutants, the rest were heterozygotes or wild-type. Abducens projections in these mice were analysed by immunohistochemistry on whole embryos bisected in the sagittal plane. Anti-neurofilament antibody was used to visualise axon tracts. The loss of both secreted semaphorins was expected to result in aberrant abducens pathfinding. Sema3C was hypothesized to provide an attractive signal guiding abducens axons towards their target and Sema3A was expected to provide a repulsive signal confining the abducens nerve to its trajectory. If the hypothesis is valid a number of possible phenotypes could be observed in the compound mutant animal: failure of axons to exit the neural tube, nerve failing to reach the target, defasciculation of the nerve or axons straying into inappropriate territory or even overshooting the target. Nine heterozygous or wild type embryos and two mutant embryos were analysed. As was the case with Sema3C mutants, no differences were identified between Sema3A/Sema3C mutant mice and their wild-type littermates (figure 5.6). In both the mutants and wild-type embryos abducens axons exited the neuroepithelium at the level of rhombomere 5 and projected rostrally to in a fasciculated nerve parallel to the neural tube to the level of rhombomere 2. There was some variability in the length, diameter and degree of fasciculation of the nerve, but any difference in the mutant embryos did not fall outside the normal range observed in wild-type or heterozygous mice.

5.3 DISCUSSION

In the *CXCR4* mutant mice most oculomotor axons fail to exit the neural tube in the appropriate ventral location and instead aberrantly project in a rostro-dorsal direction. This phenotype is consistent with the data presented in the previous two chapters. At stages 18-21 in the chick, the phase of early oculomotor nerve growth, *SDF-1* is expressed in the mesenchyme adjoining the oculomotor nerve exit point (figure 3.12). Oculomotor explants cultured *in vitro* in the presence of SDF-1 often exhibit

fasciculated bundles of oculomotor axons exiting ectopically from the rostral or lateral edges of the explant, whereas in the absence of SDF-1 all oculomotor axons exit the explants caudally (figure 4.19). Taken together these data imply that SDF-1 signalling to oculomotor axons facilitates axonal exit form the neuroepithelium. This hypothesis is further validated by the failure of oculomotor axons to exit correctly in mice lacking the receptor for SDF-1. Furthermore, these findings concur with Lieberam et al (2005) reporting a similar role for SDF-1 with respect to ventrally-exiting spinal and hindbrain motor neurons. The small subset of axons that manage to exit normally in the mutant form a much thinner nerve that nevertheless follows the correct trajectory, growing caudally towards the developing ciliary ganglion. This region is devoid of SDF-1 expression in the chick at the relevant stages. However, SDF-1 was hypothesized to play a role in the latter part of the oculomotor projection from the ciliary ganglion around the ventral edge of the eye, where the nerve branches into the target muscles. Because SDF-1 is present in some of these muscles at the stage when they are being contacted by oculomotor axons, it was hypothesised to function as an attractant promoting innervation of the muscles. It has not been possible to determine whether this aspect of oculomotor axon guidance is affected in the *CXCR4* mutant because the latter part of the oculomotor trajectory lies very close to the much larger trigeminal nerve and it is impossible to assign the oculomotor nerve with any degree of confidence.

In the case of the trochlear nerve no obvious abnormalities were observed in the peripheral projection in the absence of CXCR4. *SDF-1* is expressed in the mesenchyme adjacent to the dorsal roof plate where trochlear axons exit the neural tube (figure 3.11); and when added to the culture medium SDF-1 promotes outgrowth from trochlear explants. On this basis SDF-1 was hypothesized to facilitate trochlear axon growth towards and exit from the roof plate. *SDF-1* is also expressed in the region adjacent to the dorsal oblique, the trochlear nerve's target muscle. However, because expression of *CXCR4* in trochlear neurons doesn't persist for very long, it was thought less likely that SDF-1 is important in attracting trochlear axons to their target. Therefore, the expected phenotype in the *CXCR4* mutant was some form of misprojection of trochlear axons within the neuroepithelium with some axons possibly failing to exit the neural tube. The

fascicles of axons projecting to the ventricle may be trochlear axons that fail to grow towards the roof plate because of an inability to interpret a chemoattractive SDF-1 signal. The lack of a stronger phenotype with regard to trochlear axons can be explained in a number of possible ways. It is possible that the repulsive signals from the ventral midline including netrin and slits (Colamarino and Tessier-Lavigne 1995, Hammond et al 2005) are sufficient to drive trochlear axons to their exit point even in the absence of attractive signals. Alternatively, there may be other attractants directing trochlear axons towards the exit point compensating for the lack of SDF-CXCR4 signalling. Finally, the lack of a trochlear phenotype could be a result of species difference between mouse and chick, because while this study identified *CXCR4* expression in the trochlear nucleus of the chick at HH stage 18 (figure 3.9), Lieberam et al (2005) reported an absence of *CXCR4* expression in the trochlear nucleus of the mouse.

The examination of semaphorin mutant mice (both *Sema3C* mutants and *Sema3C/Sema3A* double mutants) failed to reveal any abnormalities in the pathfinding of the abducens nerve. This ran contrary to expectations based on the findings outlined in the previous two chapters. The *in vitro* results showed that abducens axonal growth was promoted by Sema3C and inhibited by Sema3A. This correlated with the expression patterns of the two semaphorins in the region encompassing the target muscle and the pathway of the abducens nerve. Sema3C was expressed in the target and Sema3A was expressed around the trajectory of the abducens nerve and around the muscle target. This led to the formulation of a model where Sema3C secreted from the target muscle acted as an attractant for abducens axons and the inhibitory action of Sema3A confined the extending axons to their trajectory preventing entry into inappropriate regions. If this model were to be correct, one would expect abducens pathfinding errors in mice lacking *Sema3C* or both *Sema3C* and *Sema3A*. The lack of Sema3C, if it is the key target-derived attractant, might result in a failure of axons to extend rostrally or cause them to stall and fail to reach the target. The lack of Sema3A might be expected to result in a defasciculation of the nerve or axons aberrantly entering inappropriate territory. None of these phenotypes were observed, which can be interpreted in a number of ways. Firstly, it may be the case that the loss of semaphorin signalling causes a weak phenotype that is

not apparent with the method used here. For example, while most of the axons appear to project normally, a small subset might display aberrant behaviours such as stalling or indeed extending in the wrong direction. As an example, the abducens nerve also appeared largely normal in the *CXCR4* mutant when examined with neurofilament staining, however a previous report by Lieberam and colleagues (2005), where abducens axons were specifically labelled, showed that some axons aberrantly extend dorsally within the neural tube. Thus a more sensitive detection method can reveal abnormalities which are not immediately obvious. A second possibility is that the *in vitro* growth-promoting and growth-inhibiting effects of the semaphorins on abducens axons are not physiologically relevant perhaps because the concentration of the ligand in co-culture assays is far in excess of that found *in vivo*. Personally, I find this explanation less likely because of the correlation between the expression data and the *in vitro* culture results strongly suggests a role for the semaphorins in abducens axon guidance. A third possibility is that there are compensating mechanisms involved i.e. other guidance cues participate in the control of abducens pathfinding along with Sema3A and Sema3C and are able to direct abducens axons along the correct trajectory even in the absence of semaphorin signalling. Electroporation experiments using a dominant-negative neuropilin-1 failed to shed further light on the role of semaphorins in abducens axon guidance because the results were inconclusive.

The next and final chapter will summarize all the results in this thesis, discuss what conclusions can be drawn from them and what the limitations of the findings are and suggest some avenues for future research.

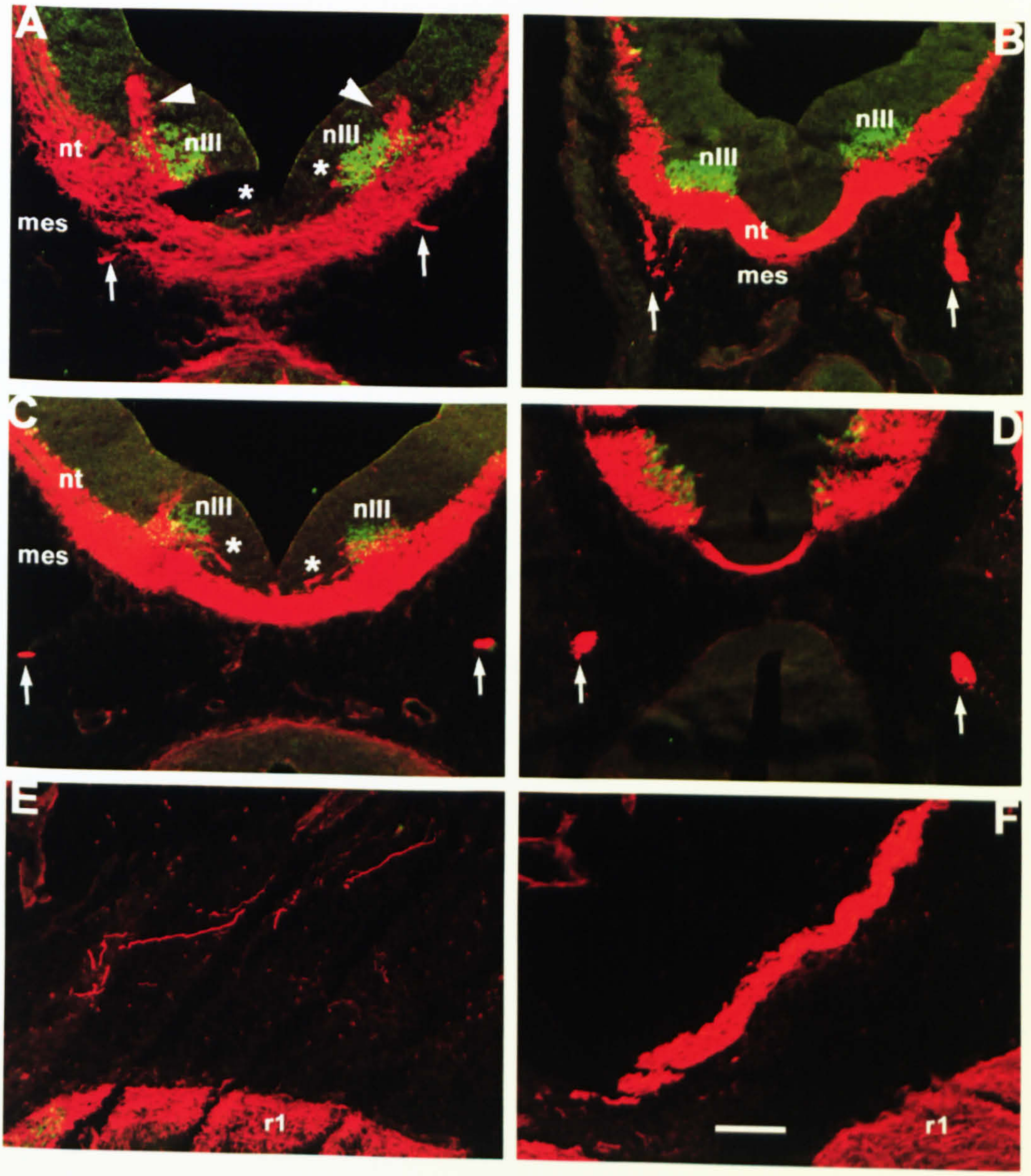
A
nt
nIII
nIII
*
*
mes
B
nIII
nIII
nt
mes
C
nt
nIII
nIII
*
*
mes
D
E
r1
F
r1
G
A-B
C-D
E-F

Figure 5.1

Figure 5.1

Oculomotor nerve in *CXCR4* mutant mice (E12.5)

Axons shown in red (neurofilament), motor neuron nuclei in green (islet). Left hand column of panels (A, C, E) shows the oculomotor nerve in homozygous mutant mice, right hand column shows the oculomotor nerve in heterozygous (B, D) or wild-type littermates (F).

A, B – Transverse section through midbrain at the level of the oculomotor nucleus. In the heterozygous mouse (B) oculomotor axons exit the neural tube ventrally (arrows). In the mutant (A) most axons emerging from the oculomotor nucleus aberrantly project dorsally within the neural tube (arrowheads). A small subset of axons exit normally (arrows) and another subset of axons project towards the midline (asterisks).

C, D – Transverse section at caudal midbrain level showing the rostral part of the oculomotor nerve (arrows). In the mutant (C) the nerve is much smaller and within the oculomotor nucleus axons can be seen projecting towards the midline (asterisks)

E, F – Sagittal section showing the oculomotor nerve. The nerve is much thinner in the mutant (E) reflecting the smaller number of axons that have exited into the periphery.

G – Schematic showing the positions of the sections

nt – neural tube, mes – mesenchyme, nIII – oculomotor nucleus, r1 – rhombomere1

Scale bar (D) – 100μm

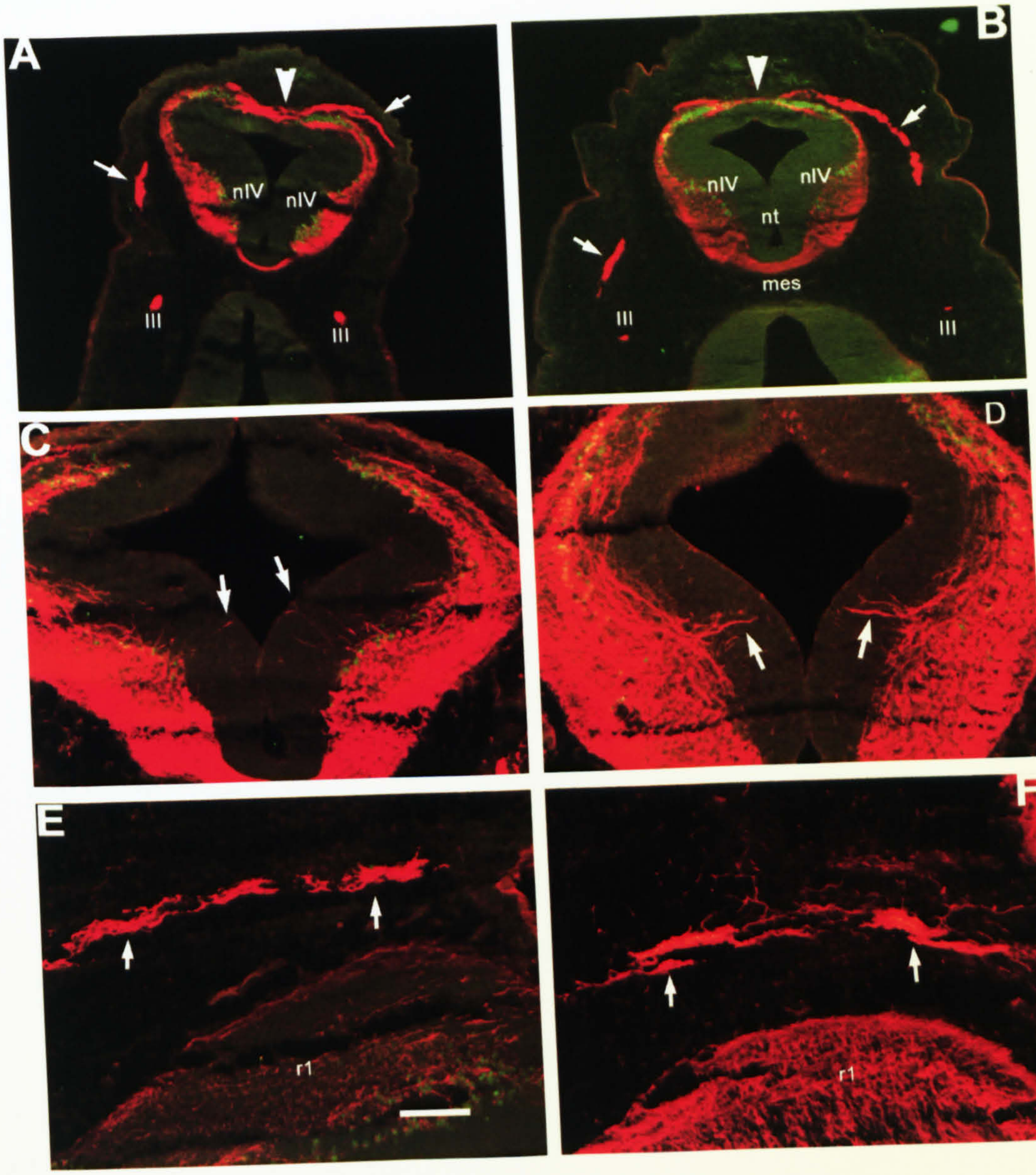

Figure 5.2

Figure 5.2

Trochear nerve in *CXCR4* mutant mice

Axons shown in red (neurofilament), motor neuron nuclei in green (islet). Left hand column of panels shows the trochlear nerve in heterozygous (A, C) or wild-type mice (E), right hand column (B, D, F) shows the trochlear nerve in homozygous mutant mice.

A, B – Transverse section at the level of the midbrain-hindbrain boundary. Trochlear axons are seen to exit from the dorsal roof plate and extend around the neural tube. No differences are apparent between the homozygous mutant (B) and the heterozygous mouse (A).

C, D – Transverse section through the trochlear nucleus. Some axons are seen projecting towards the ventricle in the heterozygote (arrows, C), but this phenotype is more striking in the mutant with fascicles of axons projecting to the ventricle (arrows, D)

E, F – Sagittal section showing the trochlear nerve. The nerve appears the same in the mutant (F) as in the wild-type embryo (E).

G – Schematic showing the positions of the sections

nIV – trochlear nucleus, nt – neural tube, mes – mesenchyme, r1 – rhombomere 1

Scale bar (C) – 240μm (A, B)
100μm (C-F)

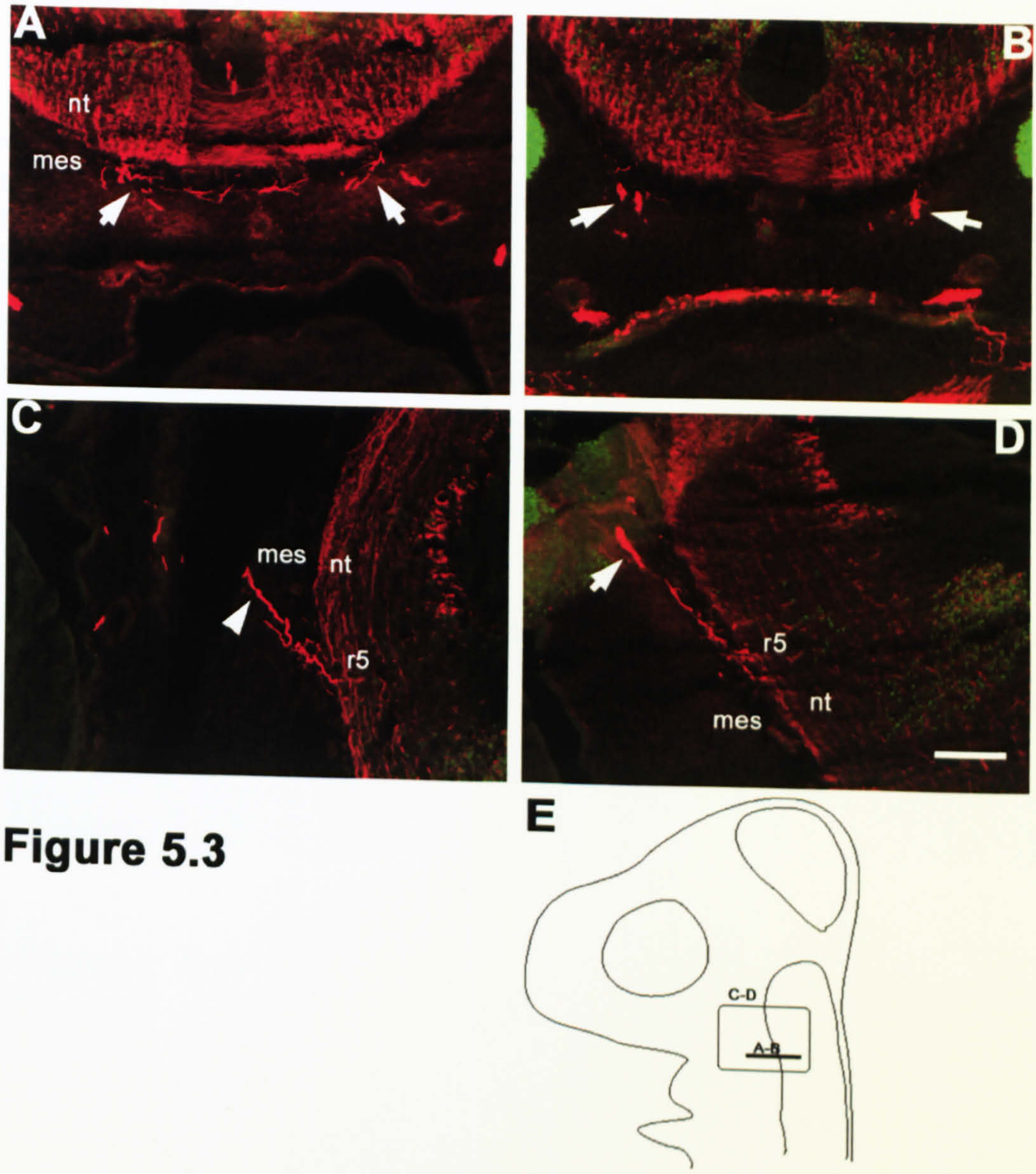

Figure 5.3

Figure 5.3

Abducens nerve in *CXCR4* mutant mice

Axons shown in red (neurofilament), motor neuron nuclei in green (islet). Left hand column of panels (A, C) shows the abducens nerve in homozygous mutant embryos, right hand column shows the abducens nerve in heterozygous (B) or wild-type (D) embryos.

A, B – Transverse section at the r5 level. Abducens axons are seen to exit ventrally from the neural tube. Arrows indicate the abducens nerve. In the mutant (A) some abducens axons project towards the midline (asterisk)

C,D – Sagittal section showing the abducens nerve. The nerve appears the same in the mutant (D) as in the wild-type embryo (C). Arrows indicate the abducens nerve.

E – Schematic showing the position of the sections

r5 – rhombomere 5, nt – neural tube, mes - mesoderm

Scale bar (D) – 100μm

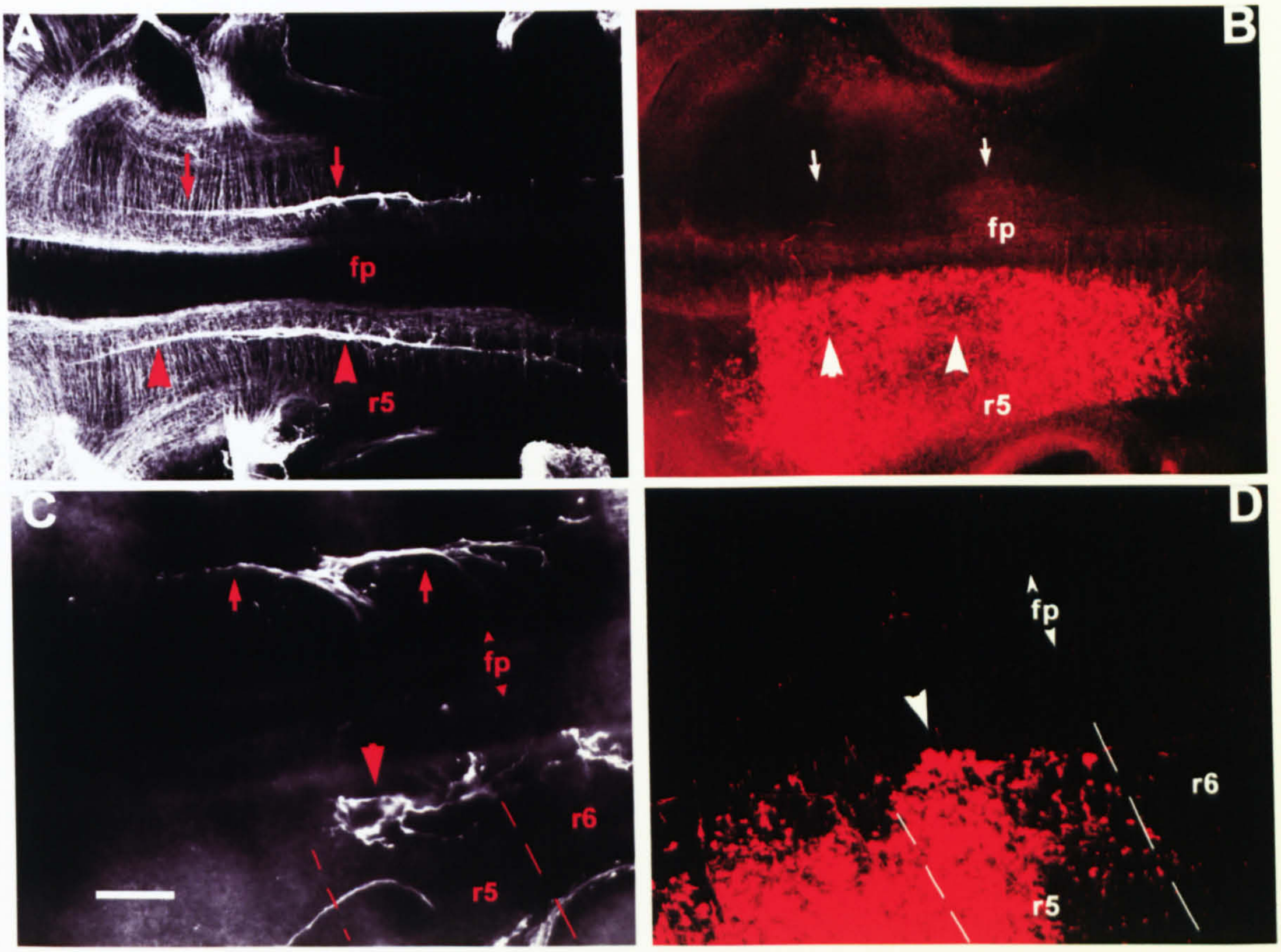

Figure 5.4

Figure 5.4

Abducens nerve in chick embryos electroporated with the dominant negative NPN-1 construct

A – Flat-mounted electroporated chick embryo with neurofilament staining in white.
B – Same field with myc staining in red, to show the cells expressing the construct. Large red arrowheads highlight the abducens nerve on the electroporated side and small red arrows show the nerve on the control side. White arrowheads and arrows indicate the same point in B. The nerve on the electroporated side appears normal

C – Flat mounted electroporated chick embryo with neurofilament staining in white. **D** – Same embryo with myc staining in red, to show the cells expressing the construct. Large red arrowheads highlight the abducens nerve on the electroporated side and small red arrows show the nerve on the control side. White arrowheads and arrows indicate the same point in B. Dotted lines indicate the boundaries of rhombomere 5. The nerve on the electroporated side is disrupted with axons failing to coalesce into rootlets which join together to project rostrally as a fasciculated nerve.

fp – floor plate, r5 – rhombomere 5, r6 – rhombomere 6.

Scale bar (C) – 120μm (A, B)
60μm (C, D)

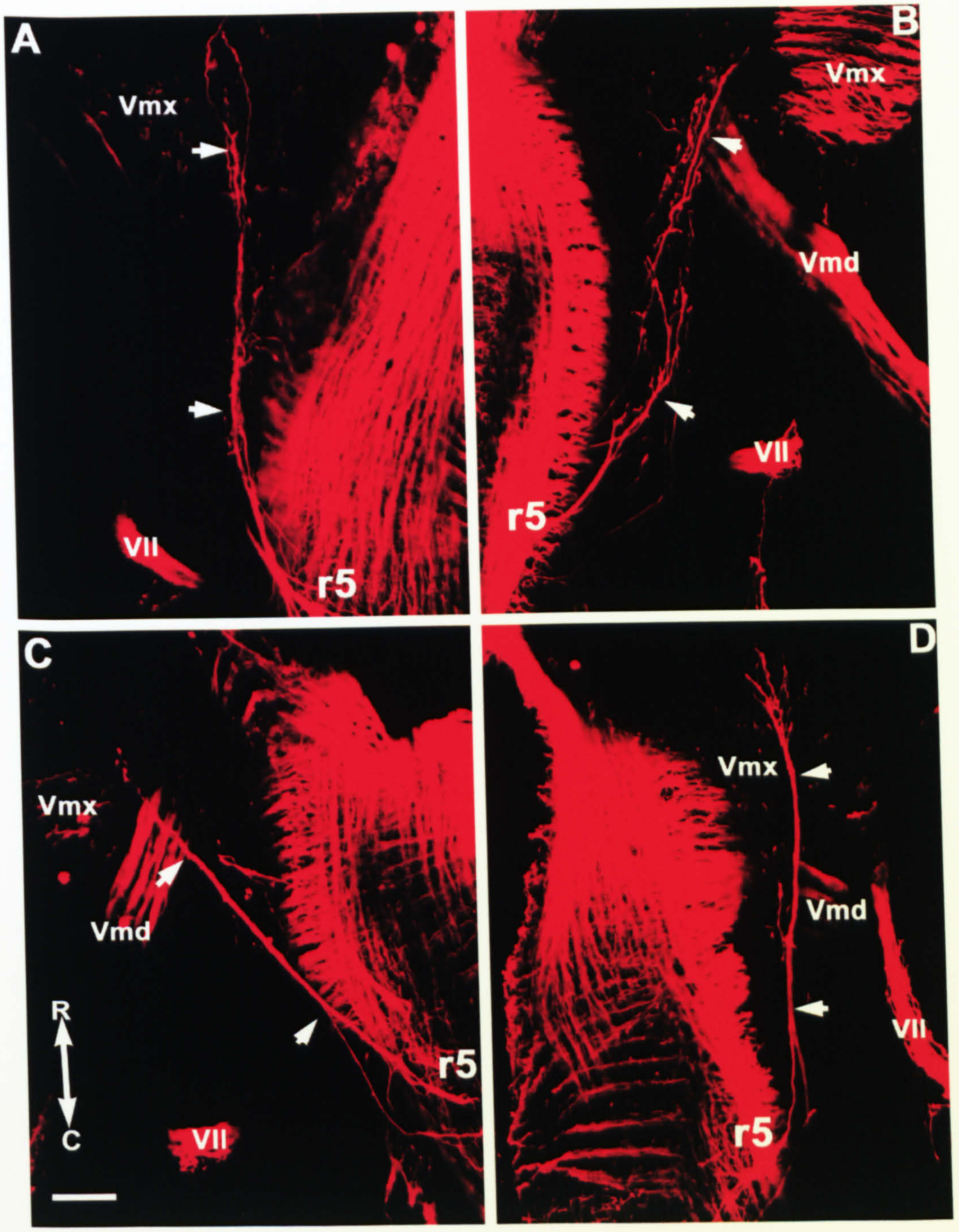

Figure 5.5

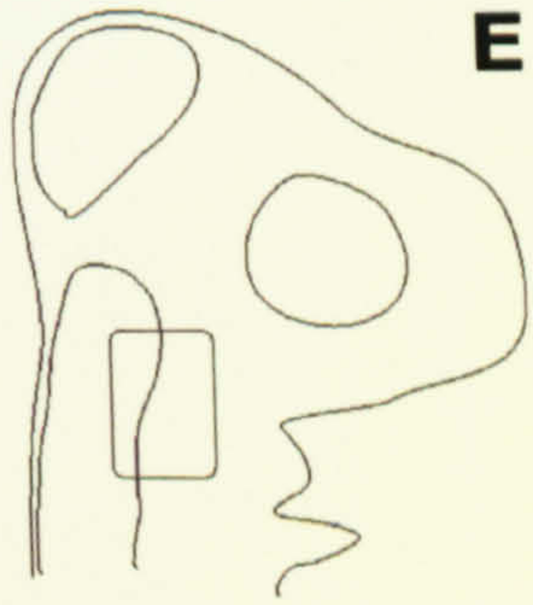

Figure 5.5

Abducens nerve in *Sema3C* mutant mouse embryos, sagittal view

A, B Wild-type E10.5 mouse embryo. Neurofilament staining in red. White arrows indicate the abducens nerve. (A – left side, B – right side).

C, D A homozygous *Sema3C* mutant E10.5 mouse embryo. Neurofilament staining in red. White arrows indicate the abducens nerve. (A – left side, B – right side). No abnormalities in abducens projection detected compared to the wild-type littermate.

E – Schematic showing position of the images in the embryo

Vmx – trigeminal nerve (maxillary branch), Vmd – trigeminal branch, VII – facial nerve, r5 –rhombomere 5, R – rostral , C – caudal

Scale bar (C) – 50μm

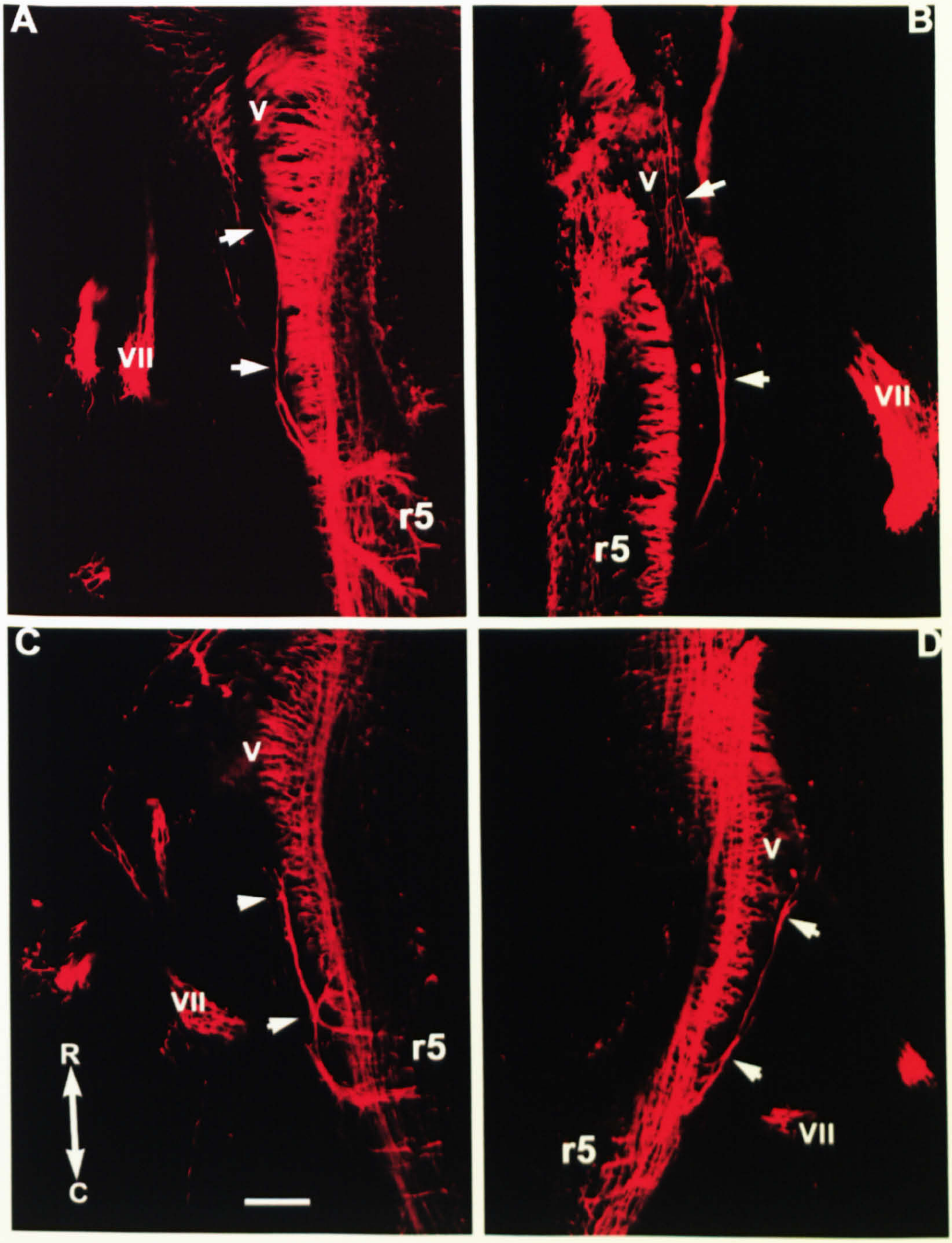

Figure 5.6

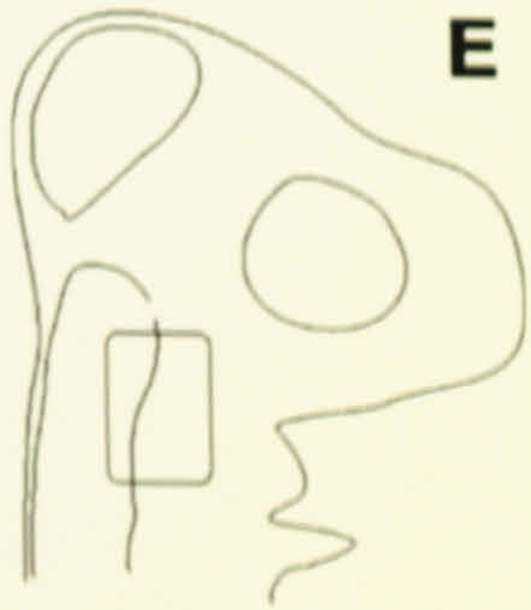

Figure 5.6

Abducens nerve in *Sema3C/Sema3A* mutant mouse embryos, sagittal view

A, B Wild-type E10.5 mouse embryo. Neurofilament staining in red. White arrows indicate the abducens nerve. (A – left side, B – right side).

C, D A homozygous *Sema3C* mutant E10.5 mouse embryo. Neurofilament staining in red. White arrows indicate the abducens nerve. (A – left side, B – right side). No abnormalities in abducens projection detected compared to the wild-type littermate.

E – Schematic showing position of the images in the embryo

V – trigeminal nerve (at the point where it exits the neural tube), VII – facial nerve, r5 – rhombomere 5, R – rostral , C – caudal

Scale bar (C) – 50μm

Chapter 6: Discussion

The aim of this study was to investigate the signals and mechanisms that govern axon guidance to the extraocular muscles. The investigation focussed on the role of five candidate guidance cues: Sema3A, Sema3C, Sema3F, HGF and SDF-1. The methods used were: analysis of the expression pattern of these molecules in the developing chick head by *in situ* hybridisation, and investigation of the functional effects of these guidance cues on oculomotor, trochlear or abducens axons' growth *in vitro* and *in vivo* to assess the physiological importance.

6.1 SUMMARY OF MAJOR FINDINGS

Sema3C was expressed in the lateral rectus muscle from HH stage 19, while at HH stages 25-28 it was also expressed in other extraocular muscles. Sema3C promoted outgrowth from abducens explants *in vitro*, but had no effect on outgrowth from oculomotor or trochlear explants. *Sema3A* was expressed around the trajectory and the target of the abducens nerve at HH stage 19 and at HH stages 25-28 it was expressed in the margins of other extraocular muscles and the adjoining mesenchyme. Sema3A inhibited abducens outgrowth *in vitro*, but had no effect on oculomotor or trochlear outgrowth. Taken together these findings suggested Sema3C and Sema3A might constitute positive and negative cues respectively for abducens growth. However, analysis of *Sema3C* mutant mice and *Sema3A/Sema3C* double mutants revealed no obvious abnormalities in the abducens projection. *Sema3F* was expressed in the mesenchyme adjoining the optic nerve exit point, dorsal to the developing ventral rectus/medial rectus at HH stages 25-28. Sema3F inhibited the outgrowth of trochlear axons and chemorepelled oculomotor axons, consistent with the idea that it limits the trajectory of these nerves.

HGF was expressed in the periocular mesenchyme in two regions at HH stage 26, one encompassed part of the dorsal oblique muscle and surrounding neural crest tissue, the

other adjoined the ventral edge of the eye and encompassed tissue flanking the ventral rectus/medial rectus and surrounding the dorsal oblique. HGF promoted axonal outgrowth from oculomotor and trochlear explants, consistent with a possible chemoattractant role. *SDF-1* was expressed in mesenchyme flanking both oculomotor and trochlear exit points from the neural tube at HH stages 18-21, and was expressed in two of the oculomotor target muscles (dorsal rectus and ventral oblique) at HH stage 26-7. SDF-1 promoted outgrowth from oculomotor and trochlear explants and induced ectopic exit from rostral and lateral edges of oculomotor explants, suggesting a role in neural tube exit as well as possible muscle targeting. Consistent with this idea, *CXCR4* mutant mice displayed major abnormalities in the abducens and oculomotor projections, with most oculomotor axons failing to exit ventrally and projecting towards the midline or dorsally instead. The peripheral trochlear projection appeared normal, but within the neural tube fascicles of trochlear axons appeared top be misprojecting towards the ventricle.

These data led to the following conclusions. Sema3C acts as a target-derived chemoattractant for abducens axons at HH stage 19, when innervation of the lateral rectus muscle is occurring. Sema3A repels abducens axons to confine them to their trajectory and prevent overshooting of the target. SDF-1 facilitates exit from the neural tube of oculomotor and trochlear axons at HH stages 18-21, and at HH stages 26-28 SDF-1 promotes oculomotor nerve growth towards the ventral oblique muscle and branching into the dorsal rectus muscle. HGF acts as a chemoattractant to promote growth of trochlear and oculomotor axons towards their targets.

6.2 MODEL OF THE INNERVATION OF EXTRAOCULAR MUSCLES

These conclusions are presented in a model shown in figure 6.1. The figure shows a schematic of a chick head at four stages: HH stage 18, HH stage 21, HH stage 26 and HH stage 28. At these stages key events in the development of this system occur. Abducens axons project from r5-r6 in the hindbrain; they start to exit the neural tube at

HH stage 16, extend rostrally and make initial contacts with the lateral rectus at stage 18 (figure 6.1A). Sema3C, which is expressed in the lateral rectus at this stage, attracts abducens axons towards their target (figure 6.1A), while Sema3A confines abducens axons to their trajectory and prevents overshooting of the target (figure 6.1A). Later the lateral rectus apparently migrates towards the lateral edge of the eye and the abducens axons extend to maintain the innervation of the muscle. It maybe the case that the early occupancy of the lateral rectus by abducens axons means that the abducens axons are unavailable to innervate other neighbouring extraocular muscles, such as the dorsal rectus, which develop later.

There are several unusual features of oculomotor axon guidance. Firstly, although oculomotor axons exit the neural tube from HH stage 16, at the same time as abducens axons and prior to trochlear axons, they do not make contacts with the ventral oblique until HH stage 27, by which stage both trochlear and abducens axons have innervated their targets. Their initial exit from the neuroepithelium is aided by SDF-1 (figure 6.1A). The reason for the subsequent delay in oculomotor innervation is not clear, but the axons appear to stall and grow slowly, until they reach the intermediate target of the ciliary ganglion by HH stage 23 (Chilton and Guthrie, 2004). This is likely to be due to the presence of a repulsive cue in the periocular mesenchyme at this stage, or an absence of an attractive cue. The nature of this signal has not been identified. It is possible that there is a requirement for the ciliary ganglion to reach a certain maturation stage before oculomotor axons can extend further. Subsequent oculomotor axon growth from the ciliary ganglion to the ventral oblique, which occurs between stages 23 and 27 is likely to be promoted by HGF expressed in this region (figure 6.1C) The ventral trajectory of the nerve is ensured by Sema3F-mediated repulsion from a region adjoining the optic nerve exit point (figure 6,1C).

The second unusual feature of oculomotor axon guidance, previously discussed, is the growth of axons towards the farthest target, the ventral oblique, and the lack of contacts with the more proximal targets. Only once the ventral oblique is contacted at HH stage 27 does the nerve branch into the other muscles. Branches to the dorsal rectus are

detectable by stage 28 and branches to the ventral rectus and medial rectus are detectable by stage 29 (Chilton and Guthrie 2004). There are several explanations that can account for this phenotype. Since the oculomotor neurons that innervate the various extraocular muscles are segregated into spatially distinct subnuclei and each neuron only sends its axon to innervate one of the muscles, one possibility that the axons of the subnuclei that innervate the proximal targets exit later or grow more slowly, thus resulting in more tardy innervation. Another possibility is that oculomotor neurons extend a primary axon to VO, and later form collateral branches into the other target muscle, which is followed by pruning back of primary axons of neurons which innervate DR, VR and MR, in order to give rise to topographically correct innervation pattern of subnuclei matching the muscles. This could be due to an activation of expression of attractive cues in the proximal target muscles, or the result of a retrograde signal from the ventral oblique, which may evoke gene expression changes that sensitise the neurons to attractive signals from the proximal muscles or induce cytoskeletal rearrangements that favour branching. *SDF-1* is expressed in the ventral oblique and dorsal rectus muscles; it might be acting as a retrograde signal from the ventral oblique, or as an attractant promoting branch formation into the dorsal rectus (figure 6.1D), or perhaps both.

The most atypical aspect of trochlear axon guidance is the dorsal trajectory of the axons, in contrast to all other somatic motor axons and the contralateral nature of the projection. Trochlear axons extend within the neural tube to the roof plate where they decussate and project contralaterally. The trajectory of trochlear axons is distinct from the dorsally-projecting branchiomotor and visceral motor axons which grow towards exit points, located about 2/3 of the distance between the floor plate and the roof plate, but do not extend all the way to the roof plate. The pattern of guidance within the neural tube has been partly attributed to the attractive action of FGF8, secreted from the midbrain-hindbrain boundary (Irving et al 2002) and partly to the repulsive action of Sema3F which prevents trochlear axons from invading the midbrain and channels them to the exit point through surround repulsion (Giger et al 2000, Watanabe et al 2004). Exit from the neural tube may be promoted by SDF-1, which is expressed in the mesenchyme

flanking the roof plate (figure 6.1B). Subsequent growth towards the target is driven by the attractive action of HGF (figure 6.1C).

An intriguing and unresolved aspect of trochlear axon guidance is what causes axons to decussate and project contralaterally? It can not be explained in conventional terms of gradients of attractants and repellents because, assuming symmetrical left and right sides, a growth cone at the midline will be exposed to identical chemorepulsive or chemoattractive stimuli from both halves of the embryo. A similar situation occurs in the guidance of spinal commissural axons, which cross the ventral midline. These axons are initially attracted to the midline by the action of netrin, but once they reach the floor plate they become sensitized to a range of repellents expressed at the midline including Slits and semaphorins, which repel the axons away from the midline once they have crossed it (Zou et al 2000). It may be that a similar mechanism enables trochlear axons to cross the dorsal midline, although nothing is currently known about what the specifics of this mechanism might be. Nonetheless, the fact that SDF-1 is capable of sensitizing oculomotor axons to Sema3A repulsion (figure 4.23 and 4.24) and that it is expressed in the region immediately adjacent to the roof plate, suggests that it is at least hypothetically possible that SDF-1 modifies the response of trochlear axons to other cues to enable them to project contralaterally.

6.3 MECHANISM OF ACTION OF THE CANDIDATE GUIDANCE CUES

6.3.1 HGF and SDF-1

HGF and SDF-1 are proposed as chemoattractants in this system. Both molecules exercise growth-promoting effects on oculomotor and trochlear axons; however they do so in different ways. HGF increases the length of oculomotor axons and the length of trochlear axons *in vitro*, in the case of trochlear axons HGF also increases defasciculation and possibly the number of axons, either by promoting branching or through neurotrophic effects on trochlear neurons (HGF is known to act as a survival

factor for motor neurons (Ebens et al 1996)) The different response of oculomotor and trochlear axons to HGF *in vitro* is interesting with reference to the expression pattern of *HGF*. *HGF* is expressed in the trochlear target muscle; therefore the increase in defasciculation/branching of trochlear axons in the presence of HGF may be indicative of the capacity of HGF to promote arborisation of trochlear axons within the target. SDF-1 also increases the length of trochlear axons and oculomotor axons *in vitro*; it may also increase the number of axons, because of increased density of axons, but it doesn't promote defasciculation. SDF-1 does however enable oculomotor axons to exit the explant ectopically. That may be a result of SDF-1 directly chemoattracting oculomotor axons towards an ectopic exit point (in the case of oculomotor axons exiting laterally and extending towards SDF-loaded beads) or through reducing the axons' sensitivity to chemorepellents within the explant (Chalasani et al 2003) (a more likely mechanism to account for the rostral exit of oculomotor explants when SDF-1 is added to the culture medium).

Chemoattraction by HGF or SDF-1, although implied by the data described, has not been demonstrated directly. A desirable experiment to carry out would be to culture explants with a focal source of HGF (such as beads or cell clusters) and assess the extent to which oculomotor and trochlear axons are able align along a gradient of HGF. Indeed, preliminary results of follow-on experiments indicate that trochlear axons are able to turn towards a focal source of HGF (P. Patel and S. Guthrie, unpublished observations). It must be noted that it is difficult to obtain conclusive proof of chemoattraction or chemorepulsion using explant experiments because the growth of an axon is influenced by neighbouring axons and cues secreted form the explant as well as the guidance molecule being tested. Furthermore, many (or all in the case of abducens explants) axons are regenerating and may behave differently to axons growing *de novo*. An alternative experiment to look for evidence of chemoattraction or chemorepulsion is to culture dissociated neurons in the presence of a guidance molecule gradient and to measure the turning responses of growth cones (Lohof et al 1992).

The difficulties encountered when attempting to demonstrate chemoattraction were also apparent in experiments with SDF-1 and oculomotor and trochlear explants. Oculomotor axons displayed turning towards SDF-loaded beads as evidenced by an increase in the angle of deflection, but the increase was not statistically significant. The result is further complicated by the propensity of oculomotor axons to exit the explant laterally towards the SDF-loaded beads, which has the consequence of increasing the angle of deflection, but is not necessarily evidence of chemoattraction because, as discussed above, it may be a result of SDF-1 acting indirectly to suppress chemorepulsion by another molecule. There is still considerable debate as to how SDF-1 exercises its effects on axons. Numerous intracellular pathways have been implicated in the transduction of SDF-1 signalling. As well as elevating cAMP (Chalasani et al 2003), SDF-1 has been reported to activate two distinct Rho-dependent pathways (Arakawa et al 2003), and two phospholipase C-dependent pathways (Xiang et al 2002). Lieberam et al (2005) also struggled to identify the mechanism by which spinal and hindbrain motor axons were misrouted from their ventral exit points in *Sdf-1* and *Cxcr4* mutants. It may be that *SDF-1* expressed in the mesenchyme adjoining the neural tube directly chemoattracts motor axons to exit into the periphery, or the shielding of chemorepellents secreted from the floor plate by SDF-1 enables motor axons to exit ventrally. Similarly, the aberrant behaviour of oculomotor axons in *Cxcr4* mutant mice observed in this study could be attributed to either mode of action of SDF-1. It is notable that SDF-1 could also sensitize oculomotor axons to the repulsive action of Sema3A *in vitro*, further increasing the diversity of effects of SDF-1 on axons and further complicating the possible mechanism which generates the axon guidance errors observed in *Cxcr4* mutants. Further research is required to clarify the mechanism of action of SDF-1.

Despite the remaining uncertainty with regard to the mode of action of SDF-1, there is an emerging pattern with respect to the roles it plays in axon guidance. The first confirmed *in vivo* role for SDF-1 came from a study which showed it acting as an attractant for retinal ganglion cells, guiding their axons out of the retina into the adjoining mesenchyme (Li et al 2005). Similarly ventrally-projecting spinal motor axons require SDF-1 for correct exit from the neural tube into the mesoderm (Lieberam et al

2005). The results presented in this study demonstrate that SDF-1 is also required for the appropriate exit of oculomotor axons from the neuroepithelium into the mesenchyme, and it may be involved in aiding the exit of trochlear axons from the neural tube. Generally, the expression of *SDF* in the developing chick head was enriched in mesenchymal tissues directly adjoining neural tissues (figure 3.10). Therefore, a key role of SDF-1 in axon guidance might be to facilitate the exit of axons from neural into mesenchymal tissues.

In addition to aiding the exit of oculomotor axons into the periphery, SDF-1 might also play a role in guiding oculomotor axons to innervate their muscle targets as suggested by the expression of SDF-1 in some of the extraocular muscles just prior to branch formation into that muscle. One possible mechanism by which this could occur is by SDF-1 inducing the formation of branch points along the axon, which leads to the formation of the nerve branches to innervate the more proximal targets of the oculomotor nerve. An interesting observation in this context is reported by Pujol et al (2004).The authors monitored the localisation of CXCR4 in hippocampal neurons – CXCR4 was initially enriched in the growth cone, but after a period of culture was distributed more evenly throughout the axon. Exposure to SDF-1 led to an increase in axonal branching preceded by the localisation of CXCR4 at the nascent branch points. Hence, SDF-1 secreted from the dorsal rectus could stimulate the branching of oculomotor axons resulting in the innervation of that muscle.

As mentioned previously, the branch formation into the proximal targets of the oculomotor nerve may require a retrograde signal from the ventral oblique muscle. The nature of such a signal, if indeed it exists, remains enigmatic, however HGF could conceivably fit the bill. There is no evidence in the published literature for the retrograde transport of HGF; however, neurotrophins such as NGF have been shown to be retrogradely transported by neurons following internalisation of Trk receptors (Claude et al 1982). Neurotrophins act in a similar fashion to HGF, signalling through tyrosine kinase receptors and activating the MAP kinase pathway to promote axonal growth and enhance neuronal survival. Once retrogradely transported to the cell body, NGF has

been shown to activate gene expression of various downstream targets including a receptor, *p75*, which recognises NGF (Kuruvilla et al 2004). Therefore, it is feasible that HGF can be internalised and retrogradely transported by a similar mechanism, and subsequently activate the expression of cell surface receptors that alter the sensitivity of oculomotor axons to guidance cues secreted from the target muscles.

A more general function of HGF could be as a non-specific target-derived chemoattractant for motor neurons. In addition to the growth-promoting effects on oculomotor and trochlear axons demonstrated here, HGF has already been shown to act as a target-derived chemoattractant for several other motor neuron populations. It is expressed in the branchial arches, promotes the outgrowth of branchiomotor axons *in vitro* (Caton et al 2000) and chemoattracts spinal motor axons that innervate the limb muscles and is expressed in the developing limb bud (Ebens et al 1996). It is notable that most motor neurons innervate muscles that develop at the same rostrocaudal axial level as the neurons themselves (Noden et al 1999). Thus HGF may be acting as a general peripheral chemoattractant for motor axons, attracting the ventral growth of motor axons within the same rostrocaudal level. The idea of non-specific chemoattractants that drive motor axon growth into the periphery is supported by the observation that both oculomotor and trochlear axons were chemoattracted by the branchial arches (A. Caton and S. Guthrie, unpublished data), which are not their normal target. Part of this chemoattraction may be mediated by HGF, which is expressed in the branchial arches. Although the effect of HGF on abducens outgrowth was not tested, it is notable that there is no expression of HGF in the lateral rectus muscle or surrounding tissue (figure 3.8), indicating that it does not function as a target-derived chemoattractant for abducens axons. If abducens axons are indeed insensitive to HGF, that may explain why they are able to turn to grow rostrally rather than extend in the same axial plane towards the branchial arches that are secreting HGF.

6.3.2 Semaphorins

Different semaphorins have been shown to exercise a wide range of effects in this system. Sema3F suppressed trochlear outgrowth and chemorepelled oculomotor axons. The differences in the response of oculomotor and trochlear axons to Sema3F could be due to distinct intracellular responses to the ligand in the two populations of axons – chemotropic turning responses in growth cones have been linked to the asymmetric distribution of receptors on growth cones in response to exposure to the ligand secreted from a focal source, sometimes mediated by localisation on lipid rafts (Guirland et al 2004). It is possible that NPN-2 or another part of the receptor complex is asymmetrically localised on oculomotor axons resulting in turning behaviour, but uniformly distributed on trochlear growth cones leading to growth cone collapse. This interpretation is consistent with the idea of Sema3F acting as a surround repellent to channel trochlear axons to their exit point (Giger et al 2000), but acting as a longer range repellent for oculomotor axons, preventing oculomotor axons from straying into too dorsal a trajectory. However, another interpretation is that the difference in the responses of oculomotor and trochlear axons is due to the experimental set up: trochlear axons are hemmed in between two repulsive gradients emanating from the Sema3F-secreting cluster and the floor plate and therefore cannot exit the explant, whereas the ventrally-projecting oculomotor axons are less sensitive to midline repulsion (Varela-Echavarria et al 1997).

The *in vivo* significance of Sema3F signalling in this system has been previously demonstrated by the disruption of oculomotor and trochlear nerves in *Sema3F* and *NPN-2* mutants (Sahay et al 2003, Chen et al 2000, Giger et al 2000). However, surprisingly no *Sema3F* expression in the mesenchyme surrounding the oculomotor nerve trajectory was detected. Therefore, another explanation for the defasciculation of the oculomotor nerve in the *NPN-2* and *Sema3F* mutant is required. *Sema3D* is expressed in that region (Chilton and Guthrie 2003), which might account for the defasciculation seen in the *NPN-2* mutant but not in the *Sema3F* mutant. Another possible explanation is that it is

due to species differences between the mouse and the chick, and while *Sema3F* is not expressed in that region in the chick it may be in the mouse.

The growth-promoting effect of Sema3C on abducens axons was surprising, especially in the light of growth inhibition by Sema3A on the same axons, and a lack of response in oculomotor and trochlear axons to Sema3C. As discussed in chapter 4.3, there are a number of possible explanations for why Sema3C induces a different response to Sema3A in abducens neurons, but it is likely that the downstream signalling cascades to these cues diverge. Sema3A has been shown to mediate growth cone collapse through cytoskeletal rearrangements induced by the activation of RhoA (Huber et al 2003), while activation of RhoA by Sema3C is yet to be reported. The divergence may occur at the level of a plexin co-receptor – NPN-1 can associate with different plexin-As, which in turn may preferentially bind Sema3A or Sema3C and evoke a distinct downstream response (Cheng et al 2001, Suto et al 2005). In fact even the idea that NPN-1 is required to mediate the effects of both ligands has been thrown into doubt by a recent report, which showed that Sema3E was capable of signalling to cells in a neuropilin-independent manner, overturning the previous paradigm that class III semaphorins require a neuropilin receptor (Gu et al 2005).

6.4 THE UNIQUE CHARACTER OF THE EXTRAOCULAR MUSCLES PLAYS A ROLE IN THE MECHANISM OF THEIR INNERVATION

As discussed in section 1.2.3, head muscles develop in a manner distinct from trunk muscles, and the regulatory cascades which govern their differentiation are poorly understood. The timing of innervation appears to be related to the timing of differentiation. The lateral rectus develops most precociously; it expresses both regulatory and structural genes before the other extraocular muscles and is the first extraocular muscle to receive innervation (Noden et al 1999, Wahl et al 1994). The ventral oblique and the dorsal oblique are the next to develop and they are innervated before the late-developing ventral rectus, medial rectus and dorsal rectus. Therefore, the

delay in innervation of the proximal oculomotor targets may be related to the maturation state of the muscles. Another question is the link between the migration and differentiation of the extraocular muscles. It is likely that the muscles require a signal from cells near their final position to complete differentiation, or they need to 'get away' from an inhibitory signal. Tzahor et al (2003) found that branchial arch muscles' differentiation is triggered by BMP and Wnt inhibitors secreted by arch neural crest cells, whilst BMPs and Wnts secreted from the neural tube prevent premature differentiation. Unpublished data from D. Noden (personal communication) suggests that FGF8 may be the signal, which is necessary for the extraocular muscles to complete their differentiation. It is also unclear how the translocation of extraocular muscles takes place. Migration of limb muscle precursors is preceded by the expression of *met*, which is in turn activated by Pax3. Extraocular muscles do not express these markers, and Borue and Noden (2004) have suggested that they do not actively migrate, but rather become embedded in a sheet of proliferating neural crest, whose expansion carries them to their final location.

The lateral rectus is an atypical muscle. Its development is precocious and it's differentiation is also controlled by a unique transcription factor cascade, which resembles the differentiation programme found in trunk muscles, with the expression of genes such as *Lbx1*, *Paraxis* and *Pax7*, but is not identical to the trunk programme because Pax3 (the crucial upstream regulator) is not expressed and because the lateral rectus primordium is unable to activate myogenesis when transplanted to the trunk. Nonetheless, the lateral rectus is unique amongst head muscles in expressing trunk regulatory genes, which has led to the suggestion that its developmental programme lies somewhere in between the classical trunk programme and head programmes (Mootoosamy and Dietrich 2002). The unique developmental programme of the lateral rectus might induce the high levels of *Sema3C* expression observed in the muscle from early stages in the chick, which has a growth-promoting effect on abducens axons and may be involved in guiding them to the lateral rectus muscle. While Sema3C is not critical for chemoattracting abducens axons because the abducens nerve still projects rostrally towards the lateral rectus in *Sema3C* mutant mice, it may be one of the factors

uniquely expressed by the lateral rectus that enable the abducens axons to correctly navigate to their target. A possible experiment to identify other factors secreted by the lateral rectus would be to carry out microarray analysis of gene expression in the lateral rectus compared to other extraocular muscles, and screen for genes known to be involved in axon guidance.

6.5 IMPLICATIONS FOR HUMAN DISEASES – CRANIAL DYSINNERVATION DISORDERS

The unique identity of the lateral rectus is important because it is directly relevant to a human genetic condition which stems from incorrect innervation of the extraocular muscles and is one of the most common causes of strabismus. Duane's syndrome causes 1-5% of all strabismus cases and if uncorrected in childhood can lead to amblyopia – a form of partial blindness (Gutowski 2000). The pathology results from an absence of the abducens nerve and an innervation of the lateral rectus by oculomotor axons. The genes responsible for Duane's syndrome have not been identified, but one of the loci has been mapped to chromosome 2 (Evans et al 2000, Appukuttan et al 1999) and contains the HoxD cluster, including HoxD3, which is involved in patterning the posterior hindbrain (Lumsden and Krumlauf 1996) where abducens cell bodies are located. No mutations in the coding regions of any of the HoxD genes have been identified (S. Ellard and N. Gutowski, personal communication), but it is possible the mutation resides in one of the regulatory or enhancer sequences, resulting in a lack of expression or inappropriate expression of HoxD3 in the developing embryo, and a consequent failure to develop the abducens nucleus. Interestingly, in the HoxA3/HoxB3 double mutant mice, which fail to develop the abducens nucleus, aberrant innervation of the lateral rectus by another nerve was observed (Gaufo et al 2003) Whilst it's unclear whether the absence of the abducens nerve is the primary cause of the pathology, it appears that the innervation of the lateral rectus by oculomotor axons is not merely opportunistic. In a chick model of Duane's syndrome where the abducens nucleus was unilaterally ablated no oculomotor innervation of the lateral rectus occurred as a result, although a few axons from the

contralateral abducens nerve contacted the muscle (Chilton and Guthrie 2004). This result suggests that despite the fact that the oculomotor nerve passes in close proximity to the lateral rectus muscle, it is not merely the fact that abducens axons have already contacted the lateral rectus muscle that prevents oculomotor nerve from branching into the lateral rectus in a similar way to its branching into the neighbouring dorsal rectus. Whether it is an absence of an attractive signal or the presence of a repulsive cue that prevent the oculomotor axons from innervating the lateral rectus is unclear. An interesting observation from Wahl and Noden (2001) in this context, was that ablation of the mesenchyme adjacent to rhombomeres 2 and 3 – a territory which the abducens axons traverse prior to innervating the lateral rectus, does not prevent abducens axons from innervating their target, but in some cases results in oculomotor axons invading the lateral rectus also, with the muscle consequently receiving innervation from two nerves. This raises the possibility that there is a repulsive cue for oculomotor axons expressed by the mesenchyme surrounding the lateral rectus and which ordinarily prevents oculomotor axons from innervating this muscle. Resolving which are the unique signals secreted by the lateral rectus or surrounding tissue would shed light on the causes of the pathology in this disease.

Congenital fibrosis of extraocular muscles (CFEOM) is a set of genetic conditions in which lack of innervation of extraocular muscles results in atrophy and fibrosis of these muscles. Symptoms that characterise these conditions usually include drooping of the eyelids and a downward gaze, lack of binocular vision and amblyopia (Engle 2002). In the less common variant of CFEOM, CFEOM2, the cause of the condition has been identified as a mutation in *ARIX*, a human version of the mouse *Phox2A* gene (Nakano et al 2001). Mice lacking *Phox2A* display an absence of the oculomotor and trochlear nuclei, the locus coerulus, a number of sensory and parasympathetic ganglia and die at birth as a result (Pattyn et al 1997). The phenotype in humans is much more restricted and is confined to an absence of the oculomotor and trochlear nuclei and the corresponding nerves, sometimes unilateral. The structures that are absent in Phox2A null mice are characterised by *Phox2A* expression preceding *Phox2B* expression in wild-type mice; it is not clear why only the oculomotor and trochlear nuclei are affected in

humans, but it highlights the difference in patterning between these rostral cranial motor nuclei and other cranial motor nuclei, whose patterning is controlled by *Hox* genes.

The more common version of CFEOM, CFEOM1, is caused by a mutation in the Kif21A gene, a novel kinesin (Yamada et al 2003). The underlying pathology is due to the loss of the superior branch of the oculomotor nerve which innervates the dorsal rectus and the levator superiore palpabrae (LPS) muscles in humans and a consequent fibrosis of these muscles. The superior branch of the oculomotor nerve is the only branch that projects contralaterally as a result of the translocation across the midline of the cell bodies of the ventromedial subnucleus, whose axons innervate the dorsal rectus (Puelles 1975, Chilton and Guthrie 2004). This translocation occurs between HH stages 27 and 35, i.e. it starts at the same time as the dorsal rectus is being innervated and possibly requires a retrograde signal from the muscle. Kinesins have been implicated in nuclear translocations, therefore it is possible that the loss of this kinesin gene prevents the midline crossing of these cell bodies which leads to the atrophy of this branch of the nerve (the other branches, which project ipsilaterally, are unaffected).

The proposed retrograde signal from the ventral oblique, which initiates branch formation into the remaining oculomotor target muscles, is likely to mediate its effects via cytoskeleton remodelling and might also feature a kinesin. The phenotype of *Kif2a* mutant mice consisted of brain abnormalities, which were caused by excessive branching of axons. It appears that this kinesin prevents inappropriate branch formation in wild-type mice by depolymerising individual microtubules and regulating microtubule dynamics (Homma et al 2003).

6.6 CONCLUDING REMARKS

In conclusion, this study has identified some of the factors involved in the control of the navigation of motor axons to the extraocular muscles, but many fascinating questions remain before regulation of axon guidance in this system can be fully understood. It is

an ideal system in which to investigate motor axon targeting; arguably it makes a much better model than targeting in the limb, which, although more extensively studied, is also vastly more complicated. The six extraocular muscles and three nerves form a sufficiently simple system to permit the principles of the different stages of innervation to be unravelled, from axon exit into the periphery to axon growth, targeting, branching and synaptogenesis.

These processes are likely to be governed by combinations of different guidance cues; furthermore each guidance cue can take on a number of roles at different stages of the innervation process. For example, SDF-1 and Sema3A might combine to prevent overshooting of the target by oculomotor and trochlear axons, while SDF-1 might promote oculomotor axon exit from the neural tube and later target oculomotor axons to the appropriate muscle and stimulate formation of collateral branches.

Some of the guidance cues investigated in this study appear to exercise generic effects on motor neurons, for example HGF might act as a non-specific target-derived chemoattractant, driving axon growth into the periphery at the same axial level, while SDF-1 enables various populations of motor axons to exit the neural tube. Other guidance cues are specific to this system, for example Sema3C attracting abducens axons to the lateral rectus. The guidance signals that govern innervation of the extraocular muscles are almost certainly not confined to the five molecules investigated in this study; other guidance cues that have been implicated in this system include members of the GDNF family (Chen et al 2003); other signals may yet be discovered.

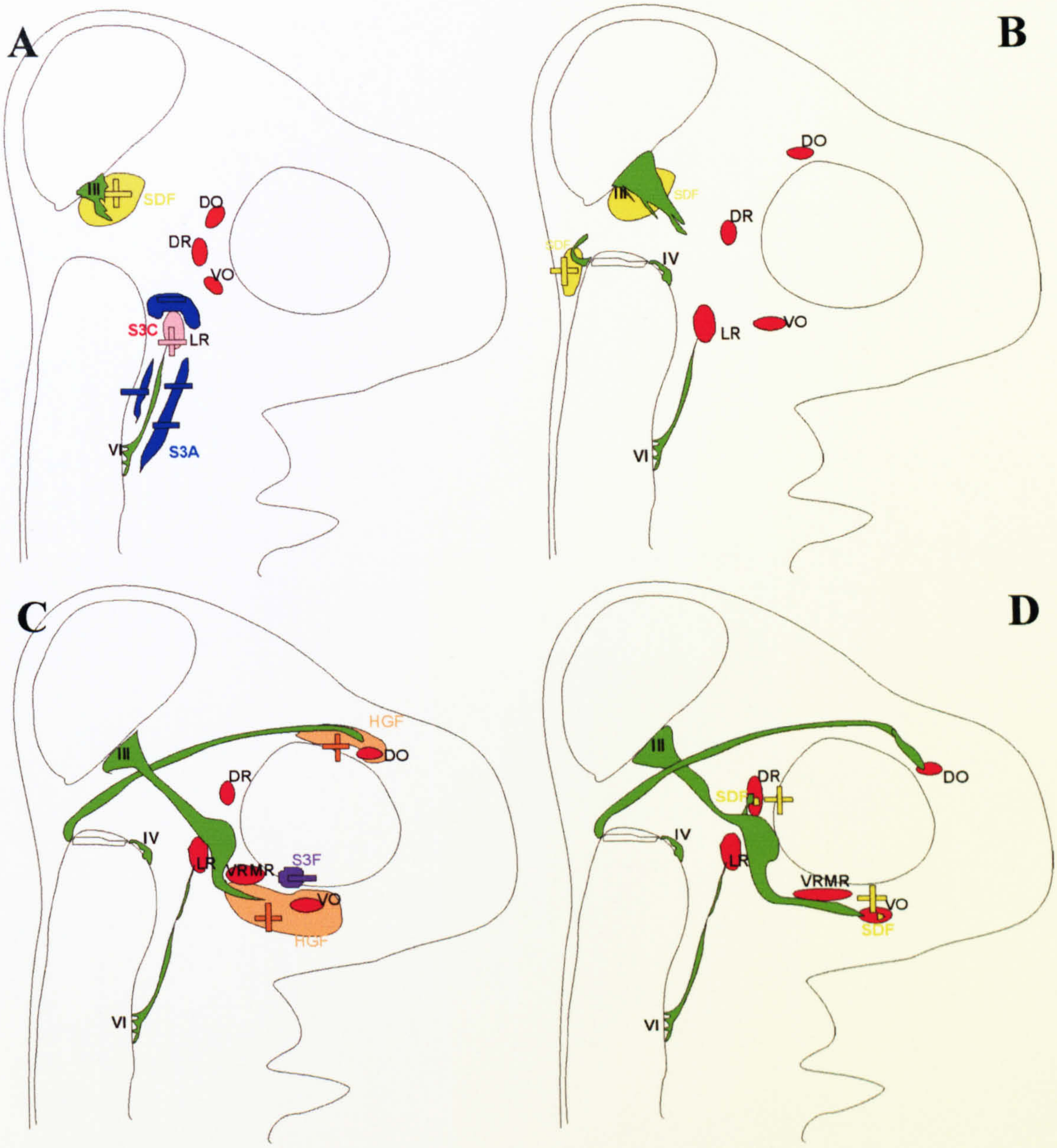

Figure 6.1

Schematic model showing the expression of key guidance molecules at different stages and their proposed effects

Figure 6.1

Schematic model showing the expression of key guidance molecules at different stages and their proposed effects

A – Stage 18. Four of the extraocular muscles are detectable at this stage, although they have not yet reached their final positions. The muscles are shown in red, with the exception of the lateral rectus which is shown in pink to indicate the expression of *Sema3C*. The pink plus sign indicates an attractive gradient of Sema3C emanating from the lateral rectus muscle and directing abducens axons to their target. The trajectory of the abducens nerve is surrounded by *Sema3A* expression (shown in blue). Blue minus signs indicate a repulsive gradient of Sema3A confining abducens axons to their course. Oculomotor axons are also emerging into the periphery at this stage. The oculomotor exit point is surrounded by *SDF-1* expression (shown in yellow). Yellow plus sign indicates SDF-1 signalling to oculomotor neurons to promote their exit from the neuroepithelium.

B – Stage 21. Still only four of the extraocular muscles are detectable, and they have advanced further towards their final position (muscles shown in red). *SDF-1* is expressed in the mesenchyme flanking the dorsal roof plate at rhombomere1 level (shown in yellow). Yellow plus sign indicates SDF-1 attracting trochlear axons to their exit point.

C- Stage 26. All extraocular muscle are now detectable, although the VRMR primordium remains fused. The trochlear nerve has reached its target and the oculomotor nerve is growing towards the most distal target. Axons of both nerves are attracted by HGF (expression shown in orange, orange plus signs indicate chemoattractive gradients). *Sema3F* is expressed adjacent to the optic nerve exit point (shown in purple), and the repulsive gradient of Sema3F confines the oculomotor nerve to its ventral trajectory (purple minus sign).

D – Stage 28. The muscles have reached their final positions. The oculomotor nerve has contacted the ventral oblique and is about to issue branches into the remaining targets. *SDF-1* expressed (at stage 26/7) in the VO and the DR (yellow) may be promoting branch formation into these muscles (yellow plus signs)

Abbreviations: DO – dorsal oblique, DR – dorsal rectus, VO – ventral oblique, LR – lateral rectus, VRMR – ventral rectus/medial rectus, III – oculomotor nerve, IV – trochlear nerve, VI – abducens nerve.

Bibliography

Anonymous (1999) Unified nomenclature for the semaphorins/collapsins. Semaphorin Nomenclature Committee. *Cell* **97**, 551-2.

Acampora, D., Mazan, S., Lallemand, Y., Avantaggiato, V., Maury, M., Simeone, A. and Brulet, P. (1995) Forebrain and midbrain regions are deleted in Otx2-/- mutants due to a defective anterior neuroectoderm specification during gastrulation. *Development* **121**, 3279-90.

Adams, R.H., Lohrum, M., Klostermann, A., Betz, H. and Puschel, A.W. (1997) The chemorepulsive activity of secreted semaphorins is regulated by furin-dependent proteolytic processing. *EMBO J* **16**, 6077-86.

Agarwala, S. and Ragsdale, C.W. (2002) A role for midbrain arcs in nucleogenesis. *Development* **129**, 5779-88.

Agarwala, S., Sanders, T.A. and Ragsdale, C.W. (2001) Sonic hedgehog control of size and shape in midbrain pattern formation. *Science* **291**, 2147-50.

Alvares, L.E., Schubert, F.R., Thorpe, C., Mootoosamy, R.C., Cheng, L., Parkyn, G., Lumsden, A. and Dietrich, S. (2003) Intrinsic, Hox-dependent cues determine the fate of skeletal muscle precursors. *Dev Cell* **5**, 379-90.

Anderson, C.N., Ohta, K., Quick, M.M., Fleming, A., Keynes, R. and Tannahill, D. (2003) Molecular analysis of axon repulsion by the notochord. *Development* **130**, 1123-33.

Appukuttan, B., Gillanders, E., Juo, S.H., Freas-Lutz, D., Ott, S., Sood, R., Van Auken, A., Bailey-Wilson, J., Wang, X., Patel, R.J., Robbins, C.M., Chung, M., Annett, G., Weinberg, K., Borchert, M.S., Trent, J.M., Brownstein, M.J. and Stout, J.T. (1999) Localization of a gene for Duane retraction syndrome to chromosome 2q31. *Am J Hum Genet* **65**, 1639-46.

Arakawa, Y., Bito, H., Furuyashiki, T., Tsuji, T., Takemoto-Kimura, S., Kimura, K., Nozaki, K., Hashimoto, N. and Narumiya, S. (2003) Control of axon elongation via an SDF-1alpha/Rho/mDia pathway in cultured cerebellar granule neurons. *J Cell Biol* **161**, 381-91.

Araujo, M., Piedra, M.E., Herrera, M.T., Ros, M.A. and Nieto, M.A. (1998) The expression and regulation of chick EphA7 suggests roles in limb patterning and innervation. *Development* **125**, 4195-204.

Arber, S., Han, B., Mendelsohn, M., Smith, M., Jessell, T.M. and Sockanathan, S. (1999) Requirement for the homeobox gene Hb9 in the consolidation of motor neuron identity. *Neuron* **23**, 659-74.

Bagnard, D., Lohrum, M., Uziel, D., Puschel, A.W. and Bolz, J. (1998) Semaphorins act as attractive and repulsive guidance signals during the development of cortical projections. *Development* **125**, 5043-53.

Bagri, A., Gurney, T., He, X., Zou, Y.R., Littman, D.R., Tessier-Lavigne, M. and Pleasure, S.J. (2002) The chemokine SDF1 regulates migration of dentate granule cells. *Development* **129**, 4249-60.

Behar, O., Golden, J.A., Mashimo, H., Schoen, F.J. and Fishman, M.C. (1996) Semaphorin III is needed for normal patterning and growth of nerves, bones and heart. *Nature* **383**, 525-8.

Bell, E., Wingate, R.J. and Lumsden, A. (1999) Homeotic transformation of rhombomere identity after localized Hoxb1 misexpression. *Science* **284**, 2168-71.

Berkes, C.A. and Tapscott, S.J. (2005) MyoD and the transcriptional control of myogenesis. *Semin Cell Dev Biol* **16**, 585-95.

Bladt, F., Riethmacher, D., Isenmann, S., Aguzzi, A. and Birchmeier, C. (1995) Essential role for the c-met receptor in the migration of myogenic precursor cells into the limb bud. *Nature* **376**, 768-71.

Borue, X. and Noden, D.M. (2004) Normal and aberrant craniofacial myogenesis by grafted trunk somitic and segmental plate mesoderm. *Development* **131**, 3967-80.

Bourikas, D., Pekarik, V., Baeriswyl, T., Grunditz, A., Sadhu, R., Nardo, M. and Stoeckli, E.T. (2005) Sonic hedgehog guides commissural axons along the longitudinal axis of the spinal cord. *Nat Neurosci* **8**, 297-304.

Brand-Saberi, B., Muller, T.S., Wilting, J., Christ, B. and Birchmeier, C. (1996) Scatter factor/hepatocyte growth factor (SF/HGF) induces emigration of myogenic cells at interlimb level in vivo. *Dev Biol* **179**, 303-8.

Briscoe, J., Pierani, A., Jessell, T.M. and Ericson, J. (2000) A homeodomain protein code specifies progenitor cell identity and neuronal fate in the ventral neural tube. *Cell* **101**, 435-45.

Briscoe, J., Sussel, L., Serup, P., Hartigan-O'Connor, D., Jessell, T.M., Rubenstein, J.L. and Ericson, J. (1999) Homeobox gene Nkx2.2 and specification of neuronal identity by graded Sonic hedgehog signalling. *Nature* **398** , 622-7.

Brittis, P.A., Silver, J., Walsh, F.S. and Doherty, P. (1996) Fibroblast Growth Factor Receptor Function Is Required for the Orderly Projection of Ganglion Cell Axons in the Developing Mammalian Retina. *Mol Cell Neurosci* **8**, 120-8.

Broccoli, V., Boncinelli, E. and Wurst, W. (1999) The caudal limit of Otx2 expression positions the isthmic organizer. *Nature* **401**, 164-8.

Brown, A., Yates, P.A., Burrola, P., Ortuno, D., Vaidya, A., Jessell, T.M., Pfaff, S.L., O'Leary, D.D. and Lemke, G. (2000) Topographic mapping from the retina to the midbrain is controlled by relative but not absolute levels of EphA receptor signaling. *Cell* **102**, 77-88.

Butler, S.J. and Dodd, J. (2003) A role for BMP heterodimers in roof plate-mediated repulsion of commissural axons. *Neuron* **38**, 389-401.

Campbell, D.S. and Holt, C.E. (2003) Apoptotic pathway and MAPKs differentially

regulate chemotropic responses of retinal growth cones. *Neuron* **37**, 939-52.

Campbell, D.S. and Holt, C.E. (2001) Chemotropic responses of retinal growth cones mediated by rapid local protein synthesis and degradation. *Neuron* **32**, 1013-26.

Carpenter, E.M., Goddard, J.M., Chisaka, O., Manley, N.R. and Capecchi, M.R. (1993) Loss of Hox-A1 (Hox-1.6) function results in the reorganization of the murine hindbrain. *Development* **118**, 1063-75.

Castellani, V., Chedotal, A., Schachner, M., Faivre-Sarrailh, C. and Rougon, G. (2000) Analysis of the L1-deficient mouse phenotype reveals cross-talk between Sema3A and L1 signaling pathways in axonal guidance. *Neuron* **27**, 237-49.

Catalano, S.M., Messersmith, E.K., Goodman, C.S., Shatz, C.J. and Chedotal, A. (1998) Many major CNS axon projections develop normally in the absence of semaphorin III. *Mol Cell Neurosci* **11**, 173-82.

Caton, A., Hacker, A., Naeem, A., Livet, J., Maina, F., Bladt, F., Klein, R., Birchmeier, C. and Guthrie, S. (2000) The branchial arches and HGF are growth-promoting and chemoattractant for cranial motor axons. *Development* **127**, 1751-66.

Chalasani, S.H., Sabelko, K.A., Sunshine, M.J., Littman, D.R. and Raper, J.A. (2003) A chemokine, SDF-1, reduces the effectiveness of multiple axonal repellents and is required for normal axon pathfinding. *J Neurosci* **23**, 1360-71.

Chang, S., Rathjen, F.G. and Raper, J.A. (1987) Extension of neurites on axons is impaired by antibodies against specific neural cell surface glycoproteins. *J Cell Biol* **104**, 355-62.

Charron, F., Stein, E., Jeong, J., McMahon, A.P. and Tessier-Lavigne, M. (2003) The morphogen sonic hedgehog is an axonal chemoattractant that collaborates with netrin-1 in midline axon guidance. *Cell* **113**, 11-23.

Chedotal, A., Del Rio, J.A., Ruiz, M., He, Z., Borrell, V., de Castro, F., Ezan, F., Goodman, C.S., Tessier-Lavigne, M., Sotelo, C. and Soriano, E. (1998) Semaphorins

III and IV repel hippocampal axons via two distinct receptors. *Development* **125**, 4313-23.

Chen, H., Bagri, A., Zupicich, J.A., Zou, Y., Stoeckli, E., Pleasure, S.J., Lowenstein, D.H., Skarnes, W.C., Chedotal, A. and Tessier-Lavigne, M. (2000) Neuropilin-2 regulates the development of selective cranial and sensory nerves and hippocampal mossy fiber projections. *Neuron* **25**, 43-56.

Chen, H., He, Z., Bagri, A. and Tessier-Lavigne, M. (1998) Semaphorin-neuropilin interactions underlying sympathetic axon responses to class III semaphorins. *Neuron* **21**, 1283-90.

Chen, J., Butowt, R., Rind, H.B. and von Bartheld, C.S. (2003) GDNF increases the survival of developing oculomotor neurons through a target-derived mechanism. *Mol Cell Neurosci* **24**, 41-56.

Chen, Y., Huang, L., Russo, A.F. and Solursh, M. (1992) Retinoic acid is enriched in Hensen's node and is developmentally regulated in the early chicken embryo. *Proc Natl Acad Sci U S A* **89**, 10056-9.

Cheng, H.J., Bagri, A., Yaron, A., Stein, E., Pleasure, S.J. and Tessier-Lavigne, M. (2001) Plexin-A3 mediates semaphorin signaling and regulates the development of hippocampal axonal projections. *Neuron* **32**, 249-63.

Chiang, C., Litingtung, Y., Lee, E., Young, K.E., Corden, J.L., Westphal, H. and Beachy, P.A. (1996) Cyclopia and defective axial patterning in mice lacking Sonic hedgehog gene function. *Nature* **383**, 407-13.

Chilton, J.K. and Guthrie, S. (2003) Cranial expression of class 3 secreted semaphorins and their neuropilin receptors. *Dev Dyn* **228**, 726-33.

Chilton, J.K. and Guthrie, S. (2004) Development of oculomotor axon projections in the chick embryo. *J Comp Neurol* **472**, 308-17.

Claude, P., Hawrot, E., Dunis, D.A. and Campenot, R.B. (1982) Binding,

internalization, and retrograde transport of 125I-nerve growth factor in cultured rat sympathetic neurons. *J Neurosci* **2**, 431-42.

Cohen, N.R., Taylor, J.S., Scott, L.B., Guillery, R.W., Soriano, P. and Furley, A.J. (1998) Errors in corticospinal axon guidance in mice lacking the neural cell adhesion molecule L1. *Curr Biol* **8**, 26-33.

Colamarino, S.A. and Tessier-Lavigne, M. (1995) The axonal chemoattractant netrin-1 is also a chemorepellent for trochlear motor axons. *Cell* **81**, 621-9.

Couly, G., Creuzet, S., Bennaceur, S., Vincent, C. and Le Douarin, N.M. (2002) Interactions between Hox-negative cephalic neural crest cells and the foregut endoderm in patterning the facial skeleton in the vertebrate head. *Development* **129**, 1061-73.

Couly, G.F., Coltey, P.M. and Le Douarin, N.M. (1992) The developmental fate of the cephalic mesoderm in quail-chick chimeras. *Development* **114**, 1-15.

Crossley, P.H., Martinez, S. and Martin, G.R. (1996) Midbrain development induced by FGF8 in the chick embryo. *Nature* **380**, 66-8.

Currie, P.D. and Ingham, P.W. (1996) Induction of a specific muscle cell type by a hedgehog-like protein in zebrafish. *Nature* **382**, 452-5.

Danielian, P.S. and McMahon, A.P. (1996) Engrailed-1 as a target of the Wnt-1 signalling pathway in vertebrate midbrain development. *Nature* **383** , 332-4.

Davenne, M., Maconochie, M.K., Neun, R., Pattyn, A., Chambon, P., Krumlauf, R. and Rijli, F.M. (1999) Hoxa2 and Hoxb2 control dorsoventral patterns of neuronal development in the rostral hindbrain. *Neuron* **22**, 677-91.

Davis, S., Gale, N.W., Aldrich, T.H., Maisonpierre, P.C., Lhotak, V., Pawson, T., Goldfarb, M. and Yancopoulos, G.D. (1994) Ligands for EPH-related receptor tyrosine kinases that require membrane attachment or clustering for activity. *Science* **266**, 816-9.

Davy, A., Gale, N.W., Murray, E.W., Klinghoffer, R.A., Soriano, P., Feuerstein, C. and Robbins, S.M. (1999) Compartmentalized signaling by GPI-anchored ephrin-A5 requires the Fyn tyrosine kinase to regulate cellular adhesion. *Genes Dev* **13**, 3125-35.

de Castro, F., Hu, L., Drabkin, H., Sotelo, C. and Chedotal, A. (1999) Chemoattraction and chemorepulsion of olfactory bulb axons by different secreted semaphorins. *J Neurosci* **19**, 4428-36.

Deiner, M.S., Kennedy, T.E., Fazeli, A., Serafini, T., Tessier-Lavigne, M. and Sretavan, D.W. (1997) Netrin-1 and DCC mediate axon guidance locally at the optic disc: loss of function leads to optic nerve hypoplasia. *Neuron* **19**, 575-89.

Demyanenko, G.P. and Maness, P.F. (2003) The L1 cell adhesion molecule is essential for topographic mapping of retinal axons. *J Neurosci* **23**, 530-8.

Denetclaw, W.F. Jr, Christ, B. and Ordahl, C.P. (1997) Location and growth of epaxial myotome precursor cells. *Development* **124**, 1601-10.

Dietrich, S. (1999) Regulation of hypaxial muscle development. *Cell Tissue Res* **296**, 175-82.

Dietrich, S., Abou-Rebyeh, F., Brohmann, H., Bladt, F., Sonnenberg-Riethmacher, E., Yamaai, T., Lumsden, A., Brand-Saberi, B. and Birchmeier, C. (1999) The role of SF/HGF and c-Met in the development of skeletal muscle. *Development* **126**, 1621-9.

Dietrich, S., Schubert, F.R., Healy, C., Sharpe, P.T. and Lumsden, A. (1998) Specification of the hypaxial musculature. *Development* **125**, 2235-49.

Dietrich, S., Schubert, F.R. and Lumsden, A. (1997) Control of dorsoventral pattern in the chick paraxial mesoderm. *Development* **124**, 3895-908.

Dontchev, V.D. and Letourneau, P.C. (2002) Nerve growth factor and semaphorin 3A signaling pathways interact in regulating sensory neuronal growth cone motility. *J Neurosci* **22**, 6659-69.

Drescher, U., Kremoser, C., Handwerker, C., Loschinger, J., Noda, M. and Bonhoeffer, F. (1995) In vitro guidance of retinal ganglion cell axons by RAGS, a 25 kDa tectal protein related to ligands for Eph receptor tyrosine kinases. *Cell* **82**, 359-70.

Dubreuil, V., Hirsch, M.R., Jouve, C., Brunet, J.F. and Goridis, C. (2002) The role of Phox2b in synchronizing pan-neuronal and type-specific aspects of neurogenesis. *Development* **129**, 5241-53.

Dupe, V., Ghyselinck, N.B., Wendling, O., Chambon, P. and Mark, M. (1999) Key roles of retinoic acid receptors alpha and beta in the patterning of the caudal hindbrain, pharyngeal arches and otocyst in the mouse. *Development* **126**, 5051-9.

Ebens, A., Brose, K., Leonardo, E.D., Hanson, M.G. Jr, Bladt, F., Birchmeier, C., Barres, B.A. and Tessier-Lavigne, M. (1996) Hepatocyte growth factor/scatter factor is an axonal chemoattractant and a neurotrophic factor for spinal motor neurons. *Neuron* **17**, 1157-72.

Eberhart, J., Swartz, M.E., Koblar, S.A., Pasquale, E.B. and Krull, C.E. (2002) EphA4 constitutes a population-specific guidance cue for motor neurons. *Dev Biol* **247**, 89-101.

Ericson, J., Rashbass, P., Schedl, A., Brenner-Morton, S., Kawakami, A., van Heyningen, V., Jessell, T.M. and Briscoe, J. (1997) Pax6 controls progenitor cell identity and neuronal fate in response to graded Shh signaling. *Cell* **90**, 169-80.

Espeseth, A., Marnellos, G. and Kintner, C. (1998) The role of F-cadherin in localizing cells during neural tube formation in Xenopus embryos. *Development* **125**, 301-12.

Evans, J.C., Frayling, T.M., Ellard, S. and Gutowski, N.J. (2000) Confirmation of linkage of Duane's syndrome and refinement of the disease locus to an 8.8-cM interval on chromosome 2q31. *Hum Genet* **106**, 636-8.

Faissner, A. (1997) The tenascin gene family in axon growth and guidance. *Cell Tissue Res* **290**, 331-41.

Falk, J., Bechara, A., Fiore, R., Nawabi, H., Zhou, H., Hoyo-Becerra, C., Bozon, M., Rougon, G., Grumet, M., Puschel, A.W., Sanes, J.R. and Castellani, V. (2005) Dual functional activity of semaphorin 3B is required for positioning the anterior commissure. *Neuron* **48**, 63-75.

Fan, J. and Raper, J.A. (1995) Localized collapsing cues can steer growth cones without inducing their full collapse. *Neuron* **14**, 263-74.

Fazeli, A., Dickinson, S.L., Hermiston, M.L., Tighe, R.V., Steen, R.G., Small, C.G., Stoeckli, E.T., Keino-Masu, K., Masu, M., Rayburn, H., Simons, J., Bronson, R.T., Gordon, J.I., Tessier-Lavigne, M. and Weinberg, R.A. (1997) Phenotype of mice lacking functional Deleted in colorectal cancer (Dcc) gene. *Nature* **386**, 796-804.

Feiner, L., Webber, A.L., Brown, C.B., Lu, M.M., Jia, L., Feinstein, P., Mombaerts, P., Epstein, J.A. and Raper, J.A. (2001) Targeted disruption of semaphorin 3C leads to persistent truncus arteriosus and aortic arch interruption. *Development* **128**, 3061-70.

Fraser, S., Keynes, R. and Lumsden, A. (1990) Segmentation in the chick embryo hindbrain is defined by cell lineage restrictions. *Nature* **344** , 431-5.

Fritzsch, B., Nichols, D.H., Echelard, Y. and McMahon, A.P. (1995) Development of midbrain and anterior hindbrain ocular motoneurons in normal and Wnt-1 knockout mice. *J Neurobiol* **27**, 457-69.

Fukamauchi, F., Mataga, N., Wang, Y.J., Sato, S., Youshiki, A. and Kusakabe, M. (1996) Abnormal behavior and neurotransmissions of tenascin gene knockout mouse. *Biochem Biophys Res Commun* **221**, 151-6.

Gage, P.J., Rhoades, W., Prucka, S.K. and Hjalt, T. (2005) Fate maps of neural crest and mesoderm in the mammalian eye. *Invest Ophthalmol Vis Sci* **46**, 4200-8.

Gale, E., Zile, M. and Maden, M. (1999) Hindbrain respecification in the retinoid-deficient quail. *Mech Dev* **89**, 43-54.

Garcia-Alonso, L., Fetter, R.D. and Goodman, C.S. (1996) Genetic analysis of Laminin

A in Drosophila: extracellular matrix containing laminin A is required for ocellar axon pathfinding. *Development* **122**, 2611-21.

Gaufo, G.O., Thomas, K.R. and Capecchi, M.R. (2003) Hox3 genes coordinate mechanisms of genetic suppression and activation in the generation of branchial and somatic motoneurons. *Development* **130**, 5191-201.

Gavalas, A., Davenne, M., Lumsden, A., Chambon, P. and Rijli, F.M. (1997) Role of Hoxa-2 in axon pathfinding and rostral hindbrain patterning. *Development* **124**, 3693-702.

Gavalas, A. and Krumlauf, R. (2000) Retinoid signalling and hindbrain patterning. *Curr Opin Genet Dev* **10**, 380-6.

Gavalas, A., Ruhrberg, C., Livet, J., Henderson, C.E. and Krumlauf, R. (2003) Neuronal defects in the hindbrain of Hoxa1, Hoxb1 and Hoxb2 mutants reflect regulatory interactions among these Hox genes. *Development* **130**, 5663-79.

Giger, R.J., Cloutier, J.F., Sahay, A., Prinjha, R.K., Levengood, D.V., Moore, S.E., Pickering, S., Simmons, D., Rastan, S., Walsh, F.S., Kolodkin, A.L., Ginty, D.D. and Geppert, M. (2000) Neuropilin-2 is required in vivo for selective axon guidance responses to secreted semaphorins. *Neuron* **25**, 29-41.

Giordano, S., Corso, S., Conrotto, P., Artigiani, S., Gilestro, G., Barberis, D., Tamagnone, L. and Comoglio, P.M. (2002) The semaphorin 4D receptor controls invasive growth by coupling with Met. *Nat Cell Biol* **4**, 720-4.

Glover, J.C. (2003) The development of vestibulo-ocular circuitry in the chicken embryo. *J Physiol Paris* **97**, 17-25.

Gould, A., Itasaki, N. and Krumlauf, R. (1998) Initiation of rhombomeric Hoxb4 expression requires induction by somites and a retinoid pathway. *Neuron* **21**, 39-51.

Goulding, M., Lumsden, A. and Paquette, A.J. (1994) Regulation of Pax-3 expression in the dermomyotome and its role in muscle development. *Development* **120**, 957-71.

Grammatopoulos, G.A., Bell, E., Toole, L., Lumsden, A. and Tucker, A.S. (2000) Homeotic transformation of branchial arch identity after Hoxa2 overexpression. *Development* **127**, 5355-65.

Gu, C., Yoshida, Y., Livet, J., Reimert, D.V., Mann, F., Merte, J., Henderson, C.E., Jessell, T.M., Kolodkin, A.L. and Ginty, D.D. (2005) Semaphorin 3E and plexin-D1 control vascular pattern independently of neuropilins. *Science* **307**, 265-8.

Guidato, S., Prin, F. and Guthrie, S. (2003) Somatic motoneurone specification in the hindbrain: the influence of somite-derived signals, retinoic acid and Hoxa3. *Development* **130**, 2981-96.

Guirland, C., Suzuki, S., Kojima, M., Lu, B. and Zheng, J.Q. (2004) Lipid rafts mediate chemotropic guidance of nerve growth cones. *Neuron* **42**, 51-62.

Gundersen, R.W. and Barrett, J.N. (1979) Neuronal chemotaxis: chick dorsal-root axons turn toward high concentrations of nerve growth factor. *Science* **206**, 1079-80.

Guthrie, S. and Lumsden, A. (1991) Formation and regeneration of rhombomere boundaries in the developing chick hindbrain. *Development* **112**, 221-9.

Guthrie, S. and Pini, A. (1995) Chemorepulsion of developing motor axons by the floor plate. *Neuron* **14**, 1117-30.

Gutowski, N.J. (2000) Duane's syndrome. *Eur J Neurol* **7**, 145-9.

Hacker, A. and Guthrie, S. (1998) A distinct developmental programme for the cranial paraxial mesoderm in the chick embryo. *Development* **125**, 3461-72.

Hadchouel, J., Carvajal, J.J., Daubas, P., Bajard, L., Chang, T., Rocancourt, D., Cox, D., Summerbell, D., Tajbakhsh, S., Rigby, P.W. and Buckingham, M. (2003) Analysis of a key regulatory region upstream of the Myf5 gene reveals multiple phases of myogenesis, orchestrated at each site by a combination of elements dispersed throughout the locus. *Development* **130**, 3415-26.

Hammond, R., Vivancos, V., Naeem, A., Chilton, J., Mambetisaeva, E., Andrews, W., Sundaresan, V. and Guthrie, S. (2005) Slit-mediated repulsion is a key regulator of motor axon pathfinding in the hindbrain. *Development* **132**, 4483-95.

Hasty, P., Bradley, A., Morris, J.H., Edmondson, D.G., Venuti, J.M., Olson, E.N. and Klein, W.H. (1993) Muscle deficiency and neonatal death in mice with a targeted mutation in the myogenin gene. *Nature* **364**, 501-6.

Hatton, W.J. and von Bartheld, C.S. (1999) Analysis of cell death in the trochlear nucleus of the chick embryo: calibration of the optical disector counting method reveals systematic bias. *J Comp Neurol* **409**, 169-86.

He, Z. and Tessier-Lavigne, M. (1997) Neuropilin is a receptor for the axonal chemorepellent Semaphorin III. *Cell* **90**, 739-51.

Heaton, M.B. (1981) The development of the oculomotor nuclear complex in the Japanese quail embryo. *J Comp Neurol* **198**, 633-48.

Heaton, M.B. and Wayne, D.B. (1983) Patterns of extraocular innervation by the oculomotor complex in the chick. *J Comp Neurol* **216**, 245-52.

Helmbacher, F., Schneider-Maunoury, S., Topilko, P., Tiret, L. and Charnay, P. (2000) Targeting of the EphA4 tyrosine kinase receptor affects dorsal/ventral pathfinding of limb motor axons. *Development* **127**, 3313-24.

Henkemeyer, M., Orioli, D., Henderson, J.T., Saxton, T.M., Roder, J., Pawson, T. and Klein, R. (1996) Nuk controls pathfinding of commissural axons in the mammalian central nervous system. *Cell* **86**, 35-46.

Heyman, I., Kent, A. and Lumsden, A. (1993) Cellular morphology and extracellular space at rhombomere boundaries in the chick embryo hindbrain. *Dev Dyn* **198**, 241-53.

Himanen, J.P., Rajashankar, K.R., Lackmann, M., Cowan, C.A., Henkemeyer, M. and Nikolov, D.B. (2001) Crystal structure of an Eph receptor-ephrin complex. *Nature* **414**, 933-8.

Holmberg, J., Clarke, D.L. and Frisen, J. (2000) Regulation of repulsion versus adhesion by different splice forms of an Eph receptor. *Nature* **408** , 203-6.

Homma, N., Takei, Y., Tanaka, Y., Nakata, T., Terada, S., Kikkawa, M., Noda, Y. and Hirokawa, N. (2003) Kinesin superfamily protein 2A (KIF2A) functions in suppression of collateral branch extension. *Cell* **114**, 229-39.

Hong, K., Hinck, L., Nishiyama, M., Poo, M.M., Tessier-Lavigne, M. and Stein, E. (1999) A ligand-gated association between cytoplasmic domains of UNC5 and DCC family receptors converts netrin-induced growth cone attraction to repulsion. *Cell* **97**, 927-41.

Hong, K., Nishiyama, M., Henley, J., Tessier-Lavigne, M. and Poo, M. (2000) Calcium signalling in the guidance of nerve growth by netrin-1. *Nature* **403**, 93-8.

Hopker, V.H., Shewan, D., Tessier-Lavigne, M., Poo, M. and Holt, C. (1999) Growth-cone attraction to netrin-1 is converted to repulsion by laminin-1. *Nature* **401**, 69-73.

Hornberger, M.R., Dutting, D., Ciossek, T., Yamada, T., Handwerker, C., Lang, S., Weth, F., Huf, J., Wessel, R., Logan, C., Tanaka, H. and Drescher, U. (1999) Modulation of EphA receptor function by coexpressed ephrinA ligands on retinal ganglion cell axons. *Neuron* **22**, 731-42.

Hu, D., Marcucio, R.S. and Helms, J.A. (2003) A zone of frontonasal ectoderm regulates patterning and growth in the face. *Development* **130**, 1749-58.

Huber, A.B., Kolodkin, A.L., Ginty, D.D. and Cloutier, J.F. (2003) Signaling at the growth cone: ligand-receptor complexes and the control of axon growth and guidance. *Annu Rev Neurosci* **26**, 509-63.

Irving, C., Malhas, A., Guthrie, S. and Mason, I. (2002) Establishing the trochlear motor axon trajectory: role of the isthmic organiser and Fgf8. *Development* **129**, 5389-98.

Irving, C. and Mason, I. (1999) Regeneration of isthmic tissue is the result of a specific

and direct interaction between rhombomere 1 and midbrain. *Development* **126**, 3981-9.

Irving, C. and Mason, I. (2000) Signalling by FGF8 from the isthmus patterns anterior hindbrain and establishes the anterior limit of Hox gene expression. *Development* **127**, 177-86.

Itasaki, N., Sharpe, J., Morrison, A. and Krumlauf, R. (1996) Reprogramming Hox expression in the vertebrate hindbrain: influence of paraxial mesoderm and rhombomere transposition. *Neuron* **16**, 487-500.

Johnson, R.L., Laufer, E., Riddle, R.D. and Tabin, C. (1994) Ectopic expression of Sonic hedgehog alters dorsal-ventral patterning of somites. *Cell* **79**, 1165-73.

Jungbluth, S., Bell, E. and Lumsden, A. (1999) Specification of distinct motor neuron identities by the singular activities of individual Hox genes. *Development* **126**, 2751-8.

Kablar, B., Asakura, A., Krastel, K., Ying, C., May, L.L., Goldhamer, D.J. and Rudnicki, M.A. (1998) MyoD and Myf-5 define the specification of musculature of distinct embryonic origin. *Biochem Cell Biol* **76**, 1079-91.

Kablar, B., Krastel, K., Ying, C., Asakura, A., Tapscott, S.J. and Rudnicki, M.A. (1997) MyoD and Myf-5 differentially regulate the development of limb versus trunk skeletal muscle. *Development* **124**, 4729-38.

Kalil, K. and Dent, E.W. (2005) Touch and go: guidance cues signal to the growth cone cytoskeleton. *Curr Opin Neurobiol* **15**, 521-6.

Kennedy, T.E., Serafini, T., de la Torre, J.R. and Tessier-Lavigne, M. (1994) Netrins are diffusible chemotropic factors for commissural axons in the embryonic spinal cord. *Cell* **78**, 425-35.

Kidd, T., Bland, K.S. and Goodman, C.S. (1999) Slit is the midline repellent for the robo receptor in Drosophila. *Cell* **96**, 785-94.

Kiernan, B.W., Garcion, E., Ferguson, J., Frost, E.E., Torres, E.M., Dunnett, S.B., Saga,

Y., Aizawa, S., Faissner, A., Kaur, R., Franklin, R.J. and ffrench-Constant, C. (1999) Myelination and behaviour of tenascin-C null transgenic mice. *Eur J Neurosci* **11**, 3082-92.

Kitsukawa, T., Shimizu, M., Sanbo, M., Hirata, T., Taniguchi, M., Bekku, Y., Yagi, T. and Fujisawa, H. (1997) Neuropilin-semaphorin III/D-mediated chemorepulsive signals play a crucial role in peripheral nerve projection in mice. *Neuron* **19**, 995-1005.

Knoll, B. and Drescher, U. (2002) Ephrin-As as receptors in topographic projections. *Trends Neurosci* **25**, 145-9.

Knoll, B., Zarbalis, K., Wurst, W. and Drescher, U. (2001) A role for the EphA family in the topographic targeting of vomeronasal axons. *Development* **128**, 895-906.

Kobayashi, H., Koppel, A.M., Luo, Y. and Raper, J.A. (1997) A role for collapsin-1 in olfactory and cranial sensory axon guidance. *J Neurosci* **17**, 8339-52.

Kolodkin, A.L., Matthes, D.J., O'Connor, T.P., Patel, N.H., Admon, A., Bentley, D. and Goodman, C.S. (1992) Fasciclin IV: sequence, expression, and function during growth cone guidance in the grasshopper embryo. *Neuron* **9**, 831-45.

Kontges, G. and Lumsden, A. (1996) Rhombencephalic neural crest segmentation is preserved throughout craniofacial ontogeny. *Development* **122**, 3229-42.

Koppel, A.M., Feiner, L., Kobayashi, H. and Raper, J.A. (1997) A 70 amino acid region within the semaphorin domain activates specific cellular response of semaphorin family members. *Neuron* **19**, 531-7.

Koppel, A.M. and Raper, J.A. (1998) Collapsin-1 covalently dimerizes, and dimerization is necessary for collapsing activity. *J Biol Chem* **273**, 15708-13.

Kullander, K., Croll, S.D., Zimmer, M., Pan, L., McClain, J., Hughes, V., Zabski, S., DeChiara, T.M., Klein, R., Yancopoulos, G.D. and Gale, N.W. (2001) Ephrin-B3 is the midline barrier that prevents corticospinal tract axons from recrossing, allowing for unilateral motor control. *Genes Dev* **15**, 877-88.

Kunz, B., Lierheimer, R., Rader, C., Spirig, M., Ziegler, U. and Sonderegger, P. (2002) Axonin-1/TAG-1 mediates cell-cell adhesion by a cis-assisted trans-interaction. *J Biol Chem* **277**, 4551-7.

Kuruvilla, R., Zweifel, L.S., Glebova, N.O., Lonze, B.E., Valdez, G., Ye, H. and Ginty, D.D. (2004) A neurotrophin signaling cascade coordinates sympathetic neuron development through differential control of TrkA trafficking and retrograde signaling. *Cell* **118**, 243-55.

Lee, K.J., Dietrich, P. and Jessell, T.M. (2000) Genetic ablation reveals that the roof plate is essential for dorsal interneuron specification. *Nature* **403**, 734-40.

Leighton, P.A., Mitchell, K.J., Goodrich, L.V., Lu, X., Pinson, K., Scherz, P., Skarnes, W.C. and Tessier-Lavigne, M. (2001) Defining brain wiring patterns and mechanisms through gene trapping in mice. *Nature* **410**, 174-9.

Lele, Z., Folchert, A., Concha, M., Rauch, G.J., Geisler, R., Rosa, F., Wilson, S.W., Hammerschmidt, M. and Bally-Cuif, L. (2002) parachute/n-cadherin is required for morphogenesis and maintained integrity of the zebrafish neural tube. *Development* **129**, 3281-94.

Li, H.S., Chen, J.H., Wu, W., Fagaly, T., Zhou, L., Yuan, W., Dupuis, S., Jiang, Z.H., Nash, W., Gick, C., Ornitz, D.M., Wu, J.Y. and Rao, Y. (1999) Vertebrate slit, a secreted ligand for the transmembrane protein roundabout, is a repellent for olfactory bulb axons. *Cell* **96**, 807-18.

Li, Q., Shirabe, K., Thisse, C., Thisse, B., Okamoto, H., Masai, I. and Kuwada, J.Y. (2005) Chemokine signaling guides axons within the retina in zebrafish. *J Neurosci* **25**, 1711-7.

Lieberam, I., Agalliu, D., Nagasawa, T., Ericson, J. and Jessell, T.M. (2005) A Cxcl12-CXCR4 chemokine signaling pathway defines the initial trajectory of mammalian motor axons. *Neuron* **47**, 667-79.

Liem, K.F. Jr, Tremml, G. and Jessell, T.M. (1997) A role for the roof plate and its

resident TGFbeta-related proteins in neuronal patterning in the dorsal spinal cord. *Cell* **91**, 127-38.

Liem, K.F. Jr, Tremml, G., Roelink, H. and Jessell, T.M. (1995) Dorsal differentiation of neural plate cells induced by BMP-mediated signals from epidermal ectoderm. *Cell* **82**, 969-79.

Lin, D.M. and Goodman, C.S. (1994) Ectopic and increased expression of Fasciclin II alters motoneuron growth cone guidance. *Neuron* **13**, 507-23.

Liu, Y., Shi, J., Lu, C.C., Wang, Z.B., Lyuksyutova, A.I., Song, X.J. and Zou, Y. (2005) Ryk-mediated Wnt repulsion regulates posterior-directed growth of corticospinal tract. *Nat Neurosci* **8**, 1151-9.

Lohof, A.M., Quillan, M., Dan, Y. and Poo, M.M. (1992) Asymmetric modulation of cytosolic cAMP activity induces growth cone turning. *J Neurosci* **12**, 1253-61.

Lu, J.R., Bassel-Duby, R., Hawkins, A., Chang, P., Valdez, R., Wu, H., Gan, L., Shelton, J.M., Richardson, J.A. and Olson, E.N. (2002) Control of facial muscle development by MyoR and capsulin. *Science* **298**, 2378-81.

Lumsden, A. and Krumlauf, R. (1996) Patterning the vertebrate neuraxis. *Science* **274**, 1109-15.

Luo, Y., Raible, D. and Raper, J.A. (1993) Collapsin: a protein in brain that induces the collapse and paralysis of neuronal growth cones. *Cell* **75**, 217-27.

Lyuksyutova, A.I., Lu, C.C., Milanesio, N., King, L.A., Guo, N., Wang, Y., Nathans, J., Tessier-Lavigne, M. and Zou, Y. (2003) Anterior-posterior guidance of commissural axons by Wnt-frizzled signaling. *Science* **302**, 1984-8.

Maina, F., Hilton, M.C., Andres, R., Wyatt, S., Klein, R. and Davies, A.M. (1998) Multiple roles for hepatocyte growth factor in sympathetic neuron development. *Neuron* **20**, 835-46.

Maina, F., Hilton, M.C., Ponzetto, C., Davies, A.M. and Klein, R. (1997) Met receptor signaling is required for sensory nerve development and HGF promotes axonal growth and survival of sensory neurons. *Genes Dev* **11**, 3341-50.

Maina, F. and Klein, R. (1999) Hepatocyte growth factor, a versatile signal for developing neurons. *Nat Neurosci* **2**, 213-7.

Maina, F., Pante, G., Helmbacher, F., Andres, R., Porthin, A., Davies, A.M., Ponzetto, C. and Klein, R. (2001) Coupling Met to specific pathways results in distinct developmental outcomes. *Mol Cell* **7**, 1293-306.

Mankoo, B.S., Collins, N.S., Ashby, P., Grigorieva, E., Pevny, L.H., Candia, A., Wright, C.V., Rigby, P.W. and Pachnis, V. (1999) Mox2 is a component of the genetic hierarchy controlling limb muscle development. *Nature* **400**, 69-73.

Manzanares, M., Nardelli, J., Gilardi-Hebenstreit, P., Marshall, H., Giudicelli, F., Martinez-Pastor, M.T., Krumlauf, R. and Chamay, P. (2002) Krox20 and kreisler co-operate in the transcriptional control of segmental expression of Hoxb3 in the developing hindbrain. *EMBO J* **21**, 365-76.

Manzanares, M., Trainor, P.A., Nonchev, S., Ariza-McNaughton, L., Brodie, J., Gould, A., Marshall, H., Morrison, A., Kwan, C.T., Sham, M.H., Wilkinson, D.G. and Krumlauf, R. (1999) The role of kreisler in segmentation during hindbrain development. *Dev Biol* **211**, 220-37.

Marin, F. and Puelles, L. (1994) Patterning of the embryonic avian midbrain after experimental inversions: a polarizing activity from the isthmus. *Dev Biol* **163**, 19-37.

Maroto, M., Reshef, R., Munsterberg, A.E., Koester, S., Goulding, M. and Lassar, A.B. (1997) Ectopic Pax-3 activates MyoD and Myf-5 expression in embryonic mesoderm and neural tissue. *Cell* **89**, 139-48.

Marquardt, T., Shirasaki, R., Ghosh, S., Andrews, S.E., Carter, N., Hunter, T. and Pfaff, S.L. (2005) Coexpressed EphA receptors and ephrin-A ligands mediate opposing actions on growth cone navigation from distinct membrane domains. *Cell* **121**, 127-39.

Marshall, H., Nonchev, S., Sham, M.H., Muchamore, I., Lumsden, A. and Krumlauf, R. (1992) Retinoic acid alters hindbrain Hox code and induces transformation of rhombomeres 2/3 into a 4/5 identity. *Nature* **360**, 737-41.

Marti, E., Bumcrot, D.A., Takada, R. and McMahon, A.P. (1995) Requirement of 19K form of Sonic hedgehog for induction of distinct ventral cell types in CNS explants. *Nature* **375**, 322-5.

Martinez, S., Crossley, P.H., Cobos, I., Rubenstein, J.L. and Martin, G.R. (1999) FGF8 induces formation of an ectopic isthmic organizer and isthmocerebellar development via a repressive effect on Otx2 expression. *Development* **126**, 1189-200.

Martinez, S., Wassef, M. and Alvarado-Mallart, R.M. (1991) Induction of a mesencephalic phenotype in the 2-day-old chick prosencephalon is preceded by the early expression of the homeobox gene en. *Neuron* **6**, 971-81.

Matsuo, I., Kuratani, S., Kimura, C., Takeda, N. and Aizawa, S. (1995) Mouse Otx2 functions in the formation and patterning of rostral head. *Genes Dev* **9**, 2646-58.

Meier, S. and Tam, P.P. (1982) Metameric pattern development in the embryonic axis of the mouse. I. Differentiation of the cranial segments. *Differentiation* **21**, 95-108.

Mellitzer, G., Xu, Q. and Wilkinson, D.G. (1999) Eph receptors and ephrins restrict cell intermingling and communication. *Nature* **400**, 77-81.

Mennerich, D., Schafer, K. and Braun, T. (1998) Pax-3 is necessary but not sufficient for lbx1 expression in myogenic precursor cells of the limb. *Mech Dev* **73**, 147-58.

Millet, S., Campbell, K., Epstein, D.J., Losos, K., Harris, E. and Joyner, A.L. (1999) A role for Gbx2 in repression of Otx2 and positioning the mid/hindbrain organizer. *Nature* **401**, 161-4.

Millonig, J.H., Millen, K.J. and Hatten, M.E. (2000) The mouse Dreher gene Lmx1a controls formation of the roof plate in the vertebrate CNS. *Nature* **403**, 764-9.

Ming, G.L., Song, H.J., Berninger, B., Holt, C.E., Tessier-Lavigne, M. and Poo, M.M. (1997) cAMP-dependent growth cone guidance by netrin-1. *Neuron* **19**, 1225-35.

Ming, G.L., Wong, S.T., Henley, J., Yuan, X.B., Song, H.J., Spitzer, N.C. and Poo, M.M. (2002) Adaptation in the chemotactic guidance of nerve growth cones. *Nature* **417**, 411-8.

Mitsui, N., Inatome, R., Takahashi, S., Goshima, Y., Yamamura, H. and Yanagi, S. (2002) Involvement of Fes/Fps tyrosine kinase in semaphorin3A signaling. *EMBO J* **21**, 3274-85.

Mizuguchi, R., Sugimori, M., Takebayashi, H., Kosako, H., Nagao, M., Yoshida, S., Nabeshima, Y., Shimamura, K. and Nakafuku, M. (2001) Combinatorial roles of olig2 and neurogenin2 in the coordinated induction of pan-neuronal and subtype-specific properties of motoneurons. *Neuron* **31**, 757-71.

Mootoosamy, R.C. and Dietrich, S. (2002) Distinct regulatory cascades for head and trunk myogenesis. *Development* **129**, 573-83.

Morin, X., Cremer, H., Hirsch, M.R., Kapur, R.P., Goridis, C. and Brunet, J.F. (1997) Defects in sensory and autonomic ganglia and absence of locus coeruleus in mice deficient for the homeobox gene Phox2a. *Neuron* **18**, 411-23.

Muhr, J., Andersson, E., Persson, M., Jessell, T.M. and Ericson, J. (2001) Groucho-mediated transcriptional repression establishes progenitor cell pattern and neuronal fate in the ventral neural tube. *Cell* **104**, 861-73.

Muhr, J., Graziano, E., Wilson, S., Jessell, T.M. and Edlund, T. (1999) Convergent inductive signals specify midbrain, hindbrain, and spinal cord identity in gastrula stage chick embryos. *Neuron* **23**, 689-702.

Muller, M., Jabs, N., Lorke, D.E., Fritzsch, B. and Sander, M. (2003) Nkx6.1 controls migration and axon pathfinding of cranial branchio-motoneurons. *Development* **130**, 5815-26.

Munsterberg, A.E., Kitajewski, J., Bumcrot, D.A., McMahon, A.P. and Lassar, A.B. (1995) Combinatorial signaling by Sonic hedgehog and Wnt family members induces myogenic bHLH gene expression in the somite. *Genes Dev* **9**, 2911-22.

Naeem, A., Abbas, L. and Guthrie, S. (2002) Comparison of the effects of HGF, BDNF, CT-1, CNTF, and the branchial arches on the growth of embryonic cranial motor neurons. *J Neurobiol* **51**, 101-14.

Nakamura, F., Tanaka, M., Takahashi, T., Kalb, R.G. and Strittmatter, S.M. (1998) Neuropilin-1 extracellular domains mediate semaphorin D/III-induced growth cone collapse. *Neuron* **21**, 1093-100.

Nakano, M., Yamada, K., Fain, J., Sener, E.C., Selleck, C.J., Awad, A.H., Zwaan, J., Mullaney, P.B., Bosley, T.M. and Engle, E.C. (2001) Homozygous mutations in ARIX(PHOX2A) result in congenital fibrosis of the extraocular muscles type 2. *Nat Genet* **29**, 315-20.

Nguyen Ba-Charvet, K.T., Brose, K., Marillat, V., Kidd, T., Goodman, C.S., Tessier-Lavigne, M., Sotelo, C. and Chedotal, A. (1999) Slit2-Mediated chemorepulsion and collapse of developing forebrain axons. *Neuron* **22**, 463-73.

Niederreither, K., Vermot, J., Schuhbaur, B., Chambon, P. and Dolle, P. (2000) Retinoic acid synthesis and hindbrain patterning in the mouse embryo. *Development* **127**, 75-85.

Nieto, M.A., Gilardi-Hebenstreit, P., Charnay, P. and Wilkinson, D.G. (1992) A receptor protein tyrosine kinase implicated in the segmental patterning of the hindbrain and mesoderm. *Development* **116**, 1137-50.

Noden, D.M. (1983) The embryonic origins of avian cephalic and cervical muscles and associated connective tissues. *Am J Anat* **168**, 257-76.

Noden, D.M. (1986) Patterning of avian craniofacial muscles. *Dev Biol* **116**, 347-56.

Noden, D.M. (1983) The role of the neural crest in patterning of avian cranial skeletal,

connective, and muscle tissues. *Dev Biol* **96**, 144-65.

Noden, D.M., Marcucio, R., Borycki, A.G. and Emerson, C.P. Jr (1999) Differentiation of avian craniofacial muscles: I. Patterns of early regulatory gene expression and myosin heavy chain synthesis. *Dev Dyn* **216**, 96-112.

Nonchev, S., Vesque, C., Maconochie, M., Seitanidou, T., Ariza-McNaughton, L., Frain, M., Marshall, H., Sham, M.H., Krumlauf, R. and Charnay, P. (1996) Segmental expression of Hoxa-2 in the hindbrain is directly regulated by Krox-20. *Development* **122**, 543-54.

Norton, W.H., Mangoli, M., Lele, Z., Pogoda, H.M., Diamond, B., Mercurio, S., Russell, C., Teraoka, H., Stickney, H.L., Rauch, G.J., Heisenberg, C.P., Houart, C., Schilling, T.F., Frohnhoefer, H.G., Rastegar, S., Neumann, C.J., Gardiner, R.M., Strahle, U., Geisler, R., Rees, M., Talbot, W.S. and Wilson, S.W. (2005) Monorail/Foxa2 regulates floorplate differentiation and specification of oligodendrocytes, serotonergic raphe neurones and cranial motoneurones. *Development* **132**, 645-58.

Novitch, B.G., Chen, A.I. and Jessell, T.M. (2001) Coordinate regulation of motor neuron subtype identity and pan-neuronal properties by the bHLH repressor Olig2. *Neuron* **31**, 773-89.

Novitch, B.G., Wichterle, H., Jessell, T.M. and Sockanathan, S. (2003) A requirement for retinoic acid-mediated transcriptional activation in ventral neural patterning and motor neuron specification. *Neuron* **40**, 81-95.

Ohta, K., Nakamura, M., Hirokawa, K., Tanaka, S., Iwama, A., Suda, T., Ando, M. and Tanaka, H. (1996) The receptor tyrosine kinase, Cek8, is transiently expressed on subtypes of motoneurons in the spinal cord during development. *Mech Dev* **54**, 59-69.

Ordahl, C.P. and Le Douarin, N.M. (1992) Two myogenic lineages within the developing somite. *Development* **114**, 339-53.

Osumi, N., Hirota, A., Ohuchi, H., Nakafuku, M., Iimura, T., Kuratani, S., Fujiwara, M.,

Noji, S. and Eto, K. (1997) Pax-6 is involved in the specification of hindbrain motor neuron subtype. *Development* **124**, 2961-72.

Panganiban, G. and Rubenstein, J.L. (2002) Developmental functions of the Distal-less/Dlx homeobox genes. *Development* **129**, 4371-86.

Pasterkamp, R.J. and Kolodkin, A.L. (2003) Semaphorin junction: making tracks toward neural connectivity. *Curr Opin Neurobiol* **13**, 79-89.

Pattyn, A., Hirsch, M., Goridis, C. and Brunet, J.F. (2000) Control of hindbrain motor neuron differentiation by the homeobox gene Phox2b. *Development* **127**, 1349-58.

Pattyn, A., Morin, X., Cremer, H., Goridis, C. and Brunet, J.F. (1997) Expression and interactions of the two closely related homeobox genes Phox2a and Phox2b during neurogenesis. *Development* **124**, 4065-75.

Pattyn, A., Vallstedt, A., Dias, J.M., Sander, M. and Ericson, J. (2003) Complementary roles for Nkx6 and Nkx2 class proteins in the establishment of motoneuron identity in the hindbrain. *Development* **130**, 4149-59.

Paulsson, M., Deutzmann, R., Timpl, R., Dalzoppo, D., Odermatt, E. and Engel, J. (1985) Evidence for coiled-coil alpha-helical regions in the long arm of laminin. *EMBO J* 4, 309-16.

Pfaff, S.L., Mendelsohn, M., Stewart, C.L., Edlund, T. and Jessell, T.M. (1996) Requirement for LIM homeobox gene Isl1 in motor neuron generation reveals a motor neuron-dependent step in interneuron differentiation. *Cell* **84**, 309-20.

Piccolo, S., Sasai, Y., Lu, B. and De Robertis, E.M. (1996) Dorsoventral patterning in Xenopus: inhibition of ventral signals by direct binding of chordin to BMP-4. *Cell* **86**, 589-98.

Pierani, A., Brenner-Morton, S., Chiang, C. and Jessell, T.M. (1999) A sonic hedgehog-independent, retinoid-activated pathway of neurogenesis in the ventral spinal cord. *Cell* **97**, 903-15.

Placzek, M., Jessell, T.M. and Dodd, J. (1993) Induction of floor plate differentiation by contact-dependent, homeogenetic signals. *Development* **117**, 205-18.

Placzek, M., Tessier-Lavigne, M., Yamada, T., Jessell, T. and Dodd, J. (1990) Mesodermal control of neural cell identity: floor plate induction by the notochord. *Science* **250**, 985-8.

Plump, A.S., Erskine, L., Sabatier, C., Brose, K., Epstein, C.J., Goodman, C.S., Mason, C.A. and Tessier-Lavigne, M. (2002) Slit1 and Slit2 cooperate to prevent premature midline crossing of retinal axons in the mouse visual system. *Neuron* **33**, 219-32.

Polleux, F., Morrow, T. and Ghosh, A. (2000) Semaphorin 3A is a chemoattractant for cortical apical dendrites. *Nature* **404**, 567-73.

Ponzetto, C., Bardelli, A., Zhen, Z., Maina, F., dalla Zonca, P., Giordano, S., Graziani, A., Panayotou, G. and Comoglio, P.M. (1994) A multifunctional docking site mediates signaling and transformation by the hepatocyte growth factor/scatter factor receptor family. *Cell* **77**, 261-71.

Porter, J.A., von Kessler, D.P., Ekker, S.C., Young, K.E., Lee, J.J., Moses, K. and Beachy, P.A. (1995) The product of hedgehog autoproteolytic cleavage active in local and long-range signalling. *Nature* **374**, 363-6.

Porter, J.D., Guthrie, B.L. and Sparks, D.L. (1983) Innervation of monkey extraocular muscles: localization of sensory and motor neurons by retrograde transport of horseradish peroxidase. *J Comp Neurol* **218**, 208-19.

Pourquie, O., Fan, C.M., Coltey, M., Hirsinger, E., Watanabe, Y., Breant, C., Francis-West, P., Brickell, P., Tessier-Lavigne, M. and Le Douarin, N.M. (1996) Lateral and axial signals involved in avian somite patterning: a role for BMP4. *Cell* **84**, 461-71.

Prin, F., Ng, K.E., Thaker, U., Drescher, U. and Guthrie, S. (2005) Ephrin-As play a rhombomere-specific role in trigeminal motor axon projections in the chick embryo. *Dev Biol* **279**, 402-19.

Prince, J.T., Nishiyama, A., Healy, P.A., Beasley, L. and Stallcup, W.B. (1992) Expression of the F84.1 glycoprotein in the spinal cord and cranial nerves of the developing rat. *Brain Res Dev Brain Res* **68**, 193-201.

Prince, V. and Lumsden, A. (1994) Hoxa-2 expression in normal and transposed rhombomeres: independent regulation in the neural tube and neural crest. *Development* **120**, 911-23.

Pringle, N.P., Yu, W.P., Guthrie, S., Roelink, H., Lumsden, A., Peterson, A.C. and Richardson, W.D. (1996) Determination of neuroepithelial cell fate: induction of the oligodendrocyte lineage by ventral midline cells and sonic hedgehog. *Dev Biol* **177**, 30-42.

Puelles, E., Acampora, D., Lacroix, E., Signore, M., Annino, A., Tuorto, F., Filosa, S., Corte, G., Wurst, W., Ang, S.L. and Simeone, A. (2003) Otx dose-dependent integrated control of antero-posterior and dorso-ventral patterning of midbrain. *Nat Neurosci* **6**, 453-60.

Puelles, L. (1978) A Golgi-study of oculomotor neuroblasts migrating across the midline in chick embryos. *Anat Embryol (Berl)* **152**, 205-15.

Puschel, A.W., Adams, R.H. and Betz, H. (1996) The sensory innervation of the mouse spinal cord may be patterned by differential expression of and differential responsiveness to semaphorins. *Mol Cell Neurosci* **7**, 419-31.

Rabacchi, S.A., Solowska, J.M., Kruk, B., Luo, Y., Raper, J.A. and Baird, D.H. (1999) Collapsin-1/semaphorin-III/D is regulated developmentally in Purkinje cells and collapses pontocerebellar mossy fiber neuronal growth cones. *J Neurosci* **19**, 4437-48.

Raper, J.A. (2000) Semaphorins and their receptors in vertebrates and invertebrates. *Curr Opin Neurobiol* **10**, 88-94.

Rashid, T., Upton, A.L., Blentic, A., Ciossek, T., Knoll, B., Thompson, I.D. and Drescher, U. (2005) Opposing gradients of ephrin-As and EphA7 in the superior colliculus are essential for topographic mapping in the mammalian visual system.

Neuron **47**, 57-69.

Rhinn, M. and Brand, M. (2001) The midbrain--hindbrain boundary organizer. *Curr Opin Neurobiol* **11**, 34-42.

Riehl, R., Johnson, K., Bradley, R., Grunwald, G.B., Cornel, E., Lilienbaum, A. and Holt, C.E. (1996) Cadherin function is required for axon outgrowth in retinal ganglion cells in vivo. *Neuron* **17**, 837-48.

Rijli, F.M., Mark, M., Lakkaraju, S., Dierich, A., Dolle, P. and Chambon, P. (1993) A homeotic transformation is generated in the rostral branchial region of the head by disruption of Hoxa-2, which acts as a selector gene. *Cell* **75**, 1333-49.

Rivas, R.J., Burmeister, D.W. and Goldberg, D.J. (1992) Rapid effects of laminin on the growth cone. *Neuron* **8**, 107-15.

Roelink, H., Porter, J.A., Chiang, C., Tanabe, Y., Chang, D.T., Beachy, P.A. and Jessell, T.M. (1995) Floor plate and motor neuron induction by different concentrations of the amino-terminal cleavage product of sonic hedgehog autoproteolysis. *Cell* **81**, 445-55.

Rosoff, W.J., Urbach, J.S., Esrick, M.A., McAllister, R.G., Richards, L.J. and Goodhill, G.J. (2004) A new chemotaxis assay shows the extreme sensitivity of axons to molecular gradients. *Nat Neurosci* **7**, 678-82.

Rudnicki, M.A., Schnegelsberg, P.N., Stead, R.H., Braun, T., Arnold, H.H. and Jaenisch, R. (1993) MyoD or Myf-5 is required for the formation of skeletal muscle. *Cell* **75**, 1351-9.

Sahay, A., Molliver, M.E., Ginty, D.D. and Kolodkin, A.L. (2003) Semaphorin 3F is critical for development of limbic system circuitry and is required in neurons for selective CNS axon guidance events. *J Neurosci* **23**, 6671-80.

Sahin, M., Greer, P.L., Lin, M.Z., Poucher, H., Eberhart, J., Schmidt, S., Wright, T.M., Shamah, S.M., O'connell, S., Cowan, C.W., Hu, L., Goldberg, J.L., Debant, A., Corfas, G., Krull, C.E. and Greenberg, M.E. (2005) Eph-dependent tyrosine phosphorylation of

ephexin1 modulates growth cone collapse. *Neuron* **46**, 191-204.

Sander, M., Paydar, S., Ericson, J., Briscoe, J., Berber, E., German, M., Jessell, T.M. and Rubenstein, J.L. (2000) Ventral neural patterning by Nkx homeobox genes: Nkx6.1 controls somatic motor neuron and ventral interneuron fates. *Genes Dev* **14**, 2134-9.

Sanders, T.A., Lumsden, A. and Ragsdale, C.W. (2002) Arcuate plan of chick midbrain development. *J Neurosci* **22**, 10742-50.

Santagati, F. and Rijli, F.M. (2003) Cranial neural crest and the building of the vertebrate head. *Nat Rev Neurosci* **4**, 806-18.

Sato, T., Araki, I. and Nakamura, H. (2001) Inductive signal and tissue responsiveness defining the tectum and the cerebellum. *Development* **128**, 2461-9.

Sato, T., Joyner, A.L. and Nakamura, H. (2004) How does Fgf signaling from the isthmic organizer induce midbrain and cerebellum development? *Dev Growth Differ* **46**, 487-94.

Scardigli, R., Schuurmans, C., Gradwohl, G. and Guillemot, F. (2001) Crossregulation between Neurogenin2 and pathways specifying neuronal identity in the spinal cord. *Neuron* **31**, 203-17.

Schilling, T.F., Walker, C. and Kimmel, C.B. (1996) The chinless mutation and neural crest cell interactions in zebrafish jaw development. *Development* **122**, 1417-26.

Schneider-Maunoury, S., Seitanidou, T., Charnay, P. and Lumsden, A. (1997) Segmental and neuronal architecture of the hindbrain of Krox-20 mouse mutants. *Development* **124**, 1215-26.

Schneider-Maunoury, S., Topilko, P., Seitandou, T., Levi, G., Cohen-Tannoudji, M., Pournin, S., Babinet, C. and Charnay, P. (1993) Disruption of Krox-20 results in alteration of rhombomeres 3 and 5 in the developing hindbrain. *Cell* **75**, 1199-214.

Schwartz, M.A. (1992) Transmembrane signalling by integrins. *Trends Cell Biol* **2**,

304-8.

Seeger, M., Tear, G., Ferres-Marco, D. and Goodman, C.S. (1993) Mutations affecting growth cone guidance in Drosophila: genes necessary for guidance toward or away from the midline. *Neuron* **10**, 409-26.

Serafini, T., Colamarino, S.A., Leonardo, E.D., Wang, H., Beddington, R., Skarnes, W.C. and Tessier-Lavigne, M. (1996) Netrin-1 is required for commissural axon guidance in the developing vertebrate nervous system. *Cell* **87**, 1001-14.

Serafini, T., Kennedy, T.E., Galko, M.J., Mirzayan, C., Jessell, T.M. and Tessier-Lavigne, M. (1994) The netrins define a family of axon outgrowth-promoting proteins homologous to C. elegans UNC-6. *Cell* **78**, 409-24.

Sharma, K., Sheng, H.Z., Lettieri, K., Li, H., Karavanov, A., Potter, S., Westphal, H. and Pfaff, S.L. (1998) LIM homeodomain factors Lhx3 and Lhx4 assign subtype identities for motor neurons. *Cell* **95**, 817-28.

Shirasaki, R., Mirzayan, C., Tessier-Lavigne, M. and Murakami, F. (1996) Guidance of circumferentially growing axons by netrin-dependent and -independent floor plate chemotropism in the vertebrate brain. *Neuron* **17**, 1079-88.

Shirasaki, R. and Pfaff, S.L. (2002) Transcriptional codes and the control of neuronal identity. *Annu Rev Neurosci* **25**, 251-81.

Shirasaki, R., Tamada, A., Katsumata, R. and Murakami, F. (1995) Guidance of cerebellofugal axons in the rat embryo: directed growth toward the floor plate and subsequent elongation along the longitudinal axis. *Neuron* **14**, 961-72.

Simeone, A., Acampora, D., Arcioni, L., Andrews, P.W., Boncinelli, E. and Mavilio, F. (1990) Sequential activation of HOX2 homeobox genes by retinoic acid in human embryonal carcinoma cells. *Nature* **346**, 763-6.

Simpson, J.H., Kidd, T., Bland, K.S. and Goodman, C.S. (2000) Short-range and long-range guidance by slit and its Robo receptors. Robo and Robo2 play distinct roles in

midline guidance. *Neuron* **28**, 753-66.

Song, H., Ming, G., He, Z., Lehmann, M., McKerracher, L., Tessier-Lavigne, M. and Poo, M. (1998) Conversion of neuronal growth cone responses from repulsion to attraction by cyclic nucleotides. *Science* **281**, 1515-8.

Stern, C.D. (2005) Neural induction: old problem, new findings, yet more questions. *Development* **132**, 2007-21.

Stern, H.M., Brown, A.M. and Hauschka, S.D. (1995) Myogenesis in paraxial mesoderm: preferential induction by dorsal neural tube and by cells expressing Wnt-1. *Development* **121**, 3675-86.

Steup, A., Lohrum, M., Hamscho, N., Savaskan, N.E., Ninnemann, O., Nitsch, R., Fujisawa, H., Puschel, A.W. and Skutella, T. (2000) Sema3C and netrin-1 differentially affect axon growth in the hippocampal formation. *Mol Cell Neurosci* **15**, 141-55.

Stoeckli, E.T. and Landmesser, L.T. (1995) Axonin-1, Nr-CAM, and Ng-CAM play different roles in the in vivo guidance of chick commissural neurons. *Neuron* **14**, 1165-79.

Strahle, U., Blader, P., Adam, J. and Ingham, P.W. (1994) A simple and efficient procedure for non-isotopic in situ hybridization to sectioned material. *Trends Genet* **10**, 75-6.

Studer, M., Lumsden, A., Ariza-McNaughton, L., Bradley, A. and Krumlauf, R. (1996) Altered segmental identity and abnormal migration of motor neurons in mice lacking Hoxb-1. *Nature* **384**, 630-4.

Sun, X., Meyers, E.N., Lewandoski, M. and Martin, G.R. (1999) Targeted disruption of Fgf8 causes failure of cell migration in the gastrulating mouse embryo. *Genes Dev* **13**, 1834-46.

Suto, F., Ito, K., Uemura, M., Shimizu, M., Shinkawa, Y., Sanbo, M., Shinoda, T., Tsuboi, M., Takashima, S., Yagi, T. and Fujisawa, H. (2005) Plexin-a4 mediates axon-

repulsive activities of both secreted and transmembrane semaphorins and plays roles in nerve fiber guidance. *J Neurosci* **25**, 3628-37.

Tajbakhsh, S., Rocancourt, D., Cossu, G. and Buckingham, M. (1997) Redefining the genetic hierarchies controlling skeletal myogenesis: Pax-3 and Myf-5 act upstream of MyoD. *Cell* **89**, 127-38.

Tamagnone, L., Artigiani, S., Chen, H., He, Z., Ming, G.I., Song, H., Chedotal, A., Winberg, M.L., Goodman, C.S., Poo, M., Tessier-Lavigne, M. and Comoglio, P.M. (1999) Plexins are a large family of receptors for transmembrane, secreted, and GPI-anchored semaphorins in vertebrates. *Cell* **99**, 71-80.

Tanabe, Y., William, C. and Jessell, T.M. (1998) Specification of motor neuron identity by the MNR2 homeodomain protein. *Cell* **95**, 67-80.

Tang, J., Landmesser, L. and Rutishauser, U. (1992) Polysialic acid influences specific pathfinding by avian motoneurons. *Neuron* **8**, 1031-44.

Taniguchi, M., Yuasa, S., Fujisawa, H., Naruse, I., Saga, S., Mishina, M. and Yagi, T. (1997) Disruption of semaphorin III/D gene causes severe abnormality in peripheral nerve projection. *Neuron* **19**, 519-30.

Tessier-Lavigne, M. and Goodman, C.S. (1996) The molecular biology of axon guidance. *Science* **274**, 1123-33.

Thaler, J., Harrison, K., Sharma, K., Lettieri, K., Kehrl, J. and Pfaff, S.L. (1999) Active suppression of interneuron programs within developing motor neurons revealed by analysis of homeodomain factor HB9. *Neuron* **23**, 675-87.

Theil, T., Frain, M., Gilardi-Hebenstreit, P., Flenniken, A., Charnay, P. and Wilkinson, D.G. (1998) Segmental expression of the EphA4 (Sek-1) receptor tyrosine kinase in the hindbrain is under direct transcriptional control of Krox-20. *Development* **125**, 443-52.

Tomaselli, K.J., Damsky, C.H. and Reichardt, L.F. (1988) Purification and characterization of mammalian integrins expressed by a rat neuronal cell line (PC12):

evidence that they function as alpha/beta heterodimeric receptors for laminin and type IV collagen. *J Cell Biol* **107**, 1241-52.

Toyofuku, T., Zhang, H., Kumanogoh, A., Takegahara, N., Suto, F., Kamei, J., Aoki, K., Yabuki, M., Hori, M., Fujisawa, H. and Kikutani, H. (2004) Dual roles of Sema6D in cardiac morphogenesis through region-specific association of its receptor, Plexin-A1, with off-track and vascular endothelial growth factor receptor type 2. *Genes Dev* **18**, 435-47.

Trousse, F., Marti, E., Gruss, P., Torres, M. and Bovolenta, P. (2001) Control of retinal ganglion cell axon growth: a new role for Sonic hedgehog. *Development* **128**, 3927-36.

Trumpp, A., Depew, M.J., Rubenstein, J.L., Bishop, J.M. and Martin, G.R. (1999) Cre-mediated gene inactivation demonstrates that FGF8 is required for cell survival and patterning of the first branchial arch. *Genes Dev* **13**, 3136-48.

Tucker, K.L., Meyer, M. and Barde, Y.A. (2001) Neurotrophins are required for nerve growth during development. *Nat Neurosci* **4**, 29-37.

Tzahor, E., Kempf, H., Mootoosamy, R.C., Poon, A.C., Abzhanov, A., Tabin, C.J., Dietrich, S. and Lassar, A.B. (2003) Antagonists of Wnt and BMP signaling promote the formation of vertebrate head muscle. *Genes Dev* **17**, 3087-99.

Varela-Echavarria, A., Pfaff, S.L. and Guthrie, S. (1996) Differential expression of LIM homeobox genes among motor neuron subpopulations in the developing chick brain stem. *Mol Cell Neurosci* **8**, 242-57.

Varela-Echavarria, A., Tucker, A., Puschel, A.W. and Guthrie, S. (1997) Motor axon subpopulations respond differentially to the chemorepellents netrin-1 and semaphorin D. *Neuron* **18**, 193-207.

Wahl, C. and Noden, D.M. (2001) Cryptic responses to tissue manipulations in avian embryos. *Int J Dev Neurosci* **19**, 183-96.

Wahl, C.M., Noden, D.M. and Baker, R. (1994) Developmental relations between sixth

nerve motor neurons and their targets in the chick embryo. *Dev Dyn* **201**, 191-202.

Wang, H.U. and Anderson, D.J. (1997) Eph family transmembrane ligands can mediate repulsive guidance of trunk neural crest migration and motor axon outgrowth. *Neuron* **18**, 383-96.

Wang, N., Butler, J.P. and Ingber, D.E. (1993) Mechanotransduction across the cell surface and through the cytoskeleton. *Science* **260**, 1124-7.

Watanabe, Y., Toyoda, R. and Nakamura, H. (2004) Navigation of trochlear motor axons along the midbrain-hindbrain boundary by neuropilin 2. *Development* **131**, 681-92.

Webber, C.A., Hyakutake, M.T. and McFarlane, S. (2003) Fibroblast growth factors redirect retinal axons in vitro and in vivo. *Dev Biol* **263**, 24-34.

Wen, Z., Guirland, C., Ming, G.L. and Zheng, J.Q. (2004) A CaMKII/calcineurin switch controls the direction of Ca(2+)-dependent growth cone guidance. *Neuron* **43**, 835-46.

Whitford, K.L., Marillat, V., Stein, E., Goodman, C.S., Tessier-Lavigne, M., Chedotal, A. and Ghosh, A. (2002) Regulation of cortical dendrite development by Slit-Robo interactions. *Neuron* **33**, 47-61.

Williams, B.A. and Ordahl, C.P. (2000) Fate restriction in limb muscle precursor cells precedes high-level expression of MyoD family member genes. *Development* **127**, 2523-36.

Williams, S.E., Mann, F., Erskine, L., Sakurai, T., Wei, S., Rossi, D.J., Gale, N.W., Holt, C.E., Mason, C.A. and Henkemeyer, M. (2003) Ephrin-B2 and EphB1 mediate retinal axon divergence at the optic chiasm. *Neuron* **39**, 919-35.

Winberg, M.L., Tamagnone, L., Bai, J., Comoglio, P.M., Montell, D. and Goodman, C.S. (2001) The transmembrane protein Off-track associates with Plexins and functions downstream of Semaphorin signaling during axon guidance. *Neuron* **32**, 53-62.

Wizenmann, A. and Lumsden, A. (1997) Segregation of rhombomeres by differential chemoaffinity. *Mol Cell Neurosci* **9**, 448-59.

Wolman, M.A., Liu, Y., Tawarayama, H., Shoji, W. and Halloran, M.C. (2004) Repulsion and attraction of axons by semaphorin3D are mediated by different neuropilins in vivo. *J Neurosci* **24**, 8428-35.

Wong, E.V., Kenwrick, S., Willems, P. and Lemmon, V. (1995) Mutations in the cell adhesion molecule L1 cause mental retardation. *Trends Neurosci* **18**, 168-72.

Wu, K.Y., Hengst, U., Cox, L.J., Macosko, E.Z., Jeromin, A., Urquhart, E.R. and Jaffrey, S.R. (2005) Local translation of RhoA regulates growth cone collapse. *Nature* **436**, 1020-4.

Xiang, Y., Li, Y., Zhang, Z., Cui, K., Wang, S., Yuan, X.B., Wu, C.P., Poo, M.M. and Duan, S. (2002) Nerve growth cone guidance mediated by G protein-coupled receptors. *Nat Neurosci* **5**, 843-8.

Xu, Q., Mellitzer, G., Robinson, V. and Wilkinson, D.G. (1999) In vivo cell sorting in complementary segmental domains mediated by Eph receptors and ephrins. *Nature* **399**, 267-71.

Yamada, K., Andrews, C., Chan, W.M., McKeown, C.A., Magli, A., de Berardinis, T., Loewenstein, A., Lazar, M., O'Keefe, M., Letson, R., London, A., Ruttum, M., Matsumoto, N., Saito, N., Morris, L., Del Monte, M., Johnson, R.H., Uyama, E., Houtman, W.A., de Vries, B., Carlow, T.J., Hart, B.L., Krawiecki, N., Shoffner, J., Vogel, M.C., Katowitz, J., Goldstein, S.M., Levin, A.V., Sener, E.C., Ozturk, B.T., Akarsu, A.N., Brodsky, M.C., Hanisch, F., Cruse, R.P., Zubcov, A.A., Robb, R.M., Roggenkaemper, P., Gottlob, I., Kowal, L., Battu, R., Traboulsi, E.I., Franceschini, P., Newlin, A., Demer, J.L. and Engle, E.C. (2003) Heterozygous mutations of the kinesin KIF21A in congenital fibrosis of the extraocular muscles type 1 (CFEOM1). *Nat Genet* **35**, 318-21.

Yamada, T., Pfaff, S.L., Edlund, T. and Jessell, T.M. (1993) Control of cell pattern in

the neural tube: motor neuron induction by diffusible factors from notochord and floor plate. *Cell* **73**, 673-86.

Yamada, T., Placzek, M., Tanaka, H., Dodd, J. and Jessell, T.M. (1991) Control of cell pattern in the developing nervous system: polarizing activity of the floor plate and notochord. *Cell* **64**, 635-47.

Ye, W., Bouchard, M., Stone, D., Liu, X., Vella, F., Lee, J., Nakamura, H., Ang, S.L., Busslinger, M. and Rosenthal, A. (2001) Distinct regulators control the expression of the mid-hindbrain organizer signal FGF8. *Nat Neurosci* **4**, 1175-81.

Yokoyama, N., Romero, M.I., Cowan, C.A., Galvan, P., Helmbacher, F., Charnay, P., Parada, L.F. and Henkemeyer, M. (2001) Forward signaling mediated by ephrin-B3 prevents contralateral corticospinal axons from recrossing the spinal cord midline. *Neuron* **29**, 85-97.

Zhu, Y., Yu, T., Zhang, X.C., Nagasawa, T., Wu, J.Y. and Rao, Y. (2002) Role of the chemokine SDF-1 as the meningeal attractant for embryonic cerebellar neurons. *Nat Neurosci* **5**, 719-20.

Zou, Y., Stoeckli, E., Chen, H. and Tessier-Lavigne, M. (2000) Squeezing axons out of the gray matter: a role for slit and semaphorin proteins from midline and ventral spinal cord. *Cell* **102**, 363-75.